Renal allograft failure: a study of the drivers of epithelial cell de-differentiation

Watchara Pichitsiri

A thesis submitted in partial fulfilment of the requirements
for the degree of Doctor of Philosophy

Applied Immunobiology and Transplantation Research Group
Institute of Cellular Medicine
Newcastle University
2011

Abstract

Kidney transplantation is the gold standard renal replacement therapy for patients with end-stage renal disease. Despite advances in immunosuppressive therapy, chronic allograft dysfunction remains the commonest cause of renal allograft failure in living recipients. The typical pathology of this disease includes chronic inflammation with tubular atrophy and interstitial fibrosis. Although the origin of the excess fibroblasts and myofibroblasts remains controversial, the process of epithelial to mesenchymal transition might play a role. This study was designed to test the linked hypotheses that the immunosuppressive drug, Cyclosporine A and graft infiltrating T cells can induce allograft pathology by alteration of the bioavailability of fibrogenic TGF-β.

An initial series of experiments examined the induction of mesenchymal transition by treatment of cultured human renal tubular epithelial cells with immunosuppressive concentrations of Cyclosporine A. Drug treated cells showed characteristic morphological changes associated with increased expression of the mesenchymal marker S100A4 and reduced expression of the epithelial marker E-cadherin; similar changes were induced by the addition of TGF-β1. The phenotypic change induced by Cyclosporine A was not the consequence of an increased response to autocrine TGF-β and could not be inhibited by specific blockade of the ALK5 component of the TGF-β receptor. Further studies showed *in vitro* that contact between activated T cells and renal tubular epithelial cells could induce mesenchymal transition by a mechanism that was dependent on activation of the TGF-β receptor complex. A final series of experiments defined a mechanism by which T cells activate latent TGF-β allowing subsequent receptor stimulation leading to either T cell or epithelial cells differentiation. The latency associated peptide binds to and inhibits native TGF-β but can be displaced by both thrombospondin-1 and neuropilin-1, producing active TGF-β. In this study it was shown that cytoplasmic thrombospondin-1 is exported and expressed on the surface of activated T cells following brief interaction with renal tubular epithelial cells; neuropilin-1 was also expressed by a mean 18% of activated human T cells. Inhibition of these two molecules with a blocking LSKL peptide sequence inhibited the normal response of activated human T cells to latent TGF-β1.

This study demonstrated that both Cyclosporine A and T cells can induce renal epithelial to mesenchymal cell transition. However, the former process seems independent of TGF-β whilst the latter requires TGF-β receptor stimulation and might be regulated *in vivo* by T cell-mediated activation of latent TGF-β within the allograft.

Acknowledgements

This thesis would not have been possible without the guidance and the help of several individuals who in one way or another contributed and extended their valuable assistance in the preparation and completion of this study.

First and foremost, I offer my utmost gratitude to my supervisor Professor John Kirby whose encouragement; supervision and support from the preliminary to the concluding level enabled me to develop an understanding of the study. His guidance helped me in all the time of research and writing of this thesis. I could not have imagined having a better advisor and mentor for my PhD study.

My sincere thanks also go to my other supervisors Dr Simi Ali and Dr Helen Robertson for helping me not only the outstanding laboratory techniques in the field of your expertise-molecular biology and immunohistochemistry- but also for yours precious support during my laboratory work period.

I would like to thank also members of flow cytometry facility and confocal bio imaging unit who also contributed to my work Ian Harvey, Susan Stamp, Brian Shenton and Trevor Booth.

I would like to thank all members of the lab, past and present, for making this three years a time to remember: David Swan, A A Alhasan, Joseph Willet, Marcin, Abdul, Julia, Sarah and Karolina. Many thanks go to others in particular to Graeme for his friendship and research support and Mo Kirkley, the most kind and patient person.

I would like to thank the Faculty of Medicine, Naresuan University who funded this research.
Finally, I would like to express my gratitude to the two most significant people in my life Mum and Dad who always give me endless support and encouragement, without them I would be nothing.

Table of content

Table of contents

Table of contents

List of figures

List of figures

List of figures

List of figures

List of tables

Chapter 1: Introduction

1.1 History of kidney transplantation

The first successful experimental kidney transplants in animals were reported in 1902 by Dr. Emmerich Ullmann in Vienna; however, the incidence of rejection was not mentioned (Druml et al., 2002). Later in 1923, Dr. Carl Williamson firstly examined a failed kidney transplant and identified the difference between autografted and allografted kidney. In addition, he introduced the term "rejection" and published the histology of a rejecting kidney (Eedy et al., 2004).

The first human-to-human kidney transplant was performed in 1933 by Yuri Voronoy, who transplanted a cadaver kidney into the medial thigh. However, the kidney graft did not function due to an ABO blood group mismatch (Matevossian et al., 2009). The first recorded event in which a transplanted kidney functioned was in 1951. David Hume in Boston performed a series of cadaveric kidney transplants into the thigh of recipient patients. All but one of these kidneys was rejected within days or weeks; the one exception was a patient in whom the kidney functioned for nearly 6 months (Hume et al., 1955). This event provided hope for the future as no immunosuppressive therapy was used in this patient. In 1953, a further advance was provided by the demonstration that tolerance to an allogeneic skin graft in an adult animal could be produced by injecting the foetus with donor strain tissue (Billingham et al., 1953).

The modern era of clinical transplantation began on December 1954, when Joseph Murray and his colleagues at Harvard performed the first kidney transplantation between identical twin brothers (Murray et al., 1958). Before 1980, the best therapeutic option for patients with kidney failure was dialysis; however, despite numerous medical and technical advances, patients with kidney failure who were treated with dialysis mostly experience a poor quality of life with increased morbidity and mortality. In recent times kidney transplantation has become the treatment of choice for patients with end-stage renal disease (ESRD). However, limitations such as an inadequate organ supply and poor long-term graft outcome remain important problems for kidney transplantation.

1.2 Kidney allograft survival

A successful transplant restores an acceptable quality of life to ESRD patients; this is due in part to the availability of potent immunosuppressive drugs. Currently, the number of patients with end-stage renal failure in the USA who might be treated by haemodialysis and transplantation comprises 350 new patients per million of population (Figure 1.1) (2010 USRD

annual report). This is consistent with the incidence of ESRD in Thailand, which increased from 30 per million of population in 1997 to 500 per million of population in 2008.

Unfortunately, the supply of kidneys for transplantation is not sufficient to meet demand. In fact, there is an attempt to expand the supply of donor kidneys by use of living donors, expanded criteria donors and non-heart beating donors. As a result, the number of kidney transplant operations has increased. Although the 1-year graft survival has increased to 92-93% (Figure 1.2 and Table 1.1) and 96% (Figure 1.3 and Table 1.2) for cadaveric and living donor transplantation respectively, the 10-year graft survival has remained unsatisfactory at approximately 67-70% for cadaveric donor (Figure 1.2 and Table 1.1) and 72-78% for living donor organs (Figure 1.3 and Table 1.2).

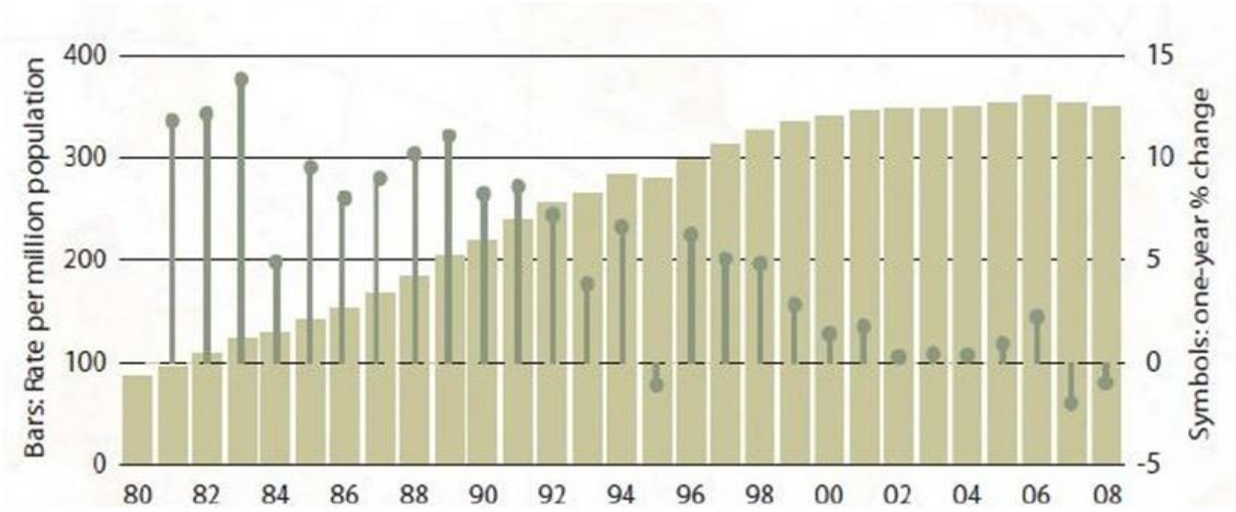

Figure 1.1 Incidence of ESRD patients from 1980-2008.

The incidence of ESRD patients has gradually increased since 1980; however, it has remained stable at around 350 per million population since 2000. These data are obtained from the 2010 USRD annual report.

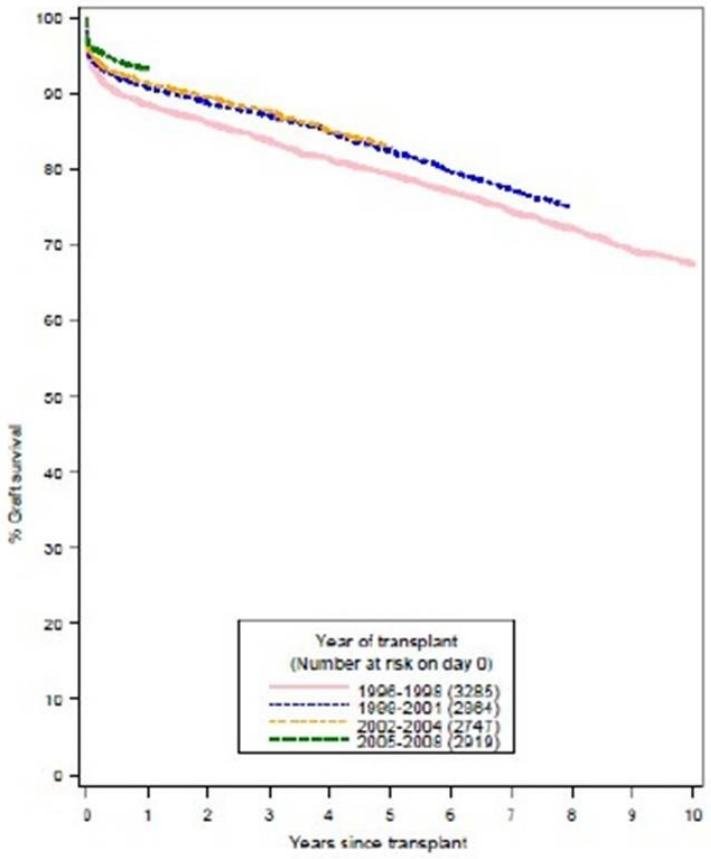

Figure 1.2 Long-term graft survivals in adult recipients for kidney transplant from donors after brain death. Data are obtained from the transplant activity report 2009-2010, UK.

Year of transplant	% Graft survival			
	One year	Two years	Five years	Ten years
1996-1998	89	86	79	67
1999-2001	91	89	82	
2002-2004	91	90	83	
2005-2008	93			

Table 1.1 The graft survival at one, two, five and ten years post kidney transplant from donors after brain death. Data are obtained from transplant activity report 2009-2010, UK.

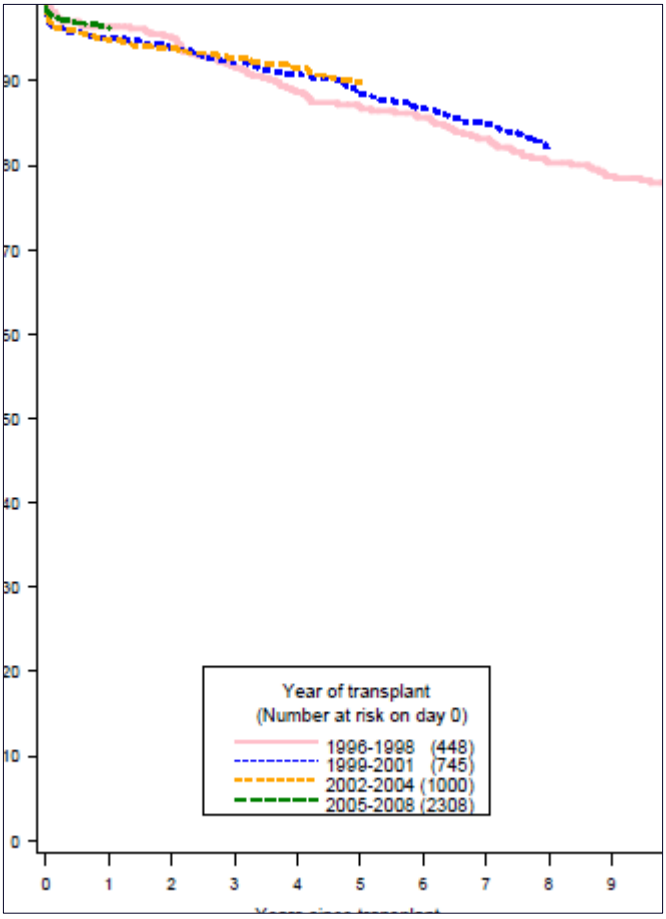

Figure 1.3 Long-term graft survivals in adult recipients for living donor kidney transplants in the UK. Data are obtained from transplant activity report 2009-2010, UK.

Year of transplant	% Graft survival			
	One year	Two years	Five years	Ten years
1996-1998	96	95	87	78
1999-2001	95	94	89	
2002-2004	96	94	90	
2005-2008	96			

Table 1.2 The graft survival for one, two, five and ten years post kidney transplant from living donors. Data are obtained from transplant activity report 2009-2010, UK.

Chapter 1: Introduction

1.3 Kidney biology

The kidney is one of the most highly differentiated organs in the body. Its functions include endocrine functions, regulation of blood pressure and intraglomerular hemodynamics, solute and water transport, acid-base balance, and the removal of waste or drug metabolites. Renal development starts when a branch of the ureteric bud invades an aggregate of mesenchymal cells called the metanephric mesenchyme. The ureteric bud cells differentiate into the epithelia of the collecting duct, whilst the metanephric mesenchymal cells differentiate into the epithelia of the rest of the nephron (Oliver et al., 2002). In the adult kidney, epithelial cells are the most frequent cells; they play a critical role in kidney function. Loss of epithelial integrity can lead to kidney dysfunction. Other cells which are contained in the kidney include mesangial, vascular smooth muscle, endothelial, renal medullary interstitial cells, myofibroblasts, fibroblasts, macrophages, and neurons (Oliver et al., 2002).

The nephron is the functional unit of the kidney. Each human kidney normally contains approximately $0.6x10^6$ - $1.4x10^6$ nephrons. These nephrons can be divided into two types based on their origins: cortical nephrons and juxtamedullary nephrons. Each nephron consists of two main components: the renal corpuscle and the renal tubules.

1.3.1 Renal tubular system

Renal tubules are composed of three main parts: the proximal tubule, the loop of Henle and the distal tubule (Figure 1.4). The main function of the tubules is maintaining homeostasis of acid-base, fluid and electrolytes by the mechanisms of secretion and reabsorption.

1.3.1.1 Proximal renal tubule

The proximal tubule is the initial part of the tubular system, connecting to the glomerulus. This tubule is divided into two parts on the basis of morphology: a proximal convoluted part (Pars convolute) and a straight part (Pars recta). The most distinctive feature of the proximal tubule is the presence of microvilli or brush border at the luminal surface. These microvilli increase the luminal surface area in order to enhance the reabsorptive capacity. Proximal tubular epithelial cells are also able to produce specific enzymes, including gamma-glutamyl transpeptidase (GGT) and alkaline phosphatase.

1.3.1.2 Loop of Henle

The loop of Henle is comprised of a thin and thick limb. The thin limb is responsible for the maintenance of a hypertonic medullary interstitium in order to dilute or concentrate the urine.

This part of the tubule originates near the corticomedullary junction and is formed by flat and simple cuboidal epithelial cells.

1.3.1.3 Distal tubule

The distal tubule is composed of three segments: the thick ascending limb of the loop of Henle, the macula densa and the distal convoluted tubule. The epithelial cells which line the ascending limb contain large mitochondria for Na^+ (sodium ion) reabsorption. These cells are attached to each other by tight junctions and adherens junctions, but desmosomes are absent. The distal convoluted tubule is lined with a cuboidal epithelium containing numerous mitochondria and is similar to the proximal tubule, except that there is no brush border in the distal tubule. The macula densa is a specialized region of the thick ascending limb which plays an important role in volume homeostasis through the rennin-angiotensin-aldosterone system. Following the distal tubule is the connecting tubule which connects the distal tubule and collecting duct.

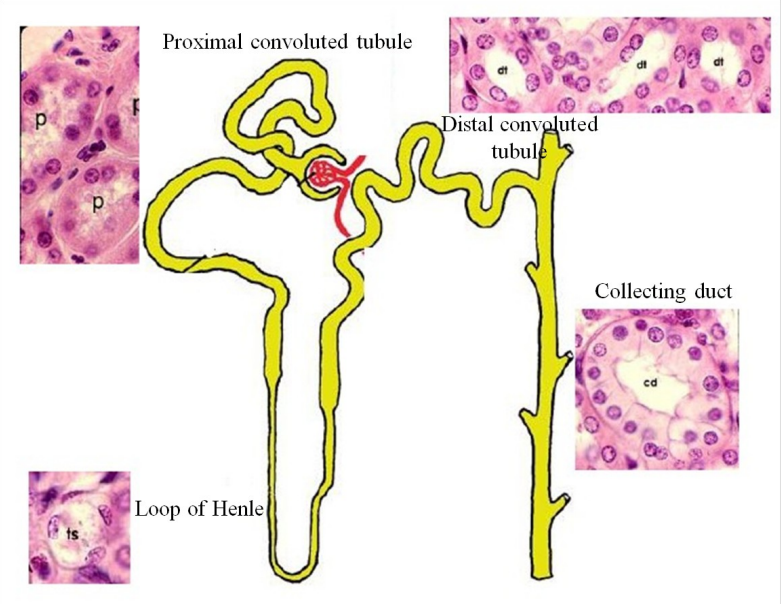

Figure 1.4 Diagram illustrating the renal tubular system. The image is adapted from Brenner and Rector's the kidney 8th edition.

1.3.2. Intercellular junctions

The renal tubular epithelium is organized as a contiguous monolayer of cuboidal cells which are attached to each other by intercellular junctions on the apical side and connected to the basement membrane on the basal side. The intercellular junctions of the epithelium, which play a major role in maintaining cell polarity and integrity, comprise three different cell-cell contact structures: tight junctions, adherens junctions and desmosomes (Xu et al., 2009) (Figure 1.5).

1.3.2.1 Tight junctions

A tight junction is an intercellular junction structure at the lateral side close to the apical surface of the epithelial cell. Functions of tight junctions include providing intercellular sealing, controlling paracellular diffusion and preventing intramembrane diffusion between the apical and basolateral surfaces. Tight junctions consist of transmembrane proteins, including occludin, claudins and junctional adhesion molecules, and peripheral membrane proteins such as zonula occludens (ZO), which interact with each other to form a complex network (Shin et al., 2006). Occludin and claudins are essential structures of the intercellular tight junction strands. ZO provides the strength and integrity of tight junctions by interacting with actin filaments (Xu et al., 2009).

1.3.2.2 Adherens junctions

Adherens junctions are located immediately below the tight junctions on the basolateral surface of the epithelial cells. Previous studies suggest that the formation of adherens junctions is essential for the assembly of tight junctions (Troxell et al., 2000); thus, alteration of the adherens junctions modulates tight junction formation and the epithelial paracellular barrier. The adherens junctions are important for normal functions of epithelium such as providing strong adhesive links between cells via homotypic interaction of E-cadherin, and maintaining apical-base axis and polarity (Baum et al., 2011).

Cadherins are Ca^{2+}-dependent adhesion molecules essential for the induction and maintenance of the adherens junctions (Angst et al., 2001). The transmembrane adhesion protein E-cadherin is the major cadherin expressed by epithelial cells, including renal epithelial cells (Veerasamy et al., 2009). The extracellular domain of E-cadherin interacts with the adjacent cells through homotypic interactions, whereas the cytoplasmic tail is associated with β-catenin, an intercellular protein that binds to α-catenin, which interacts with the actin cytoskeleton (Xu et al., 2009). Loss of E-cadherin expression is recognized as one of the key events of epithelial transformation (Yang et al., 2001).

β-catenin is also an intracellular signal transduction molecule that mediates signalling in the Wnt growth factor pathway. Signalling through the canonical Wnt pathway is initiated by secreted Wnt proteins which bind to a transmembrane receptors encoded by frizzled genes. Activation of the receptor leads to phosphorylation of dishevelled protein which associates with axin and this complex prevents glycogen synthase kinase 3β (GSK3β) from phosphorylating β-catenin (Liu et al., 2010). Unphosphorylated β-catenin escapes E3 ubiquitin ligase-mediated proteosomal degradation, forms a complex with transcription factors and regulates gene

expression. The complex of β-catenin with T cell factor (TCF) has been shown in a number of studies to promote epithelial to mesenchymal transition (EMT) (Liu et al., 2010).

1.3.2.3 Desmosomes

Desmosomes are intercellular adhesion complexes located on the lateral surface of epithelial cells. A desmosome is characterized by transmembrane proteins and desmosomal plaque proteins that link the structure to the intermediate filament cytoskeleton (Delva et al., 2009). Desmogleins and desmocollins are cadherin transmembrane proteins which mediate cell adhesion by their extracellular domains, whereas the cytoplasmic domains interact with the plakophilin and plakoglobin proteins, which are also associated with desmosomal plaque protein, desmoplakin, providing a link to keratin intermediate filaments (Delva et al., 2009).

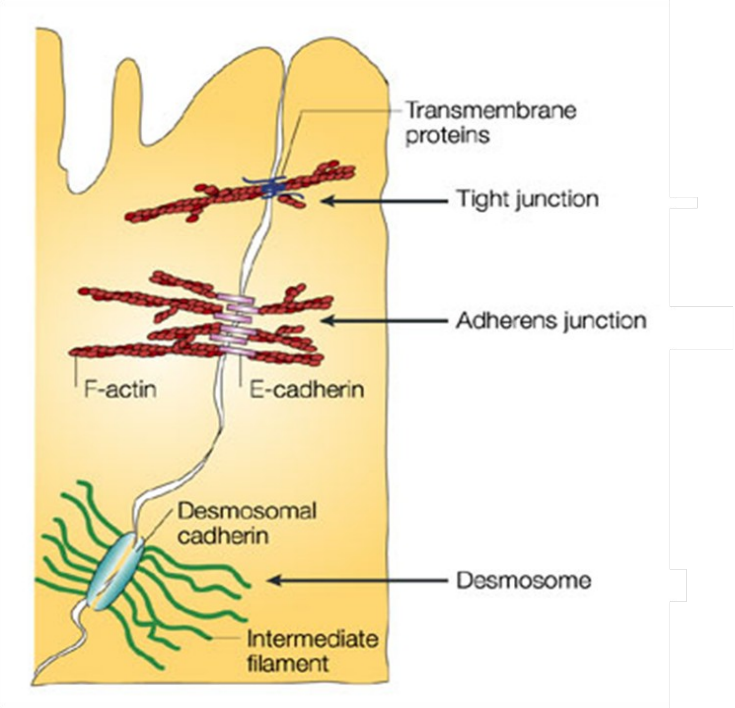

Figure 1.5 Schematic demonstrating the main types of intercellular junction in epithelial cells.

The tight junction contains transmembrane proteins that link to the actin cytoskeleton. Adherens junctions are formed by homophilic interaction between E-cadherin molecules and are associated to the actin filament through β and α-catenins. Desmosomes consist of desmosomal cadherins linked to keratin intermediate filaments and integrate the intermediate filament network across the epithelial sheet. This image is from Kobielak and Fuchs, 2004.

1.4 Mechanism of T cell activation

T lymphocytes (T cells) play a key role in cell-mediated immune responses, including cell-mediated rejection following kidney allotransplantation. Most graft-infiltrating T cells

during acute renal allograft rejection are effector T cells which are generated by the activation of naive or cross-reactive memory T cells. This T cell activation involves the recognition of allogeneic class I and class II MHC antigens on appropriate antigen presenting cells.

1.4.1 Major histocompatibility complex

The major histocompatibility complex (MHC) contains a series of genes which encode class I MHC antigens which are present on the surface of almost every cell in the human body. Class II MHC antigens are also encoded by genes in the MHC, but the expression of these antigens is normally restricted to haematogenous antigen presenting cells. Together these histocompatibility antigens play an important role in determining the outcome of organ allotransplantation. When the donor and recipient differ in their histocompatibility antigens, there is a potential for allograft rejection (Apostolopoulos et al., 2008). The human MHC genes are present on chromosome 6. In humans, the MHC antigens are called human leukocyte antigens (HLA). The class I antigens include HLA-A, HLA-B, and HLA-C, and the class II antigens include HLA-DP, HLA-DQ and HLA-DR (Figure 1.6).

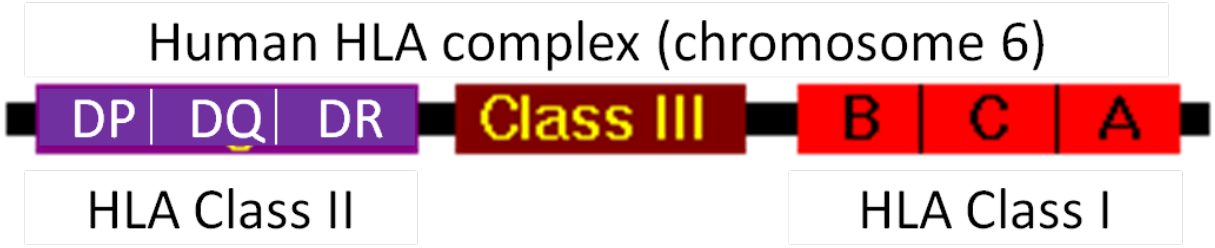

Figure 1.6 Human leukocyte antigens are encoded on chromosome 6.

1.4.1.1 MHC class I molecules

Class I MHC antigens are composed of a polymorphic glycosylated heavy α chain which is noncovalently bound to nonpolymorphic light chain β2-microglobulin. The heavy chain anchors the MHC complex to the cell membrane and contains three extracellular domains (α1, α2 and α3), a hydrophobic transmembrane region and a short cytoplasmic tail (Figure 1.7A). The MHC class I molecules are expressed on the cell surface of almost all nucleated cells. The foreign antigens presented by MHC class I molecules are recognized by host $CD8^+$ T cells. In addition, MHC class I molecules typically bind peptide epitopes derived from proteins in the cytoplasm of cells, including viral proteins (Apostolopoulos et al., 2008).

1.4.1.2 MHC class II molecules

The class II MHC antigens have a similar overall structure to class I antigens, but are composed of polymorphic α and β chains (Figure 1.7 B). The class II molecules are normally

expressed only on professional antigen-presenting cells (APCs), including dendritic cells, B lymphocytes and macrophages. However, during an inflammatory response, some other cell types may be induced to express MHC class II proteins by the action of cytokines such as interferon (IFN)-γ (Kimmel et al., 2003). MHC class II molecules typically bind extracellular peptides.

1.4.2 Minor histocompatibility antigens (miHA)

The observation that T cells recognize peptide epitopes in the context of presentation by MHC antigens explains why MHC-matched graft tissues can be rejected on the basis of the expression of minor histocompatibility antigens (miHA). These antigens are now understood to consist of graft-specific peptides which are presented by MHC antigens. The classical example is the H-Y antigen which allows female recipients to recognize MHC-matched male cells. This was first demonstrated in animal models (Barth et al., 1956), but may also play a role in acute rejection of human kidney allograft tissue (Kim et al., 2009).

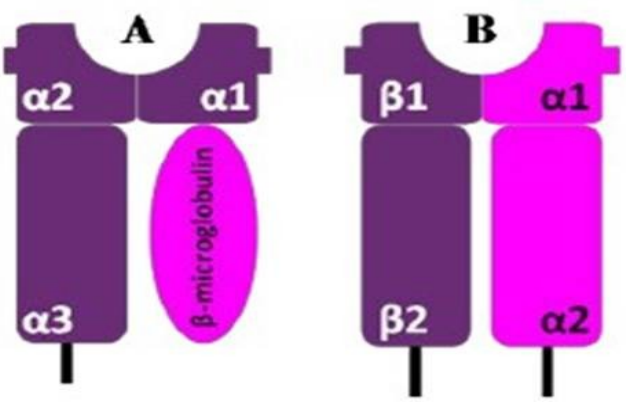

Figure 1.7 Structure of MHC class I and class II antigens

(A) MHC class I antigens consists of polymorphic α chains (α1, α2 and α3) noncovalently attached to β2-microglobulin. (B) MHC class II antigens consists of polymorphic α chains (α1 and α2) attached to polymorphic β chains (β1 and β2). This image is taken from Alfzali et al., 2007.

1.4.3 Antigen presenting cells

T cell activation is achieved by specific recognition of a peptide-MHC antigen complex displayed on the surface of specialized antigen presenting cells. APC can be divided into two groups: professional APC and non-professional APC. Professional antigen presenting cells are defined as cells of haematopoietic origin which express costimulatory molecules and MHC class

I and class II molecules. These cells include dendritic cells (DC), macrophages and B cells, and are specialized to initiate T cell activation (Resigno, 2010). Among the professional APC, activated DC are the most potent stimulators of naïve T cells due to their high level expression of MHC class I and class II antigens and costimulatory molecules (Ingulli, 2010). Non-professional APC include epithelial cells, endothelial cells and stromal cells which normally do not express MHC class II unless they are stimulated by the proinflammatory cytokine IFN-γ (Resigno et al., 2010). Activation of naive T cells requires two signals delivered by the APC. The first signal is antigen-specific and delivered by the T cell receptor. The second signal is an antigen nonspecific signal triggered by the interaction of cell-surface costimulatory molecules on a professional APC with corresponding receptors on the T cell (Pilat et al., 2011).

1.4.4 Allorecognition

T cells need to be activated in order to proliferate and differentiate to effector T cells. However, the activation process requires an encounter between T cells and foreign peptide-MHC complexes on antigen presenting cells. Three pathways of alloantigen recognition have been described (Safinia et al., 2010): the direct pathway in which recipient T cells recognize intact allogeneic peptide-MHC complexes expressed on the surface of donor APC (Game et al., 2002), the indirect pathway in which recipient T cells recognize peptides derived from allogeneic MHC molecules presented by self APC (Gökman et al., 2008), and the semi-direct pathway in which recipient DC acquire intact allogeneic antigen-MHC complexes from donor cells and present these to recipient T cells (Herrera et al., 2004) (Figure 1.8).

1.4.4.1 Direct allorecognition

In order for recipient T cells to directly bind to intact allogeneic peptide-MHC complexes, donor APC must migrate out of the graft to make direct contact with recipient T cells within secondary lymphoid tissue. The importance of donor APC in causing graft rejection was demonstrated by prolonged survival of donor-derived APC-depleted allogeneic thyroid grafts in the absence of immunosuppression (Lafferty et al., 1976). This result supports the importance of the direct pathway, as stimulation of recipient T cells is dependent on donor APCs. In addition, an adoptive transfer experiment in T cell deficient SCID and $Rag^{-/-}$ mice showed that acute $CD4^+$ T cell-mediated rejection required donor MHC class II molecules. Furthermore, MHC class II deficient mice also rejected grafts when reconstituted with $CD4^+$ T cells, suggesting that direct recognition plays an important role during acute rejection (Pietra et al., 2000). It is believed that the direct pathway is responsible for early rejection because of the high frequency

of T cells capable of recognizing allogeneic MHC on donor dendritic cells (DCs) (Caballero et al., 2006). However, donor DCs are depleted rapidly after engraftment due to apoptosis and elimination by the recipient immune system (Hornick et al., 1998; Caballero et al., 2006).

1.4.4.2 Indirect allorecognition

In contrast to the direct pathway, the indirect pathway of allorecognition describes recipient APC presenting donor MHC-derived peptides complexed with self-MHC molecules to recipient T cells. Foreign antigens can be processed by three mechanisms. Firstly, antigens from the graft are shed into the circulation and engulfed by recipient DC within secondary lymphoid tissues. Secondly, donor cells migrate to secondary lymphoid organs and are captured by recipient DC for antigen processing and presentation. Thirdly, recipient APC migrate into the graft, take up antigens and then migrate to secondary lymphoid tissues.

Evidence supporting the indirect pathway was provided by MHC class II-deficient skin grafts which were rejected rapidly by normal recipients (Auchincloss et al., 1993). Importantly, removal of recipient $CD8^+$ cells or $CD4^+$ cells showed that $CD4^+$ cells were involved in, and required for, this rapid rejection (Auchincloss et al., 1993). Since the donor grafts lacked class II MHC molecules, recipient $CD4^+$T cells must recognize donor antigens presented in association with recipient class II molecules.

1.4.4.3 Semi-direct allorecognition

Recently, a number of publications have shown that intact donor cell-surface molecules, including MHC, can be transferred to recipient APC leading to activation of T-cells which can directly recognise allograft cells (Jiang et al., 2004).

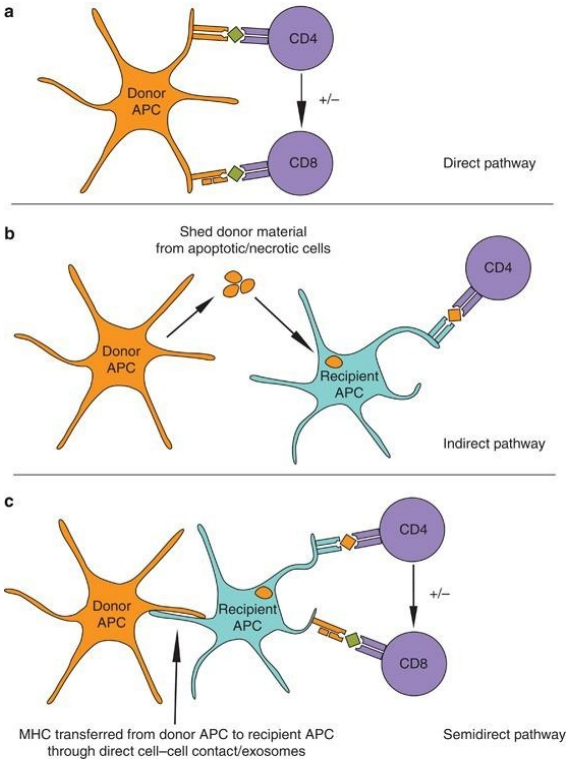

Figure 1.8 Diagram shows direct, indirect and semi-direct allorecognition pathways.

(A) Direct pathway. Intact foreign MHC on donor APC binds $CD4^+$ and $CD8^+$ recipient T cells; $CD4^+$ T cells provide help for the effector function of $CD8^+$ T cells. (B) Indirect pathway. Recipient APCs present processed donor peptides to $CD4^+$ T cells. (C) Semi-direct pathway. Cell-to-cell contact between donor and recipient APC may transfer intact allogeneic MHC antigens. The image is taken from Safinia et al., 2010.

1.4.5 The immune response

When an alloantigen is recognized by any of the pathways described above, effector T cells are activated leading to allograft destruction. This alloresponse results from the activation of either naïve T cells or memory T cells. It has been reported that 40-50% of circulating T cells in humans has a memory phenotype (McFarland et al., 2000). A re-transplant model in mice demonstrated a more severe immune response resulting from the activation of memory T cells than from naïve T cells (Liang et al., 2010). Activated T cells can generate a range of effector mechanisms. These include cellular (delayed-type) hypersensitivity (DTH), contact-dependent T-cell cytotoxicity and humoral (antibody and complement) immunity (Afzali et al., 2007) (Figure 1.9).

Following activation, $CD4^+$ T cells secrete interleukin (IL)-2 which induces naive T cells to become T helper 0 (Th0) cells. Combination of IL-2 with IFN-γ and IL-12 or IL-4 causes

these Th0 cells to differentiate into two subsets: T helper 1 (Th1) and T helper 2 (Th2) cells respectively. Th1 cells help $CD8^+$T cell activation and macrophage-dependent DTH responses, whilst Th2 cells are typically responsible for humoral responses and eosinophil activation (Le Moine et al., 2002). Following activation, $CD8^+$T cells become cytotoxic and destroy target cells by two main mechanisms: the release of perforin and granzymes and activation of the Fas-Fas ligand system.

Naive B cells can be activated in a T cell-dependent and T cell-independent manner depend on the nature of antigens (Benson et al., 2007). Most alloantigens are T cell-dependent. Therefore, B cells need to process antigen and present antigen-MHC class II complex to Th2 cells resulting to B cell proliferation, plasma cell differentiation and the production of allospecific antibodies.

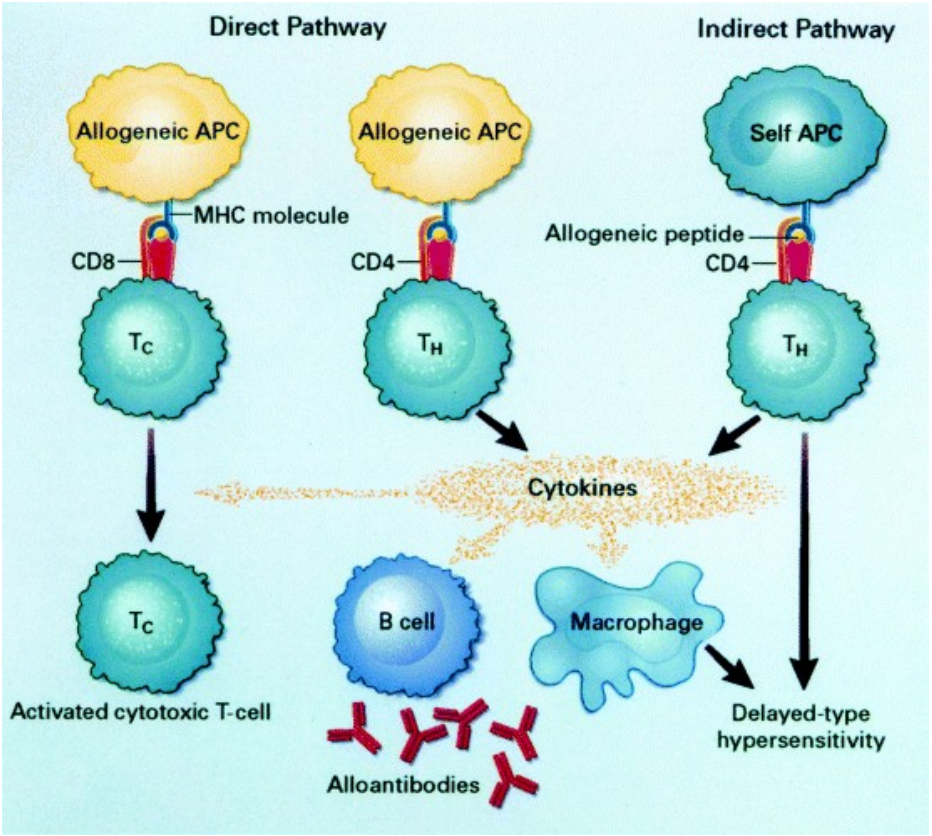

Figure 1.9 The central role played by T cell activation in allograft immunity.
$CD8^+$T cells become activated cytotoxic T cells. Activated $CD4^+$T cells differentiate to T helper cells and secrete multiple cytokines leading to delayed-type hypersensitivity and alloantibody responses. This image is obtained from Sayegh, 1999.

1.5 Banff classification of renal allograft pathology

Kidney allograft biopsy provides essential information for diagnosis among many causes of acute or chronic allograft dysfunction. Therefore, standardization of renal allograft biopsy interpretation is necessary for treatment decisions and also for clinical trials. In 1991, a group of pathologists, nephrologists and transplant surgeons met in Banff, Canada, to formulate the nomenclature and classification of renal allograft pathology. Since then, a Banff meeting has been held every two years to review and update the criteria for the diagnosis of renal allograft pathology. The most recent update of the Banff classification was published in 2009 and is detailed below (Sis, 2010).

1.5.1 Banff 2009 classification

In order to define the Banff rejection adequate biopsy specimens are required. These must contain two cores of tissue with cortex containing ≥ 10 glomeruli and ≥ 2 arteries. The pathology is scored as follows:

1. Normal kidney

2. Antibody-mediated rejection (ABMR)

2.1 C4d deposition and the presence of circulating anti-donor antibodies but without morphologic evidence of acute rejection.

2.2 Acute ABMR

a. Type I: C4d+, presence of anti-donor antibodies with ATN (acute tubular necrosis)-like minimal inflammation.

b. Type II: C4d+, presence of anti-donor antibodies and leukocytes in peritubular capillaries (PTC).

c. Type III: C4d+, presence of anti-donor antibodies with transmural arteritis.

2.3 Chronic active ABMR: C4d+, presence of anti-donor antibodies with morphological changes including glomerular double contour, peritubular capillary basement membrane multilayering, interstitial fibrosis and tubular atrophy (IF/TA) and arterial fibrous thickening.

3. Borderline changes: tubulitis (mononuclear cell infiltration in tubular epithelial cells) with minimal interstitial infiltration

4. T cell-mediated rejection (TCMR)

4.1 Acute TCMR

a. Type IA: interstitial infiltration (>25%) with moderated tubulitis (>4 mononuclear cells/ tubular cross section)

b. Type IB: interstitial infiltration (>25%) with severe tubulitis (>10 mononuclear cells / tubular cross section)

c. Type IIA: mild to moderate intimal arteritis

d. Type IIB: severe intimal arteritis (>25% of lumen occlusion)

e. Type III: transmural arteritis

4.2 Chronic TCMR: arterial intimal fibrosis with mononuclear cell infiltration in fibrosis (chronic allograft arteriopathy).

5. Interstitial fibrosis and tubular atrophy (IF/TA) without specific causes.

5.1 Grade I: Mild IF/TA (<25% of cortical area)

5.2 Grade II: Moderate IF/TA (26-50% of cortical area)

5.3 Grade III: Severe IF/TA (>50% of cortical area)

6. Other: change not due to rejection

1.6 T-cell mediated rejection (TCMR)

According to the Banff classification (section 1.5.1), TCMR is defined by infiltration of recipient mononuclear cells into the renal tubules (tubulitis), arterioles (endotheliolitis) and interstitium (Figure 1.10), followed by functional deterioration of the renal allograft. According to recent data, 19% of renal allograft fibrosis resulted from TCMR. In addition, 5.8% of this subgroup eventually progressed to renal allograft loss (El-Zoghby et al., 2009)

1.6.1 Mechanism of leukocyte recruitment

Infiltration of inflammatory cells into the renal allograft tubular epithelium is the hallmark of the alloimmune response leading to tubular injury, interstitial fibrosis and subsequent chronic allograft dysfunction. Leukocyte recruitment from the blood into the graft tissues is essential for development of TCMR. Recruitment of lymphocytes across the vascular endothelium is a complex process, as described below.

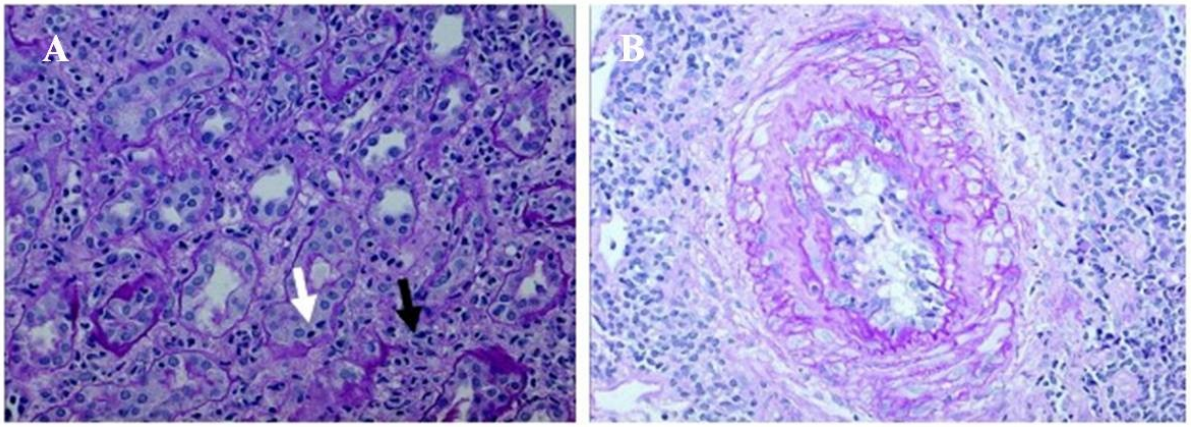

Figure 1.10 Microscopic analysis demonstrating histology of TCMR.
(A) Periodic acid-Schiff staining showing mononuclear cells infiltrating renal tubules (tubulitis; white arrow) and the interstitial tissues (black arrow). (B) Periodic acid-Schiff staining showing subendothelial infiltration with >25% luminal occlusion (severe intimal arteritis). These images were obtained from Dr Helen Robertson, personal communication.

1.6.1.1 Leukocyte tethering and rolling

The first steps of T cell recruitment include leukocyte tethering and rolling along the vessel wall, which is mediated primarily by interactions between selectin and selectin ligands. The selectins are a calcium-dependent, type I transmembrane glycoproteins. Three selectins have been identified: E-selectin, P-selectin and L-selectin which were originally discovered in endothelial cells, platelets and leukocytes respectively (Kelly et al., 2007). The selectins are upregulated on the surface of endothelial cells by inflammatory cytokines such as tumor necrosis factor (TNF)-α and IL-1β (Thurman, 2007).

1.6.1.2 Leukocyte adhesion

*Chemo*attractant cyto*kines* or chemokines are responsible increasing leukocyte adhesion to the apical surface of endothelial cells. Chemokines induce specific leukocyte recruitment to the affected area during inflammation. In the early phase after transplantation, the proinflammatory cytokines TNF-α and IL-1β are released by allograft endothelial cells and renal epithelial cells as a consequence of ischemia/reperfusion injury and tissue trauma (Thurman et al., 2006). Subsequently, proinflammatory cytokines induce local chemokine secretion. Several chemokines have been observed in renal allograft biopsies during acute rejection and chronic allograft nephropathy, including CCL-2 (MCP-1), CCL-3 (MIP-1α), CCL-4 (MIP-1β), CCL-5 (RANTES) (Robertson et al., 2000), CCL-13 (MCP-4) (Chakravorty et al., 2001), CCL-20 (MIP-

3α) (Woltman et al., 2005), CXCL-5 (ENA-78) (Schmouder et al., 1995), CXCL-8 (IL-8) (Sibbring et al., 1998), CXCL-10 (Lazzeri et al., 2005), MIF (Lan et al., 1998) and CX3CL1 (Gao et al., 2006).

Proinflammatory cytokines and chemokines activate integrin expression by leukocytes and also increase integrin adhesion. Critical adhesion molecules on leukocytes include the integrins leukocyte function associated molecule-1 (LFA-1) and very late antigen-4 (VLA-4). Endothelial counter-receptors for these adhesion molecules are intercellular adhesion molecules (ICAM)-1 and ICAM-2, and vascular cell adhesion molecule-1 (VCAM-1) respectively; these are also up-regulated by cytokine stimulation (Kelly et al., 2007), leading to firm adhesion between recipient leukocytes and allograft endothelial cells.

1.6.1.3 Intraluminal crawling

This is a step in which leukocytes move from the primary adhesion site to the nearest endothelial cell junction in order to begin diapedesis (Schenkel et al., 2004).

1.6.1.4 Leukocyte transendothelial migration

This is a final step in which leukocytes cross the endothelial wall and enter the interstitium. This process can occur by two different pathways: paracellular or transcellular migration. Paracellular diapedesis is a process by which leukocytes and endothelial cells co-ordinately disassemble endothelial cell-cell junctions leading to a gap formation between endothelial cells. However, transcellular diapedesis is the process by which leukocytes migrate directly through individual endothelial cells via a transcellular pore without disrupting the endothelial cell-cell junction (Carman, 2009).

1.6.2 $CD103^+CD8^+$ T cells: a predominant T cell population in renal tubulitis

A characteristic of TCMR is deterioration of the renal allograft associated with interstitial infiltration by mononuclear cells and penetration of T lymphocytes through the tubular basement membrane to contact the epithelial cells (Racusen et al., 1999). It has long been recognized that $CD8^+$ T cells are the predominant intratubular T cell population (Robertson et al., 1996). Previous studies have shown the expression of CD8 mRNA by T cells in urine during acute renal allograft rejection (Vasconcellos et al., 1998; Yannaraki et al., 2006), suggesting a role for these cells during graft rejection. Although $CD8^+$ T cells are a main population of graft infiltrating T cells, CD8 blockade could not abolish graft rejection whilst blockade of CD4 did reduce the severity of rejection (Lee et al., 1994; Pietra et al., 2000). It remains unclear whether $CD4^+$ T

cells provide help for a $CD8^+$ T cell effector response or $CD4^+$ T cells play a key role in the effector phase of an immune response.

Previous studies have shown that the $\alpha E(CD103)\beta_7$ integrin (termed CD103) defines a subset of largely intratubular $CD8^+$ effector T cells during renal allograft rejection (Hadley et al., 1997). This integrin was first identified by its expression on T cells in the gut mucosa where it is expressed by >95% of intestinal intraepithelial lymphocytes and ~40% of lymphocytes in the lamina propia (Cerf-Bensussan et al., 1987). In addition, it has been shown that E-cadherin is the adhesive counter-receptor for CD103. The majority of $CD103^{-/-}$ mice accept islet cell allografts, suggesting a potential role for CD103 in CD8-mediated allograft destruction.

In humans, CD103 is expressed by only a small number (2%) of circulating T cells (Cerf-Bensussan et al., 1987), but it is strikingly up-regulated on intratubular T cells during allograft rejection (Hadley et al., 1997). It has been demonstrated *in vitro* that TGF-β can induce the expression of CD103 by activated human T cells (Wong et al., 2003). In addition, $CD8^+$ T cells expressing a dominant-negative TGF-β receptor showed little CD103 expression following migration into the allograft, suggesting a role of TGF-β as a key factor in the regulation of CD103 (Wang et al., 2005).

1.6.3 The role of $CD103^+CD8^+$ T cells in renal allograft rejection

Normally, cytotoxic T lymphocytes (CTL), which include predominantly CD8 and some of CD4 T cells, mediate lysis of target cells by two main mechanisms: exocytsis of cytotoxic granules and receptor-ligand binding between Fas and Fas ligand (Groscurth et al., 1998). Cytotoxic granules contain perforin and granzymes; perforin is a pore-forming protein which is inserted into target cell membranes leading to pore formation, granzymes are serine proteases which enter the target cell via a perforin pore leading to apoptotic cell death. T cells expressing mRNA encoding perforin have been identified within the tubules during renal allograft rejection (Robertson et al., 1996). Following antigen recognition, CTL also express Fas ligand (FasL) on their cell surface either by de novo synthesis or transformation of inactive FasL to an active form (Groscurth et al., 1998). The FasL binds to its receptor expressed on surface of target cells resulting in caspase activation and target cell apoptosis. This is consistent with cytotoxic profile found in rejecting graft biopsies (Robertson et al., 1996; Einecke et al., 2005). Both of these processes require adhesive interaction between T cells and their target. During tubulitis this adhesion could be stabilised by interaction between the CD103 integrin and E-cadherin.

Recent studies have suggested that CD103 is not essential for tubular damage following kidney transplantation since $CD103^{-/-}$ recipient mice develop similar histological lesions to wild-

type mice (Einecke et al., 2006). It has also been shown that expression of the CD103 receptor, E-cadherin is reduced during allograft rejection, indicating a reduced potential for tubular epithelial cells to bind CD103+ T cells (Einecke et al., 2006). Interestingly, the extent of tubulitis and tubular damage was unchanged in mice lacking perforin, granzymes and CD103, suggesting a cell contact-dependent cytotoxic mechanism is not required for graft destruction (Einecke et al., 2006). However, the Fas/FasL interaction and $CD4^+$ T cell-mediated delayed-type hypersensitivity could still contribute to graft failure in this system.

1.6.4 The role of T cells in renal fibrosis

It has been reported that tubulointerstitial fibrosis is associated with renal infiltration by inflammatory cells such as T cells and macrophages in human and experimental kidney diseases (Strutz et al., 1994). This suggests a role for immune cells in the development of fibrosis. A recent study showed evidence to support a direct role for $CD4^+$ T cell in renal fibrosis (Tapmeier et al., 2010). Depletion of $CD4^+$ T cells reduced interstitial expansion and collagen deposition following unilateral ureteric obstruction (UUO). In addition, $RAG^{-/-}$ mice, which are T cell deficient, showed a reduction of interstitial collagen deposition in the UUO model. This protective effect was decreased after reconstitution by $CD4^+$ T cells (Tapmeier et al., 2010). Interestingly, the expression of TGF-β was similar in both $RAG^{-/-}$ mice and after $CD4^+$ T cells reconstitution. However the expression of TGF-β does not reflect TGF-β activity. It is possible that latent TGF-β might be activated in $CD4^+$ T cell reconstitution mice more than in $RAG^{-/-}$ mice.

A previous study showed a close association between intratubular T cells and epithelial cells showing characteristics associated with early EMT in human renal allograft biopsy sections. This study also demonstrated *in vitro* that a model intraepithelial T-cell line could induce EMT by a TGF-β-dependent mechanism (Robertson et al., 2004). However, it is not clear whether these T cells secreted active TGF-β or activated latent TGF-β that was already generated in the cell culture model.

1.7 Specific causes of renal allograft loss

The reason for the lack of improvement in long-term outcome of kidney transplantation remains unclear but is likely to be multifactorial. A recent longitudinal study, mainly of living donor kidney allograft recipients (72.5%), has identified specific causes of late kidney graft loss (El-Zoghby et al., 2009). According to this study, death with a functioning graft is the leading cause of late renal allograft loss (43.4%). The causes of graft loss not due to patient death differ

between living and cadaveric donors. Following live donation, most grafts are lost as a consequence of glomerular diseases (40%) and interstitial fibrosis and tubular atrophy (IF/TA) (24%), whereas for cadaveric donors, IF/TA (43%) and glomerular diseases (32%) are the most common causes of graft failure (Figure 1.11). Although the once common term "chronic allograft nephropathy" has now been changed in order to identify the specific causes of renal allograft fibrosis, it is clear that graft fibrosis remains a major problem following kidney transplantation.

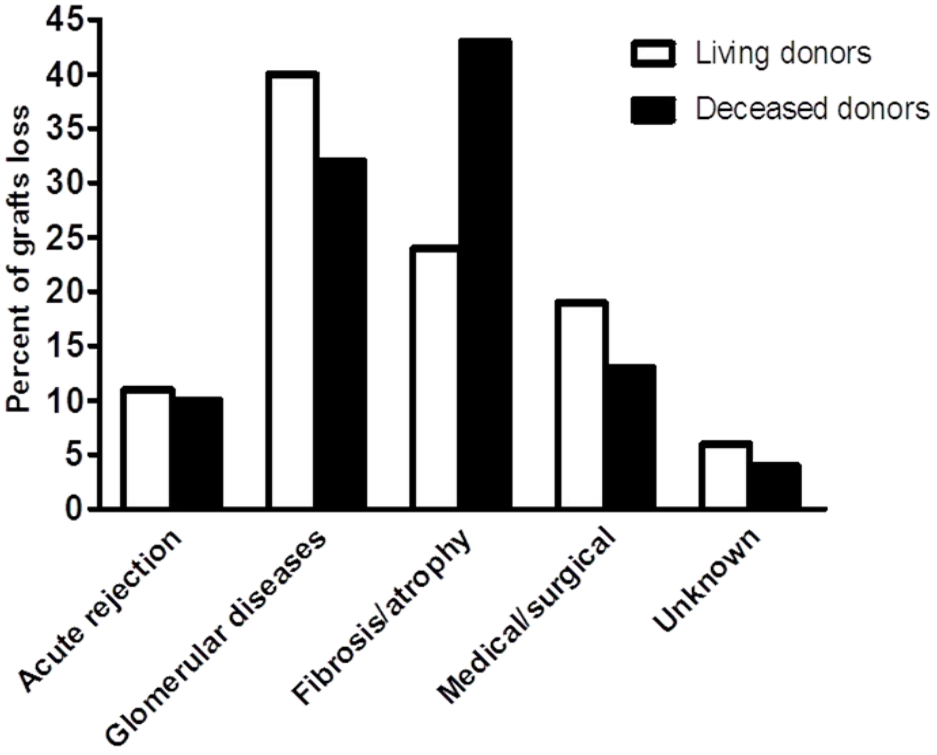

Figure 1.11 Causes of loss of functioning grafts in recipients of allogeneic kidneys from living donors (open bars) or deceased donors (black bar). This image is from EL-Zoghby et al., 2009.

1.7.1 Causes of renal allograft loss due to interstitial fibrosis and tubular atrophy (IF/TA).

In the subgroup of graft loss due to fibrosis, rejection (predominantly cell-mediated rejection), is the leading cause of failure; this is followed by BK virus nephropathy (Figure 1.12). Interestingly, the incidence of calcineurin inhibitor nephrotoxicity observed in this study was very low compared to a previous study performed using kidney graft biopsies from patients who received kidney-pancreas transplants during the period 1987-2000 (Nankivell et al., 2003). Most of the patients in this earlier study received Cyclosporine-based immunosuppression (77.5% Cyclosporine, 22.5% Tacrolimus) and 98.6% of this cohort showed some evidence of calcineurin

inhibitor nephrotoxicity after 10 years. Cyclosporine-induced nephrotoxicity will be discussed in chapter 3.

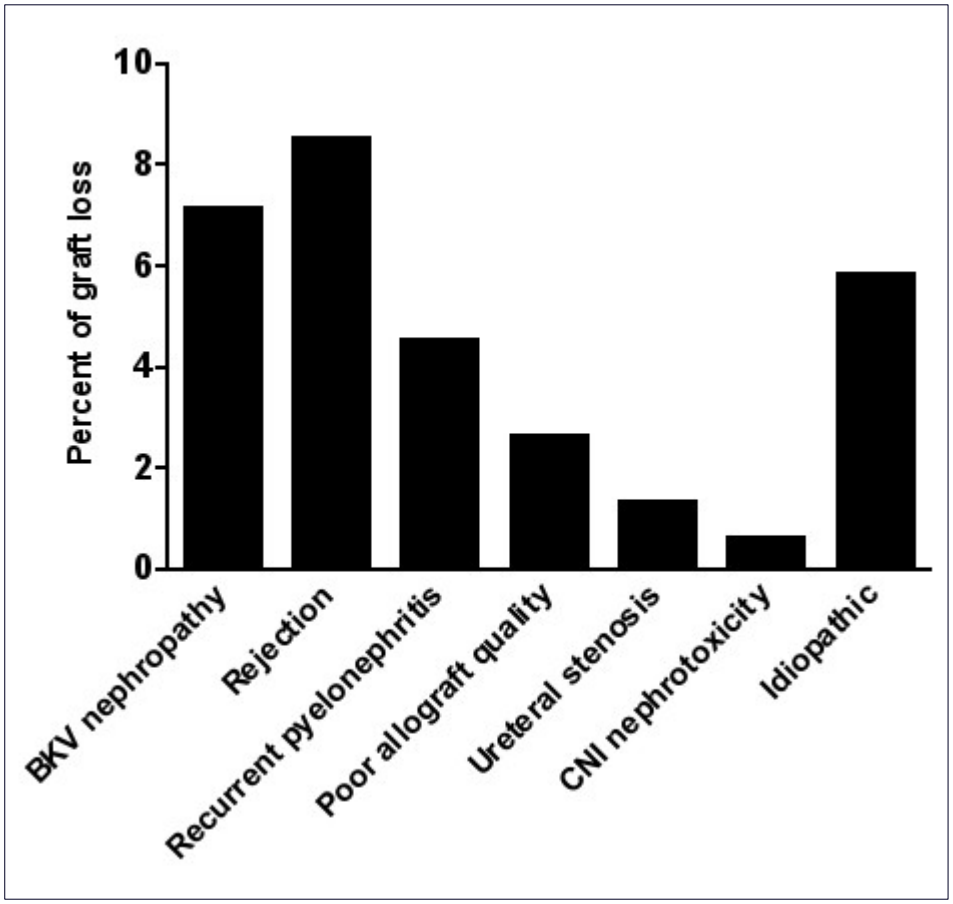

Figure 1.12 Bar graph demonstrating the specific causes of renal allograft loss due to interstitial fibrosis and tubular atrophy. This image is adapted from El-Zoghby et al., 2009.

1.8 Interstitial fibrosis and tubular atrophy (IF/TA)

In kidney allograft biopsies, the extent of renal IF/TA is one of the most important prognostic factors of graft failure (Müller et al., 2000). Protocol biopsies studied between 1998 and 2004 showed that the prevalence of moderate to severe fibrosis was 13% at 1 year and 17% at 5 years. In addition, mild fibrosis at 1 year progressed to severe fibrosis at 5 years in 23% of allografts (Stegall et al., 2011). These results demonstrate that interstitial fibrosis remains a major problem in the current era of transplantation.

Fibrosis is part of the kidney's normal response to injury. This wound healing process is normally resolved with restoration of renal architecture and the recovery of function. However, in some circumstances this process can lead to irreversible loss of tissue function. Fibrosis involves an excessive accumulation of extracellular matrix (ECM), primarily collagen type

I, in response to sustained inflammation after injury, and usually results in loss of function when normal tissue is replaced with scar tissue (Wynn et al., 2007). Previously, it was believed that the fibrogenesis process resulted from an imbalance between collagen synthesis and degradation and that a reduction in protease activity can result in fibrosis. However, it is now clear that fibrosis is a multifactorial process of which abnormal matrix synthesis is only a part. An experimental study has shown that abnormal collagen synthesis in kidneys is transient whilst the density of the matrix can continue to increase (Hewitson et al., 1998). Some studies have also shown that whilst the matrix metalloproteinases (MMP) are responsible for ECM degradation, knockout mice do not have a fibrotic phenotype (Ronco et al., 2007). Additionally, overexpression of MMP2 can induce fibrosis (Cheng et al., 2006). Despite the controversial role for MMPs in the pathogenesis of fibrosis, MMP expression has often presented in experimental models (Lovett et al., 1992) of human renal disease (Shiau et al., 2006).

1.8.1 Origin of the fibroblast

Mesenchymal cells are the principle ECM-producing cells involved in fibrosis (Becker et al., 2001). In kidney fibrosis, the interstitial fibroblasts activate glomerular mesangial cells and vascular smooth muscle cells which are associated with interstitial fibrosis, glomerulosclerosis and vascular sclerosis (Becker et al., 2001). However, the interstitial fibroblasts are more crucial for IF/TA in progressive renal diseases than other cell types. Fibroblasts can be derived from several sources. These include local proliferation of resident fibroblasts (Hewitson et al., 1995), recruitment of blood-borne precursors (Grimm et al., 2001), transformation of renal tubular epithelial and endothelial cells by epithelial to mesenchymal transition (EMT) (Liu et al., 2004) and endothelial to mesenchymal transition (Zeisberg et al., 2008) respectively, and migration of precursors from the perivascular region (Humphrey et al., 2010) (Figure 1.13).

1.8.1.1 Local interstitial fibroblasts

Initial data concerning the origin of fibroblasts was obtained from experiments using parabiotic rats which suggested that fibroblasts were unlikely to derive from hematogenous precursors but from resident interstitial fibroblast (Ross et al., 1970). More recent data using a murine unilateral ureteric obstruction (UUO) model demonstrated during the first day following UUO that resident peritubular fibroblasts also differentiate into myofibroblasts (Picard et al., 2008).

1.8.1.2 Bone marrow-derived fibroblasts

A study using bone marrow transgenic mice demonstrated that after myocardial ischemia, 24% of all myofibroblasts involved in scar formation are derived from the bone marrow (van Amerongen et al., 2008). Furthermore, a recent study using the UUO model of renal fibrosis demonstrated that stressed renal tubular epithelial cells induced expression of the chemokine CXCL16, leading the recruitment of bone marrow-derive fibroblast precursors (Chen et al., 2011).

1.8.1.3 Endothelial mesenchymal transition (EndoMT)

It has been reported that endothelial cells can transform to fibroblasts and contribute to renal fibrosis. Zeisberg and colleagues observed that 30-50% of fibroblasts co-expressed the endothelial marker CD31 and markers of fibroblasts and myofibroblasts, including S100A4 and α-SMA, in three different models of renal fibrosis (Zeisberg et al., 2008). A transgenic, endothelial cell fate-tracing technique also confirmed the presence of EndoMT in fibrotic kidneys (Zeisberg et al., 2008).

1.8.1.4 Transition from epithelial cells

Evidence of epithelial to mesenchymal transition (EMT) was first provided in 1995 by the cloning of fibroblast specific protein-1 (FSP-1 or, more generally, S100A4), a member of the S100 protein family (Strutz et al., 1995). The promoter/enhancer region driving this gene is active in fibroblasts but not in epithelium, mesangial cells or embryonic endoderm, indicating that FSP-1 is a specific marker for fibroblasts (Strutz et al., 1995). A landmark study supporting the existence of EMT was performed by Iwano and colleagues who used genetic mapping to investigate EMT *in vivo* (Iwano et al., 2002). This study used the GGT-Cre driver to label proximal tubular cells and the Rosa26 reporter (R26R) with the bacterial LacZ gene as a marker of cell fate. Following UUO-induced renal fibrosis, approximately 38% of S100A4-positive cells expressed LacZ staining, suggesting that many interstitial fibroblasts were derived from GGT-labelled tubular epithelial cells (Iwano et al., 2002). Most *in vitro* studies support a role for EMT in fibrogenesis, however a recent *in vivo* fate-tracing study has raised some doubt by demonstrating that pericytes are a major source of interstitial fibroblasts during renal fibrosis (Humphrey et al., 2010).

1.8.1.5 Pericytes or perivascular fibroblasts

A recent study used transgenic mice with three different cre-driver lines: Six2-cre labelled all epithelial cells except those of the collecting duct, Hoxb7-cre labelled epithelial cells from the collecting duct and FoxD1-cre labelled renal pericytes or perivascular fibroblasts. Following UUO injury there was no evidence that any α-SMA-positive cells expressed LacZ staining, suggesting that no myofibroblast was derived from renal epithelial cells. In contrast, FoxD1-cre labelled cells expressed α-SMA predominantly in the interstitial area. This suggests that FoxD1-labelled cells or pericytes were converted into myofibroblasts in this model of UUO-induced renal fibrosis (Humphrey et al., 2010).

Although the origin of renal interstitial fibroblast in renal fibrosis remains controversial, numerous previous papers and ongoing studies have supported the existence of EMT *in vitro*. The details of EMT will be discussed in section 1.8.

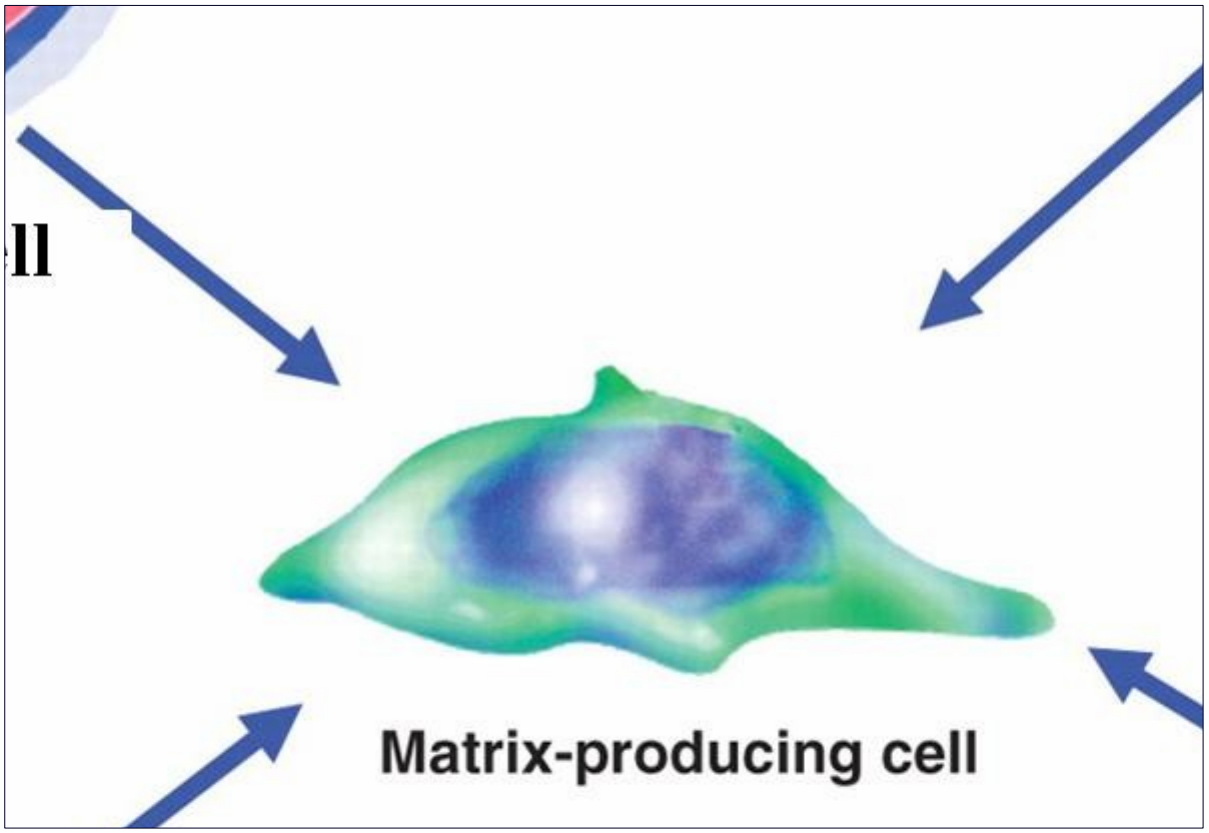

Figure 1.13 Potential origins of matrix-producing cells causing renal allograft fibrosis. The image is obtained from Strutz et al., 2006.

1.9 Epithelial to mesenchymal Transition (EMT)

EMT is a biological process that allows a mature epithelial cell to undergo the biochemical changes required to produce a mesenchymal cell. These include: enhanced

migratory capacity, invasiveness, elevated resistance to apoptosis, and increased production of ECM components (Yang J and Liu Y, 2001). Multiple processes are required in order to complete EMT. These include activation of transcription factors, expression of specific cell-surface proteins, reorganization and expression of cytoskeletal proteins, production of ECM-degrading enzymes, and changes in the expression of specific microRNAs, for example miR-200a and miR-141 which are known to prevent renal fibrosis (Wang et al., 2011).

1.9.1 Characteristics of EMT

Four key steps at the cellular level are essential for EMT (Figure 1.14):

1.9.1.1 Loss of the epithelial intercellular junction

Tubular epithelial cells are normally polygonal in shape and tightly attached to each other, forming an epithelial sheet through cell adhesion mechanisms. One of the first changes in epithelial cell transformation is the suppression of E-cadherin expression (Yang J and Liu Y, 2001). E-cadherin, a transmembrane glycoprotein predominantly located in adherens junctions, is considered a marker of differentiated epithelial phenotype by several studies (Zeisberg et al., 2003; Arias et al., 2001); E-cadherin is essential for maintaining epithelial polarity and tight junction development (Tunggal et al., 2005). The cytoplasmic domain of E-cadherin associates with the actin cytoskeleton through β-catenin molecules (section 1.3.2). Disassembly of the E-cadherin/catenin interaction leads to epithelial disruption, phenotypic alteration and enhanced cell proliferation (section 1.3.2.2). Although several papers have suggested that loss of E-cadherin results in EMT, a recent paper showed that E-cadherin reduction may not always lead to this transition as a consequence of the activation of an antagonistic BMP-7 signalling pathway (Veerasamy et al., 2009).

1.9.1.2 De novo expression of mesenchymal markers

One of the important features of EMT is the acquisition of fibroblast or myofibroblast markers by cells which retain a recognizable epithelial phenotype. This is termed intermediate stage EMT. Several molecules have been used to identify fibroblasts in both *in vivo* and *in vitro* studies; these include S100A4, α-SMA, vimentin and HSP47.

1.9.1.2.1 S100A4/FSP-1

Fibroblast specific protein 1 (FSP-1) in mouse or S100A4 in human was identified as a gene specifically expressed in fibroblasts by subtractive and differential mRNA hybridization (Strutz et al., 1995). S100A4 belongs to the S100 superfamily of cytoplasmic calcium-binding

proteins (Garrett et al., 2006). The S1004 protein monomer has a molecular weight of 10-12 kDa but generally forms homodimers or heterodimers within cells (Marenholz et al., 2006). S100A4 is localized in the nucleus, cytoplasm, and the extracellular space. However cytoplasmic expression is observed in the majority of S100A4-expressing cells. S100A4 protein plays a role in the regulation of a wide range of biological effects including cell motility, contractility, differentiation and survival (Schneider et al., 2008).

S100A4 has both intracellular and extracellular effects which are likely to involve different mechanisms. It has been shown that intracellular S100A4 interacts with cytoskeletal proteins such as actin and myosin leading to increased cell motility (Tarabykina et al., 2007). It has also been shown that S100A4 protein is released from several cell types (Schmidt-Hansen et al., 2004; Cabezón et al. 2007). The paracrine effects of S100A4 can be divided into 3 groups: firstly, increasing cell motility by a direct effect on cytoskeletal gene expression (Belot et al., 2002) and by increasing the expression of matrix metalloproteinases (MMPs) which degrade extracellular matrix proteins allowing cell migration (Schmidt-Hansen et al., 2004); secondly, increasing cell proliferation and differentiation, at least in neurons and cardiac myocytes (Fang et al., 2006; Schneider et al., 2007); and thirdly, preventing apoptotic cell death (Schneider et al., 2007).

S100A4 was first introduced as a marker for epithelial cells undergoing EMT in kidney fibrosis in 1995 (Strutz et al., 1995). However, the use of S100A4 expression to define all fibroblasts produced by EMT is now debatable since it has been observed that the interstitium of kidney contains fibroblasts which do not express S100A4 (Le Hir et al., 2005). It has also been reported that myofibroblasts do not express S100A4 (Picard et al., 2008). Furthermore, several studies have reported the expression of S100A4 by various normal human cells, including monocytes (Cabezón et al., 2007), macrophages (Österreicher et al., 2011), T lymphocytes (Cabezón et al., 2007), neutrophilic granulocytes (Cabezón et al., 2007), and endothelial cells (Semov et al., 2005).

1.9.1.2.2 Vimentin

Vimentin is an intermediate filament protein which forms one of the components of the cytoskeleton. It is normally expressed by mesenchymal cells (Steinert et al., 1988). However, a study of human kidney biopsies has reported the presence of vimentin staining in normal glomerular epithelial cells (Essawy et al., 1997). In addition, adult epithelial cells transiently express vimentin in response to various insults (Witzgall et al., 1994). Furthermore, *in vivo*

studies have demonstrated that vimentin is commonly expressed in injured tubular cells (Gröne et al., 1987). Damaged renal tubular cells, which express vimentin, can retain an epithelioid basolateral border (Witzgall et al., 1994; Zhu et al., 1996).

1.9.1.2.3 α-smooth muscle actin (α-SMA)

Alpha-smooth muscle actin (α-SMA) is the characteristic actin isoform found in several cell types, including vascular smooth muscle cells, pericytes, lens epithelial cells, mesengial cells, and myofibroblasts. However, α-SMA has not been recognized in nomal tubular epithelial cells (Gabbiani et al., 1981; Skalli et al., 1989). The expression of α-SMA is an excellent marker of myofibroblasts (Desmouliere et al., 1992). The role of α-SMA expression is to upregulate the contractility of cells, and increased expression of α-SMA directly correlates with increased force generation by myofibroblasts (Hinz et al., 2001). α-SMA expression is upregulated by several growth factors, including fibroblast growth factor (FGF)-2, angiotensin II and TGF-β1; conversely, platelet-derived growth factor (PDGF) and epidermal growth factor (EGF) can inhibit α-SMA expression (Barrientos et al., 2008).

1.9.1.2.4 Heat shock protein 47 (HSP47)

HSP47 is a member of the serpin superfamily of serine proteinase inhibitors. This protein is thought to be a molecular chaperone involved in the synthesis of collagen molecules. Expression of HSP47 in injured tubules has been used as a marker for collagen synthesis in EMT. However, HSP47 is not specific for collagen type I (Nagata et al., 2003), which is commonly found in fibrotic tissue, but is also associated with collagen type IV which is present in the normal tubular basement membrane.

1.9.1.3 Disruption of the tubular basement membrane (TBM)

The renal tubular basement membrane contains an abundance of collagen type IV. Integrity of the TBM is required for the maintenance of a polarized epithelial phenotype, with the disruption of type IV collagen leading to EMT (Zeisberg et al., 2001). It has been reported that infiltrating mononuclear cells and interstitial fibroblasts secrete MMP-2 and MMP-14 which specifically cleave collagen type IV and laminin in the basement membrane. This facilitates degradation of the tubular basement membrane and enhances EMT (Yang et al., 2001; Zeisberg et al., 2004). Furthermore, *in vitro* studies demonstrate that, without TGF-β, MMP-2 alone is capable of inducing renal tubular epithelial cell transformation (Cheng et al., 2003).

1.9.1.4. Enhanced migration and the invasive capacity of transformed cells

Disruption of the TBM is of fundamental importance for clearing a path for transformed renal tubular epithelial cells to migrate towards the interstitium. In addition, reorganization of the actin cytoskeleton and induction of α-SMA expression provides the potential for these cells to acquire the capacity for contractility, leading to migration and invasion (Yang et al., 2001). Furthermore, transformed epithelial cells acquire S100A4, which also promotes motility.

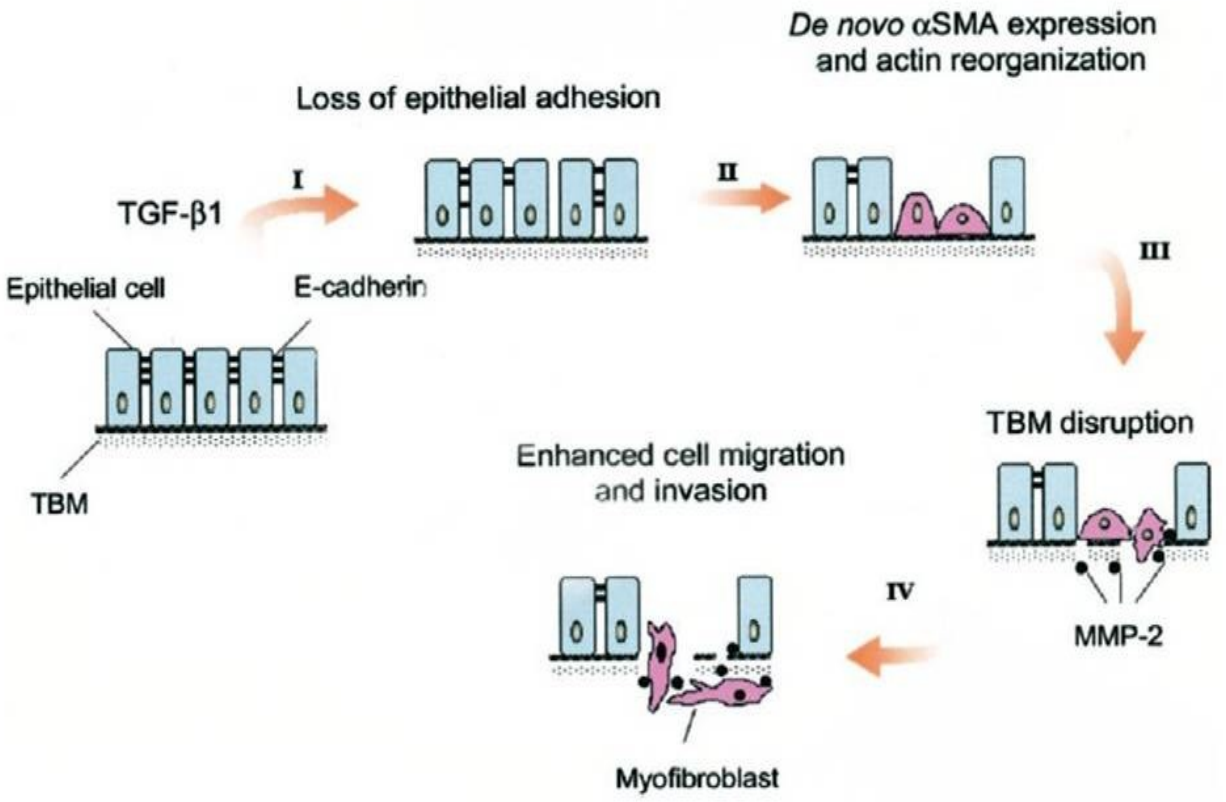

Figure 1.14 Diagram showing four key steps during tubular epithelial to mesenchymal transition.

EMT is a multi-step process which includes: 1) loss of epithelial adhesion properties, 2) *de novo* expression of α-SMA and actin reorganization, 3) disruption of the TBM, and 4) enhanced migration and invasive capacity of the transformed cells. This image is obtained from Yang et al., 2001.

1.9.2 Classification of EMT

Since March 2008, EMT has been categorized into three subtypes based on the biological process and biomarker expression (Figure 1.15).

1.9.2.1 Type 1 EMT

EMT type I is associated with implantation, embryo formation and organ development processes which are organized in order to produce diverse cell types with mesenchymal phenotypes (Zeisberg et al., 2009). Type 1EMT normally does not cause fibrosis or induce an invasive phenotype but transforms primitive epithelial cells into mesenchymal cells (primary mesenchyme) required for gastrulation, organogenesis and subsequent development of secondary epithelia.

1.9.2.2 Type 2 EMT

This type of EMT initially starts as a part of a normal wound healing process which produces fibroblasts in order to repair damaged tissue following injury. However, type II EMT can be associated with chronic inflammation which prolongs the process leading to excessive fibrosis and damage of the tissue architecture. This process might be relevant to the chronic renal allograft dysfunction associated with IF/TA (Robertson et al., 2004).

1.9.2.3 Type 3 EMT

This type of EMT occurs in epithelial cancer cells that have previously undergone genetic and epigenetic changes which lead to the development of tumours. Cells generated by type 3 EMT may invade and metastasize via the circulation or lymphatic system.

1.9.3 Mediators of type 2 EMT

EMT can be induced or regulated by various growth and differentiation factors, including TGF-β, fibroblast growth factor (FGF)-2, hepatocyte growth factor (HGF) and PDGF (Zavadil et al., 2005). Among these, TGF-β is a major inducer of EMT during embryogenesis, cancer progression and fibrosis. The molecular pathways activated by TGF-β during the development of type 2 EMT in renal tubular epithelial cells are complex and may not be the same in different cell types (Fan et al., 1999; Okada et al., 1997).

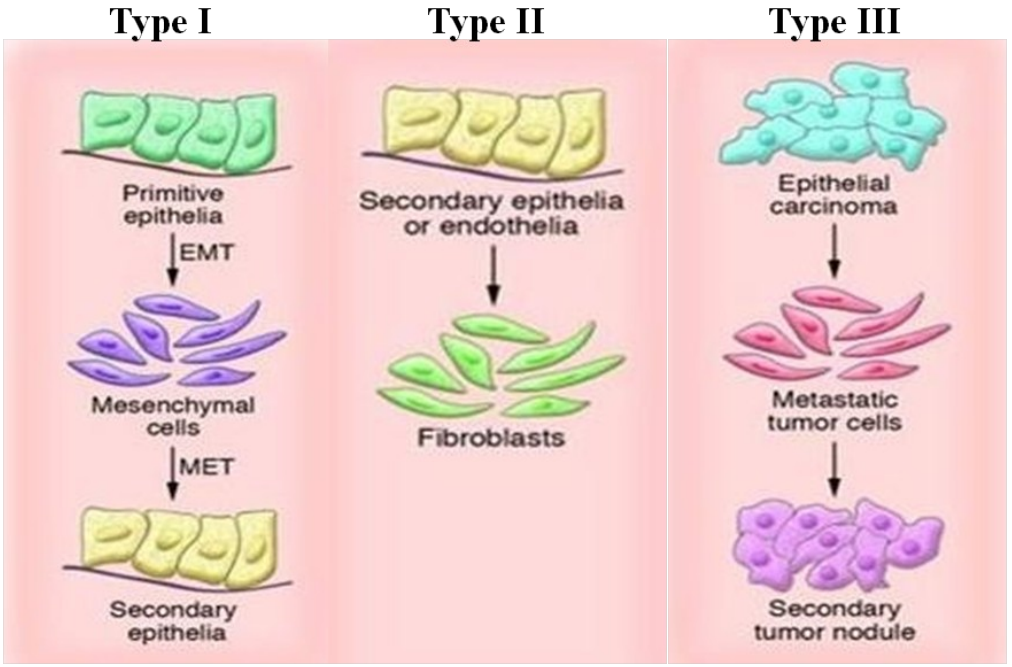

Figure 1.15 Diagram shows different types of EMT.

Type 1 EMT is seen when primitive epithelial cells transition into mesenchymal cells that form the diaspora of the basic body plan, following gastrulation or neural crest migration. This primary mesenchyme can be re-induced to form secondary epithelia by an MET. Type 2 EMT is seen when secondary epithelial cells populate interstitial spaces with resident or inflammation-induced fibroblasts. Type 2 EMT can occur over extended periods of time and can eventually destroy an affected organ if the primary insult is not removed or attenuated. Type 3 EMT is seen when secondary epithelial cells transform into cancer cells that later undergo the EMT with migration and invasive capacity. This image is taken from Zeisberg et al., 2009.

1.9.3.1 Transforming growth factor β (TGF-β)

TGF-β is a multifunctional cytokine that exerts a variety of biological activities depending on the target cell type. It is well known that TGF-β is central to the induction of fibrosis in many tissues, including the kidney. TGF-β-induced EMT was first recognized by modelling *in vitro*. Following addition of TGF-β, the morphology of mouse mammary epithelial cells changed from cuboidal to an elongated spindle shape. In addition, these TGF-β-treated cells showed increased expression of the mesenchymal markers fibronectin and vimentin and decreased expression of the epithelial markers E-cadherin, ZO-1 and desmoplakin (Miettinen et al., 1994). All isoforms of TGF-β (TGF-β1, TGF-β2 and TGF-β3) share the capacity to induce EMT in epithelial cells (Miettinen et al., 1994; Valcourt et al., 2005).

Several observations have indicated that activation of the Smad signalling pathway is strongly associated with EMT. An *in vitro* study using transfected murine mammary epithelial cells showed that increased ectopic expression of Smad2 or Smad3 with Smad4 induces EMT whereas a dominant-negative Smad2, Smad3 and Smad4 blocked TGF-β-induced EMT (Valcourt et al., 2005). Moreover, a study in human proximal tubular cells demonstrated that inhibitory RNA against Smad2/3 can block TGF-β-induced EMT *in vitro* (Phanish et al., 2006).

1.9.3.2 Connective tissue growth factor (CTGF)

CTGF is a matrix-associated, heparin-binding protein which was originally isolated from the conditioned medium of human umbilical vein endothelial cells (Bradham et al., 1991). CTGF plays an important role in the regulation of cell proliferation, apoptosis, embryogenesis, differentiation, and wound healing and is expressed in various human tissues, including the kidney (Goldschmeding et al., 2000).

It has been reported that CTGF functions as a downstream mediator of TGF-β, acting specifically on connective tissue cells (Grotendorst et al., 1997). Blockade of CTGF partially inhibits TGF-β induced EMT *in vitro* and *in vivo* (Burns et al., 2007; Burns et al., 2006). In addition, blocking CTGF by using CTGF antisense oligonucleotides can decrease the expression of fibronectin, collagen type I and α-SMA gene expression and also reduces the development of interstitial fibrosis areas in the UUO model, despite the sustained expression of TGF-β (Yokoi et al., 2004).

1.9.3.3 Integrin-linked kinase (ILK)

ILK is a serine/threonine kinase that regulates various cellular processes including adhesion, migration, differentiation and survival (Wu et al., 2001). It has been reported that the induction of ILK plays a role in TGF-β1 and CTGF-mediated EMT (Liu et al., 2008). In addition, TGF-β can induce ILK expression in renal tubular epithelial cells by a mechanism that is dependent on intracellular Smads (Li et al., 2003) and CTGF (Liu et al., 2007).

1.10 Transforming growth factor-β

TGF-β is a ubiquitously expressed and multifunctional cytokine that not only plays a central role in EMT regulation, but also regulates the development, differentiation, and survival of most cell types and tissues (Blobe et al., 2000).

The TGF-β superfamily contains two subfamilies defined by structural similarity and their specific signalling pathway: firstly, the TGF-β, Activin and Nodal subfamily and secondly,

the BMP (bone morphogenetic protein), GDF (growth and differentiation factor) and MIS (muellerian inhibiting substance) subfamily. Members of the TGF-β superfamily play crucial roles in biological and immunological functions through activation of complex signalling pathways. Disturbance of their signalling has been implicated in several developmental disorders and in various human diseases including cancer, fibrosis and auto-immune diseases (Blobe et al., 2000).

There are three isoforms of TGF-β termed TGF-β1, TGF-β2, and TGF-β3, which all act through an intracellular signalling cascade of Smad family proteins via ligand-induced activation of TGF- β receptor kinases (Böttinger et al., 2002). The three TGF-β isoforms TGF- β1, TGF-β2 and TGF-β3 have different functions which do not overlap. For example, TGF-β1 knockout mice develop severe autoimmune-like inflammatory diseases (Kullkarni et al., 1993). TGF-β2 deficient mice suffer from perinatal mortality and a wide range of developmental defects including cardiac, lung, craniofacial, limb, spinal cord, eye, inner ear and urogenital defects (Sandford et al., 1997). TGF-β3 null mice have cleft palates and delayed lung development due to defects in branching morphogenesis and cell differentiation (Kaartinen et al., 1995). This suggests that a large number of TGF-β functions cannot be compensated for by other family members.

1.10.1 Latent TGF-β

Normally, almost all TGF-β isoforms are secreted as an inactive latent complex called small latent complex (SLC), which contains the C-terminal mature TGF-β (molecular weight 25kDa) and the N-terminal latency associated peptide (LAP) (molecular weight 75-80kDa) (Annes et al., 2003). Before secretion, mature TGF-β is cleaved from the LAP by a furin-like endoproteinase in the Golgi apparatus (Dubois et al., 1995). However, the LAP remains associated with the TGF-β dimer by non-covalent interactions (Annes et al., 2003), and this interaction inhibits the activity of TGF-β (Figure 1.16). The LAP domain contains three N-glycosylated asparagine residues and three cysteine residues which are essential for dimerization of LAP monomers (Lawrence et al., 2001). Mutation of these cysteines prevents the association of LAP and mature TGF-β, leading to active TGF-β secretion (Lawrence et al., 2001). In addition to conferring latency, LAP is essential for the folding and secretion of the TGF-β precursor. In most cells, the SLC is bound to a large glycoprotein, latent TGF-β binding protein (LTBP) via disulphide bonds between LAP and LTBP. This complex is called the large latent complex (LLC) which was first discovered in platelets in 1988 (Miyazono et al., 1988; Wakefield et al., 1988). Most cells secrete TGF-β in the form of the large latent complex (LLC) (Koli et al., 2001).

LTBP-1 plays a central role in the processing and secretion of TGF-βs (Miyazono et al., 1992), and LTBP-1 is co-expressed with TGF-β1 in the kidney (Taipale et al., 1994; Koski et al., 1999). A study using a phorbol ester-stimulated human erythroleukemia cell line showed that the small latent TGF-β complex is secreted very slowly with the majority retained in the Golgi apparatus (Miyazono et al., 1991). However, LTBPs are secreted rapidly, and association with the SLC enhances the secretion of latent TGF-β (Taipale et al., 1994; Miyazono et al., 1991). LTBPs also have a role in targeting latent TGF-β to the extracellular matrix (Saharinen et al., 1998). Interaction between growth factors and ECM molecules is a major mechanism for regulation of growth factor activity. Fibronectin is required for the assembly of LTBP-1 to ECM (Dallas et al., 2005). This interaction is mediated by heparan sulphate proteoglycan through the heparin binding sites on both fibronectin and LTBP-1 (Chen et al., 2007). Mature TGF-β needs to be released from the latent complex in order to bind to TGF-β receptor and subsequently trigger biological responses. The detail of latent TGF-β activation is in section 1.10.

1.10.2 TGF-β receptors

TGF-βs transduce their signals across the cell membrane into the nucleus through type I (TβR-I) and type II (TβR-II) serine/threonine kinase receptors (Derynck and Zhang, 2003). To date, five type II receptors and seven type I receptors (Activin-receptor-like kinases, ALKs) have been identified in humans. At least two type II receptors and two type I receptors are needed for signalling (Luo and Lodish, 1996). Both type I and type II receptor kinases are organized sequentially into an N-terminal extracellular ligand binding domain, a transmembrane region, and a C-terminal serine/threonine kinase domain. Besides type I and type II receptors, TGF-β ligands can bind to type III receptors (Betaglycans). Betaglycan is the most abundant TGF-β receptor on the cell surface where it functions as an accessory receptor that binds and presents TGF-β to its signalling receptors (Derynck and Zhang, 2003). The type III receptor can bind all three TGF-β isoforms, though it has a higher affinity for TGF-β2 than TGF-β1 and TGF-β3 (Chiefetz and Massague, 1991).

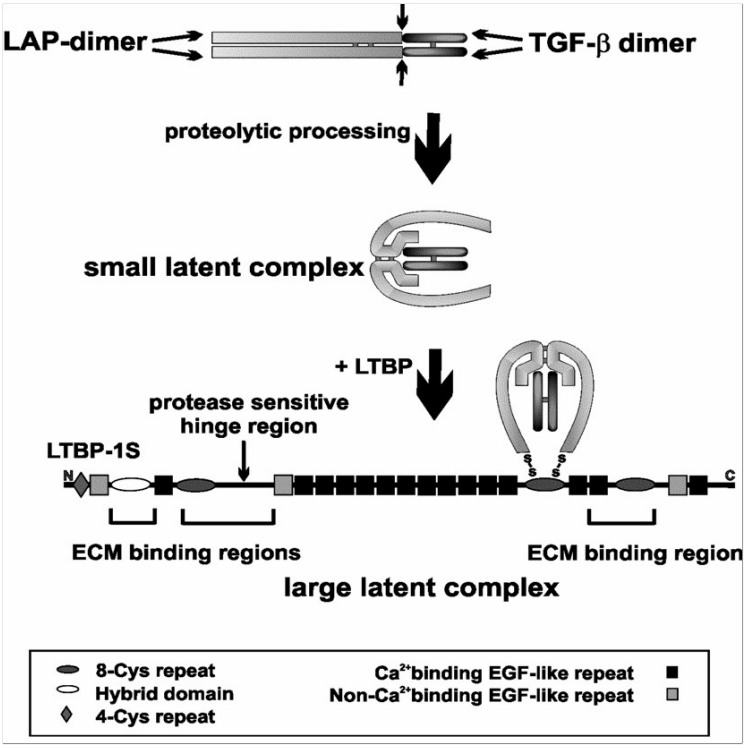

Figure 1.16 Structure of the small and large latent TGF-β complexes.

TGF-β is synthesized as a precursor molecule consisting of the C-terminal mature TGF-β and N-terminal LAP. TGF-β is cleaved from its propeptide by furin-like endoproteinase during secretion; however, mature TGF-β remains associated with LAP by non-covalent binding, forming the small latent complex. The large latent complex contains the small latent complex which is covalently bound to an LTBP. This image is taken from Hyytiäinen et al., 2004.

1.10.2 TGF-β receptors

TGF-βs transduce their signals across the cell membrane into the nucleus through type I (TβR-I) and type II (TβR-II) serine/threonine kinase receptors (Derynck and Zhang, 2003). To date, five type II receptors and seven type I receptors (Activin-receptor-like kinases, ALKs) have been identified in humans. At least two type II receptors and two type I receptors are needed for signalling (Luo and Lodish, 1996). Both type I and type II receptor kinases are organized sequentially into an N-terminal extracellular ligand binding domain, a transmembrane region, and a C-terminal serine/threonine kinase domain. Besides type I and type II receptors, TGF-β ligands can bind to type III receptors (Betaglycans). Betaglycan is the most abundant TGF-β receptor on the cell surface where it functions as an accessory receptor that binds and presents TGF-β to its signalling receptors (Derynck and Zhang, 2003). The type III receptor can bind all

three TGF-β isoforms, though it has a higher affinity for TGF-β2 than TGF-β1 and TGF-β3 (Chiefetz and Massague, 1991).

1.10.3 Smads

Smads are a group of transcription factors that interact with and modulate the activity of the TGF-β receptor complex. The Smad proteins are homologues of the drosophila protein, mothers against decapentaplegic (MAD) and the *C. elegans* protein SMA. The name is a combination of these two. The Smad proteins are a family of transcription factors found in vertebrates, insects and nematodes (Heldin et al., 1997). The Smad family can be divided into three subfamilies:

1.10.3.1 Receptor-regulated (R)-Smads

R-Smads are directly phosphorylated by type 1 TGF-β receptors through their intracellular kinase domain, leading to R-Smad activation. R-Smads include Smad2 and Smad3, which are normally activated by TGF-β (Figure 1.20), activin and nodal signalling, except in endothelial cells in which TGF-β signalling can also activate Smad1 and Smad5 (Miyazawa et al., 2002). Smad1, Smad5 and Smad8 are normally activated by the BMP/GDP subfamily.

1.10.3.2 Common partner (Co)-Smads

Smad4 is the only known mammalian Co-Smad. Smad4 binds to the activated R-Smads and facilitates translocation of the heterotrimeric complex into the nucleus.

1.10.3 Inhibitory (I)-Smads

Smad6 and Smad7 function by inhibiting the downstream signal from type I TGF-β receptors, thereby acting as negative regulators of signalling mediated by the TGF-β superfamily of ligands.

1.10.4 The TGF-β/Smad signalling pathway

A TGF-β ligand initiates signalling by binding the type II receptor on the cell surface. This interaction allows type II receptors to recruit the type I receptor to form a hetero-tetrameric complex with the ligand. Upon recruitment, the type II receptor phosphorylates the type I receptor on a specific GS domain which contains a series of glycine-serine repeats. The activated type I receptor then propagates the signal inside the cell through phosphorylation of the R-Smads (Smad2 and Smad3) which then form a heteromeric complex with the Co-Smad (Smad4) to facilitate translocation into the nucleus, where they associate and cooperate with transcription

factors to activate or repress target gene transcription (Figure 1.17) (Feng and Derynck, 2005). For regulation, there are I-Smads (Smad6 and Smad7) which negatively regulate TGF-β signalling. Smad7 competes with R-Smad to bind to the type I receptor, whereas Smad6 prevents the R-Smad from binding to the Co-Smad by interacting with Smad4.

1.10.5 Non-Smad signalling-mediated EMT

Although most studies report that Smads are necessary for the development of TGF-β-dependent EMT in tubular epithelial cells, activation of non-Smad pathways such as the RhoA (RHOA; Ras homologue gene family, member A), MAPK and PI3K signalling cascades (Derynck and Zhang, 2003) can also contribute to development and progression of the epithelial transition (Zhang et al., 2009).

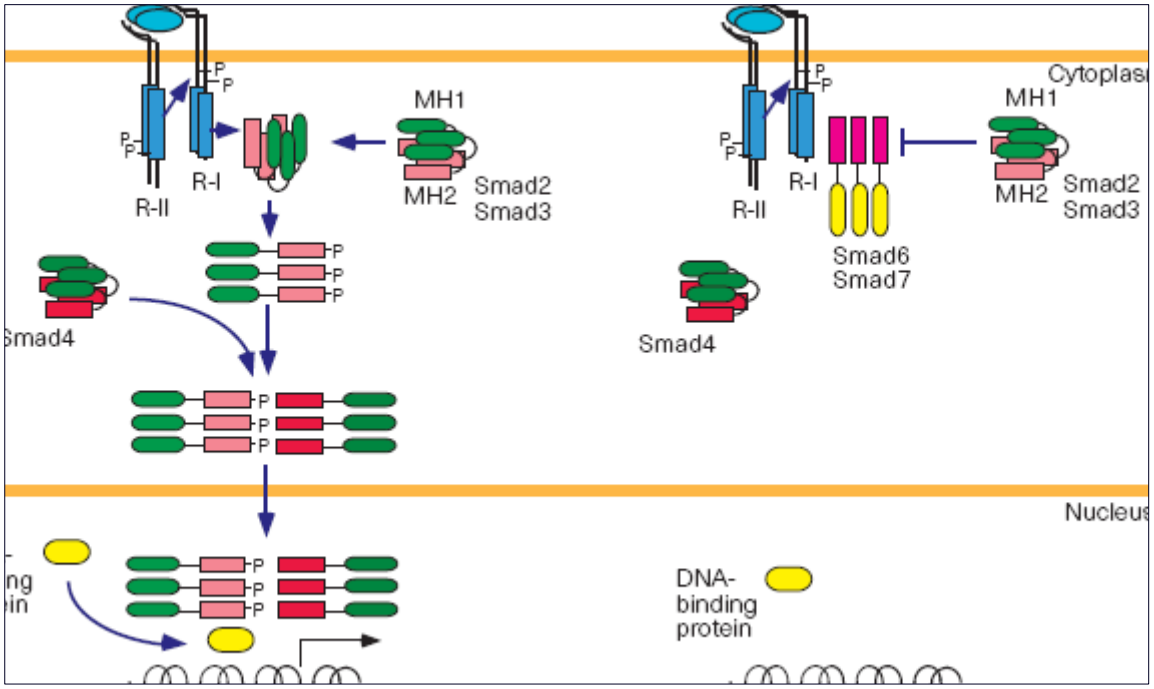

Figure 1.17 Diagram showing the intracellular signaling mechanism of the TGF-β/Smad pathway.

(a) TGF-β binds to TβR-II with the aid of TβR-III. After the binding, TβRII recruits and phosphorylates TβR-I, resulting in the phosphorylation (P) of Smad2 and Smad3. Phosphorylated Smad2 and Smad 3 then form a heteromeric complex with Smad4 and translocate to the nucleus. This Smad complex regulates gene transcription with the association

of transcription factors, co-activators and co-repressors. (b) Smad6 and Smad7 bind to the receptor and inhibit phosphorylation. The image is taken from Heldin et al., 1997.

1.11 Latent TGF-β activation

Increased TGF-β expression is seen in conditions including fibrotic diseases and neoplastic disorders, and often correlates with clinical disease severity (Wang et al., 2005). However, increased expression of TGF-β is not sufficient to increase TGF-β activity, because all three TGF-β isoforms are expressed in tissues as inactive latent precursors. The extracellular activity of TGF-β is regulated by the conversion of latent TGF-β to active TGF-β. This activation can occur through physical processes and biological activation.

1.11.1 Physical activation of latent TGF-β

1.11.1.1 Activation by pH

Many studies have shown that latent TGF-β is activated by acid (Lyons et al., 1988; Miyazono et al., 1988; Brown et al., 1990). This probably results from denaturation of the LAP protein, which disturbs the interaction between LAP and TGF-β. Previous studies of the activation of latent TGF-β in a fibroblast-conditioned medium have demonstrated that a small fraction of total TGF-β was active over the range of pH 4-5 (Lyons et al., 1988). Another study of the activation of purified human platelet-derived latent TGF-β1 by pH suggested that no activation was observed above pH 3.5 (Miyazono et al., 1988). More recently it was shown that latent TGF-β was activated both below pH 3.1 and above pH 11.9 (Brown et al., 1990).

1.11.1.2 Heat activation

Heating is an effective method for activating latent TGF-β. According to an *in vitro* study, heat activation of latent TGF-β generates greater activity than acid activation (Brown et al., 1990). The optimal temperature is 70-80°C for 10 minutes; thermal denaturation of mature TGF-β occurs above 80°C (Brown et al., 1990).

1.11.1.3 Activation by reactive oxygen species (ROS)

It has been shown that latent TGF-β1can be activated by ROS both *in vitro* by ionizing radiation or using a metal-catalyzed ascorbate system, and *in vivo* by irradiation, (Barcellos-Hoff et al., 1996). It has been suggested that hydroxyl radicals induce modifications which disable LAP binding, leading to exposure of the active growth factor.

1.11.2 Activation of TGF-β by integrins

Integrins are a large family of cell adhesion and signalling receptors. Individual integrins comprise an α and β subunit in non-covalent interaction; there are 18 α subunits and 8 β subunits that can form at least 24 different heterodimeric transmembrane receptors. These transmembrane receptors provide a structural and functional bridge between the extracellular matrix and the intracellular cytoskeleton. In addition, they can transfer information from the ECM to the cell interior or vice versa and are also involved in cell adhesion, maintenance of morphology, migration, proliferation, survival, differentiation, and invasion (Hynes, 2004). Four integrins, including αvβ3 (Asano et al., 2005), αvβ5 (Asano et al., 2006), αvβ6 (Munger et al., 1999) and αvβ8 (Mu et al., 2002) have been shown to bind latent TGF-β *in vitro* via an integrin-binding RGD amino acid sequence motif present in the LAP region of the latent complex.

A study in mice carrying a mutation in the RGD integrin-binding motif (*Tgfb1* $^{RGE/RGE}$ mice) demonstrated a similar phenotype to *Tgfb1*$^{-/-}$ mice (Yang et al., 2007). This finding suggests that integrin-mediated activation of latent TGF-β1 is absolutely essential for TGF-β1 to function during development and to control the immune system *in vivo*. However, as the integrin-binding RGD motif is present in the latent forms of TGF-β1 and TGF-β3, but not TGF-β2, it seems that an alternative mechanism must be responsible for the activation of latent TGF-β2.

Besides the β subunit, the αv integrins are also important in TGF-β activation. Mice lacking a functional integrin αv gene (*Itgav*$^{-/-}$ mice) develop identical abnormalities in vasculogenesis and cleft palate as seen in *Tgfb1*$^{-/-}$ and *Tgfb3*$^{-/-}$ mice (Dickson et al., 1995; Kaartinen et al., 1995). This suggests αv integrins are necessary for the activation of TGF-β *in vivo*.

1.11.2.1 αvβ3 and αvβ5 integrins

αvβ3 and αvβ5 integrins can be expressed by many different cell types. Mice lacking either αvβ3 or αvβ5 do not show any defect associated with decreased TGF-β activation (Huang et al., 2000; Reynolds et al., 2002). However, evidence suggests that both αvβ3 and αvβ5 can activate latent TGF-β expressed by fibroblastic cells. Dermal fibroblasts from patients with the autoimmune disease scleroderma show enhanced expression of αvβ3 and αvβ5, and increased TGF-β activation; this was inhibited by antibodies against the αvβ3 and αvβ5 integrins (Asano et al., 2006; Wipff et al., 2007). The expression of αvβ5 by dermal fibroblast results in transformation to a myofibroblastic phenotype as a consequence of increased TGF-β activity (Asano et al., 2006). Moreover, αvβ5 integrin-mediated activation of TGF-β produces lung fibroblast to myofibroblast differentiation during pulmonary fibrosis (Scotton et al., 2009).

However, this area remains controversial as recent data have shown that mice lacking both the αvβ3 and αvβ5 integrins are not protected from bleomycin-induced pulmonary fibrosis (Atabai et al., 2009).

1.11.2.2 αvβ6 integrin

The αvβ6 integrin is predominantly expressed by activated epithelial cells. This integrin is thought to be important for localized activation of latent TGF-β on the epithelial surface (Munger et al., 1999). Study of *Itgb6*$^{-/-}$ mice demonstrated a mild inflammatory phenotype which was limited to the skin and lung (Huang et al., 1996). Additionally, macrophages from *Itgb6*$^{-/-}$ mice showed defects in lung phospholipid clearance, resulting from reduced αvβ6 integrin-mediated activation of TGF-β (Koth et al., 2007). Furthermore, *Itgb6*$^{-/-}$ mice developed periodontal disease due to reduced TGF-β activation by αvβ6 integrin-expressing oral epithelial cells (Ghannad et al., 2007). Thus, αvβ6-mediated TGF-β activation seems important for controlling the functions of this cytokine at epithelial barriers. Normally, basal expression of the αvβ6 integrin is low, but expression of this integrin is increased when tissue injury occurs. The αvβ6 integrin has been implicated in the pathology of several different models of disease resulting from tissue damage. Studies using integrin *Itgb6*$^{-/-}$ mice, or blocking antibodies against αvβ6 show protection from pulmonary fibrosis (Munger et al., 1999), renal fibrosis (Hahm et al., 2007) and liver fibrosis (Patsenker et al., 2006; Wang et al., 2007).

1.11.2.3 αvβ8 integrin

The αvβ8 integrin is expressed by many different cell types, including neurons and neuroepithelial cells (Proctor et al., 2005), astrocytes (Cambier et al., 2005), airway epithelial cells and fibroblasts (Araya et al., 2006; Neurohr et al., 2006), and dendritic cells and $CD4^+$ T-cells of the immune system (Travis et al., 2007). Expression of the αvβ8 integrin and αvβ8-mediated TGF-β activation by astrocytes is important in controlling brain angiogenesis, with activated TGF-β acting upon endothelial cells (Cambier et al., 2005). TGF-β activation by the αvβ8 integrin is also required to regulate neurovascular homeostasis in the adult brain (Su et al., 2010). These findings suggest an essential role for αvβ8 integrin-mediated TGF-β activation in regulating brain vascular development and function in health and disease. *Itgb8*$^{-/-}$ mice show cleft palate, as occurred in *Tgfb3*$^{-/-}$mice, and defects in yolk sac vasculogenesis similar to *Tgfb1*$^{-/-}$ mice (Dickson et al., 1995; Kaartinen et al., 1995). Interestingly, mice that express a non-integrin-responsive TGF-β1 and lack TGF-β3 (*Tgfb1*$^{RGE/RGE}$; *Tgfb3*$^{-/-}$) have abnormal vascular

morphogenesis identical to *Itgb8*$^{-/-}$ mice, as well as the expected abnormalities of the single TGF-β null mice (Cambier et al., 2000). Expression of the αvβ8 integrin has also been reported for some dendritic cells. Failure of the expression of this integrin by dendritic cells allows autoimmune colitis to develop in mice, suggesting a specific role for TGF-β activation by αvβ8 integrin expressing dendritic cells in the development of immunoregulatory T cells (Travis et al., 2007).

1.11.2.4 The mechanism of integrin-mediated TGF-β activation

As described above, almost all latent forms of TGF-β interact with integrins via an RGD integrin-binding motif in the LAP region of the latent complex. However, evidence suggests that different integrins can activate TGF-β by two different methods.

1.11.2.4.1 Mechanical induction of active TGF-β by integrins

Cell culture models have shown that activation of the latent TGF-β complex by the αvβ5 (Wipff et al., 2007) and αvβ6 (Munger et al., 1999) integrins is not prevented by protease inhibitors, indicating that cleavage of latent TGF-β is not required. Furthermore, active TGF-β is not released into the culture medium from cells expressing the αvβ6 integrin (Munger et al., 1999), leading to the hypothesis that integrin binding to the latent complex induces a conformational change to allow active but still complex-bound TGF-β to bind to its specific receptor. Evidence now points to a role for cell contraction in the activation of TGF-β via the αvβ5 and αvβ6 integrins. An intact actin cytoskeleton is required for TGF-β activation by these integrins, as TGF-β activation is reduced by treatment with the actin polymerization inhibitor cytochalasin D (Munger et al., 1999; Wipff et al., 2007), whereas cell contraction stimulating agents such as thrombin, angiotensin-II and endothelin-1, can enhance TGF-β activation by the αvβ5 integrin (Wipff et al., 2007). Stimulation of the protease-activated receptor-1 (PAR1) pathway in lung epithelial cells by thrombin or other PAR1 agonists enhances TGF-β activation by the αvβ6 integrin (Jenkins, 2006) (Figure 1.18). This enhancement requires signalling via the Rho kinase (ROCK) signalling pathway (Jenkins et al., 2006), which is important in actin–myosin cell contractility.

These data suggest that activation of TGF-β via αvβ5 and αvβ6 integrins requires: (i) the binding between LAP and integrin on the outside of the cell, which allows generation of a force by the actin cytoskeleton connected to the cytoplasmic domain of the integrin, and (ii) binding between LTBP-1 and the ECM which creates an opposing holding force. Applying both of these

forces to the LLC may lead to a conformational change in the complex that allows TGF-β to bind to its receptor.

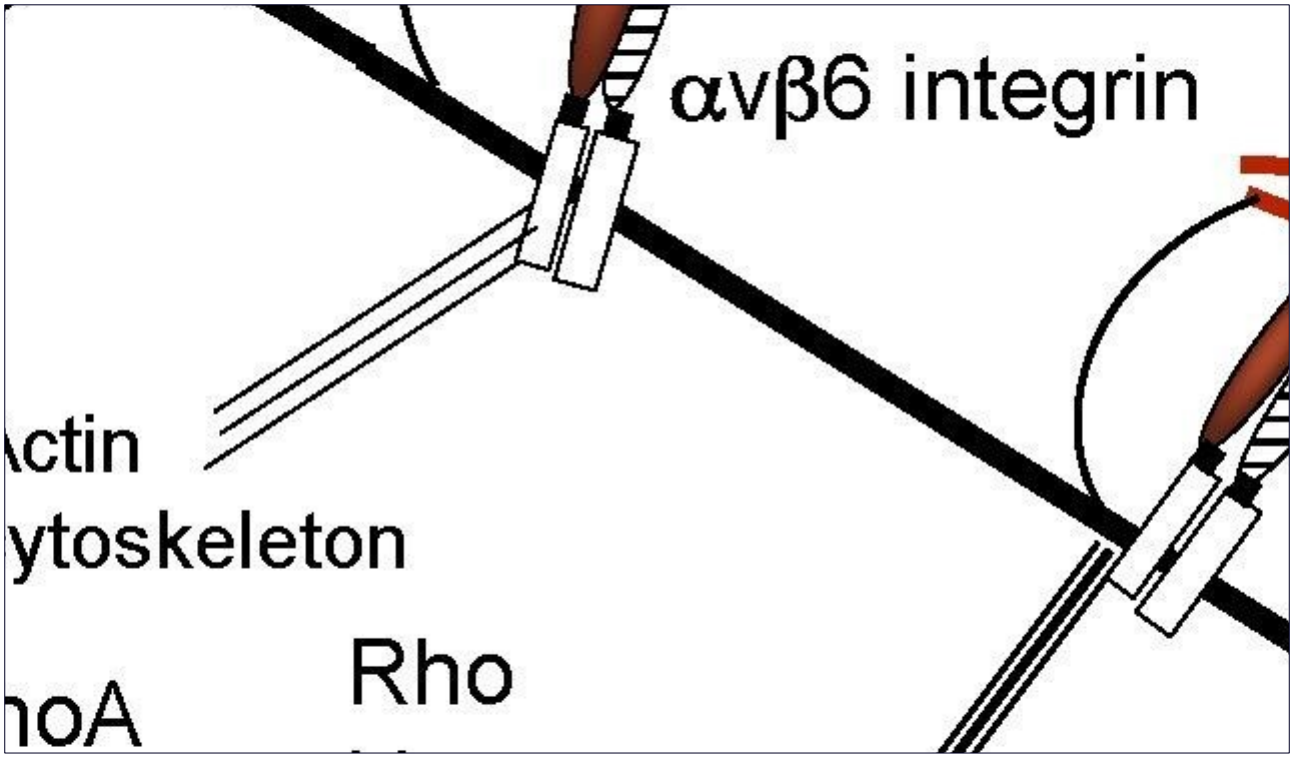

Figure 1.18 The association between thrombin and the αvβ6 integrin in latent TGF-β activation.

Platelets release thrombin which acts on epithelial PAR1, leading to RhoA-induced actin polymerization and cytoskeletal contraction against the cytoplasmic domain of the β6 subunit of the αvβ6 integrin. This interaction results in conformational changes in the integrin-latent TGF-β complex which allow active TGF-β to bind to its specific receptor. This image is taken from Jenkins, 2008.

1.11.2.4.2 Protease-mediated activation of TGF-β by αvβ8 integrins

It has been observed that not all integrins activate latent TGF-β by inducing a conformational change. The cytoplasmic domain of the αvβ8 integrin does not connect to the actin cytoskeleton, suggesting that actin-mediated cell contraction does not play a major role in TGF-β activation by this integrin (Mu et al., 2002). It has been observed that proteolytic cleavage of LAP by the cell surface MMP14 or transmembrane matrix-metalloprotease-1 (MT-MMP1) is crucial in the generation of active TGF-β in αvβ8-expressing cells (Mu et al., 2002). Furthermore, a study using a co-culture model of foetal tracheal epithelial cells and fibroblasts showed a high level of active TGF-β, which was significantly inhibited by anti-MMP and anti-

αvβ8 (Araya et al., 2006). A further study using human bronchial epithelial cells suggested that IL-1β may have a role in αvβ8-mediated TGF-β activation by an MMP14 dependent mechanism (Araya et al., 2007). The transcription factors SP1 and SP3, and the activating transcription factor 2 (ATF2) have been identified as key promoters of β8 integrin transcription (Markovic et al., 2010). A study in fibroblasts using SP3 knockdown showed a reduction in αvβ8 expression. Furthermore, the αvβ8 integrin may function by presenting latent TGF-β to MMP14, which causes proteolytic cleavage LAP and releases active TGF-β (Figure 1.19). However, the particular stimuli that enhance β8 integrin and MMP14 expression in different cell types leading to αvβ8-mediated TGF-β activation are unknown.

The activation of TGF-β by the αvβ8 integrin releases active TGF-β from the latent complex. However, the role of MMP14 in αvβ8-mediated TGF-β activation has only been tested in cells originating from the lungs and airways (Mu et al., 2002; Araya et al., 2007) and the generality of this mechanism remains to be established.

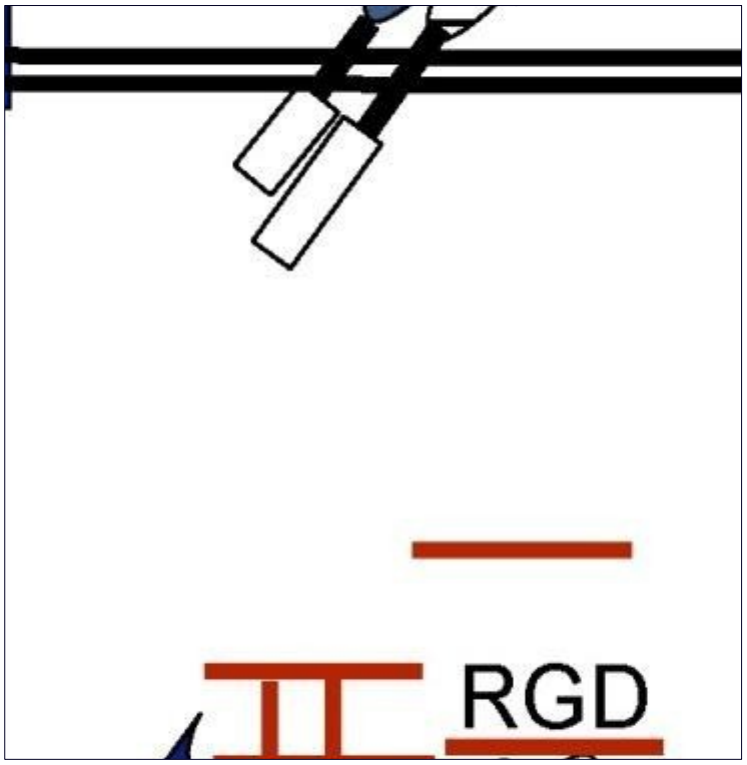

Figure 1.19 Role of MMP14 in αvβ8-mediated latent TGF-β activation.

The αvβ8 integrin binds the RGD sequence on latent TGF-β. The αvβ8 integrin then presents the latent TGF-β to MMP14, which proteolytically digests LAP and allows the active TGF-β molecule to bind with the receptor. This image is obtained from Jenkins et al., 2006.

1.11.3 Activation of TGF-β by Thrombospondin-1

Thrombospondin-1 (TSP-1) is a matricellular glycoprotein which is expressed in conditions such as wound healing, angiogenesis and neoplasia (Bornstein, 2001). It has been shown *in vitro* that TSP-1 expression is regulated by growth factors including PDGF, FGF-2 and TGF-β (Soula-Rothhut et al., 2005).

A previous study comparing TSP-1 null mice with TGF-β1 null mice demonstrated a similarity of organ pathology, in particular in the lung and pancreas (Crawford et al., 1998). Moreover, administration of a TSP-1 inhibitor to wild type mice showed similar pathology to TGF-β null mice (Crawford et al., 1998). It has also been shown that TSP-1 activates latent TGFβ by forming a direct interaction with the latent TGF-β complex which induces a conformational rearrangement which exposes active TGF-β. The mechanism of TSP-1-induced latent TGF-β activation is discussed in chapter 5.

1.12 Evidence of latent TGF-β activation during kidney allograft rejection

A number of reports have demonstrated increased expression of TGF-β mRNA and protein associated with the tubules after kidney transplantation (Robertson et al., 2001; Özdemir et al., 2005). However it is also clear that the biological response to this growth factor is dependent on activation of the latent growth factor within the kidney.

1.12.1 The role of the αvβ6 integrin in kidney transplantation

The αvβ6 integrin has been implicated in the pathogenesis of several kidney diseases, including chronic fibrosis after transplantation. The normal adult kidney expresses only low levels of the αvβ6 integrin but it has been suggested that this integrin is expressed by tubular epithelial cells of the proximal tubule, loop of Henle and collecting duct during kidney development (Arend et al., 2000).

A recent study of gene expression in renal allograft biopsy specimens has demonstrated that increased expression of a set of genes is prognostic of late graft failure (Einecke et al., 2007) Importantly, the gene with the fourth greatest prognostic value in this study encoded the β6 integrin chain, suggesting an important role for activation of latent TGF-β in the progression of this disease. It is notable that increased expression of the β3 integrin chain (see section 1.10.2.1) was also prognostic of graft failure, but less so than the β6 integrin. This result is consistent with a previous immunohistochemical study which showed increased expression of the β6 integrin

kidney allografts with subclinical or clinical rejection. Importantly, the expression of this integrin was greatly increased on remnant tubular epithelial cells during the development of fibrosis associated with chronic allograft rejection (Trevillian et al., 2004).

Col4A3$^{-/-}$ mice provide a model of the autosomal recessive Alport syndrome and develop progressive glomerulonephritis accompanied by the accumulation of extracellular matrix and fibroblasts, resulting in kidney fibrosis. It has been demonstrated that these mice express high levels of the αvβ6 integrin. Addition of an αvβ6 blocking antibody inhibited the accumulation of activated fibroblasts and deposition of extracellular matrix, as well as the expression of TGF-β, suggesting a role for the αvβ6 integrin in TGF-β regulation in this disease (Hahm et al., 2007).

Another study using UUO-induced renal fibrosis showed that interstitial fibrosis was reduced in β6 integrin$^{-/-}$ mice compared to wild-type mice. In addition, phosphorylated Smad 2 and active TGF-β were markedly reduced in the β6 integrin deficient mice, indicating that inhibition of the function of the β6 integrin can prevent renal fibrosis through TGF-β regulation (Ma et al., 2003).

1.12.2 Thrombospondin-1-induced latent TGF-β in kidney fibrosis

Recent data suggest that thrombospondin-1 plays a potential role in latent TGF-β activation by mesangial cells in the kidney (Tada and Isogai, 1998). A previous study showed that experimental mesangial cell proliferative glomerulonephritis induced by an anti-Thy1 antibody was associated with de novo expression of TSP-1 and increased TGF-β expression (Hugo et al., 1995). However, addition of a TSP-1 blocking peptide reduced active TGF-β expression and the level of phosphorylated Smad 2 (Daniel et al., 2004). Furthermore, TSP-1 siRNA-transfected cells decreased their expression of active TGF-β and deposited less extracellular matrix (Daniel et al., 2003). Besides the anti-Thy1 model, diabetic nephropathy in TSP-1$^{-/-}$ mice showed less expression of active TGF-β and structural changes compared to wild type mice (Daniel et al., 2007). These suggest that TSP-1 is an endogenous activator of TGF-β in experimental glomerulonephritis and diabetic nephropathy *in vivo*.

1.13 The association between Cyclosporine A and TGF-β production

Recent protocol biopsy data has shown that 0.6% of renal allografts are lost by interstitial fibrosis resulting from Cyclosporine nephropathy (El-Zoghby et al., 2009). Although it seems that the recent incidence of Cyclosporine nephrotoxicity has been markedly decreased, it is clear that Cyclosporine nephropathy is associated with tubular atrophy and interstitial

fibrosis (see Chapter 3). It has also been suggested that Cyclosporine is associated with increased production of TGF-β. A study of human renal graft biopsies demonstrated increased expression of TGF-β in biopsies from patients with Cyclosporine treatment (Mohamed et al., 2000). Furthermore, the renal function and structural damage was improved by administrating a specific TGF-β neutralising antibody in a mouse model of chronic Cyclosporine nephropathy (Ling et al., 2003).

The exact mechanism of Cyclosporine-induced TGF-β secretion is incompletely understood. However, several factors have been shown to increase TGF-β secretion during Cyclosporine-induced renal graft fibrosis. A study in rats on a low sodium diet showed the deposition of extracellular matrix and increased expression of TGF-β following Cyclosporine treatment, whilst rats on a normal sodium diet remained normal (Shihab et al., 1997). This suggests a role for the renin-angiotensin system in TGF-β expression in Cyclosporine-induced renal fibrosis. In addition, it has been shown that addition of L-arginine reduced TGF-β expression and deposition of extracellular matrix in rat with chronic Cyclosporine nephrotoxicity, indicating a role of nitric oxide in TGF-β expression (Shihab et al., 2000). Aldosterone has also been reported to induce TGF-β expression. Treatment of rats with Cyclosporine and a mineralocorticoid receptor antagonist down-regulated TGF-β expression compared to rats with Cyclosporine treatment (Macunluoglu et al., 2008). Chronic Cyclosporine nephrotoxicity is often associated with macrophage infiltration. A study using macrophage depleted rats showed a reduction of TGF-β expression, although expression of the myofibroblast marker, α-SMA did not change (Carlos et al., 2010**)**. Interestingly, an *in vitro* study showed a direct effect of Cyclosporine on TGF-β production by several cell lines, including renal tubular epithelial cells (Esposito et al., 2000; Mohamed et al., 1999). This observation suggests that calcineurin might be involved in regulating TGF-β expression (Esposito et al., 2000). Since TGF-β is a key cytokine for EMT-mediated organ fibrosis, renal allograft fibrosis associated with Cyclosporine nephrotoxicity may be induced by EMT following activation of the TGF-β signalling pathway.

1.14 **Hypothesis**

Kidney transplantation is the treatment of choice for patients with end-stage renal disease. Despite advances in transplant medicine, late allograft loss is still a major problem. Recent data has shown that 10-year renal graft survival is approximately 65% in cadaveric transplantation and 80% in living donor transplantation. Besides death with a functioning graft,

chronic allograft failure is the most common cause of renal allograft loss in living recipients. The typical pathology of chronic allograft dysfunction includes chronic inflammation with tubular atrophy and interstitial fibrosis.

Interstitial fibrosis is defined by an accumulation of extracellular matrix proteins in the interstitium leading to distortion of the renal architecture. This ECM is produced by active fibroblast or myofibroblasts. Currently, the origin of these interstitial fibroblasts remains controversial although, several sources of fibroblasts have been proposed, including epithelial mesenchymal transition (EMT), endothelial mesenchymal transition (EndoMT), resident interstitial fibroblasts, bone marrow-derived fibroblasts and pericytes or perivascular fibroblasts. However, the process of epithelial to mesenchymal transition might play a role in renal allograft fibrosis since a previous study has shown that 30% of interstitial fibroblasts are derived from renal epithelial cells (Iwano et al., 2002).

This study was designed to test the linked hypotheses that Cyclosporine A and graft-infiltrating T cells can induce allograft fibrosis through induction of epithelial mesenchymal transition by alteration of the bioavailability of fibrogenic TGF-β.

1.15 Aim and Objectives

The overall aim of this study was to investigate the pathogenic role of epithelial to mesenchymal transition in allograft fibrosis after kidney transplantation. Initial investigations were designed to demonstrate the development of EMT by specific causes including Cyclosporine A and graft-infiltrating T cells, and also to understand the involvement of the key profibrotic cytokine TGF-β in this process. In the final part of this study, the mechanism by which activated T cells can activate latent TGF-β leading to either T cell or epithelial cell differentiation was determined.

1.15.1 Objectives

The main experimental objectives of this study are to:

- Investigate the possibility that Cyclosporine A can induce epithelial to mesenchymal transition of renal proximal tubular epithelial cell lines.
- Determine the mechanism by which a model intraepithelial T-cell line induces epithelial to mesenchymal transition of a renal proximal tubular epithelial cell line.
- Identify the potential mechanisms by which activated T cells mediate the activation of latent TGF-β.

Chapter 2: Materials & Methods

2.1 Tissue culture techniques

Tissue culture was performed under aseptic conditions in a class II laminar flow cabinet (Telstar Life Sciences). All items used were sprayed with 70% ethanol on entry and removal from the cabinet, including gloves. Tissue culture materials were either purchased as sterile or were sterilised by autoclaving at 121°C and 15 PSI (pound per square inch) for 15 minutes prior to use. Cell lines were routinely passaged (dependent on cell type; see subsequent individual sections for details) and frozen stocks were maintained in liquid nitrogen. Each of the seven cell lines used in this study required different cell culture media (Table 2.1). All culture medium was pre-warmed in a water bath at 37°C prior to use. All cells were cultured in a humidified 5% CO_2 incubator at 37ºC. Cells were seeded into either 25cm^2 or 75cm^2 tissue culture flasks. Cells were monitored daily using an inverted microscope.

2.1.1 General maintenance of cell lines

2.1.1.1 Adherent cells

Adherent cells are anchorage-dependent and grow as a monolayer on the horizontal surface of tissue culture flasks (CELLSTAR, Greiner Bio-One). When they reached approximately 80% confluence, the cells were passaged at a ratio of 1:3-1:4 depending on cell type. Briefly, cell culture medium was removed and the cells were washed gently two times with 10ml of sterile, pre-warmed PBS (Sigma). The cells were harvested from the culture flask by incubation with 5ml of pre-warmed 0.25% (v/v) trypsin and 0.02% (v/v) ethylenediaminetetraacetic acid (Trypsin/EDTA; Sigma) solution for 5 minutes at 37°C. Following incubation, 15ml of pre-warmed complete culture medium (section 2.1.2) was added to the flask in order to neutralise trypsin activity and the suspension was agitated gently. The cell suspension was then centrifuged at 500 x g for 5 minutes. The supernatant was discarded and the cell pellet resuspended in 1ml of pre-warmed appropriate culture medium (section 2.1.2). Cells were counted by using a haemocytometer (section 2.1.3) and an optimum number seeded (section 2.2) into either 25cm^2 flasks or 75cm^2 culture flasks.

2.1.1.2 Suspension cells

Suspension cells are free-floating in culture medium and many are hematogenous cell lines. These cells were cultured in vertical culture flasks. They were passaged when the cell

density reached 2×10^6 cells/ml. Briefly cells were collected in a plastic universal container (Scientific Laboratory Supplies, UK) and centrifuged at 500 x *g* for 5 minutes. The supernatant was discarded and the cell pellet was resuspended in 1ml pre-warmed appropriate culture medium. Cells were counted by using a haemocytometer and an optimal number was transferred to new flasks.

2.1.2 Culture medium

2.1.2.1 Roswell Park Memorial Institute (RPMI)-1640 Medium, HEPES Modification

RPMI-1640 medium was developed by Moore et al. at Roswell Park Memorial Institute (Moore and Hood, 1993). RPMI-1640 medium, HEPES (4-(2-hydroxyethyl)-1-piperazineethanesulfonic acid) Modification (Sigma, UK) contains 25mM HEPES buffer. For complete RPMI-1640 medium, buffered medium was supplemented with 10% heat- inactivated foetal bovine serum (FBS), antibiotics (100IU/ml Penicillin and 100µg/ml Streptomycin) and 2mM L-glutamine (all obtained from Sigma). Complete RPMI 1640 medium was stored at 4°C for further use.

2.1.2.2 Dulbecco's Modified Eagle Medium (DMEM)/Nutrient F-12 Ham

This medium contains a 1:1 mixture of DMEM and Ham's F-12 Nutrient with 3.15g/l D-glucose, 15mM HEPES, L-glutamine and sodium bicarbonate (Sigma). It was supplemented with 100IU/ml Penicillin, 100µg/ml Streptomycin, 5% FBS and 5ml of ITS-X (10mg/l insulin, 5.5mg/l transferrin, 6.7µg/l sodium selenite and 2.0g/l ethanolamine) (Gibco, Invitrogen); this medium is referred to as complete DMEM/F-12 medium, when used for cell culture. This medium was used to grow renal tubular epithelial cell lines including HKC-8 and HK-2 cells.

2.1.2.3 Renal Epithelial Cells Growth Medium (REGM™) BulletKit

This is a defined medium for growing primary human renal tubular epithelial cells. It contains renal epithelial cell basal medium (REBM™, Lonza) and the following growth supplements (SingleQuots™, Lonza); human Epidermal Growth Factor (hEGF) 0.5 ml, Hydrocortisone 0.5 ml, Epinephrine 0.5 ml, Insulin 0.5 ml, Triiodothyronine 0.5 ml, Transferrin 0.5 ml; GA-1000 (Gentamicin and Amphotericin-B) 0.5 ml and FBS 2.5 ml per 500ml of REBM™.

2.1.2.4 Dulbecco's Modified Eagle Medium (DMEM)

The DMEM used in this study contained 1g/l D-glucose and 3.7g/l sodium bicarbonate (Sigma) but no phenol red. The complete DMEM was supplemented with 2mM L-glutamine, 100IU/ml Penicillin, 100µg/ml Streptomycin and 10% FBS when it was used to grow cells.

2.1.2.5 X-VIVO™ Medium

X-VIVO™ (Lonza) is a serum-free medium specific for T lymphocytes. It contains Lglutamine, gentamicin and phenol red.

Medium and Supplements	**Cell lines**				
	HK-2 and HKC-8	**HRCE**	**MOLT-16, MFB-F11 and PBMC**	**T cell**	**MDA-231**
Medium	DMEM/F-12	REBM™	RPMI 1640	X-Vivo™	DMEM phenol red-free
FBS	5%	-	10%	-	10%
Glutamine	2mM	-	2mM	-	2mM
Penicillin Streptomycin	100IU/ml 100µg/ml	- -	100IU/ml 100µg/ml	- -	100IU/ml 100µg/ml
ITS-X (100x)	5 ml	-	-	-	-
SingleQuots™	-	1 set	-	-	-

Table 2.1 Medium and supplements used for cell culture.

2.1.3 Cell counting

Cell density was evaluated by using a Neubauer Haemocytometer (Weber England) which consists of two chambers, each containing 9 squares (Figure 2.1A). The central counting area of the haemocytometer contains 25 large squares. When counting, only those cells on the

lines of two sides of the large square were counted (Figure 2.1B). Cells were harvested, resuspended in phosphate buffer saline (PBS) and a 10µl aliquot was transferred to the haemocytometer. The number of cells was counted in the four corners plus the middle square in the central square and the average was taken and multiplied by 5 to include all 25 squares and 1 x 10^4 to obtain the number of cells per ml. For example, if total cell count is 50 cells in 5 squares:

$$\text{Total cell number} = 5 \times 50 \times 10^4 = 2.5 \times 10^6 \text{ cells/ml}$$

Trypan blue (a potent carcinogen) is a dye used to distinguish viable and dead cells. Viable cells exclude the dye while non-viable cells absorb the dye and appear blue. In order to check cell viability, cells were mixed with 0.1% Trypan blue (Sigma) and the proportion of viable (dye excluding) cells was recorded.

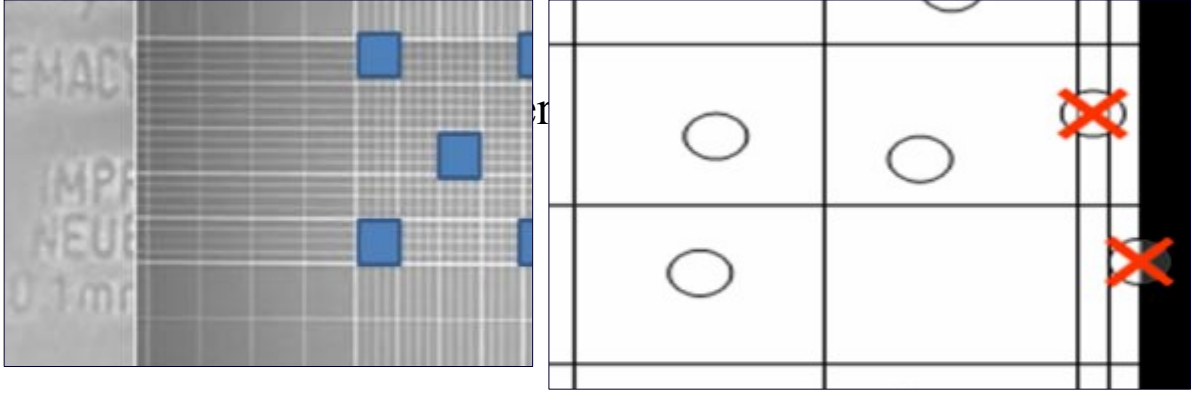

B

Figure 2.1 Cell counting by haemocytometer.

(A) Haemocytometer counting chamber with nine large squares and five counting areas in the central square. (B) For cells on the borders on counting areas, only two sides of border lines were counted.

2.1.4 Mycoplasma testing

Cell lines were tested for mycoplasma infection using the MycoAlert Mycoplasma Detection Assay (Promega) according to the manufacturer's instruction. Briefly, 2ml of culture supernatant was transferred into a plastic universal tube and centrifuged at 500 x g for 5 minutes. Then, 100µl of cleared supernatant was transferred into a microcentrifuge tube, with the addition of 100µl of the mycoplasma reagent, and incubated at room temperature for 5 minutes. The microcentrifuge tube was inserted into a luminometer and the result was recorded as reading A. Then, 100µl of mycoplasma substrate was added and incubated for 10 minutes. The luminescence was read again and recorded as reading B. The ratio between reading A and reading B was then calculated. A ratio < 1 indicated an uninfected cell line. No infected cell lines were detected during this study.

2.1.5 Cell storage

To maintain a stock of cryopreserved cell lines, cell stocks were preserved in liquid nitrogen. Cells were frozen at ~90% confluence (determined by light microscopy). Cell culture medium was removed and cells washed gently with 10 ml of pre-warmed PBS. Cells were detached from the surface of the flask using 5ml trypsin/EDTA. 15ml of pre-warmed culture medium were then added to the flask and the cell suspension was agitated gently. The cell suspension was centrifuged at 500 x g for 5 minutes. The supernatant was discarded and the cell pellet was resuspended in 1ml of freezing medium containing 10% dimethylsulfoxide (DMSO) (Sigma) and 90% FBS (v/v), and then 0.5ml of cell suspension was transferred to conservation vials (Corning). The vials were cooled at a rate of -1°C per minute by holding in a freezing

container (Mr. Frosty, Nalgene, Hereford, UK) at -80°C for 24 hours. Following this, the vials were transferred and stored in a liquid nitrogen freezer until required.

2.1.6 Reviving frozen cells

Cell stocks (see section 2.1.5) were removed from the liquid nitrogen store and rapidly thawed in a 37°C water bath. Cells were resuspended in 10ml pre-warmed culture medium and agitated gently. The cell suspension was centrifuged at 500 x g for 5 minutes to form a pellet. The supernatant was discarded and the pellet resuspended in pre-warmed complete culture medium. Cells were seeded as required into 75cm^2 tissue culture flasks. The final volume of the culture flask was made up to 20ml with pre-warmed culture medium. Cells were maintained at 37°C in a humidified atmosphere (5% CO_2 in air). Once the cells had reached ~90% confluence or a cell density of 2x10^6 cells/ml (determined by light microscopy), they were passaged as detailed in section 2.1.1 and routine culture commenced.

2.2 Cell lines

2.2.1 HKC-8 cell line

This is an immortalised human renal tubular epithelial cell line developed by Dr. Johng S. Rhim (Racusen et al., 1997). The parental cells were isolated from normal renal cortex and then exposed to adenovirus 12:SV40 hybrid virus. This cell line is a non-producer of the immortalising virus and is non-tumorigenic. In addition, the properties of proximal renal tubular epithelium, including biochemical parameters, transport activities and immunohistochemical staining for epithelial markers, have been demonstrated in this cell line (Racusen et al., 1997). Furthermore, this cell line has been widely used as a model for renal proximal tubular epithelial cells in other studies, for example Ca^{2+} signalling (Turvey et al., 2010) and fibrosis (Tan et al., 2008). HKC-8 cells were cultured in DMEM/F-12 HAM medium supplemented with 0.5µg insulin, 0.275µg transferrin, 0.385pg selenium (ITS-X, GIBCO, Invitrogen), 100IU/ml Penicillin, 100µg/ml Streptomycin and 5% FBS. This cell line was split in a 1:3 ratio and cultured in 75cm^2 tissue culture flasks. Originally, HKC-8 cells were maintained in DMEM/F-12 HAM with 2% FBS, insulin, transferrin, selenite and hydrocortisone (Racusen et al., 1997). However, it has also been shown that HKC-8 cells grown in DMEM/F-12 HAM with 5% FBS displayed characteristics of differentiated proximal renal tubular epithelial cell (Bland et al., 1999).

2.2.2 HK-2 cell line

This line of immortalised human proximal renal tubular epithelial cells was produced from primary renal tubular cells which were extracted from normal adult human renal cortex, then exposed to a recombinant retrovirus containing the human papilloma virus (HPV 16) E6/E7 genes. This cell line has functional and phenotypic characteristics of proximal renal epithelial cells (Ryan et al., 1994) which are comparable to the HKC-8 cell line (Racusen et al., 1997). In this study HK-2 cells were cultured in DMEM/F-12 HAM with 5% FBS and similar supplements to those used for the HKC-8 cell line. Although this medium differs from the supplemented serum-free keratinocyte medium suggested in the original paper, more recent studies of differentiated cell functions have routinely used the DMEM/F12 HAM medium described in the current report (Shimizu et al., 2011).

2.2.3 Human renal cortical epithelial cells (HRCE)

Clonetic™ HRCE was purchased from Lonza. These primary renal cells were extracted from normal renal cortex. The characteristics of epithelial cells were demonstrated by positive cytokeratin staining (Clonetic™ Renal Epithelial Cell System, Lonza). Clonetic™ HRCE cells arrived frozen and were thawed at 37° in a water bath for less than 2 minutes or until the ice was melted. The cells were then resuspended in the cryovial and seeded at a density of 2,500 cells/cm^2 into 75cm^2 tissue culture flasks which contained 15ml of a specific culture medium (BulletKit®) with supplement (SingleQuots®) solution (section 2.1.2.3). HRCE cells were sub-cultured as described above (section 2.1.1), except the centrifugation was decreased to 220g. The seeding density for HRCE was 2,500 cells/cm^2 and the culture medium was changed every second day. Cells were used for between 3-5 passages.

2.2.4 Peripheral Blood Mononuclear cells (PBMC)

Human peripheral blood mononuclear cells (PBMC) are circulating blood cells which have a single nucleus, such as lymphocytes and monocytes. PBMC was isolated from the venous blood of healthy volunteers in accordance with Ethics committee approval. Blood was heparinised and separated by density centrifugation (Noble et al., 1967) as described in section 3.3.1. PBMC were cultured in RPMI 1640 complete medium.

2.2.5 T cells

T cells were isolated from the whole blood of healthy volunteers in accordance with Ethics committee approval, using the RosetteSep® human T cell enrichment cocktail (StemCell

Technologies) as described in section 2.2.5.1. These cells were activated using Dynabeads® Human T-Activator CD3/CD28 (Invitrogen). T cells were routinely cultured in serum-free X-VIVO™ medium (Lonza).

2.2.5.1 Human T cell isolation from whole blood

The RosetteSep® Human T cell Enrichment Cocktail isolates T cells from whole blood by a negative selection mechanism. Tetrameric antibody complexes (TACs) play a key role by cross-linking CD16, CD19, CD36, CD56, CD66b and glycoprotein A on red blood cells (RBCs) to form "immunorosettes" containing unwanted cells and RBCs (Figure 2.2). The increased density of the unwanted cell-RBC complex allows separation by density gradient centrifugation. T cells were isolated from the venous blood of healthy volunteers by using RosetteSep® T Cell Enrichment Cocktail.

Blood was mixed with heparin (Sigma) at a final concentration of 100units/ml to prevent coagulation. RosetteSep® T cell Enrichment Cocktail was added to heparinised blood at 50µl/ml and incubated at room temperature for 20 minutes. The sample was then diluted with an equal volume of sterile PBS (phosphate buffered saline) containing 2% BSA (2% BSA/PBS), followed by layering over a Lympholyte®-H (density gradient 1.077g/ml, Cedarlane, VHBio). The sample was centrifuged at 1200 x g for 20 minutes to separate the unwanted cells and RBCs. The density medium : plasma interface layer, which contained enriched T cells, was removed. The enriched cells were washed with 2% BSA/PBS by centrifugation at 600 x g for 10 minutes. The T cells pellet was resuspended in complete RPMI 1640 medium. (Figure 2.3)

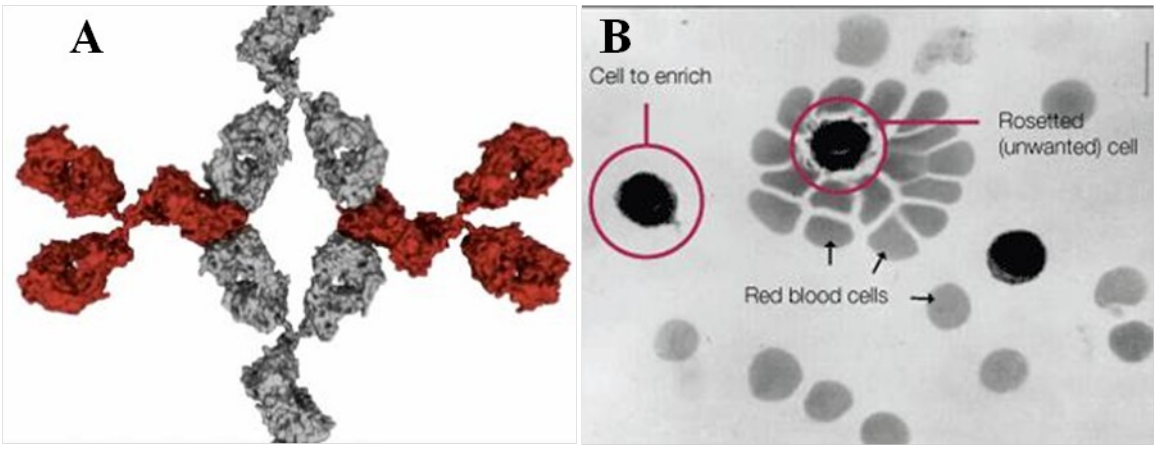

Figure 2.2 Mechanism of T cell isolation from whole blood by RosetteSep® Human T cell Enrichment Cocktail.

Panel A shows the structure of the tetrameric antibody complex which consists of two binding domains which recognize RBCs and unwanted cells. Panel B shows the crosslinked complex between unwanted cells and multiple RBCs forming the immunoresette. This image is taken from the RosetteSep® information sheet.

2.2.6 MDA231 cell line

MDA231 is a breast cancer cell line which was established from the pleural effusion of a 51-year-old Caucasian female patient with breast adenocarcinoma (Brinkley et al., 1980). This cell line was cultured in phenol red-free DMEM complete medium since phenol red has an oestrogenic activity which might disturb cell proliferation (Walsh-Reitz and Toback, 1992). These cells were split at a ratio of 1:3 and grown in 75cm^2 tissue culture flasks. MDA231 cells are used widely as a cell model for neuropilin-1 (NRP-1) expression (Glinka et al., 2011).

2.2.7 MFB-F11 cell line

MFB-F11 cells are embryonic fibroblasts from *Tgfb*$^{-/-}$ mice transfected with a plasmid containing TGF-β responsive Smad-binding elements coupled to a secreted alkaline phosphatase reporter gene (SBE-SEAP). The MFB-F11 cell line was produced in order to assess the activity of TGF-βs, including TGF-β1, TGF-β2 and TGF-β3. These cells are not induced by latent TGF-β or other members of the TGF-β family such as activin, nodal, BMP-2 and BMP-6 (Tesseur et al., 2006). MFB F-11 cells were cultured in RPMI 1640 complete medium. Cells were passaged twice a week at the ratio 1:4-1:5 in 75cm^2 tissue culture flasks.

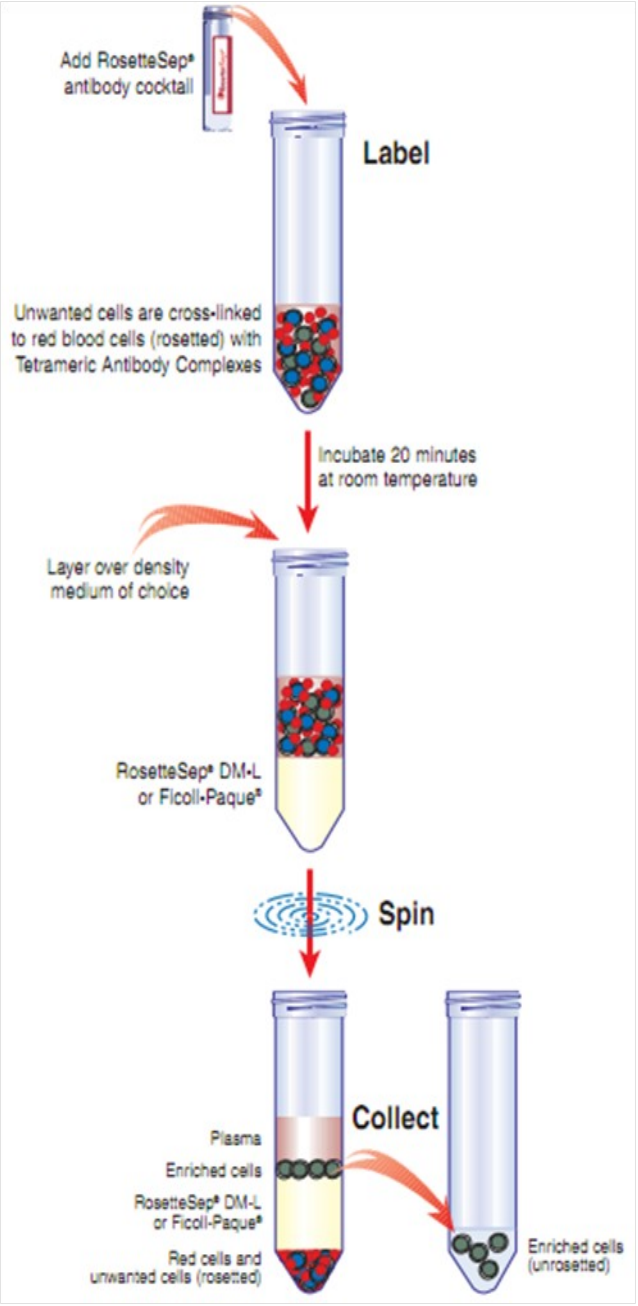

Figure 2.3 T cells isolation procedure.

The purity of isolated T cells was measured after staining with a fluorochrome-conjugated anti-CD3 antibody (Dako) and analyzed by flow cytometry as described in section 2.7. The percentage of $CD3^+$ T cells in the enriched cell population was routinely greater than 97%. This image is taken from the RosetteSep® information sheet.

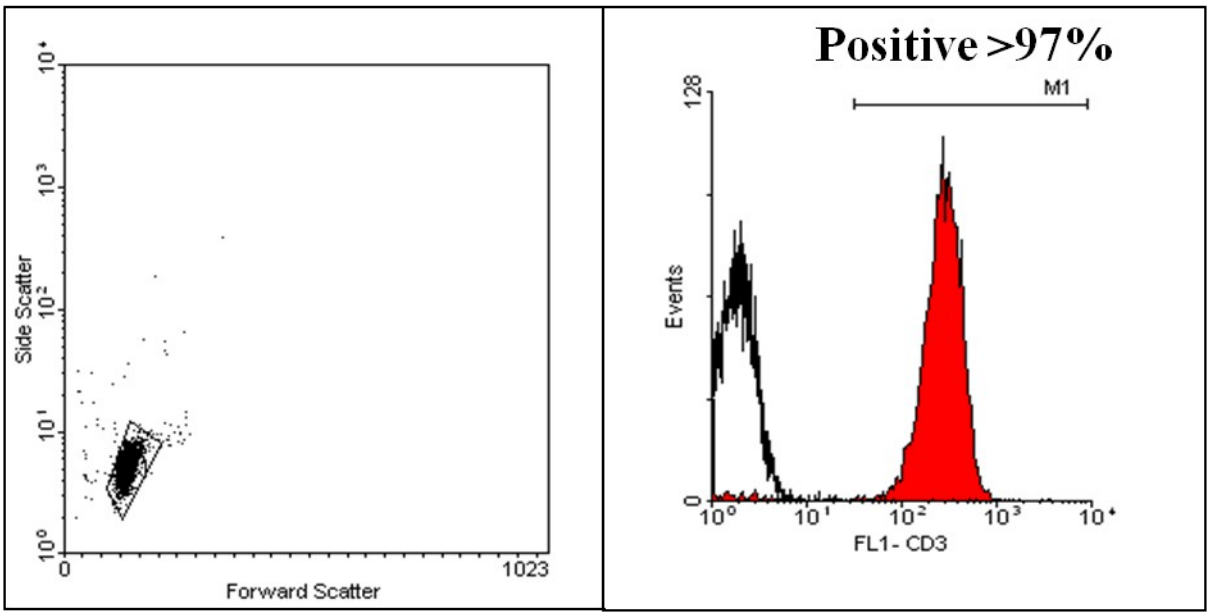

Figure 2.4 Flow cytometric analysis of the percentage of $CD3^+$ T cells after whole blood isolation.

T cells were isolated according to the RosetteSep® T cell Enrichment Cocktail protocol. Then, the isolated T cells were stained with monoclonal anti-CD3 antibody (red histogram) and an

appropriate isotype control (open histogram). Analysis showed that the isolated cells contained more than 97% $CD3^+$ T cells.

2.3 Molecular biology techniques

2.3.1 RNA biology

Ribonucleic acid (RNA) is made up of a long chain of nucleotides. Each nucleotide consists of a nucleobase, a ribose sugar and a phosphate group. RNA can be divided into 3 types based on their functions. (i) Messenger RNA (mRNA) is transcribed from DNA by RNA polymerase enzyme and serves as a template for the synthesis of proteins. (ii) Ribosomal RNA (rRNA) is one of 2 main components of ribosomes; the other is proteins (ribosomes = rRNA + proteins). These ribosomes become associated with mRNA in the cytoplasm. (iii) Transfer RNA (tRNA) contains a specific amino acid at one end and anticodon region which recognises and binds mRMA at one end. The tRNA binds to the mRNA codon and transfers amino acids to the ribosomes in order to synthesise protein. It is mRNA that was of particular interest in this study, since it represents gene expression in physiological and pathological conditions. Therefore, it allows measurement of changes in gene expression after the treatment of cells with a variety of cytokines. The TRI-Reagent technique was used to extract cellular RNA.

2.3.2 RNA extraction

Total RNA was extracted following an adaptation of the TRI-Reagent method (technical bulletin MB205, Sigma). Confluent cells in 25cm^2 tissue culture flasks were washed twice with 5ml of ice-cold PBS. 1ml of ice-cold PBS was added to the flasks and the cells were harvested mechanically from the surface using a cell scraper. The cell suspension was centrifuged at 500 x g for 5 minutes to form a pellet. The supernatant was removed by pipetting. The cell pellet was lysed in an Eppendorf tube using 1ml of TRIzol-Reagent (Sigma), and the lysate was passed several times through a pipette until homogeneous. The lysate was allowed to stand at room temperature for 5 minutes to ensure complete dissociation of nucleoprotein complexes. 200µl of chloroform was added and the sample shaken vigorously by hand for 15 seconds. The sample was left at room temperature for 15 minutes and was then centrifuged at 12000 x g for 15 minutes at 4°C. The centrifugation separates the sample into 3 phases: a red bottom organic phase (containing proteins), an interphase (containing DNA) and a colourless upper aqueous phase (containing RNA). The aqueous phase was transferred to a fresh tube and 0.5ml of 2-propanol was added to the sample and gently mixed together. The sample was left at room temperature for 10 minutes and then centrifuged at 12000 x g for 10 minutes at 4°C. The

supernatant was removed by aspiration and the RNA pellet washed in 1ml of 75% ethanol. The sample was vortexed briefly and centrifuged at 7500 x g for 5 minutes at 4°C. The supernatant was aspirated and the RNA pellet was allowed to air dry for 10-15 minutes. The RNA was dissolved by resuspension in 20µl of RNase (Ribonuclease)-free water (Sigma). The RNA was either reverse transcribed immediately or stored at -80°C until required.

2.3.3 Determination of quality and quantity of RNA

The RNA sample should be free of contaminating substances, including proteins, DNA, phenol, ethanol and salts. Contamination can decrease the efficiency of reverse transcription, leading to reduced amplification. RNA purity can be evaluated from the ratio of the absorbance at 260nm and 280nm (A_{260}/A_{280}); this was measured using a nanodrop spectrophotometer (No-1000 NanoDrop®) (Figure 2.5). In the spectrophotometer, a sample is exposed to ultraviolet light at 260nm (for nucleic acid) and 280nm (for proteins), and a photo-detector measures the light that passes through the sample. Pure RNA should have an A_{260}/A_{280} ratio in the range of 1.7-2.1. In addition, the $A_{260}/_{A230}$ ratio can be used to exclude contamination with proteins, phenol and chaotropic salts such as guanidinium isothiocyanate, which absorb UV light at 230nm. The value of the A_{260}/A_{230} ratio should be around 2. The nanodrop spectrometer can also be used to estimate RNA concentrations.

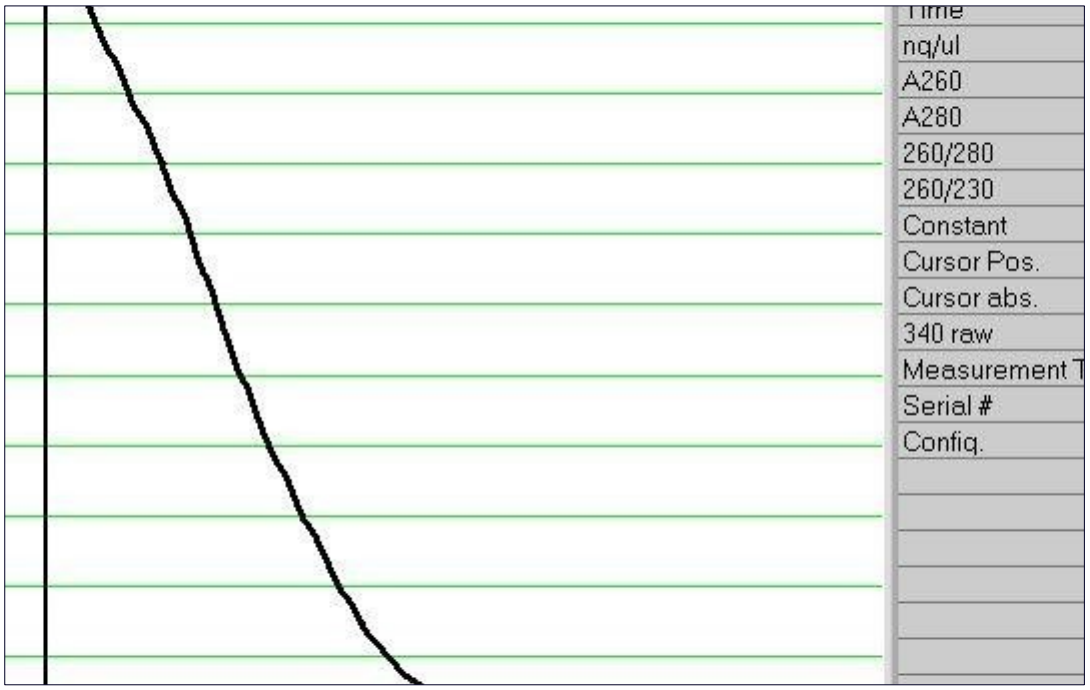

Figure 2.5 RNA purity and concentration measurement by Nanodrop specrophotometry. This image is representative of RNA samples, and shows an A260/280 ratio of 2.00, The 260/230 ratio was 2.16 and the RNA concentration was 2183.38ng/µl.

2.3.4 Determination of RNA integrity

Isolation of intact RNA is essential for gene expression analysis. The method used to assess the integrity of total RNA is to run an RNA sample on an agarose gel stained with ethidium bromide (EtBr) (Sigma). Briefly, a 1% agarose gel was made by combining 1g agarose powder (Sigma) with 100ml of 1xTAE (Tris-acetate-EDTA) buffer solution. The agarose was completely dissolved by heating in a microwave oven at high power for 2 minutes and then partly cooled in running tap water. 3µl of 25mM EtBr was added to the warm 1% agarose and mixed well together. The 1% agarose solution was poured into a minigel electrophoresis tray with a 20-well separation comb. The agarose solution was allowed to solidify for at least 45 minutes at room temperature. The agarose gel tray was put into an electrophoresis tank (Mini-Sub® Cell GT, BIO-RAD) and submerged in 1 x TAE buffer solution. The comb was removed from the gel. 12µl of 1 kilobase pair (kb) DNA ladder was applied to the first well. 1µg of RNA sample was mixed with 2µl of 6x gel loading dye and RNase-free water to a total volume of 12µl. 100V of electricity was applied to run the gel for 1 hour. The gel was viewed under UV light. Intact RNA should display clear ribosomal bands of 28s rRNA and 18s rRNA at ~1.7kb and ~ 800bp (base pair), respectively (Figure 2.6) with little degradation or smearing of the bands.

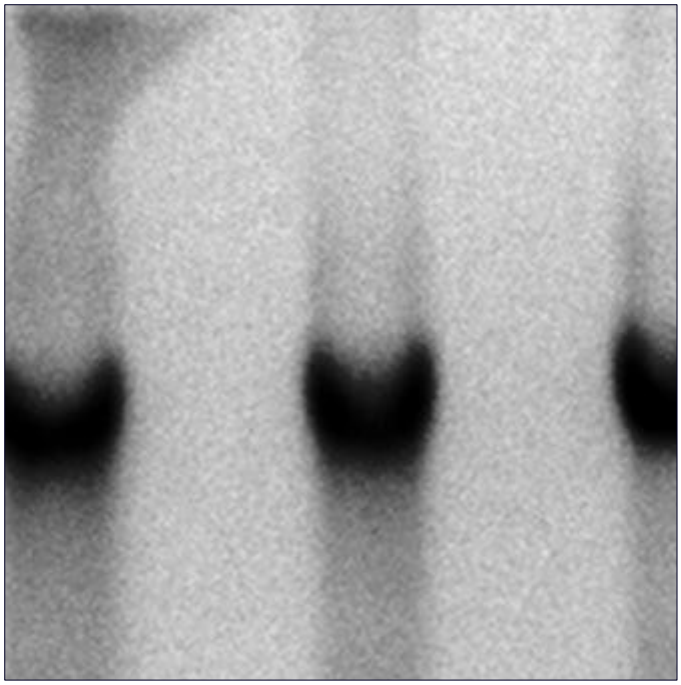

Figure 2.6 Quality of representative RNA samples.

This image shows the ethidium bromide stained RNA separated in a 1% agarose gel. The two clear bands in each lane are 28s rRNA and 18s rRNA which are located at 1.7 Kb and 800bp respectively.

2.3.5 Reverse transcription of RNA

Reverse transcription (RT) is a process in which single-stranded RNA is reverse transcribed into double-stranded complementary DNA (cDNA). The cDNA produced from this reaction can be used for PCR amplification. Four reagents are needed for cDNA production. These include mRNA as a template, dNTPs (dGTP, dCTP, dATP and dTTP), reverse transcriptase and primers. Three different types of primers can be used for the RT reaction:

(1) Oligo (dT), which binds only at the poly-A tail of mRNA; therefore, cDNA from this primer predominantly contains the 3' end of the gene. If the gene is very long, the 5' end is probably not transcribed.

(2) Random hexamers prime randomly along the entire length of mRNA, producing short cDNA fragments. The benefit of this primer is increasing the probability of transcription of the 5' end of the gene to cDNA. It also produces cDNA even if there is no poly (A) tail in the sequence, such as 18s rRNA.

(3) Sequence-specific primers bind only to one specific mRNA sequence.

This study used oligo $(dT)_{12-18}$ and random hexamers as primers for real-time PCR, depending on the sequence. The oligo $(dT)_{12-18}$ was used routinely, whereas random hexamers were used to prime 18s rRNA because of the absence of poly (A) tail in 18s rRNA. Reverse transcriptase is an RNA dependent DNA polymerase which synthesises cDNA from RNA in the 5′ to 3′direction. SuperScript®III Reverse Transcriptase (Invitrogen) is purified from *E. coli* expressing the gene of Moloney-Murine Leukaemia Virus (M-MLV). To generate cDNA from mRNA for a 20µl reaction volume, 1µg of starting RNA template was first denaturated for 10 minutes at 70°C in the presence of 200ng random hexamer (Fermentas) or 0.5µg oligo (dT_{12-18}) (Invitrogen) primers and 0.5mM dNTPs (Invitrogen). The mixture was cooled to 4°C for 2 minutes and then 1×First-Stand buffer (Invitrogen), 0.01M DTT (Dithiothreitol) (Invitrogen) and 200units SuperScript™ III reverse transcriptase (Invitrogen) were added, followed by subsequent incubation at 50°C for an hour. The DTT is used to stabilise enzymes and other proteins which posses free sulfhydryl (Chen et al., 2004). It is used in reverse transcriptase reaction to reduce disulphide bonds in RNases which are needed for maintaining stability, thereby inhibiting RNase activity and preserving mRNA for the reaction. The reaction was inactivated by heating at 70°C for 15 min. When the reaction was primed by random hexamers, the mixture was incubated for 5 min at 25°C before incubating at 50°C.

Component	**Volume/Reaction (µl)**

Oligo(dT)$_{12-18}$ (0.5µg/µl) or random hexamer (0.2µg/µl)	1.0
dNTPs (10mM each dNTP)	1.0
5 x first strand buffer (250 mM Tris-HCl (pH 8.3), 375 mM KCl, 15 mM $MgCl_2$)	4.0
DTT (0.01M)	1.0
SuperScript™ III (200units/µl)	1.0
RNase free water	2.0
Template RNA (100ng/µl)	10.0
Total volume	20.0

Table 2.2 Components required for the cDNA synthesis process.

2.4 Polymerase Chain Reaction

The polymerase chain reaction (PCR) is a technique to amplify a piece of DNA by *in vitro* enzymatic replication in order to generate thousands or millions of copies of a specific

DNA sequence. Typically, PCR consists of a series of 20-40 cycles. Before the cycle is started, the reaction mixture is heated to 95°C for 5 minutes in order to activate DNA polymerase. The cycle then begins with a denaturation step which consists of heating the reaction to 95°C for 1 minute. This disrupts the DNA strands by breaking the hydrogen bonds. After denaturing the DNA, the temperature is reduced to around 60°C for 30 seconds in order to allow binding between the primers and the single strand DNA template. This is the annealing step. Then, the temperature is increased to 72°C, which is an optimum temperature for DNA polymerase to synthesise a new DNA strand in the 5′ to 3′ direction. This is the extension or elongation step.

2.4.1 Real-time PCR

Real-time PCR is a technique for detection and quantification of the amplified DNA as the reaction progresses in real time, in contrast to standard PCR, in which the product of the reaction is detected at the end. A basic PCR reaction consists of three phases: (i) the exponential phase, which shows the exact accumulation of PCR product at every cycle, (ii) the linear phase, in which the reaction is slowing due to consumed components and (iii) the plateau phase, in which the reaction stops and the products start to degrade (Figure 2.7). Real-time PCR detects the accumulation of specific PCR products during the reaction; thus, the data is measured during the exponential phase of the PCR reaction. Standard PCR measures the accumulation of the PCR products after the PCR reaction or the plateau phase, which provides less quantitative data than the real-time PCR.

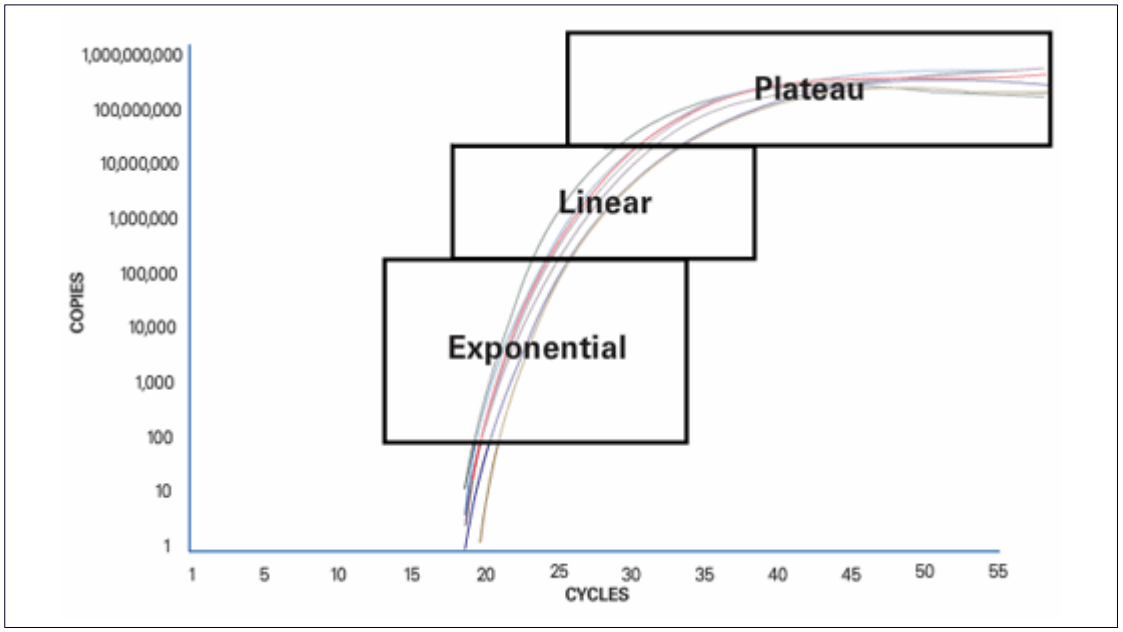

Figure 2.7 Three phases of the PCR reaction.

The PCR process can be divided into three stages (i) exponential amplification, (ii) linear and (iii) plateau stage. (Image taken from the Applied Biosystems tutorial)

2.4.2 Real-time PCR detection chemistry

Several methods have been developed for the detection of DNA amplification. The method used in this study is called TaqMan®-based detection or fluorogenic 5′ nuclease chemistry. This method was first reported by researchers at Cetus Coporation in 1991 (Holland et al., 1991) and subsequently developed by Applied Biosystems for research applications. Principally, the TaqMan® chemistry uses a fluorogenic probe to enable detection of the accumulating PCR product during PCR cycles. TaqMan probes are oligonucleotides 20-30 bases long containing a reporter fluorescent dye on the 5′ end and a quencher dye on the 3′ end. As long as the quencher and the fluorophore are close together, the fluorescence emitted by the reporter dye is inhibited by the quencher by a process termed FRET (Fluorescence Resonance Energy Transfer). However, during the PCR reaction, the TaqMan probe is cleaved by the 5′ nuclease activity of DNA polymerase, resulting in separation of the reporter and quencher dye which allows the signal emission from the reporter dye (Figure 2.8).

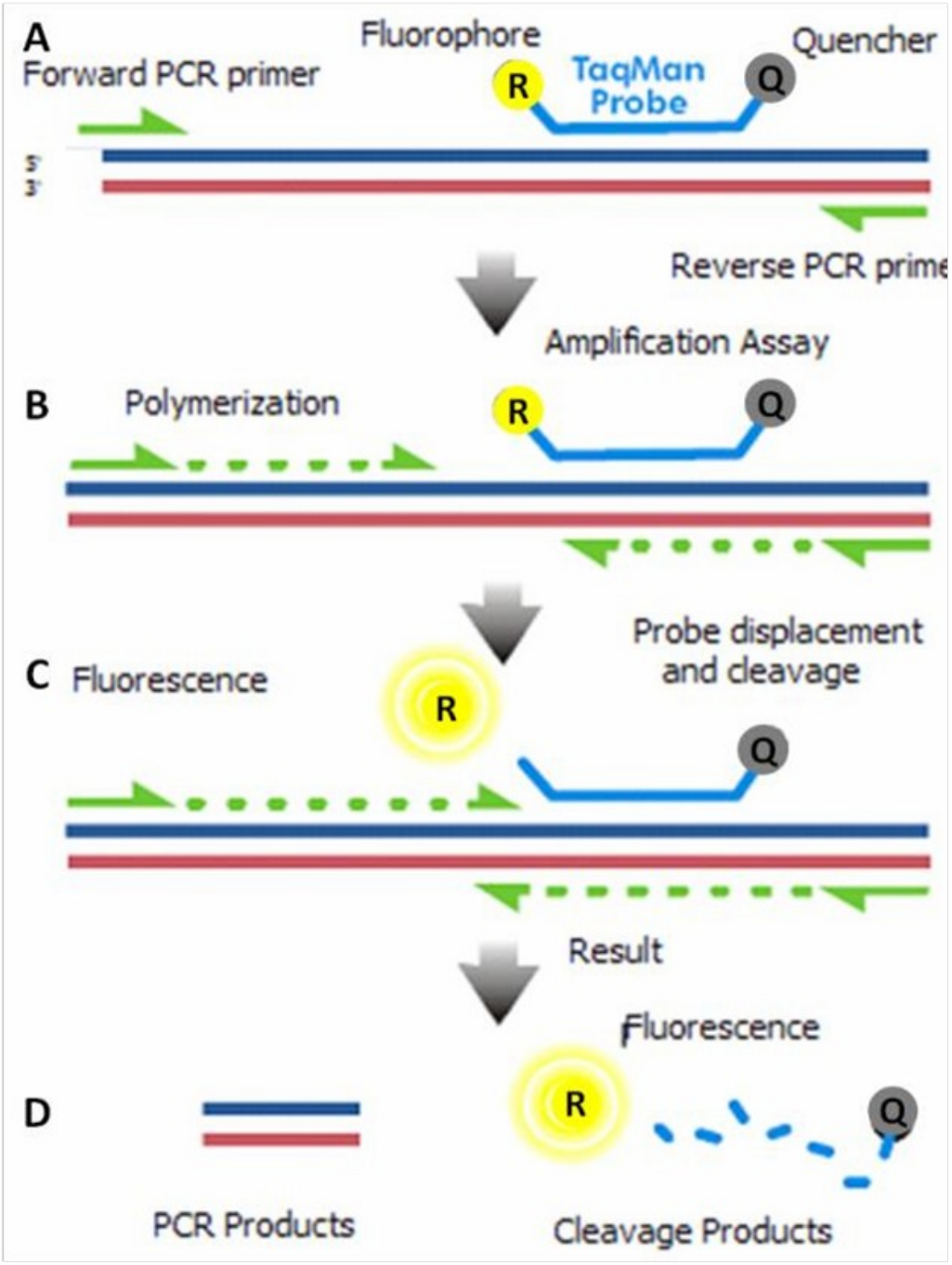

Figure 2.8 TaqMan® Probe based assay.

TaqMan® probe contains a fluorescent reporter (R) dye and a quencher (Q) at the 5´and 3´ ends respectively (A). When the probe is intact, the proximity of the quencher dye reduces the fluorescent emitted by the reporter dye by FRET (B). During the extension step, the DNA polymerase cleaves the reporter dye from the probe (C). Once separated for the quencher, the reporter dye emits its characteristic fluorescence (D). Image taken from the Applied Biosystems tutorial.

2.4.3 TaqMan® Gene Expression Assays

This study used TaqMan® gene expression assays with predesigned and preformulated primers and probes by Applied Biosystem (Table 2.3). Most of the used primers were intron spanning primers as indicated by the "_m1" suffix (Table 2.3); therefore they could not detect genomic DNA sequences. TaqMan® Gene Expression assays contain a 20x mix of 2 unlabelled PCR primers and FAM™ dye-labelled TaqMan® MGB probes. Quantification of gene expression using TaqMan® gene expression assays is performed as the second step in a two-step reverse transcription-polymerase chain reaction (RT-PCR) protocol on any ABI PRISM® Sequence Detection System Instrument.

All TaqMan® gene expression assays were optimised to work with TaqMan® universal PCR master mix and with complementary DNA (cDNA). The real-time PCR reaction components for a single 20µl reaction 96-well plate were prepared. Briefly, TaqMan® gene expression probes and primers, TaqMan® gene expression master mix and cDNA template were mixed together in an RNase-free 1.5ml microcentrifuge tube by brief centrifugation (Table 2.4). Then, 20µl of each PCR reaction was transferred into the well of a 96-well plate (in triplicate) including no template controls (NTCs) followed by centrifugation. The plate was then loaded into the ABI PRISM® Sequence Detection System instrument. The PCR reactions were run with the universal thermal cycling parameters (Table 2.5).

ASSAY ID	REPORTER DYE	REPORTER QUENCHER	GENE NAME

Hs99999901_s1	FAM	NFQ	**18S rRNA** Human 18S rRNA
Hs99999905_m1	FAM	NFQ	**GAPDH** Glyceraldehyde-3-Phosphate Dehydrogenase
Hs00171257_m1	FAM	NFQ	**TGF-β1** Transforming growth factor beta1
Hs00559580_m1	FAM	NFQ	**CD103** Integrin, alpha E (human mucosal lymphocyte antigen 1)
Hs00203958_m1	FAM	NFQ	**FOXP3** Forkhead box P3
Hs01546494_m1	FAM	NFQ	**NRP-1** Neuropilin-1
Hs00386448_m1	FAM	NFQ	**LTBP-1** Latent TGF –β binding protein 1
Hs00962908_m1	FAM	NFQ	**TSP-1** Thrombospondin 1

Table 2.3 TaqMan® Gene Expression Assays (TaqMan® MGB probes, FAM™ dye-labeled)

PCR reaction mix component	**Volume per well (20µl reaction)**	**Final concentration**

2x TaqMan® Universal Master Mix	10µl	1x
20x TaqMan® Gene Expression Assay	1µl	1x
cDNA template diluted in RNase-free water	9µl	-
Total	20µl	-

Table 2.4 PCR reaction mix components.

Real-time PCR system	**Reaction plate**	**Reaction volume**	**Thermal cycling reaction**			
			Parameter	Polymerase activation	PCR (40 cycles)	
					Denature	Anneal/extend
			Temp.(°C)	95	95	60
ABI PRISM® 7000 system	96-well standard	20µl	Time (mm:ss)	10:00	0:15	1:00

Table 2.5 Standard parameters for TaqMan® Gene Expression Assays.

2.4.4 Real-time PCR quantification

The two general types of real-time PCR quantification strategies are termed absolute and comparative quantification. This study used the latter method to measure changes in the level of

gene expression. The relative quantification method determines the changes of target gene levels in a sample of interest compared to a control or untreated sample, and expresses this relative to the level of an endogenous control gene. Ideally, the endogenous control gene should be stably expressed at the same level in all study samples and unaffected by other parameters such as experimental conditions. A housekeeping gene encodes a protein essential for basic cellular function in all human cells and is normally selected for use as an endogenous control. Common endogenous sequences used in real-time PCR are 18s ribosomal RNA (18s rRNA), β-actin and glyceraldehydes 3-phosphate dehydrogenase (GAPDH). However, it has been reported that the expression level of these genes may vary among tissues or cell types during cell proliferation and organ development (Thellin et al., 1999). In this study, the GAPDH gene, which is the most common endogenous control gene used for analysis of renal tissue (Schmid et al., 2003) and shows the lowest variability (Cui et al., 2009), was used as an endogenous control for renal cell lines. For T lymphocytes, 18s rRNA, which has been reported as the most stable housekeeping sequence in these cells (Bas, 2004), was used as the endogenous control.

2.4.4.1 Relative quantification by the arithmetic formulas.

The relative or comparative quantification method requires the C_T (Cycle threshold) value and application of arithmetic formulas to achieve a result. The C_T is defined as the number of cycles required for the fluorescence signal to exceed the background level. Calculation of the level of expression of the target gene is based on comparison of the C_T values of activated and control cells. The C_T values of both the control and the samples of interest are first normalised to the endogenous housekeeping or reference gene. In order to obtain a valid result, the efficiency of both the target amplification and the reference amplification used in the experiment has to be greater than 90% and approximately equal. The method of PCR efficiency assessment is described in section 2.4.4. Below are the steps used to calculate the comparative C_T ($\Delta\Delta C_T$)

Step 1: To calculate the mean and standard deviation values of the replicate samples.

The mean C_T values and standard deviations are calculated by using Microsoft® Excel software.

Step 2: To calculate the ΔC_T value.

The ΔC_T is calculated as follows:

$$\mathbf{\Delta C_T = C_T\,(target) - C_T\,(reference)}$$

Step 3: To calculate the standard deviation of the ΔC_T value.

The standard deviation (SD) of the ΔC_T value is calculated from the standard deviations of the target and the reference values by using the following formula:

$$\mathbf{SD = (SD_{target}^2 + SD_{reference}^2)^{1/2}}$$

Step 4: To calculate the $\Delta\Delta C_T$ values.

The $\Delta\Delta C_T$ value is calculated as:

$$\mathbf{\Delta\Delta C_T = \Delta C_T (treated\ sample) - \Delta C_T (non\text{-}treated\ sample)}$$

Step 5: To calculate the standard deviation of $\Delta\Delta C_T$ values.

The calculation of $\Delta\Delta C_T$ involves the subtraction of the ΔC_T calibrator (non-treated) sample. This is subtraction of an arbitrary constant; thus, the SD of the $\Delta\Delta C_T$ value is similar to the SD of the ΔC_T value.

2.4.4.2 Relative quantification by REST 2009 software

In 2002, the relative expression software tool (REST) was established as a new tool for relative gene quantification (Pfaffl et al., 2002). REST compares two samples, with replicate data in the treated and non-treated groups, and calculates the relative expression ratio between them (Figure 2.9). The mathematical model is based on the mean C_T deviation between the treated and non-treated group of target genes, normalised by the mean C_T deviation of the reference gene (Pfaffl et al., 2002). Furthermore, the reaction efficiency is calculated on the basis of the dilution method (see 2.4.5). The statistical significance is tested by a Pair Wise Fixed Reallocation Randomisation Test and plotted using standard error (SE) estimation via a complex Taylor algorithm (from REST-gene quantification information).

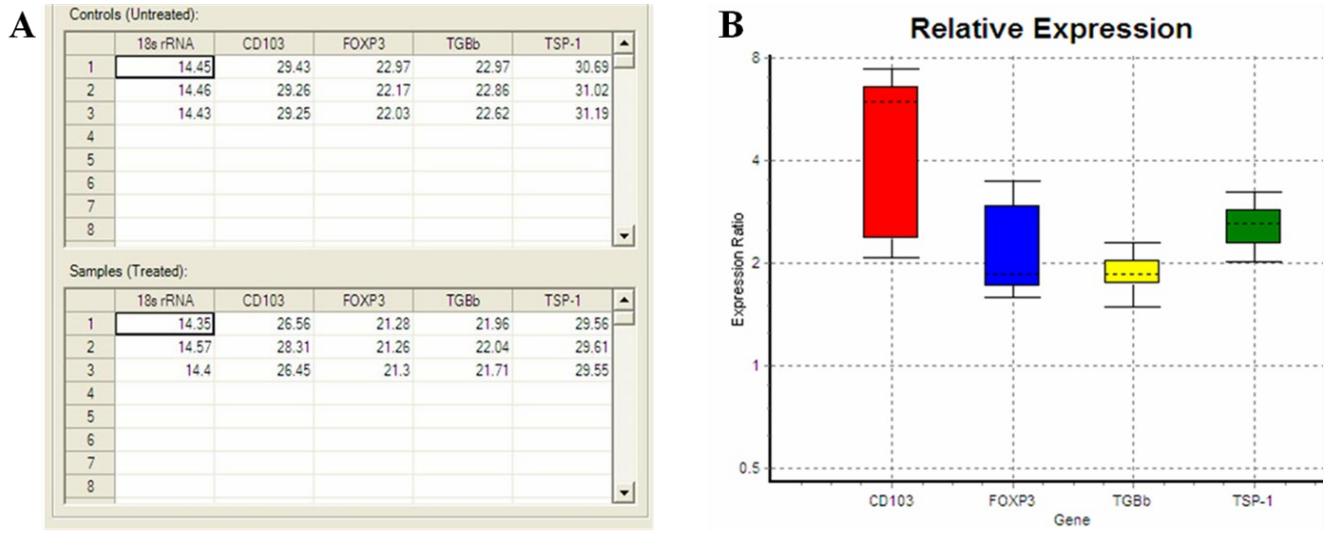

Figure 2.9 Comparative quantification of gene expression using REST software.

Panel A shows a comparison of CD103, Foxp3, TGF-β1 and TSP-1 mRNA between treated and non-treated samples in triplicate data, and was normalised to the C_T value of 18s rRNA. Panel B is a box and whisker plot showing the median change (and interquartile ranges) in relative gene expression.

2.4.5 Real-time PCR amplification efficiency

2.4.5.1 Amplification efficiency calculated using an arithmetic formula.

In order to obtain the valid $\Delta\Delta C_T$ values, the amplification efficiency must be determined and both the target and reference genes should have approximately equal values. The efficiency of PCR can be evaluated by performing a dilution series experiment. The C_T values are plotted against cDNA concentration and the slope of the plot is calculated to determine the amplification efficiency. The efficiency of the PCR should be between 90-100%, which means that the slope between the linear phases of amplification graphs should be between -3.6 and -3.1. The efficiency of the PCR reaction depends on some variables, including the quality of the primers and length of the amplicon (Wong et al., 2005). Less than 90% efficiency does not exclude valid results but an optimised system is recommended. Assays used in the present work were designed by Applied Biosystems. The efficiency of PCR reaction was determined from the equation:

$$\text{Efficiency} = 10^{(-1/\text{slope})} - 1$$

The slope -3.25 indicates that the efficiency of the real-time PCR reaction was higher than 90% (Figure 2.10).

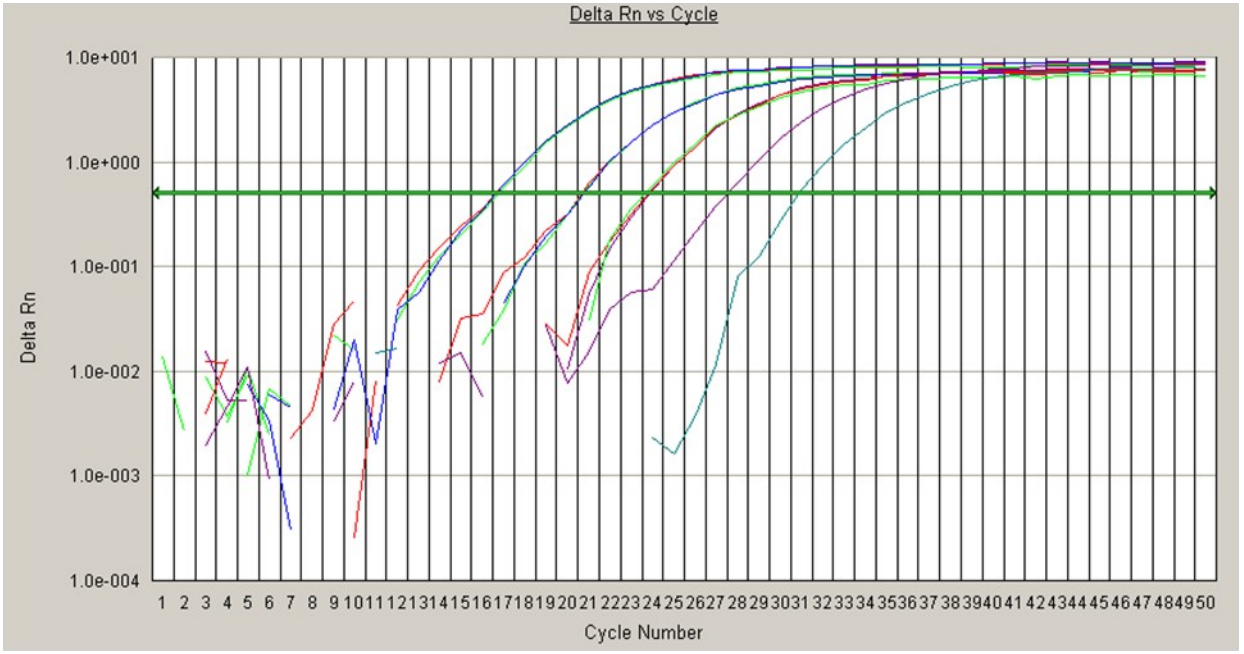

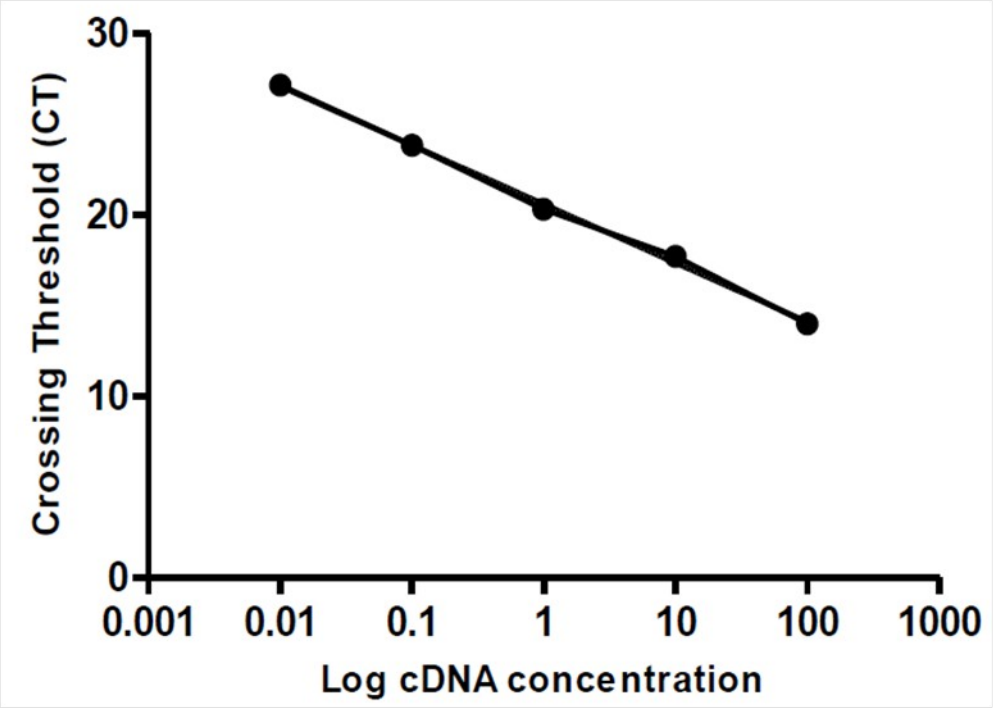

Figure 2.10 Representative amplification plots and a standard curve for real-time PCR detection of 18s rRNA in diluted samples.

The standard curve is graphically represented by a semi-log regression line plot of C_T value versus log of input nucleic acid (a slope of -3.25 indicates a PCR reaction with 100% efficiency).

2.4.5.2 Amplification efficiency calculated using REST software

PCR efficiency values are not only determined by fitting a regression line to a subset of data points in the log-linear phase, but also by applying REST software. The dilution series experiment was performed in triplicate. The mean C_T values and the standard concentration were completed, and then the software calculated the reaction efficiency which should be in a range between 0.9-1.0 (Figure 2.11).

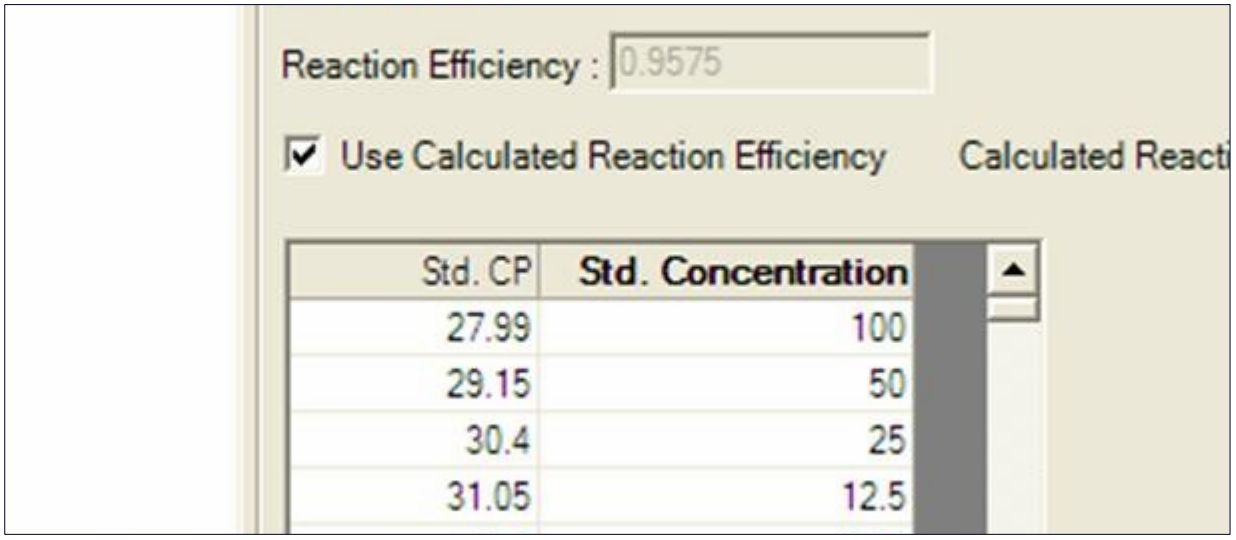

Figure 2.11 Reaction efficiency of TaqMan® Gene Expression Assay calculated using REST 2009 software.

Each standard concentration was performed in triplicate and the standard CP (crossing point, equivalent terminology for C_T) results are mean (n=3). The good value of reactive efficiency should be in range 0.9-1. This high efficiency result (0.9575) is representative of all the gene expression values assayed in this study.

2.5 Immunohistochemistry

Immunohistochemistry is a technique which demonstrates the localisation of antigens in tissue sections or cells in culture (immunocytochemistry), by the use of specific antibodies to detect individual antigens. Bound antibodies can be visualised by means of a marker such as a fluorescent dye or enzyme. This study used both immunofluorescence and immunoperoxidase

staining; the latter method was used specifically for the experiments in chapter 5 and will be described later.

2.5.1 Immunofluorescence staining

This technique was used to detect antigens on cultured cells using specific primary antibodies. The distribution of the antigens was visualised by laser scanning confocal microscopy after the addition of fluorochrome-labelled secondary antibodies.

2.5.1.1 Gelatin coating 4-chamber slides

In the initial stages of this research, there was a problem with cell attachment, in particular HKC-8 and HK-2 cells, during the washing steps involved in immunofluorescence staining experiments. In order to improve cell attachment, the chamber slides were coated with a 0.1% gelatin solution (Sigma). Gelatin is a heterogeneous mixture of water soluble proteins which contains collagen. The 0.1% gelatin solution was prepared from 2% gelatin solution (G1393, Sigma) by diluting in PBS and was sterilised in the autoclave (at 121°C for 15 minutes) before use. The 4-chamber slides for immunofluorescence staining were coated with a sterile 0.1% gelatin solution. Briefly, 0.5ml of 0.1% gelatin solution was added to each well and left at room temperature in the tissue culture hood for a minimum of 1 hour. Excess solution was removed and the slides were allowed to air dry in a sterile area for 1 hour.

2.5.1.2 Cell preparation

Cells were grown on 0.1% gelatin coated chamber slides until 80% confluence was reached. For some experiments the cells were then treated with cytokines such as TGF-β1 for 72 hours. The culture medium was removed and the cells were washed twice with PBS buffer. The cells were then fixed, as described in section 2.5.1.3.

2.5.1.3 Cell fixation

In order to ensure free access of the antibody to its antigen, cells must be fixed and permeabilized. The fixation immobilises the antigens and retains the cellular architecture. Several fixatives are commonly used, with selection dependent on the nature of the antigen being examined and on the properties of the antibody used. Fixation methods are generally divided into two classes: organic solvents and cross-linking reagents. Organic solvents such as alcohols and acetone remove lipids, dehydrate the cells and precipitate proteins within the cellular architecture. Cross-linking reagents (such as paraformaldehyde) form intermolecular bridges, normally through free amino groups, thus creating a network of linked antigens. Cross-linkers preserve cell structure better than organic solvents, but may reduce the antigenicity of some cell components, and require the addition of a permeabilization step, to allow access of the antibody

to the specimen. This study used acetone and paraformaldehyde fixation for HKC-8 and MDA231 cells respectively.

Briefly, HKC-8 cells were fixed in pre-cooled acetone at -20°C for 10 minutes. The fixed cells were allowed to air dry before washing in PBS. MDA231 cells were fixed in 4% paraformaldehyde at room temperature for 10 minutes and were then rinsed briefly with PBS before being permeabilized with 0.2% Triton X-100 in PBS for 10 minutes at 4°C.

2.5.1.4 Immunofluorescence procedure

In order to reduce non-specific binding of immunoglobulin (IgG), fixed cells were incubated in 1% bovine serum albumin (BSA, Sigma) in PBS at room temperature for 1 hour. Cells were then incubated with primary antibodies (Table 2.6) diluted in 1%BSA/PBS overnight at 4°C. Primary antibodies were mouse monoclonal anti-E-cadherin 1:50 (BD Biosciences), mouse monoclonal anti-α SMA 1:100 (Sigma), rabbit polyclonal anti-S100A4 1:100 (Dako) and rabbit polyclonal anti-pSmad 2/3 1:100 (Santa Cruz). Control sections were incubated with 1%BSA/PBS in place of primary antibodies. Slides were washed in PBS for 15 minutes with 3 changes of PBS. The cells were then incubated with secondary antibodies (Table 2.6); polyclonal rabbit anti-mouse IgG FITC-conjugated (1:100) or polyclonal goat anti-rabbit IgG FITC-conjugated (1:150) in the dark at room temperature for 1 hour. The cells were washed in PBS for 15 minutes with 3 changes of PBS. A nuclear counterstain with 4', 6- diamidino-2-phenylindole (DAPI) was applied by incubating with cells at room temperature for 2 minutes. Cells were washed again in PBS for 5 minutes. Cells were covered with anti-fade mounting medium (DAKO), overlaid with a coverslip and stored at 4°C in the dark until analysis.

2.5.2 Laser scanning confocal microscopy (LSCM)

Immunofluorescence staining was analysed by laser scanning confocal microscopy (LSCM). LSCM is a technique for obtaining high-resolution optical images with depth selectivity (Paddock, 2000). The basic concept of confocal microscopy was originally developed by Marvin Minsky from the mid-1950s until the late 1980s (Minsky, 1988); advances in computer and laser technology have now been applied to confocal microscopy (Amos et al., 2003). The basis for confocal microscopy is the elimination of out-of-focus light or flare in the specimen by spatial filtering. Briefly, a laser beam passes through a light source pinhole and is then focused by an objective lens into a small focal volume on the surface of the specimen. The returning light is focused by an objective lens into a detector pinhole. Any light that passes though the second pinhole stimulates a low noise photomultiplier. This second pinhole prevents light from above or

below the plane of focus from striking the photomultiplier (Paddock, 2000). The LSCM uses a laser for a light source; illumination and detection are confined to a single, diffraction-limited, point in the specimen. This point is focused in the specimen by an objective lens and scanned using some form of scanning device. Points of light from the specimen are detected by sensitive photomultiplier tube detectors (PMT), which are positioned behind a pinhole, and the output from the PMT is built into an image by the computer.

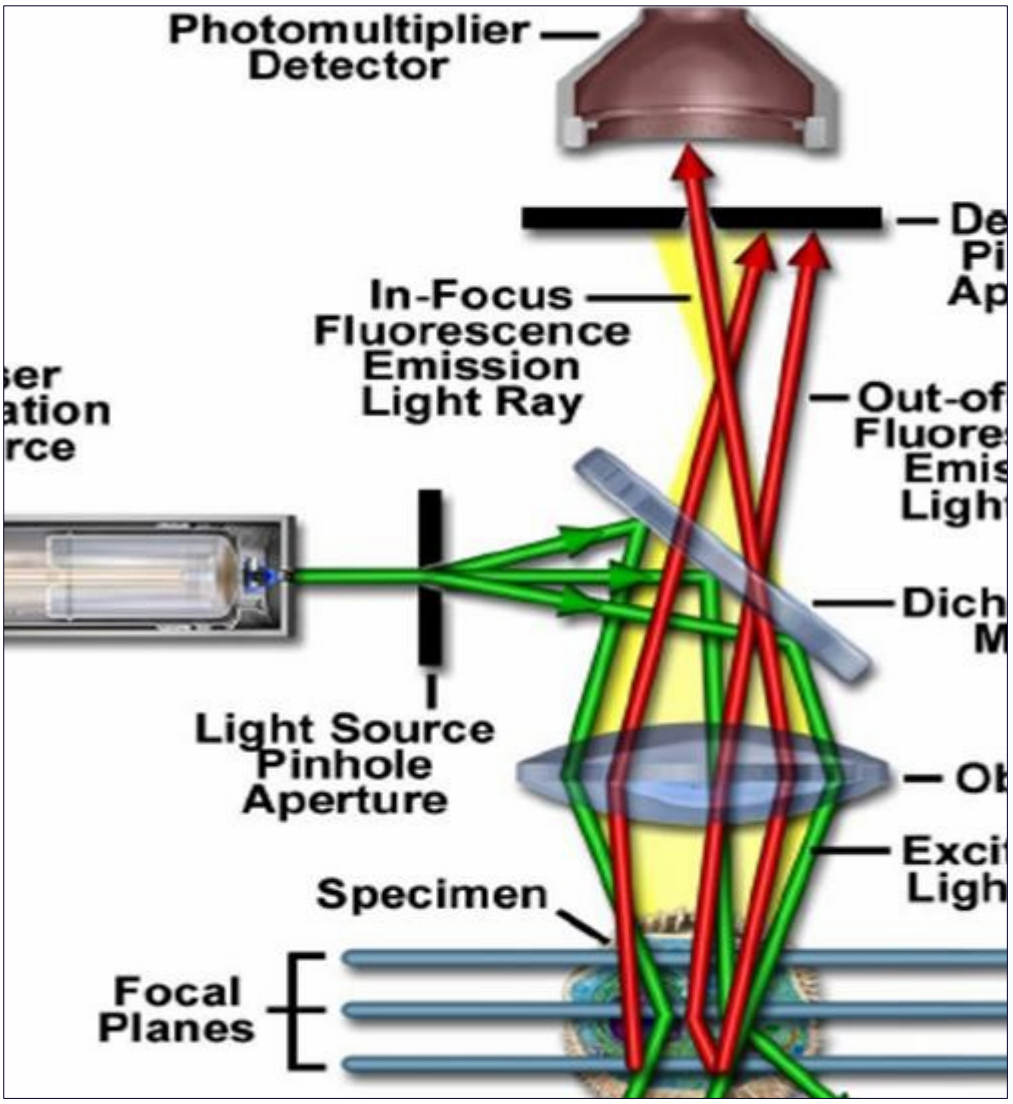

Figure 2.12 The principle of confocal microscopy.

The confocal microscope eliminates the out- of-focus light by means of a confocal "pinhole" situated in front of the photomultiplier detector which acts as a spatial filter and allows only the in-focus part of the light to be imaged. Light from above and below the plane of focus of the object is eliminated from the final image. This image is taken from Paddock, 2000**.**

This study used the confocal microscopy technique to detect antibody conjugated with fluorescent markers to show the relative distribution of epitopes of interest in cells or tissues. A control section, which showed negative staining, was obtained from cells stained only with fluorescent dye-conjugated secondary antibody (Figure 2.13). In addition, quantitative measurement of fluorescence intensity was performed using Leica software.

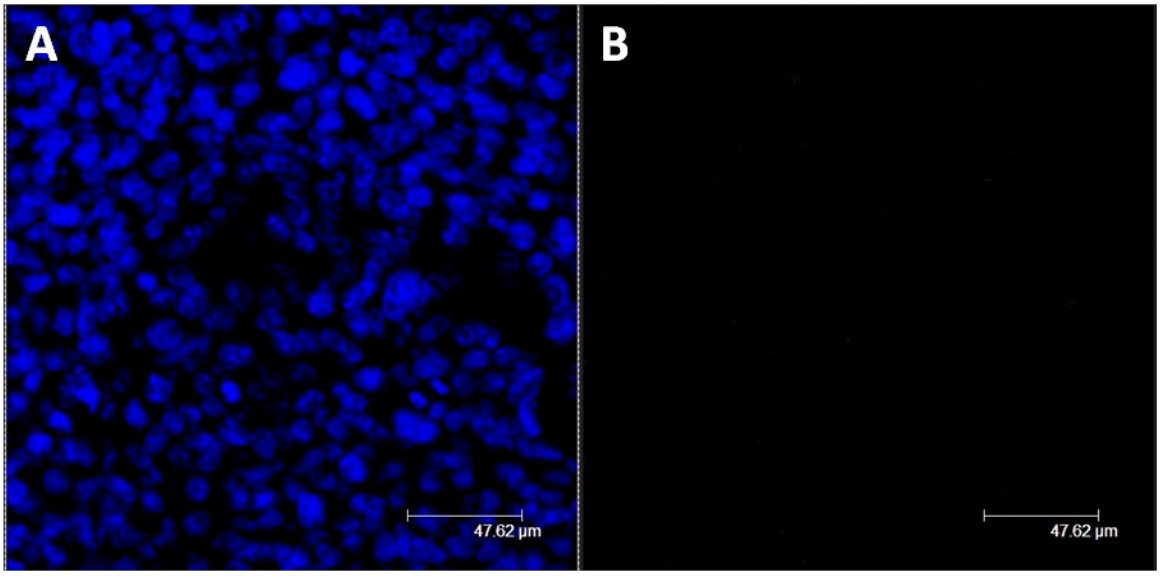

Figure 2.13 Microscopic immunofluorescence staining image of a control monolayer.
The blue nuclear label conferred by DAPI was visualized via ultraviolet laser excitation (A), while (B) was visualized for fluorescein labelling via laser excitation at 480nm. Cells were stained by FITC-conjugated secondary antibody and DAPI without primary antibody. The slides were visualized by confocal microscopy with x63 objective lens magnification.

2.5.3 Quantification of immunofluorescence intensity

To quantify the immunofluorescence intensity from the microscopic immunofluorescence image, 20 areas were randomly selected and measured for immunofluorescence intensity by Leica confocal softwate (LCS Lite version 2.6). The results were reported as mean ± SEM.

	Concentration	Company
Primary antibodies		
Mouse monoclonal anti-E-cadherin	1:50	BD Biosciences Dako
Rabbit polyclonal anti-S100A4	1:100	Sigma
Mouse monoclonal anti-α SMA	1:100	Abcam
Rabbit monoclonal anti-neuropilin-1	1:100	Dako
Mouse monoclonal anti-CD3	1:50	Santa Cruz
Mouse polyclonal anti-pSmad 2/3	1:100	
Secondary antibodies		
Polyclonal rabbit anti-mouse immunoglobulin (FITC conjugated)	1:100	Dako
Polyclonal goat anti-rabbit immunoglobulin (FITC conjugated)	1:150	Sigma

Table 2.6 Primary and secondary antibodies used for microscopic immunofluorescence staining.

2.6 Western Blotting

Western blotting or protein immunoblotting is a technique used to detect specific proteins in tissue or cell preparations. Polyacrylamide gel electrophoresis is used first to separate native or denatured proteins, and then the proteins are transferred to a hydrophobic polyvinylidene difluoride (PDVF) (GE Health Life Sciences) membrane where they are detected using antibodies specific for the target protein.

2.6.1 Preparation of protein lysates from cultured cells

A lysis buffer containing detergent, salt, buffer, protease inhibitor and phosphatase inhibitor is generally required to lyse cells, solubilise protein and prevent protein and phosphoprotein degradation. In addition to lysis, cells can be broken down mechanically by sonication. To prepare lysates, confluent cells from 25cm^2 tissue culture flasks were washed twice in cold PBS and tharvested with a cell scraper. The cells were then resuspended in 50-

100µl of lysis buffer which contained CelLytic M (Sigma), Protease Inhibitor Cocktail (Roche) and Halt Phosphatase Inhibitor Cocktail (Pierce). The lysate was vortexed every 10 minutes for a total of 30 minutes on ice. The lysate was then sonicated at amplitude 10 (MSE Soniprep 150, SANYO) for 30 seconds on ice. The lysate was then centrifuged at 16000 x g at 4°C for 20 minutes. The clear supernatant was transferred to a new tube and the protein lysate was stored at -80°C.

2.6.2 Protein quantification

Protein concentration was measured using the Pierce BCA protein assay kit (Thermo Scientific). The Pierce BCA Protein Assay is a detergent-compatible formulation based on bicinchoninic acid (BCA) for the colorimetric detection and quantitation of total protein. This method combines the reduction of Cu^{+2} to Cu^{+1} by protein in an alkaline medium (the biuret reaction) with a highly sensitive and selective colorimetric detection of the cuprous cation (Cu^{+1}) by bicinchoninic acid. The protein quantification was performed according to the instructions for the Pierce BCA protein assay kit. Briefly, 200µl of BCA working solution was loaded into the well of a flat 96-well plate and 25µl of standard or unknown proteins were added into each well in triplicate. The mixture was incubated at 37°C for 30 minutes. The protein concentration was measured with a microplate reader at a wavelength of 562nm (Figure 2.15). A standard curve of protein concentrations against absorbance was plotted using known concentrations of bovine serum albumin (Sigma).

Figure 2.14 Pierce BCA protein assay procedure.

200µl of BCA working reaction was loaded into 96-well plate and then 25µl of standard or unknown proteins were added to each well. The mixture was incubated at 37°C for 30 minutes.

The protein concentration was measured using a microplate reader at 562nm. (This image is taken from the Pierce BCA protein assay kit instructions)

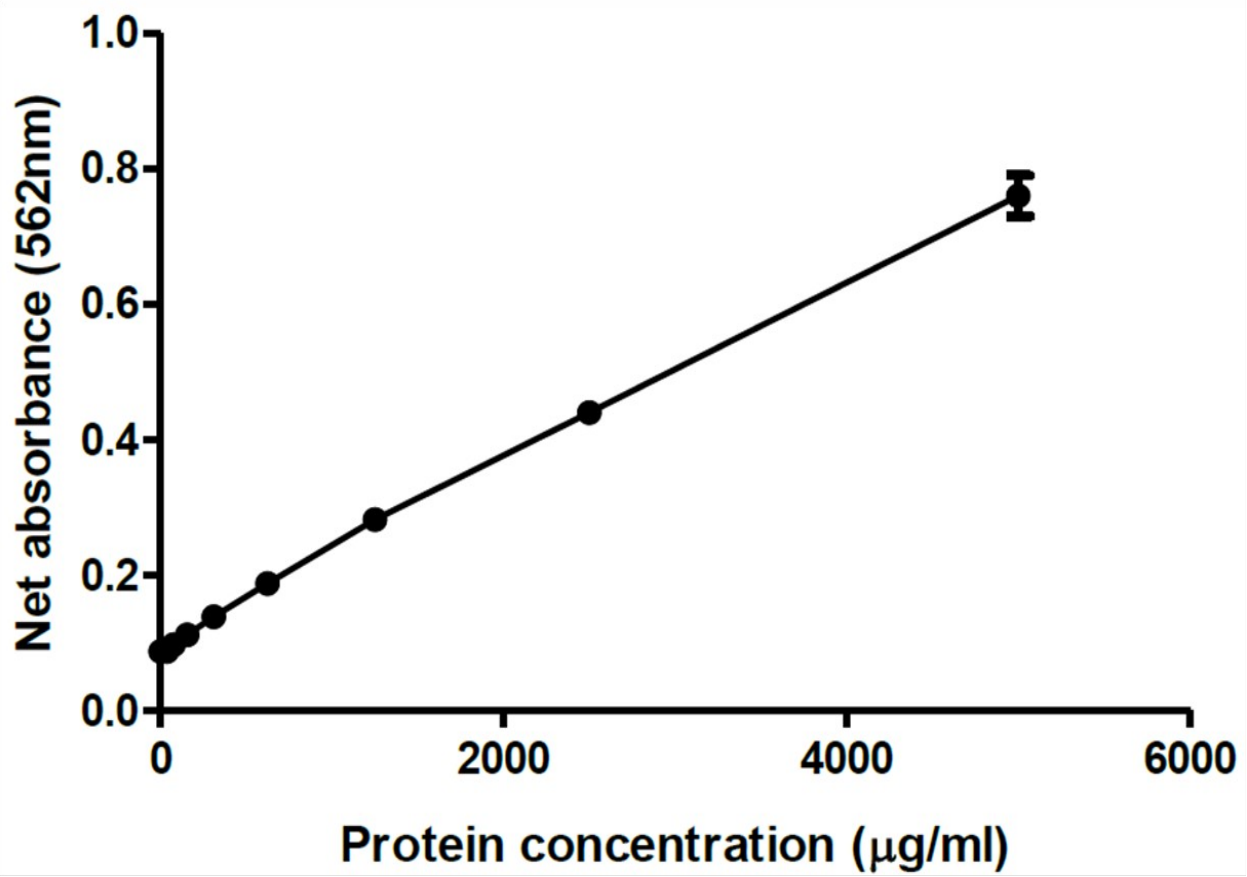

Figure 2.15 Standard protein dose response curve generated using the Pierce BCA assay.

2.6.3 Separation of proteins by sodium dodecyl sulphate-polyacrylamide gel electrophoresis (SDS-PAGE).

Antibodies used for western blotting typically recognise epitopes within denatured proteins. In order to denature protein, the anionic detergent sodium dodecyl sulfate (SDS) is added to the loading buffer, and the mixture boiled at 95°C for 5 minutes. After the denaturing process, SDS-PAGE maintains the denatured state of polypeptides and allows the separation of proteins by their molecular weight. In the presence of SDS, proteins become negatively charged and move towards a positively charged electrode through the polyacrylamide mesh of the gel. Proteins move differently through the gel matrix depending on their size: the smaller the protein the more rapid the movement. Gels containing a low percentage of acrylamide are used to separate larger proteins, whereas small proteins separate better in high percentage gels. The proteins in this study were separated by SDS-PAGE using the Hoefer Mighty Small™ gel

apparatus (GE Healthcare). Gels for SDS-PAGE were made from 10% resolving or separating gels and 5% stacking gels (Table 2.7). Protein samples were treated with an equal volume of sample loading dye (Table 2.8) heated to 95°C for 5 minutes and briefly spun prior to loading onto the gel. Prestained protein molecular weight markers (Fermentas) were used in one lane to determine the molecular weight of the proteins. SDS-PAGE was performed in 1x running buffer (Table 2.8), with protein migration driven at 100V through the stacking gel and then at 150V through the resolving gel.

2.6.4 Coomassie Blue staining of polyacrylamide gels

It is possible to visualise protein bands within SDS-PAGE gels by coomassie blue staining. Briefly, gels were stained for 1 hour with a solution containing 30% methanol, 10% acetic acid and 0.1% coomassie-brilliant-blue R250 (Sigma). The gels were then destained with 30% methanol and 10% acetic acid for a further 2 hours, or for longer if required.

2.6.5 Western blotting

Following separation by SDS-PAGE, the proteins were transferred from the gel onto a PVDF membrane (Hybond-P, GE Health Science) by wet transfer. Prior to the transfer, the membrane was pre-soaked in methanol for 10 seconds, rinsed in water and equilibrated in 1×transfer buffer. The gel and the aligned PVDF membrane were sandwiched between pre-soaked sponges and pre-soaked filter papers in a blotting tank (Hoefer TE series, Pharmacia) and protein transfer was carried out at 4˚C at 100V overnight. After transfer, the PVDF membrane was blocked in 5% dried skimmed milk (Marvel) in Tween-Tris buffer solution (TTBS) (pH7.6) for total protein or 5%BSA/TTBS (for phosphoprotein) for 1 hour at room temperature and incubated overnight with primary antibodies in 5% milk/TTBS or 5% BSA/TTBS rocking at 4°C. Primary antibodies and their working dilutions are indicated in the appropriate results chapter. To remove unbound antibodies, blots were washed 3 times in TTBS for 5 minutes each. Appropriate HRP (Horseradish peroxidise)-conjugated secondary antibodies were then applied in 5% milk/TTBS or 5%BSA/TTBS for 1 hour at room temperature, followed by 3 washes in TTBS. The ECL-Plus reagent (GE Healthcare) was used for signal development according to the manufacturer's instructions. Signals were captured on x-ray film (Fuji, NIF RX-100).

Reagent	5% Stacking gel (ml)	10% Resolving gel (ml)
Deionised water	5.5	7.90
1.5M Tris-base, pH 8.8	-	5.00
1M Tris-HCl, pH 6.8	1.00	-
10% SDS	0.08	0.20
30% Acrylamide (29:1 Acrylamide:Bisacrylamide)	1.30	6.70
10% Ammonium Persulphate	0.08	0.20
TEMED	0.008	0.008
Total	8ml	20ml

Table 2.7 Components of the resolving and separating gels

Buffer recipes	
6x Loading buffer	
Tris HCl, pH 6.8	300 mM
SDS	12%
Bromophenol blue	0.6%
Glycerol	60%
Dithiothreitol (DTT)	600 mM
5x Running Buffer	
Tris base	15.1g
10% SDS	50ml
Glycine	94g
Water	1000ml
10x Transfer Buffer	
Tris base	30.3g
Glycine	144g
Water	1000ml
1x TTBS	
Tris base	2.42g
NaCl	8.4g
Tween 20	1ml

Water	1000ml

Table 2.8 Composition of Western blot buffer solutions.

2.7 Bioactive TGF-β measurement

TGF-β is secreted as a latent pro-peptide complex, which requires activation to expose or release bioactive TGF-β peptides (section 1.4.6). Several methods have been developed to detect bioactive TGF-β, such as enzyme-linked immunosorbent assay (ELISA), radioimmunoassay and the use of reporter cells (Abe, 1994).

One of the most popular TGF-β bioassays is based on an ability to induce expression of plasminogen activator inhibitor-1 (PAI-1). Mink lung epithelial cells were transfected with a truncated PAI-1 promoter fused to the firefly luciferase reporter gene (Abe et al., 1994). However, the disadvantage of this assay is that these cells can be induced by other growth factors (Abe et al., 1994; Van Waarde et al., 1997). Recently, a highly sensitive and specific bioassay has been described (Tesseur et al., 2006). This TGF-β bioassay uses a specific cell line called MFB-F11, which is a fibroblast cell line isolated from TGF-$\beta^{-/-}$ mouse embryos which has been stably transfected with a construct consisting of a synthetic promoter element containing twelve Smad responsive CAGA boxes, and a TGF-β-inducible DNA sequence, linked to a secreted alkaline phosphatase (SEAP) reporter gene (Figure 2.16). This assay has been shown to be specific for TGF-β1, TGF-β2 and TGF-β3 but not for other related TGF-β family members. In addition, MFB-F11 cells detect bioactive TGF-β in biological samples and in cell co-culture systems, but do not respond to latent TGF-β. The MFB-F11 cell line was kindly provided for this study by Dr Ina Tesseur (Stanford University, USA). This study used MFB-F11 to detect active TGF-β present in cell culture supernatants of renal epithelial cells and T cells unless otherwise indicated.

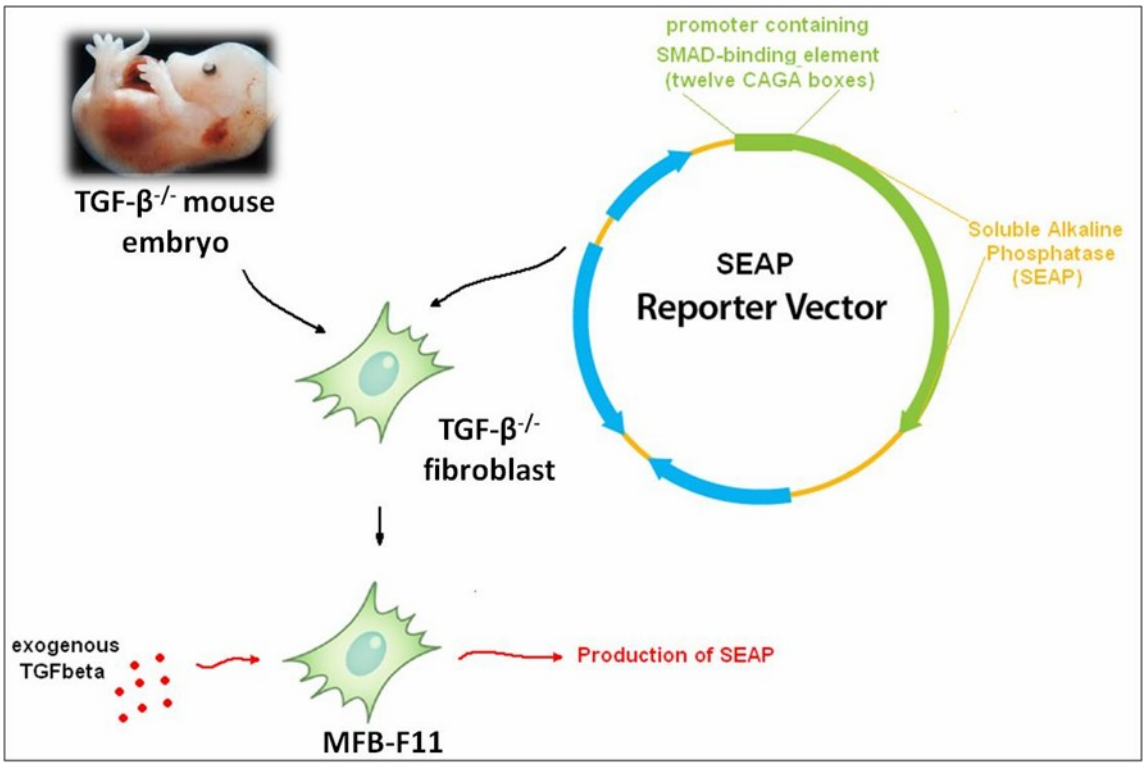

Figure 2.16 Scheme showing the establishment of the MFB-F11 cell line.

An embryonic fibroblast cell line obtained from TGF-$\beta^{-/-}$ mice (MFB-F11) was transfected with a construct consisting of a promoter containing SMAD binding elements linked to a secreted alkaline phosphatase reporter gene (SEAP). After stimulation with exogenous TGF- β, MFB-F11 cells produce SEAP which can be further quantified following reaction with pNPP or Phospha-Light™ (section 5.3).

2.7.1 TGF-β bioassay protocol

The TGF-β bioassay procedure was adapted from an original publication (Tesseur et al., 2006). This study used 2 different substrates for alkaline phosphatase detection: P- Nitrophenyl Phosphate (pNPP, Sigma) and Phospha-Light™ (Applied Biosystem). Details of the Phophs-Light™ assay will be described in section 5.3. pNPP is the most common substrate used in alkaline phosphatase-based enzyme immunoassays, allowing colour changes to be easily quantified using a spectrophotometer.

Briefly, $4x10^4$ MFB-F11 cells were seeded in 96-well, flat bottom plates using cell culture conditions optimal for the MFB-F11 cell line (section 2.2.7). Following overnight culture, the cells were washed twice with PBS and incubated in 50µl serum-free RPMI for 4 hours at 37°C. Following this incubation, serial dilutions of human recombinant TGF-β (0-

1000pg/ml) or test samples were added to the MFB-F11 cells in a total volume of 100µl. To test the putative presence of the latent form of TGF-β, heat activation of some samples was performed by heating to 80°C for 5 minutes (Zamora et al., 2007). The MFB-F11 cells were incubated with test samples and a standard serial dilution of TGF-β for 48 hours. After 48 hours, 100µl of supernatant was transferred to a new plate for 10 minutes at 65°C for heat inactivation of endogenous alkaline phosphatase activity. The samples were then mixed with four times concentrated pNPP solution prepared according to the manufacturer's instructions. The reaction was incubated at 37°C for various periods and absorbance at 405nm was analysed. A standard curve was established in each assay using known concentrations of TGF-β from 0- 1000pg/ml (Figure 2.17).

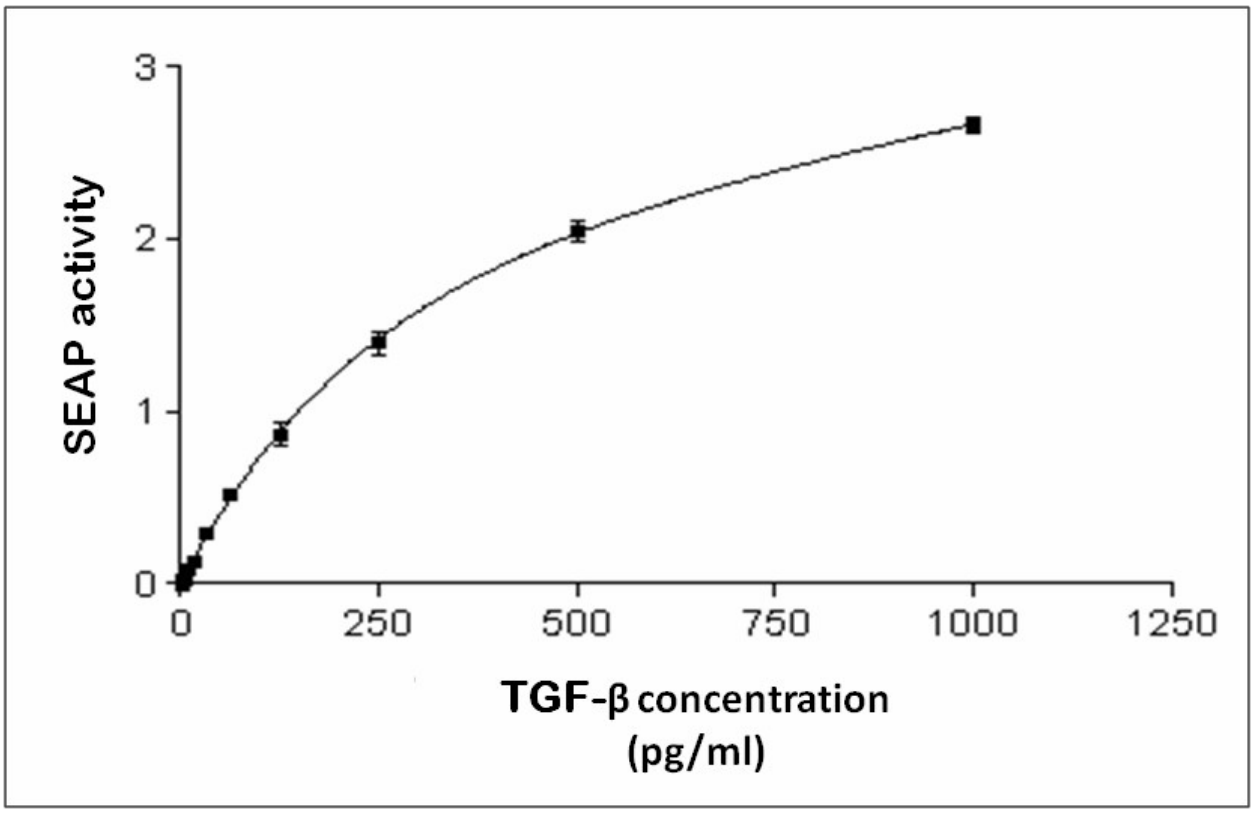

Figure 2.17 Standard curve of TGF-β concentration using the MFB-F11 bioassay.

MFB-F11 cells were incubated with TGF-β for the period of 48 hours. Following heat-inactivation, cell culture supernatants were mixed with pNPP substrate. The reaction was read at 405nm after 24 hour incubation. The results show the mean and the error bars are SEM (n=3). This graph is a representative of 3 separate experiments.

2.7.2 Efficacy of a TGF-β receptor type I inhibitor assessed using the MFB-F11 bioassay

As described in section 1.4.6, signalling by the TGF-β family is mediated by type I and type II transmembrane TGF-β receptors. Ligand interaction with a homodimer of type II receptors recruits and activates the homodimeric type I receptor (activin receptor-like kinase; ALK). The unique combination of type I and type II receptors confers the specificity of ligand signalling (Piek et al., 2001). For example, TGF-βs preferentially activate ALK-5. To inhibit signalling, an ALK-5 inhibitor was applied in some experiments in order to determine the potential role of TGF-β signalling.

SB-505124 is a small molecule inhibitor which was developed as a competitive inhibitor of the ATP binding site of ALK-5 (DaCosta et al., 2004). According to a previous study, SB-505124 selectively inhibits ALK-4 and ALK-5 which respond to activin and the TGF-βs respectively; these receptors do not respond to the BMPs (DaCosta et al., 2004).

The MFB-F11 bioassay was used to test efficacy and optimise the concentration of SB-505124. Briefly, $4x10^4$ MFB-F11 cells were seeded in 96-well flat bottom plate. After overnight culture, semi-confluent cells were pre-treated with SB-505124 (0-5μM) for 1 hour. Following this pre-treatment, 0.5ng/ml of TGF-β was added to each well and incubated for 48 hours. The supernatant was collected and processed as described in section 2.7.2. From this experiment, it is clear that a concentration of 0.5-1.0μM of the AKL-5 inhibitor inhibits TGF-β signalling to baseline levels (Figure 2.12); this concentration is consistent with published results (DaCosta et al., 2004).

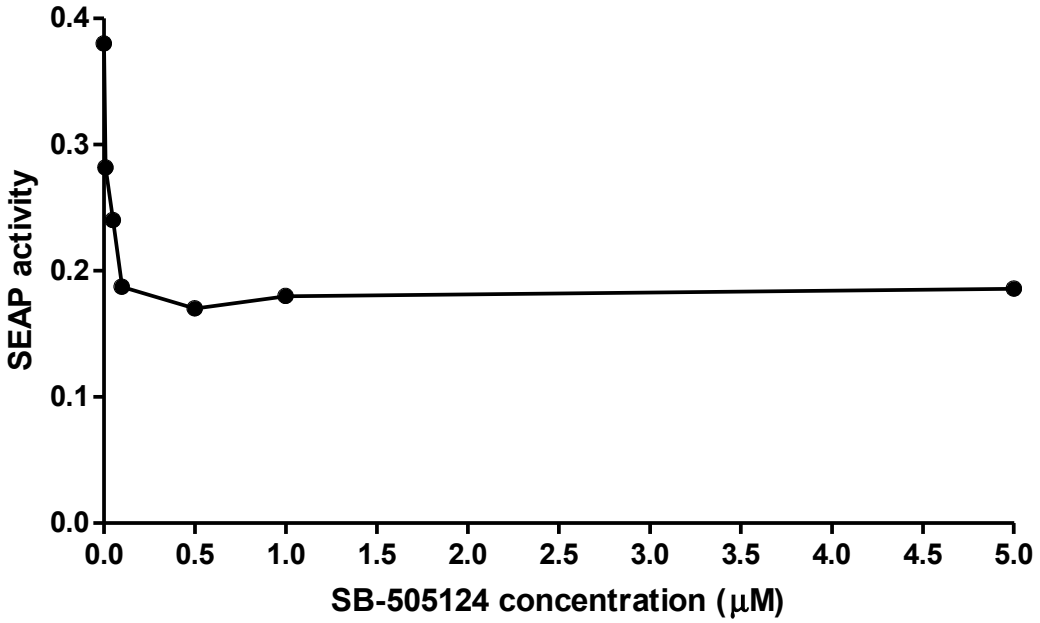

Figure 2.18 TGF-β bioassay analysis to optimize use of the ALK-5 inhibitor

Confluent MFB-11 cells were incubated with a concentration range of ALK-5 inhibitor (0-5μM) in the presence of TGF-β1 at a fixed concentration of 0.5ng/ml for 48 hours. The response to TGF-β1 was evaluated by measuring SEAP activity at 405nm after incubation with pNPP. The plot shows mean values (N=3) and the error bars are SEM. These results are from a single experiment.

2.8 Immunofluorescence Flow cytometry

Immunofluorescence flow cytometry is a powerful technique for the measurement of a range of parameters for single cells within a suspension. The flow cytometer uses laminar flow and hydrodynamic focusing to generate a fluid stream containing cells, which are constrained within a limited cross sectional area as they pass through one or more beams of monochromatic (typically laser) light. Some of this light is unaltered in wavelength but either reflected or scattered by the cells and measured using photomultipliers. The reflected or forward scatter (FSC) signal is proportional to the area or size of the cells, whilst the side scatter (SSC) provides a measure of cytoplasmic granularity. Depending on the instrument used, further light can be absorbed, re-emitted and detected at a different wavelength by a range of fluorochromes, which can be attached to individual cells either chemically or immunochemically. These fluorescence signals provide a measure of the amount of each fluorochrome associated with individual cells.

The flow cytometers used in this project used excitation wavelengths of 488 and 635nm and were able to collect fluorescence signals emitted by the following fluorochromes: FITC (519nm), PE (phycoerythrin) (576nm), PI (617nm) and APC (allophycocyanin) (660nm) (Table 2.9).

Fluorochrome	Laser	Laser Excitation (nm)	Florescence channel	Excitation peak (nm)	Emission peak (nm)
Fluorescein (FITC)	Argon	488	FL-1 Green	495	519
Phycoerythrin (PE)	Argon	488	FL-2 Yellow	566	576
Propidium Iodide (PI)	Argon	488	FL-3 Orange	351	617
Allophycocyanin (APC)	Red Diode	635	FL-4 Red	650	660

Table 2.9 Fluorochrome absorption and emission spectra for the BD FACSCalibur™.

2.8.1 Immunofluorescence staining for flow cytometry

Flow cytometry was performed using a BD FACSCalibur™ with twin laser and four colour detection (BD Biosciences). Cells were labelled with fluorochrome-conjugated antibodies and prepared as single cells in suspension (details of labelling intracellular antigens appear in section 5.3). Briefly, adherent cells were harvested by incubating with pre-warmed non-enzymic dissociation solution (Invitrogen) for 5-10 minutes. These cells were then washed in 2%FBS/PBS twice and resuspended in 2%FBS/PBS at a concentration of $1x10^6$ cells/ml. 100µl of cells were incubated with fluorochrome-conjugated antibodies (Table 2.9) at an appropriate concentration (Table 2.10) for 30 minutes on ice. Following this incubation, the cells were washed twice in 2%FBS/PBS by centrifugation at 500xg for 5 minutes. If a secondary antibody was required, it was incubated with cells at 4°C in the dark for 1 hour and the washing step was repeated. Then, the cell pellet was resuspended in 400µl of 2%BSA/PBS.

For control samples, cells were incubated with isotype control antibodies at an appropriate concentration.

Antibodies	Concentration	Company
Primary antibodies		
Mouse monoclonal anti-neuropilin-1 APC-conjugates	1:10	Miltenyi Bioec
Mouse monoclonal anti-CD103 FITC-conjugated	1:10	EuroBiosciences
Mouse monoclonal anti-LAP (TGF-β1) PE-conjugated	1:10	R&D System
Mouse monoclonal anti-TSP-1 Biotin-conjugated (A6.1)	1:10	Abcam
Isotype control		
Mouse IgG1 isotype control APC-conjugated	1:10	Miltenyi Biotec
Mouse IgG2A isotype control FITC-conjugated	1:10	Ebioscience
Mouse IgG1 isotype control PE-conjugated	1:10	Ebioscience
Mouse IgG1 isotype control biotin-conjugated	1:10	R&D System
Secondary antibody		
Streptavidin FITC-conjugated	1:50	Ebioscience

Table 2.10 Details of the isotype control antibodies, primary antibodies and secondary antibodies used in flow cytometry experiments.

2.8.2 Flow cytometric analysis

This study analysed FCM data using WinMDI (Window Multiple Document Interface) version 2.9, which was produced by Joe Trotter of the Scripps Research Institute. Cells are commonly analysed for five parameters including forward scatter (FSC), side scatter (SCC), FITC, PE and APC fluorescence (Figure 2.19).

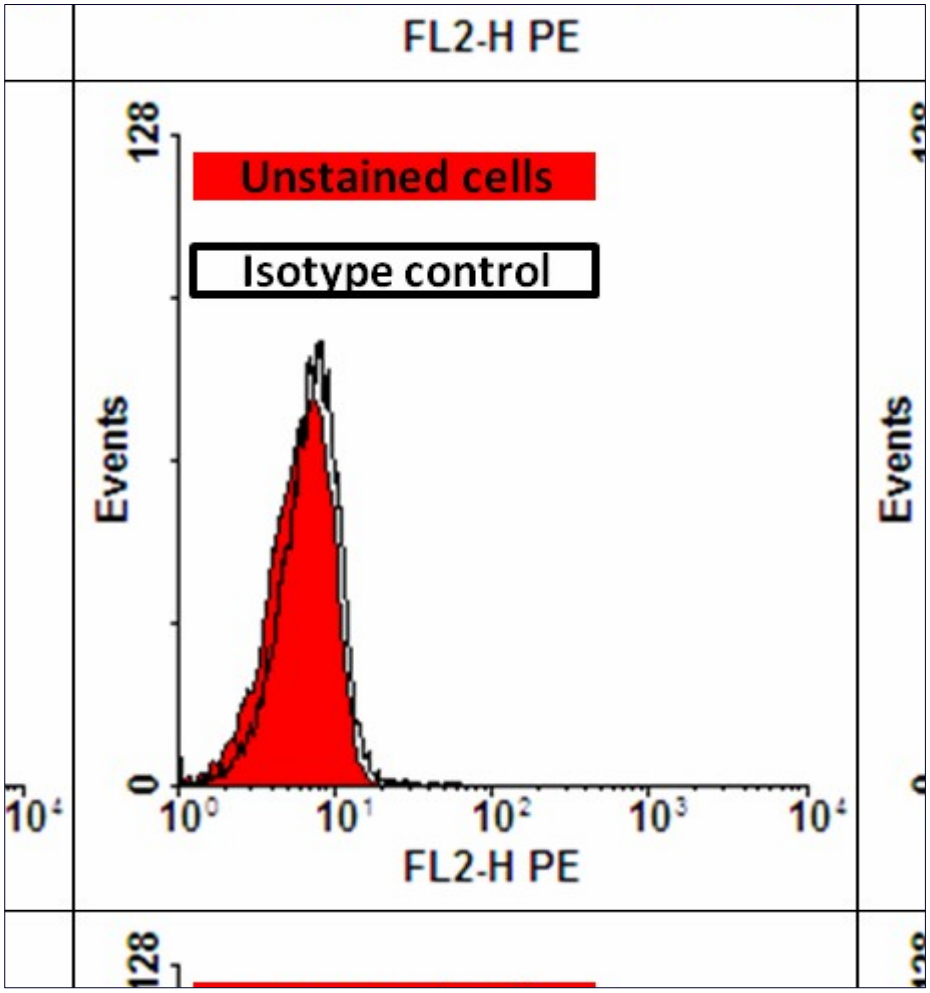

Figure 2.19 Histogram analysis of flow cytometry by WinMDI 2.9 software.
Cells were processed for immunofluorescence staining as describe above. This image shows the histogram of unstained cells (red) overlayed with an isotype control-stained sample. This is a representative control sample for all flow cytometry experiments.

2.8.3 Flow cytometric analysis of cell death using Propidium Iodide (PI)

PI is an agent which can penetrate dead cells followed by alteration of its fluorescence characteristics after intercalation into genomic DNA. Following this intercalation, PI can be excited using the argon laser with fluorescence detected in channels FL2 or FL3.

Briefly, cells were harvested as described in 2.9.1. After the last washing step, the cell pellet was resuspended in a PBS buffer containing PI at a concentration of 1µg/ml. This suspension was immediately analysed by flow cytometry.

2.9 Statistical Analysis

Before choosing a statistical test to analyse experimental results, the nature of the data must first be considered. Parametric data conform to a normal or Gaussian distribution, whilst non-parametric data do not. Whilst it is difficult formally to demonstrate the normality of small sample sizes, most biological processes do conform to this distribution. However, non-parametric tests must be used for obviously skewed data, perhaps containing off-scale values. The statistical tests used to analyse data in this study have been divided into 3 groups.

2.9.1 Description of the scatter of individual data samples

Most of the results in this study were judged parametric and were described as mean ± standard error of the mean (SEM).

2.9.2 Comparison between two samples

2.9.2.1 Parametric distribution

- The unpaired Student's *t* test was used to compare the mean of two unmatched groups of data.
- The paired Student's *t* test was used to compare two matched groups of data containing paired samples handled in parallel. For example, values collected with and without cytokine stimulation of T cells isolated from individual blood donors are treated as paired data.

2.9.2.2 Nonparametric distribution

- Mann-Whitney test. This is the nonparametric equivalent to the unpaired Student's *t* test.
- Wilcoxon test. This is the nonparametric equivalent to a paired Student's *t* test.

2.9.3 Comparison between three or more groups of experimental data.

One-way analysis of variance or ANOVA was used to determine the significance of differences between multiple groups of data. The significance of differences between individual sets of data was examined by application of an appropriate post-test.

2.9.4 P value

All statistical analysis was performed using GraphPad Prism version 5 (GraphPad Software, San Diego, USA) with the threshold probability (P) value (alpha) set at 0.05. With a P value of less than 0.05 there is less than a 5% chance of observing between identical groups a

difference as large as was actually measured. At this level, differences between groups were considered significant.

2.9.5 Statistical Power

The statistical power shows the probability of which the test will reject null hypothesis when the null hypothesis is false. This study calculated the statistical power by using a calculator from DSS research web site.

(http://www.dssresearch.com/KnowledgeCenter/toolkitcalculators/statisticalpowercalculators.aspx)

Chapter 3: A Potential Role of EMT in Cyclosporine-induced Renal Allograft Fibrosis

3.1 Introduction

The suppression of allograft rejection is a goal of organ transplantation. Thus, the development of efficient immunosuppressive drugs is the key for maintaining successful allograft function. Since the introduction of calcineurin inhibitors (CNI), short-term renal allograft survival has improved, though long-term renal allograft survival remains a major problem. CNI, which act by inhibiting calcineurin function, consists of two main drugs, Cyclosporine and Tacrolimus. This study focuses on Cyclosporine because it has been widely used and is associated with more complications.

Cyclosporine and Tacrolimus differ in molecular structure and intracellular binding receptors. Cyclosporine ($C_{62}H_{111}N_{11}O_{12}$,) is a hydrophobic, cyclic undecapeptide, with a molecular weight of 1202.64 Daltons. It was first discovered during a screening programme for new antibiotics and isolated from the soil fungus, *Tolypocladium inflatum Gams*. Its immunosuppressive activity was discovered later by J.F. Borel in 1976 (Borel and Baumann, 1994; Stähelin, 1996) and it was subsequently approved for clinical use to prevent rejection in organ transplantation in 1983 (Kapturczak et al., 2004). Tacrolimus was discovered in 1984 from the fermentation broth of a Japanese soil sample containing the bacterium *Streptomyces tsukubaensis* (Kino et al., 1987). Since its introduction in clinical practice, Cyclosporine has had a significant impact on immune modulation therapy in transplant medicine, autoimmune diseases and inflammatory disorders. Currently, both Cyclosporine and Tacrolimus are important in the prevention of allograft rejection. In addition, approximately 90% of patients have been discharged post transplantation on a CNI-based immunosuppressive regimen (Andreoni et al., 2007).

3.2 Mechanism of action of Cyclosporine

During an immune response, activation of the T cell receptor (TCR) results in an increase of intracellular free calcium ion which then triggers the activation of calcinuerin, a calcium-dependent serine/threonine phosphatase enzyme. In the physiological state, activated calcineurin dephosphorylates the cytoplasmic component of the nuclear factor of activated T cells (NFATc). After this dephosphorylation, NFATc translocates from cytoplasm to the nucleus, where it associates with the nuclear NFAT (NFATn) causing activation of the

transcription of genes coding for IL-2 and related cytokines (Gaffen and Liu, 2004). These cytokines, in particular IL-2, play an important role in the proliferation and differentiation of effector T cells which destroy the donor graft.

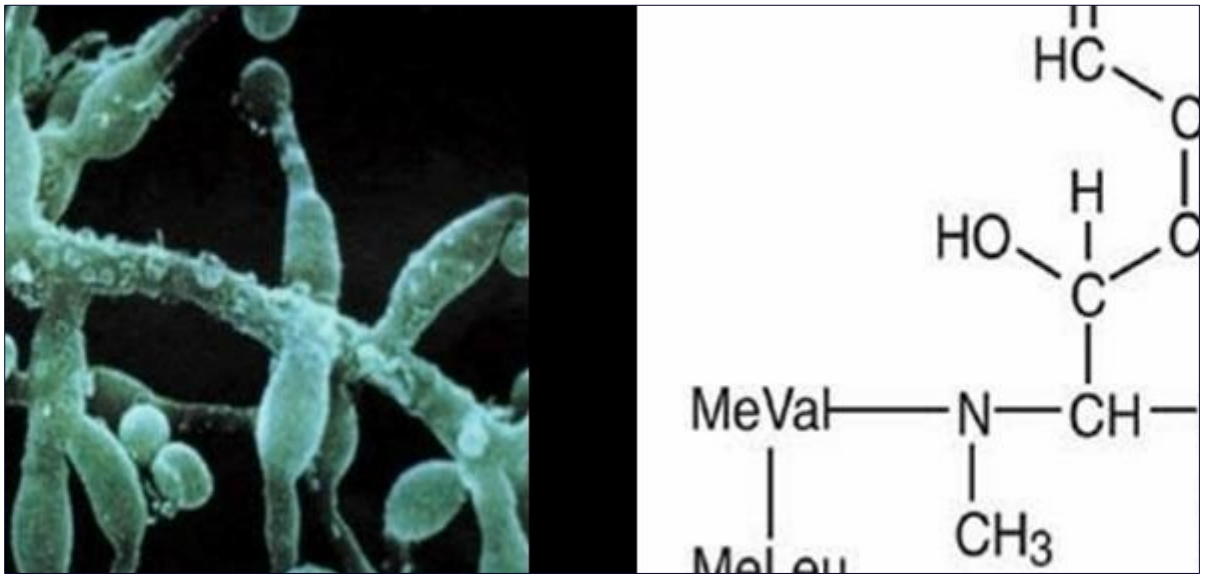

Figure 3.1 Scanning electron microscopy image of *Tolypocladium inflatum Gams* (A) and the structure of cyclic polypeptide Cyclosporine (B). These images are from Petcher et al. 1976.

Following administration, Cyclosporine enters through the cell membrane and binds to its receptor, cyclophilin, in the cytoplasm. Tacrolimus forms a complex with its cytosol receptor FKBP-12. Both cyclophilin and FKBP-12 are immunophilins, a highly conserved family of proteins which have peptidyl-prolyl cis-trans isomerase (PPIase) activity (Fisher et al., 1989; Wang and Heitman, 2005). Cyclophilin and FKBP-12 are present abundantly in most cells in the human body (Ryffel, 1993) and have high affinity for calcineurin. Blocking calcineurin by Cyclosporine-cyclophilin and Tacrolimus-FKBP-12 complexes leads to inhibition of NFATc dephosphorylation. As a result, the migration of NFATc to the nucleus is inhibited and the association of NFATc with NFATn cannot occur (Figure 3.2). Consequently, IL-2 production is inhibited, which is essential for activation and proliferation of lymphocytes (Ho et al., 1996). Inhibition of the calcineurin-NFAT pathway by Cyclosporine and Tacrolimus is not specific to immune cells but can also lead to toxic changes in other organs, including nephrotoxicity (Liu et al., 2007).

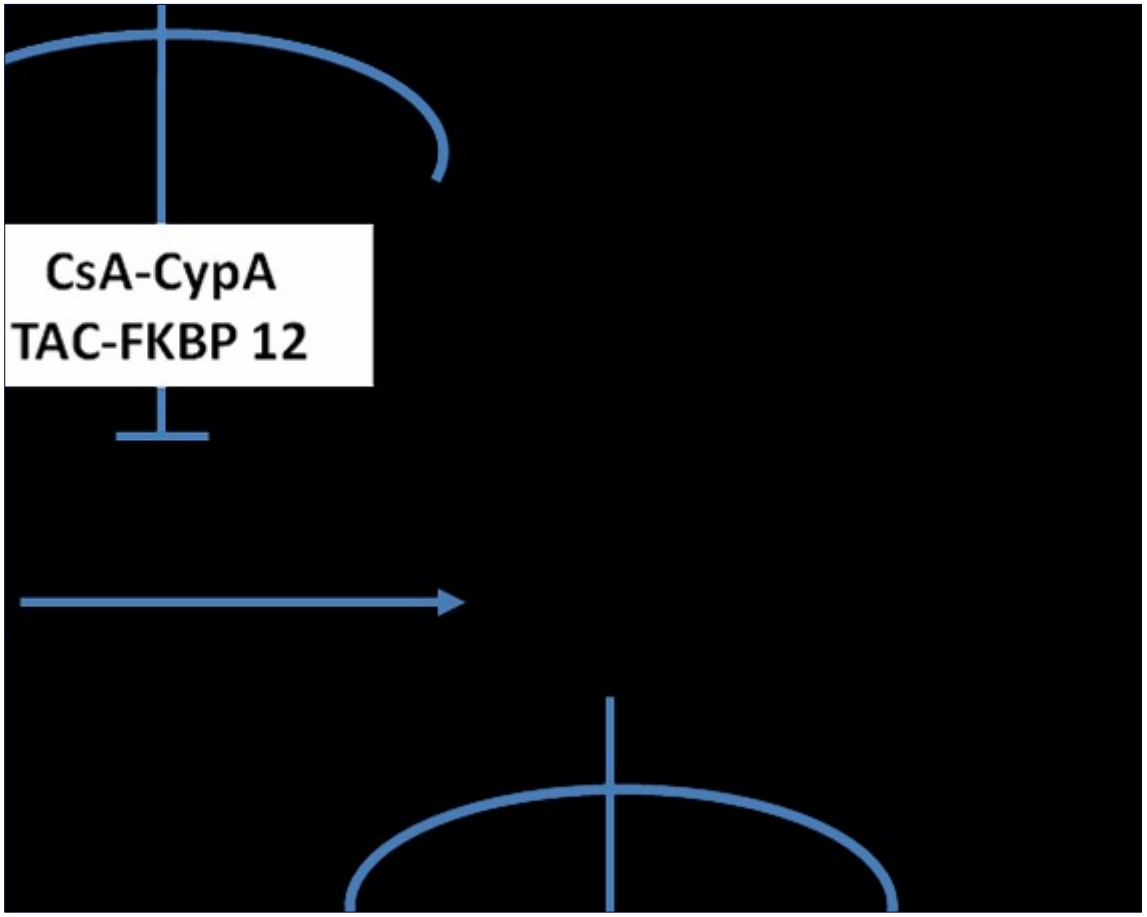

Figure 3.2 Mechanism of action of Cyclosporinend Tacrolimus.
Cyclosporine binds to Cyclophylin, whereas Tacrolimus binds to FKBP-12 in cell cytoplasm. These complexes block calcineurin activity leading to the inhibition of IL-2 production.

3.3 Incidence of Cyclosporine nephrotoxicity

Since 1988, the short-term outcome of kidney grafts has substantially improved (Hariharan et al., 2000). Hariharan and co-workers reported that one-year graft survival from deceased donors increased from 75.7% to 87.7% and also the rate for living donor grafts increased from 88.8% to 93.9% (Hariharan et al., 2000). This significant improvement is due in part to the potent immunosuppressive effect of Cyclosporine, which has contributed to a significant reduction in acute rejection episodes. However, there have been several studies which report potential renal toxicity in kidney and other organ transplantation (Myers et al., 1988; Nankivell et al., 2004).

Chapter 3: A potential role of EMT in Cyclosporine-induced renal allograft fibrosis

In fact, Cyclosporine has been associated with numerous adverse reactions including hypertension, hyperlipidemia, gingival hyperplasia, kidney (Marcén et al., 2001) and liver dysfunction (Klintmalm et al., 1981). However, nephrotoxicity is a major side effect of Cyclosporine. The clinical nephrotoxicity of Cyclosporine was first reported in patients receiving kidneys from cadaveric donors who showed the characteristics of acute toxicity, such as reversible renal dysfunction mediated by hemodynamic change (Klintmalm et al., 1981). Two years later, long term nephrotoxicity of Cyclosporine including tubulointerstitial injury followed by focal glomerular sclerosis was described in heart transplant patients who received Cyclosporine for longer than 12 months (Myers et al., 1984). Since then, several studies involved in chronic Cyclosporine nephrotoxicity have been published and strategies to reduce toxicity have emerged (Nankivell et al., 2004).

The incidence of chronic Cyclosporine nephrotoxicity has been reported by several groups. For example, kidney-pancreas transplant patients were studied by protocol biopsy for up to 10 years. Evidence of CNI toxicity, including arteriolar hyalinosis, glomerulosclerosis and interstitial damage, was reported as 76.4%, 93.5% and 96.8% at 1 year, 5 years and 10 years, respectively (Nankivell et al., 2004). However, a more recent study was conducted using a larger patient cohort and showed that 31% of graft loss at 5 years after transplantation resulted from interstitial fibrosis and tubular atrophy (IF/TA). In contrast to the other studies, CNI nephrotoxicity (0.6%) was not a major contributor to late graft loss (El-Zoghby et al., 2009). The different incidences of CNI nephrotoxicity might be explained according to the following factors:

(1) Subjects: Nankivell et al (2004) performed kidney biopsies in patients with kidney and pancreas transplantation, whilst the more recent study (El-Zoghby et al., 2009) recruited only patients with kidney transplantation. The different transplant procedures might affect the dosage and level of calcineurin inhibitors.

(2) Immunosuppressive drugs: Although both studies used calcineurin inhibitors as immunosuppressive drugs, Cyclosporine was a main drug in Nankivell study and Tacrolimus was used in another study.

(3) Improved diagnostic techniques, such as molecular diagnosis for BK polyomavirus, or C4d marker for humoral rejection, allow more specific identification of the causes of graft failure.

Several papers have suggested that Tacrolimus has an ability to induce nephrotoxicity similar to that of Cyclosporine (Khanna et al., 2002; Shimizu e al., 2008). However, human

(Cantarovich et al., 2005) and animal studies (Bagnis et al., 1997) have shown a weaker vasoconstrictive and fibrogenic effect of Tacrolimus than Cyclosporine. In addition, clinical trials in renal transplantation have shown better renal function and graft survival in Tacrolimus treated patients compared with Cyclosporine (Cantarovich et al., 2005; Shihab et al., 2008). Furthermore, a recent protocol biopsy study reported fewer, less severe and less progressive chronic histological change in kidney transplantation patients, despite using Tacrolimus as the main immunosuppressive drug (Stegall et al., 2011). To date, the reasons for these differences are still incompletely understood.

3.4 Cyclosporine nephrotoxicity

Two types of Cyclosporine nephropathy have been described: acute nephrotoxicity and chronic nephrotoxicity, based on the time of onset of toxicity and histological manifestations.

3.4.1 Acute Cyclosporine nephropathy

The acute form of Cyclosporine nephrotoxicity results from renal vasoconstriction, which is induced by an imbalance of local vasoactive substances. Rat models of experimental Cyclosporine nephrotoxicity demonstrated the constriction of afferent arterioles following Cyclosporine treatment. As a result, there is constriction of renal arterioles, followed by a decline in renal function. This acute toxicity is reversible and depends on the concentration of Cyclosporine. There are three forms of acute Cyclosporine nephrotoxicity: functional toxicity, tubular toxicity and vascular toxicity.

3.4.1.1 Functional toxicity

This is the earliest form of acute Cyclosporine nephrotoxicity. The typical characteristics of functional toxicity include clinical renal allograft dysfunction, such as glomerular filtration rate reduction and increased serum creatinine but without histological abnormality.

3.4.1.2 Toxic tubulopathy

Patients usually present with acute renal allograft dysfunction with high serum Cyclosporine levels. The typical histological finding of tubular toxicity is isovolumetric vacuolisation in most of the proximal tubules. These symmetrical vacuoles in the tubular cytoplasm result from an enlargement of endoplasmic reticulum and an increase of lysosomes (Mihatsch et al., 1998).

3.4.1.3 Vascular toxicity

Cyclosporine has direct toxicity to endothelial cells, resulting in two types of vasculopathy: acute arteriolopathy and thrombotic microangiopathy (Liptak and Ivanyi, 2006). Acute arteriolopathy usually affects only afferent arterioles. A common histological finding is swelling and vacuolation of endothelial cells and also vacuolation, necrosis and apoptosis of myocytes which are then replaced by plasma protein insudates (hyalinisation). Thrombotic microangiopathy can be characterised by the existence of thrombi in the lumen of arterioles and glomerular capillaries.

3.4.2 Chronic Cyclosporine-induced nephrotoxicity

The chronic toxicity of Cyclosporine usually presents with slow, insidious and irreversible renal allograft dysfunction. In contrast to the acute form, chronic Cyclosporine toxicity is not only characterised by renal vasoconstriction, but also by permanent structural damage. This chronic form typically involves 3 parts of the kidney graft, including nodular hyalinosis (vessels), striped fibrosis (interstitium and tubule) and glomerular sclerosis (glomerulus).

3.4.2.1 Nodular hyalinosis

This arteriopathy is characterised by nodular hyaline (glassy translucent substance) deposition in the tunica media of afferent arterioles, which contain smooth muscle cells and elastic fibre, leading to smooth muscle cell damage. The necrotic arteriolar smooth muscle cells are then replaced by focal or circular or bead-like plasma protein deposits on the walls of the afferent arterioles (Figure 3.3).

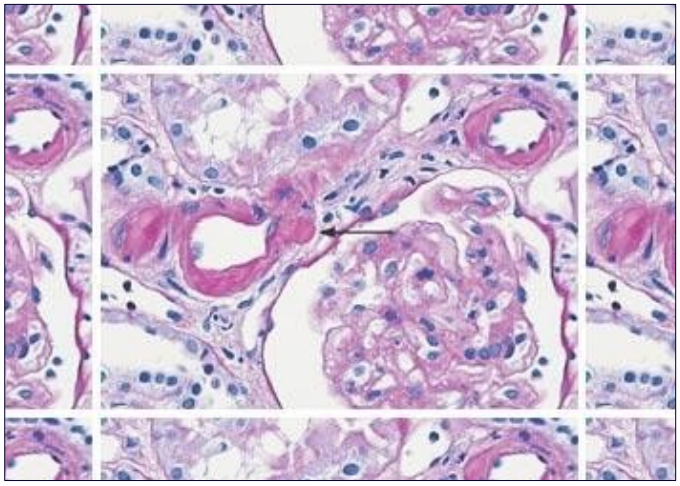

Figure 3.3 Microscopic image of chronic Cyclosporine nephrotoxicity.
The black arrow shows nodular or beads-like medial hyalinosis of afferent arteriole. The image is from Liptak and Ivanyi, 2006.

3.4.2.2 Interstitial fibrosis and tubular atrophy

Recently, the IF/TA caused by non-immunologic factors has been classified as a subtype of medullary ray injury (MRI) (Kobayashi et al., 2010). Striped fibrosis in renal allograft is reported as a consequence of chronic Cyclosporine nephrotoxicity-associated MRI. The striped fibrosis is defined by the presence of ischemic tubular atrophy and interstitial fibrosis areas, alternating with relatively normal tubules and interstitium (Figure 3.4).

3.4.2.3 Glomerular sclerosis

There are many manifestations of glomerular involvement, such as glomerular hypertrophy, mesangial matrix expansion, capillary collapse and/or focal segmental or focal global sclerosis.

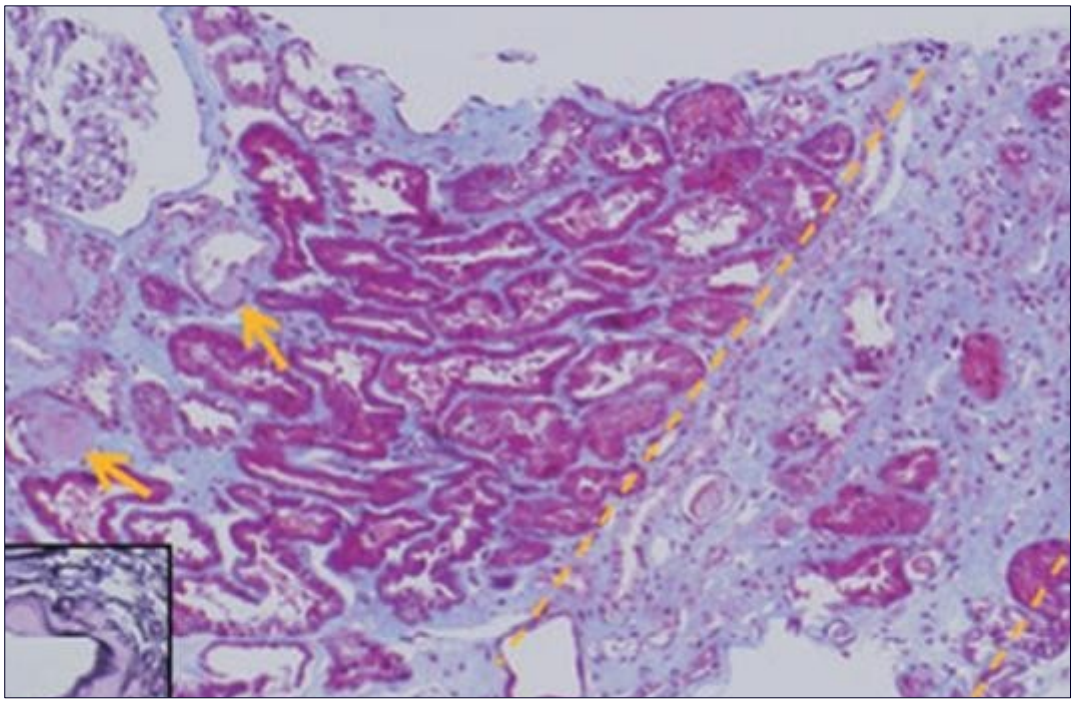

Figure 3.4 Microscopic image of chronic Cyclosporine-induced nephrotoxicity.
The dotted line shows the transition between areas of IF/TA and intact tubule. The yellow arrows demonstrate the nodular hyalinosis. The image is obtained from Kobayashi et al. 2010.

3.5 Pathogenesis of chronic Cyclosporine-induced nephrotoxicity

To date, several hypotheses have been proposed to explain the pathogenesis of chronic Cyclosporine nephrotoxicity. However, the exact mechanisms are not clearly understood. Nevertheless, the most likely aetiologies are chronic low grade ischemia and TGF-β up-regulation (Ling et al., 2003).

3.5.1 Chronic low grade ischemia

It has been demonstrated that chronic ischemia induced by Cyclosporine resulted from an imbalance of vasoactive substances by increasing the expression of vasoconstrictive mediators including renin-angiotensin aldosterone system (RAAS), endothelin-1 (ET-1) (Ramirez et al., 2000) and TXA2 (Thromboxane A2) (Kim et al., 1997), as well as a reducing

vasodilators such as PGI2 (Prostacyclin), PGE2 (Prostaglandin E2) (Rogers et al., 1988) and NO (Nitric oxide) (Kurus et al., 2005).

Consequently, the resulting renal vasoconstriction results in both renal dysfunction and hypoxia. Renal ischemia promotes reactive oxygen species (ROS) production that contributes to structural damage by increasing apoptosis and cellular tubular injury.

3.5.2 TGF-β up-regulation

TGF-β is a key cytokine implicated in the pathogenesis of fibrosis in chronic kidney diseases, including chronic Cyclosporine nephropathy. Studies from our group and others have shown that Cyclosporine is associated with an up-regulation of TGF-β expression (Mohamed et al., 2000). Furthermore, the renal function and structural damage were ameliorated by administrating a specific TGF-β neutralising antibody in a mouse model of chronic Cyclosporine nephropathy (Ling et al., 2003).

The exact mechanism of Cyclosporine-induced TGF-β secretion is incompletely understood. However, multiple hypotheses have been proposed, such as angiotensin II (Pichler et al., 1995; Shihab et al., 1997) and aldosterone activation (Bobadilla and Gamba, 2007), macrophage infiltration (Lim et al., 2004) and direct cell toxicity (Esposito et al., 2000). However, a study using rat model of type I diabetes showed that inhibition of calcineurin reduced glomerular extracellular matrix accumulation (Gooch et al., 2003). In addition, TGF-β induced accumulation of extracellular matrix via ROS generation, calcium influx and calcineurin activation (Gooch et al., 2004). Therefore, a mechanism of Cyclosporine induced TGF-β production by renal tubular epithelial has remained controversy.

3.5.3 Role of Cyclosporine on CTGF expression

CTGF is a pro-fibrotic growth factor which acts downstream of TGF-β. Previous studies suggested that CTGF played a role in TGF-β1-induced EMT during organ fibrosis (Burns et al., 2006; Burns et al., 2007). Blocking CTGF expression reduced the expression of fibronecin, collagen and α-SMA in the UUO mouse model (Yokoi et al., 2004). In addition, a study using human renal cell line (HK-2) showed increased CTGF mRNA expression following Cyclosporine treatment during Cyclosporine-induced EMT *in vitro* (McMorrow et al., 2005). However, some paper showed a negative role of CTGF in chronic Cyclosporine nephrotoxicity. Rat experimental chronic nephrotoxicity showed no difference of CTGF mRNA expression

between control and rats with Cyclosporine treatment (Shihab et al., 2006). Therefore, it seems that a role of Cyclosporine in CTGF regulation remains unknown.

3.5.4 Calcineurin-NFAT pathway

Nodular hyalinosis is one of the manifestations of chronic Cyclosporine-induced renal injury (section 3.4.2). This arterial hyalinosis results from the replacement of necrotic smooth muscle cells in the vascular wall by plasma proteins. A study in a rat model of Cyclosporine nephrotoxicity demonstrated the process of arteriolar hyalinosis, starting with the granular eosinophilic transformation of smooth muscle cells in afferent arterioles, followed by the vacuolisation of smooth muscle cells and subsequent hyaline deposition (Young et al., 1995). The underlying mechanisms responsible for smooth muscle cell necrosis are not yet clear. However, it has been observed that the changes in smooth muscle cells may be associated with several factors, including the function of calcineurin-NFAT in smooth muscle cells (Graef et al., 2001; Nieves-Cintrón et al., 2007), prolonged arteriolar vasoconstriction and direct toxicity of Cyclosporine.

Recent data have suggested an important role for the calcineurin-NFAT signalling pathway in chronic Cyclosporine nephropathy, though this has not been fully defined. It has been suggested that nuclear localisation of NFAT plays an important role in the acquisition and maintenance of smooth muscle cell differentiation and arterial remodelling. Moreover, it also has been reported that there is an association between NFAT and COX-2; the COX-2 gene promoter contains binding sites for NFAT, indicating that NFAT is involved in the regulation of COX-2 gene expression (Sugimoto et al., 2001). NFAT is inhibited by Cyclosporine, leading to a decrease in COX-2 expression and, consequently, renal vasoconstriction.

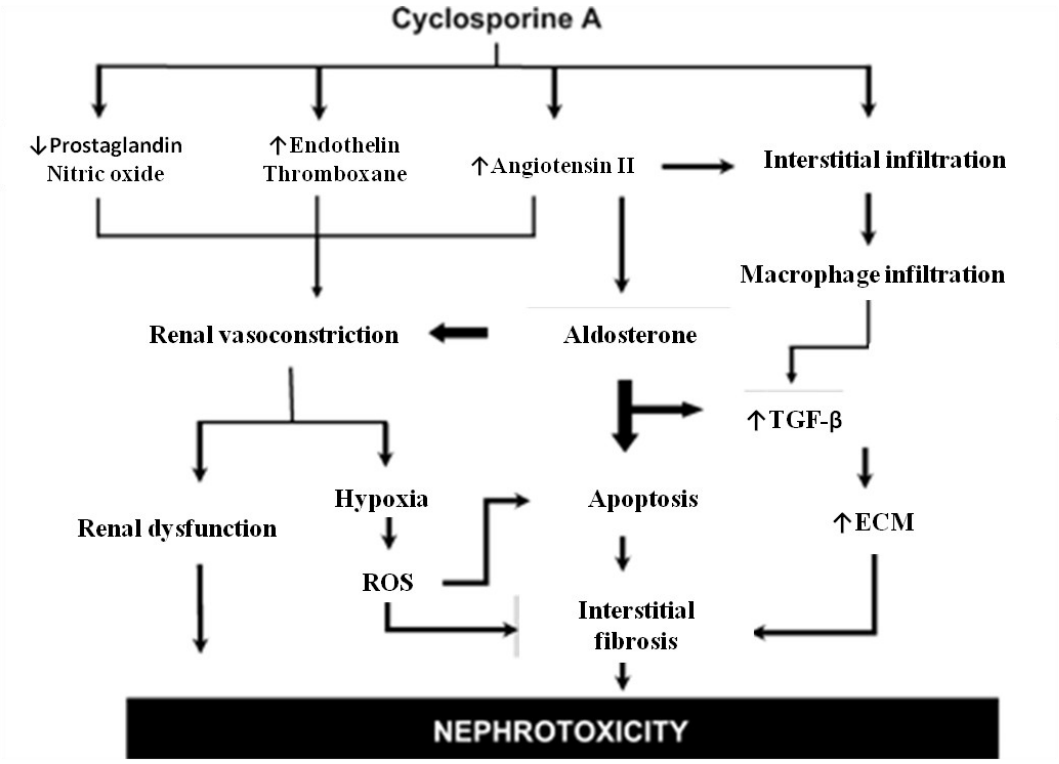

Figure 3.5 Diagram demonstrating the pathogenesis of chronic Cyclosporine nephrotoxicity.

3.5.5 Cyclosporine-induced epithelial mesenchymal transition

It is widely accepted that TGF-β is a key cytokine for fibrogenesis including renal allograft fibrosis due to Cyclosporine nephrotoxicity. TGF-β induces interstitial fibrosis by several mechanisms, including:

(i) Accelerating fibroblast proliferation which leads to an increase in the production of extracellular matrix.

(ii) Decreasing the degradation of ECM by down regulating the matrix metalloproteinase enzymes.

Current evidence shows that EMT is one of the important mechanisms for TGF-β induced organ fibrosis (Kalluri and Neilson, 2003). EMT is described as a multistep process in which epithelial cells lose their epithelial phenotypes and acquire mesenchymal characteristics (see section 1.8). The losses of epithelial characteristics which are commonly observed during EMT are morphological change from typical cuboidal-shaped epithelia to elongated spindle-shaped fibroblast-like cell and reduction of intercellular adhesion molecules

such as E-cadherin. The mesenchymal markers which are commonly used to identify fibroblasts include S100A4 and α-SMA.

According to the previous data, TGF-β is up-regulated in chronic Cyclosporine nephrotoxicity both *in vivo* and *in vitro* (Mohamed et al., 2000; Esposito et al., 2000). Therefore, Cyclosporine might have a direct effect on renal tubular epithelial cells by inducing EMT. This is supported by *in vitro* studies in renal proximal tubular epithelial cell lines (Slattery et al., 2005; McMorrow et al., 2005). In addition, recent data has shown that Cyclosporine-induced EMT is inhibited by BMP-7, which is a TGF-β antagonist, by down regulating the expression of connective tissue growth factor, a downstream mediator of TGF-β1 (Xu et al., 2010). Since the effect of Cyclosporine-induced TGF-β production is most likely cell/tissue specific, thus this study chose a different cell line to investigate this issue.

Chapter 3: A potential role of EMT in Cyclosporine-induced renal allograft fibrosis

3.6 Aim

EMT has been proposed as an important mechanism for fibrogenesis. This leads to the hypothesis that Cyclosporine may induce EMT in renal tubular cells, resulting in interstitial fibrosis in chronic Cyclosporine nephrotoxicity.

This study will determine the pathogenic role of EMT in chronic Cyclosporine nephrotoxicity by:

- Demonstration that EMT can be induced in renal epithelial cell lines by TGF-β1.
- Demonstration of the characteristics of EMT in renal epithelial cell lines at both protein and molecular levels after Cyclosporine treatment.
- Demonstration of the association between Cyclosporin and bioactive TGF-β1 levels.

3.7 Materials and Methods

All detail of materials used in this chapter is shown in chapter 2. The following methods were designed for experiments performed only in this chapter.

3.7.1 Peripheral blood mononuclear cell (PBMC) preparation

All PBMCs contain a single round nucleus. These cells primarily include lymphocytes and monocytes. They are usually isolated from anti-coagulated whole blood by density gradient centrifugation in a ficoll-400/sodium metrizoate solution of density 1.077g.cm^{-3}, with the PBMCs floating at the interface.

3.7.1.1 PBMC preparation procedure

Briefly, the fresh whole blood was supplemented with heparin at a concentration of 1unit/ml of blood. The heparinised blood was then diluted with serum free RPMI at a ratio of 1:1. After that, 7 ml of Lympholyte®-H was layered under 10 ml of diluted blood followed by centrifugation at 800g at room temperature for 20 minutes with the brake off. The interfacial cells were collected and transferred into a new universal tube (Figure 3.11). The cells were washed twice in serum free RPMI by centrifugation at 600g for 10 minutes at room temperature. The cells were then resuspended in complete RPMI at 1 x 10^{6}cells/ml for experiments.

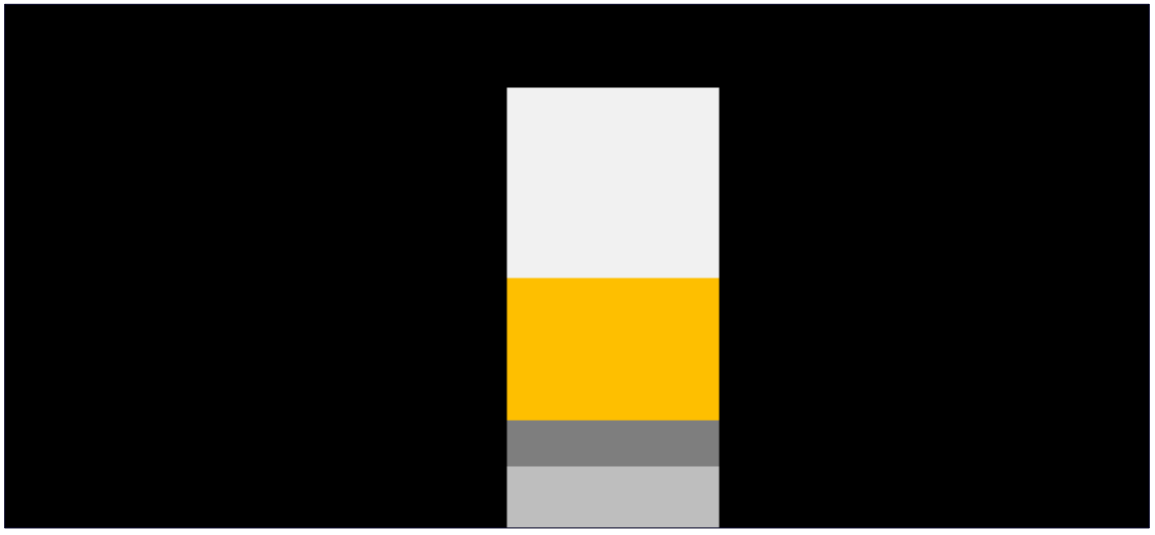

Figure 3.6 Peripheral mononuclear cells preparation

3.7.2 Thymidine incorporation assay

The amount of DNA in a cell must double prior to mitotic division. This process involves the systhesis of new DNA which provides a route to the quantification of cell division within a population of cells in a culture. Thymidine is a nucleoside which is incorporated specifically into DNA. If an excess of thymidine, which has been labelled with a radioactive isotope (typically tritium), is provided in the cell culture medium, this isotope will be incorporated during DNA synthesis. Subsequent detection of the decay of this isotope in DNA, which has been isolated from the cells, provides a signal which is proportional to the rate of cell proliferation.

3.7.2.1 Thymidine incorporation assay procedure

Safety rules for working with radioisotopes include wearing protective clothes, the use of suitable shielding materials while handling the radioisotope, monitoring contamination before and after experiments, disposing of radioactive waste appropriately and recording used radioisotopes in a log book. These rules were obeyed throughout this work. 1μCi (37 kBq) of ^{3}H-thymidine was added to each well of stimulated-PBMCs in a 96-well plate and incubated for 6 hours in a humidified 5% CO_2 incubator at 37ºC for 6 hours. The 3H-thymidine-exposed cells were harvested by filtration onto the glass fibre filter. Following drying in an oven (60°C/4 hours), the filter was placed in a plastic bag with β scintillation fluid and analysed in a β scintillation counter. Data were recorded as counts per minute (cpm).

3.8 Results

3.8.1 Morphological changes in HKC-8 cells after exposure to TGF-β1

One of the key characteristics of EMT is morphological changes from epithelial cobblestone-like to fibroblast-like appearance. Since TGF-β1 is recognised as a key mediator of EMT, treatment of renal epithelial cells with TGF-β1 might result to changes of renal epithelial morphology.

Initially, the features of EMT were examined in the HKC-8 cell line following TGF-β1 treatment. HKC-8 cells were grown in 25 cm^2 tissue culture flasks until they reached 80% confluence. Then these semi-confluent cells were incubated with 5ng/ml of TGF-β1 for 72 hours. The morphology of cells was viewed by inverted microscopy.

Normally, like other epithelial cells, HKC-8 appeared as a single layer of cube-like cells with large spherical nuclei (Figure 3.7A). Changes in morphology became apparent after 48 hours. However, the epithelial cells were strikingly transformed to elongated spindle-shaped cells following 72 hours of TGF-β1 treatment (Figure 3.7B). This suggests that TGF-β1 induces reorganization of the epithelial cell's cytoskeleton.

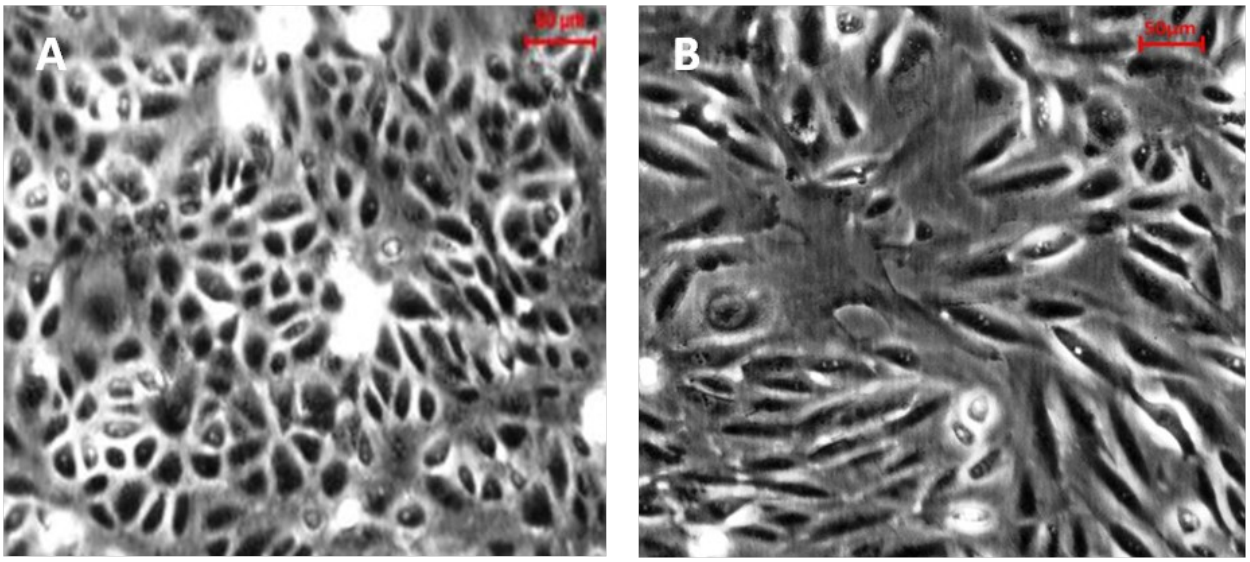

Figure 3.7 Morphological manifestations of renal tubular epithelial cells following TGF-β1 treatment.

The light microscopic analysis of the morphology of HKC-8 incubated in complete medium or medium containing TGF-β1 at a final concentration 5ng/ml for 72 hours. The normal cells (A) exhibited the cobblestone-like appearance, whereas the cells with TGF-β1 treatment (B) adopted a bipolar morphology. The images were taken at x 200 magnification. The results are representative of 2 similar experiments.

3.8.2 TGF-β1 disrupted cell-cell adhesion between renal epithelial cells

Cell junctions are a specific characteristic of epithelial cells. These structures consist of protein complexes, especially E-cadherin, which maintains cell-cell contact and epithelial cell polarity (section 1.3.2). It has been suggested that loss of epithelial adhesion molecule is an early sign of EMT development (Aresu et al., 2008). Therefore, E-cadherin expression might be reduced following TGF-β1 treatment. In this experiment, cells were grown on 0.1%gelatin-coated slides in order to increase the attachment between epithelial cells and the surface of the slides. Gelatin, which mainly consists of hydrolysed collagen type I, is commonly used to enhance cell attachment during *in vitro* study. It has been shown that gelatine has no effect on epithelial monolayer and tight junction molecule expression (Zhang et al., 2009).

1 x 10^5 HKC-8 cells were seeded onto 0.1% gelatine-coated chamber slides until semi-confluence was reached. TGF-β1 was then added at the concentration 5ng/ml and incubated with HKC-8 cells for 72 hours. After washing, the cells were fixed in cold acetone at -20˚C for 10 minutes, and the slides were air-dried. Non-specific antibody binding was blocked by incubating with 1%BSA/PBS for 1 hour. Subsequently, the cells were incubated with mouse monoclonal anti-E-cadherin antibody (clone Ber-ACT8) for 1 hour, followed by FITC-conjugated monoclonal anti-mouse IgG antibody for 1 hour; control sections were incubated with secondary antibody only. The slides were viewed by confocal microscopy at times 63 magnifications.

Most of normal renal tubular epithelial cells contacted each other and formed typical cobblestone-like islands. The linear staining pattern of E-cadherin was apparent along the points of cell-cell contact (Figure 3.8A). In contrast, with TGF-β1 treatment, the cells became scattered with no expression of E-cadherin on the cell membranes. In addition, E-cadherin molecules seemed to move from the cell surface into the cytoplasm of treated cells (Figure 3.8B).

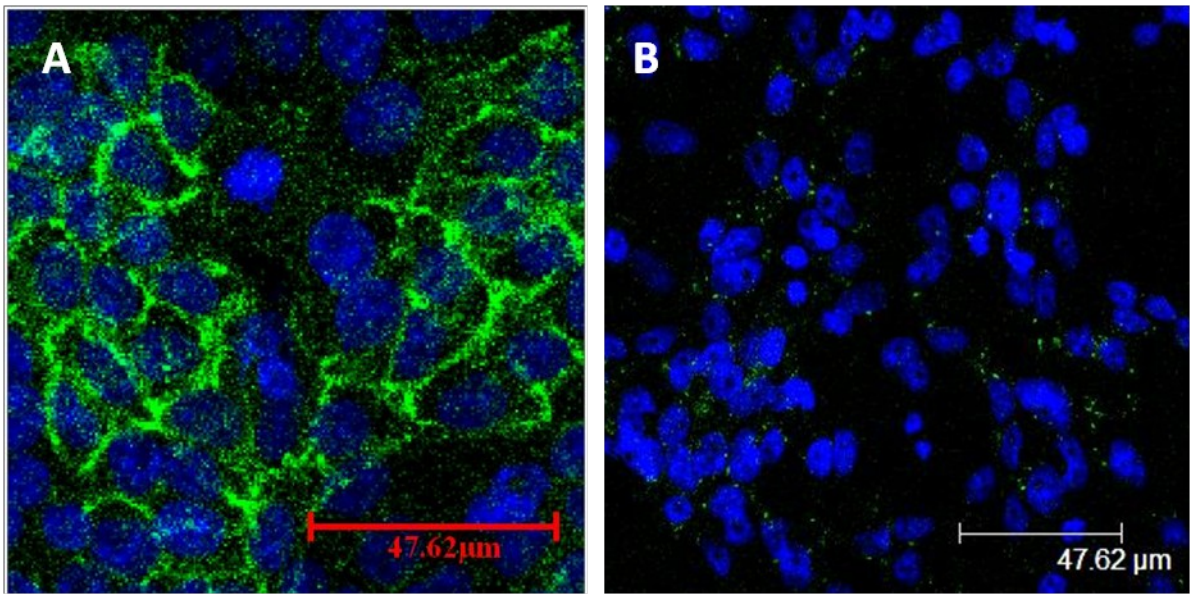

Figure 3.8 Confocal immunofluorescence analysis of E-Cadherin expression in renal tubular cells.

Semi-confluent HKC-8 cells were incubated in complete medium (A) or medium containing 5ng/ml of TGF-β1 for 72 hours (B). In normal cells, the E-cadherin was predominantly localized at cell-cell junction (Green). After TGF-β1 treatment, E-cadherin almost disappeared from the cell junction. Nuclei were visualized by 4', 6-diamidino-2-phenylindole DAPI stain (Blue). The images were taken at x63 magnification. The results are the representative of 3 similar experiments.

3.8.3 TGF-β1-induced de novo expression of mesenchymal markers

Another feature of EMT is de novo expression of mesenchymal markers. It is accepted that S100A4/FSP-1 and α-SMA are markers for fibroblast and myofibroblast respectively (Vongwiwatana et al., 2005). Other cell types can express S100A4 such as macrophage and leukocytes (Le Hir, et al. 2005). However, S100A4 appears as a marker of cells in fibrogenesis, at least in epithelial cells undergoing EMT because S100A4 expression precedes complete EMT (Okada et al., 1997), transfection of S100A4 in tubular epithelium results in conversion to mesenchymal phenotypes (Strutz et al., 1995) and siRNA S100A4 reduces fibrosis (Okada et al., 1997). Since there were only renal tubular epithelial cells present in this experiment, thus S100A4 was chosen as one of the markers of mesenchymal cells.

HKC-8 cells were grown in chamber slides until semi-confluence (70-80% confluence) was reached. They were then incubated with 5ng/ml of TGF-β1 for 72 hours. The expression of S100A4 and α-SMA were detected by microscopic examination after immunofluorescence staining. Cells were stained with polyclonal rabbit anti-human S100A4 antibody and monoclonal mouse anti-human α-SMA (clone 1A4) antibodies and their appearance was visualised by confocal microscopy and compared with non-treated control cells.

S100A4 expression appeared at a low level in the cytoplasm of normal HKC-8 cells while α-SMA expression was absent. Following TGF-β1 treatment, S100A4 expression was generally increased in cytoplasm of HKC-8 cells (figure 3.9). However, α-SMA was present as microfilament-like structures in only a proportion of the cells (figure 3.10).

This study observed a different pattern of S100A4 and α-SMA expression by renal epithelial cells. S100A4 was generalized present by nearly all HKC-8 cells, while α-SMA was expressed by some HKC-8 cells. This probably suggested that some S100A4-positive fibroblasts were transformed into a reversible activated state. However, it was clear that TGF-β1 was able to induce both S100A4 and α-SMA expression in renal tubular epithelial cells.

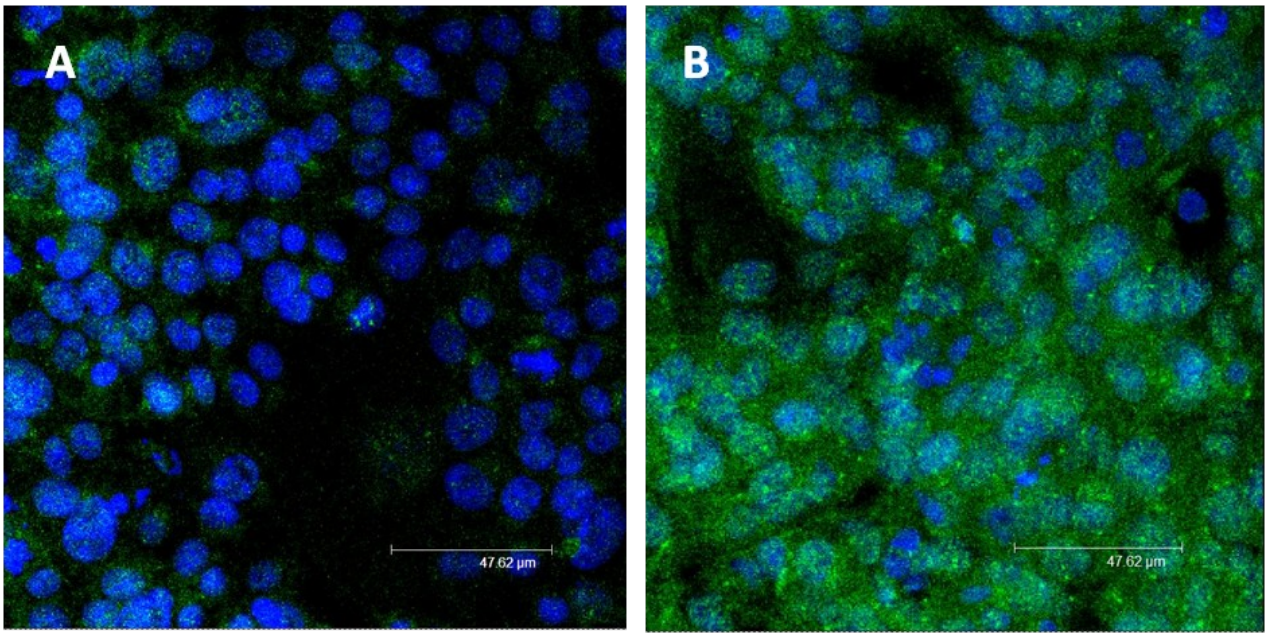

Figure 3.9 Microscopic immunofluorescence analysis of S100A4 expression in renal tubular epithelial cells.

Semi-confluent HKC-8 cells were incubated in complete medium (A) or medium containing 5ng/ml of TGF-β1 for 72 hours (B). The S100A4 was faintly appeared in cytoplasm of normal cells (Dark green). However, the significant expression of S100A4 was observed in TGF-β1 treated cells (Bright green). Nuclei were visualized by DAPI stain (Blue). The images were taken at x63 magnification. The results are the representative of 3 similar experiments.

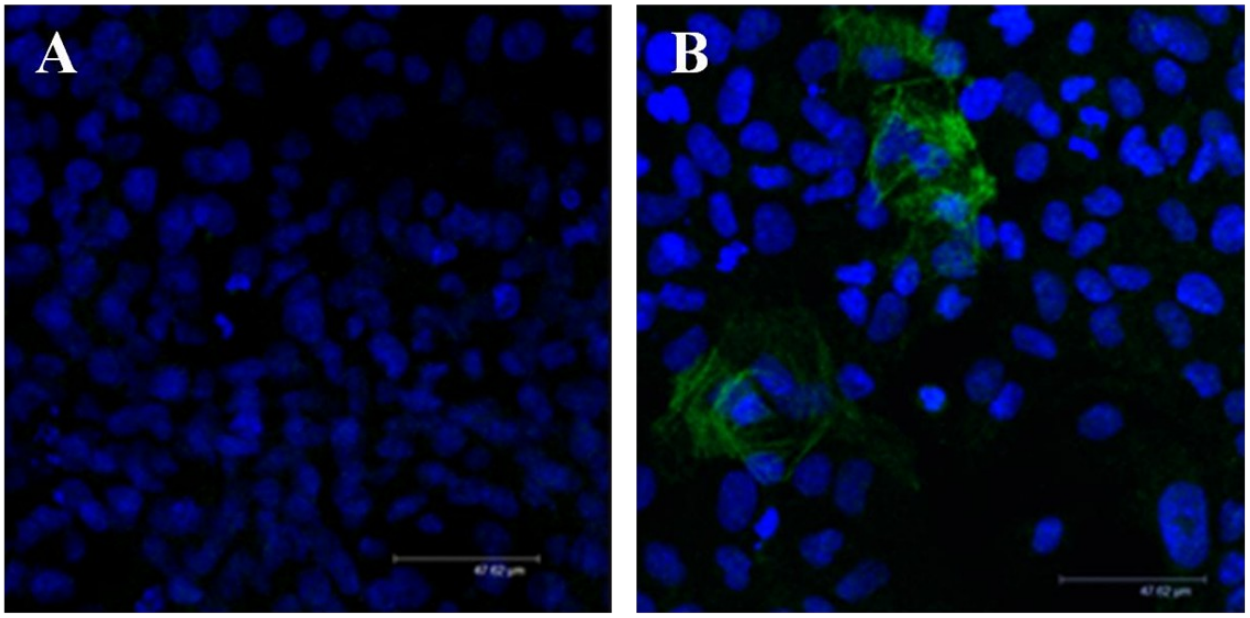

Figure 3.10 Microscopic immunofluorescence analysis of α-SMA expression in renal tubular epithelial cells.

Semi-confluent HKC-8 cells were incubated in complete medium (A) or medium containing 5ng/ml of TGF-β1 for 72 hours (B). There was no α-SMA expression observed in normal cells. However, the microfilamentous bundles of α-SMA were expressed after TGF-β1 treatment. Nuclei were visualized by DAPI stain (Blue). The images were taken at x 63 magnification. The results are the representative of 2 similar experiments.

3.8.4 The effect of TGF-β1 on E-cadherin expression by Western blot.

This experiment was performed in order to confirm that E-cadherin expression was reduced in the presence of TGF- β1. Semi-confluent HKC-8 cells were incubated with 5ng/ml of TGF-β1 for 72 hours before performing protein lysis (section 2.6.1). The E-cadherin expression was detected by Western blot analysis and compared to control cells. Equal protein loading was demonstrated by probing for the expression of the 50kDa housekeeping protein, α-tubulin.

The western blot showed a single band of E-cadherin protein in normal HKC-8 cells. However, following TGF-β1 treatment, the 120kDa E-cadherin band was less dense compared to the one of normal cells (Figure 3.11). This confirmed that TGF-β1 could induce the loss of this epithelial cell marker, one of key features of EMT

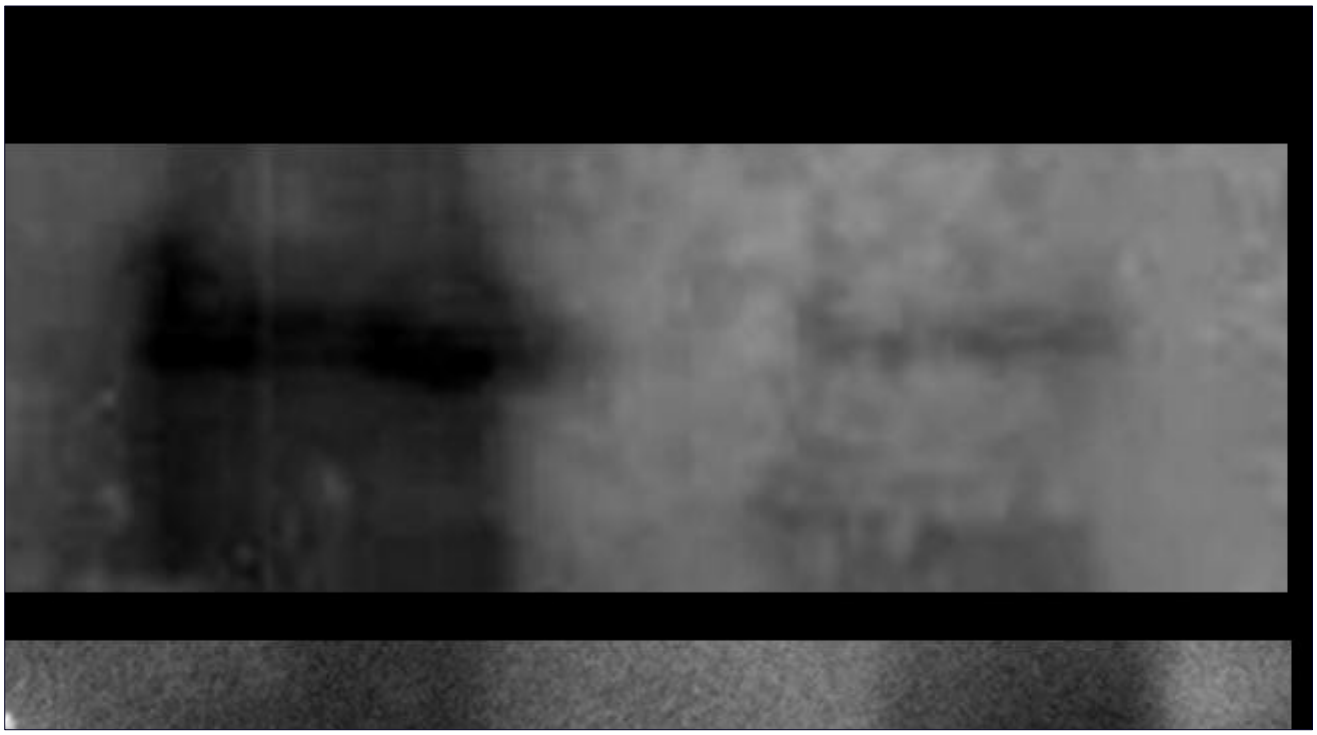

Figure 3.11 Comparison of E-cadherin expression between normal cells and TGF-β1-treated cells by Western Blotting.

Western blot analysis demonstrated that normal HKC-8 cells expressed the E-cadherin (lane A); however this adhesion protein was reduced in the presence of TGF-β1 5ng/ml for 72 hours (lane B). Equal loading between the lanes was validated by the detection of α-tubulin. These results are representative of 2 similar experiments.

3.8.5 The mitogenic response of PBMCs to Muromonab-CD3 (OKT3) and Cyclosporine

Before starting experiments with Cyclosporine, the immunosuppressive effect of Cyclosporine was examine by ^{3}H-Thymidine incorporation assay to demonstrate the activity of the drug.

OKT3 is a murine monoclonal antibody that specifically reacts with the T cell receptor-CD3 complex on the surface of T cells. Human T cells are activated by interaction with plate-bound OKT3, leading to mitogenic T cell proliferation.

This study was performed in 2 stages. Firstly, a mitogenic concentration of OKT3 was defined by measurement of the proliferative response of treated human T cells. Secondly, the concentration of Cyclosporin required to inhibit this mitogenic response was measured.

PBMCs were isolated from human whole blood and then incubated with OKT3 at a concentration ranging from 0-10µg/ml for 72 hours. T cell proliferation was then measured by quantification of 3H-thymidine incorporation. Stimulation of PBMC with OKT3 induced a marked proliferative response (Figure 3.12). It was clearly seen that OKT3 at 10ng/ml could induce proliferation of PBMCs; however, this study chose OKT3 at concentration 20ng/ml for induction of PBMC proliferation because it is a widely recommended concentration (Lee and Molinaro, 2003).

Next, PBMCs were incubated with 20ng/ml of OKT3 in the presence of a range of concentrations of Cyclosporine for 72 hours followed by application of the ^{3}H-thymidine incorporation assay protocol (section 3.8.2). Cyclosporine was able to inhibit OKT3-induced PBMC proliferation with an IC50 value of between 0.01 and 0.1ng/ml (Figure 3.13). In addition, the maximal inhibition of T cell proliferation was at a concentration above 1µg/ml. However, Cyclosporine at a concentration 5µg/ml was used in further experiments on the basis of results from a previous study (McMorrow et al., 2005).

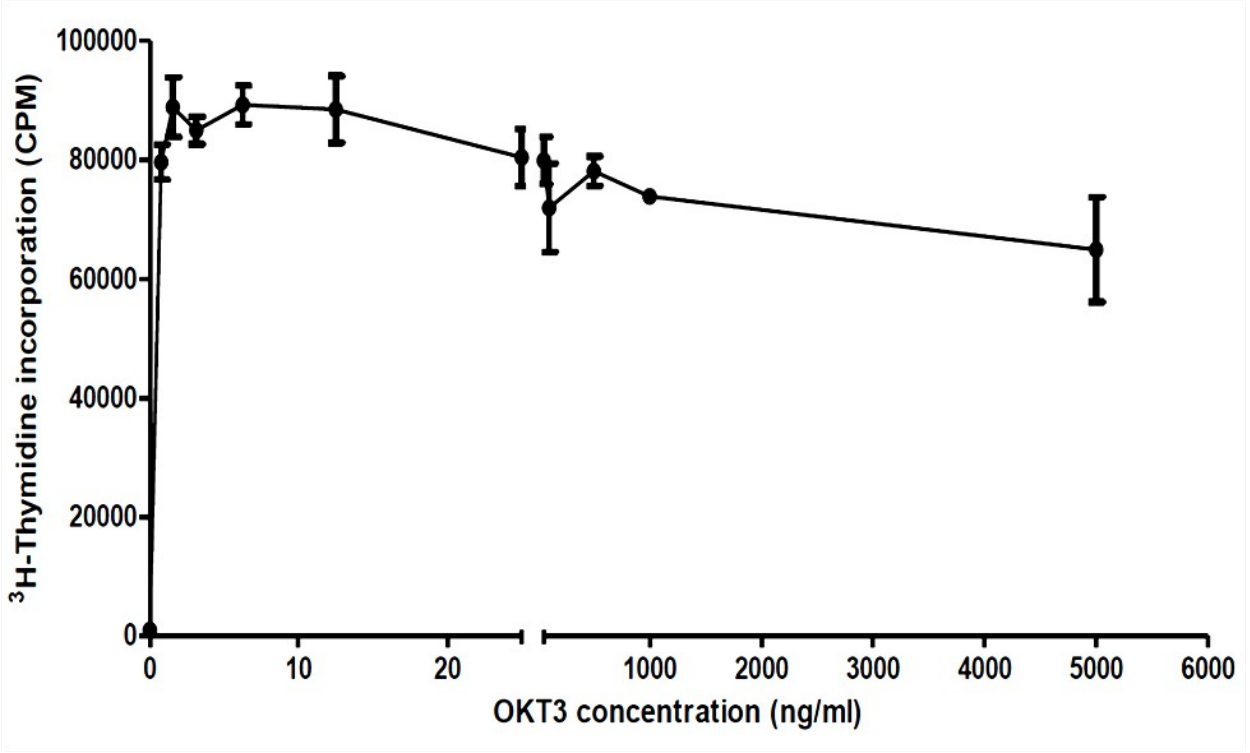

Figure 3.12 ^{3}H-Thymidine incorporation analysis of the mitogenic response of T cells to OKT3.

Peripheral blood mononuclear cells (PBMC) were isolated from whole blood followed by incubating with OKT3 20ng/ml for 72 hours. The stimulated leukocytes were incubated with ^{3}H-Thymidine for 6 hours before counting radioactivity. The plots show mean results, the error bars represent the SEM. These results are from one of 2 similar experiments.

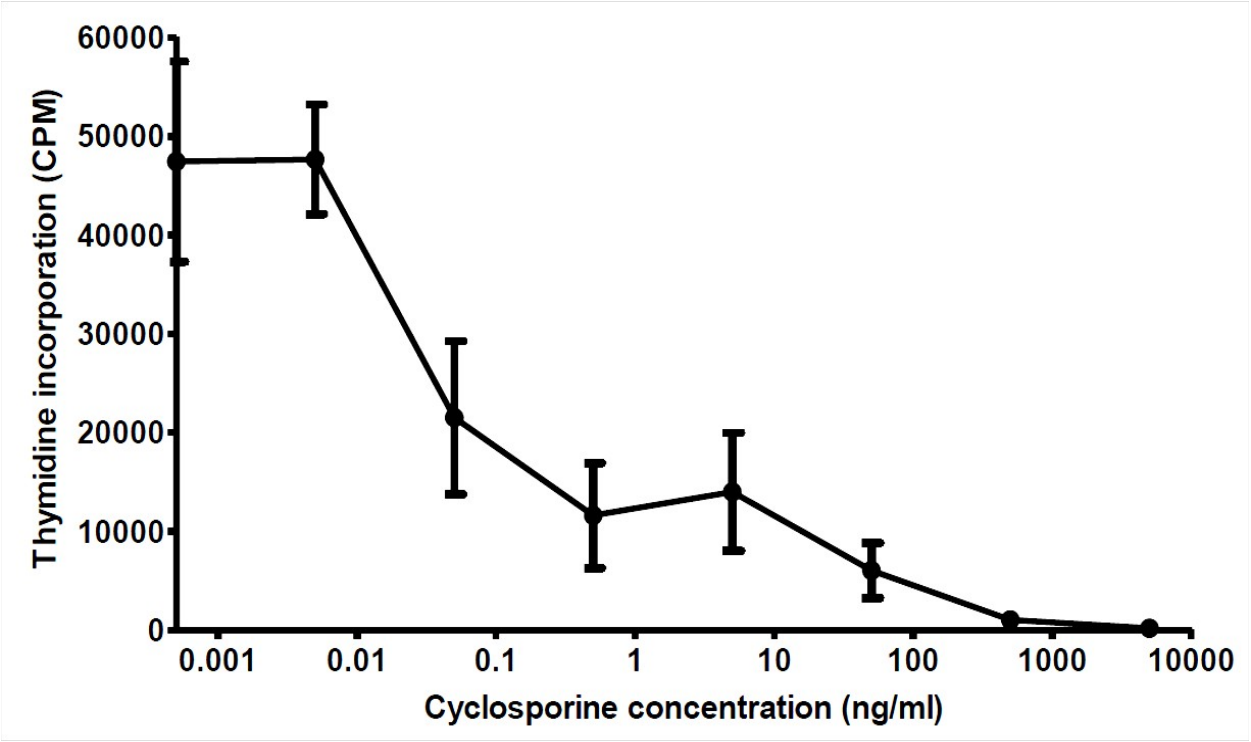

Figure 3.13 ^{3}H-Thymidine incorporation analysis showing suppression of the mitogenic response of T cells by Cyclosporine.

Peripheral blood mononuclear cells were isolated from human whole blood and followed by incubating with OKT3 at an optimal 20ng/ml in the presence of different concentrations of Cyclosporine for 72 hours. The stimulated leukocytes were incubated with ^{3}H-Thymidine for 6 hours before counting the radioactivity. The plots show mean results and the error bars are the SEM. The results are representative of 2 similar experiments.

3.8.6 Effect of Cyclosporine on renal epithelial cell proliferation.

The effect of Cyclosporine on proliferation of renal tubular epithelial cells was investigated by counting cells in culture. Briefly, $2x10^{4}$ of HKC-8 cells were grown in a 12-well

plate until 80% confluence was reached. Then, the cells were incubated with Cyclosporine at a concentration of 10ng/ml, 100ng/ml, 1μg/ml and 5μg/ml. Control cells were grown in medium and a medium containing 0.1% ethanol (vehicle control, VC). Cells were harvested in trypsin/EDTA and directly counted using a haemocytometer at 0, 24, 48 and 72 hours after Cyclosporine treatment.

Cyclosporine had no effect on growth and proliferation of HKC-8 cells at concentration less than 5μg/ml. However, Cyclosporine at concentration 5μg/ml inhibited the proliferation of HKC-8 cells at 48 and 72 hours after treatment (Figure 3.14). It was clear that the suppressive effect on renal tubular epithelial cells required a very high concentration of Cyclosporine compared to immune cells. The proliferative capacity of epithelial cells seemed to be calcineurin-independent since the immunosuppressive activity was much lower around 0.05ng/ml (Figure 3.13). Normally, the therapeutic level of Cyclosporine used in humans is approximately 200ng/ml in whole blood. This observation suggested that the suppressive effect of Cyclosporine on the proliferation of non-lymphocytic cells, renal tubular cells was much higher than the human blood Cyclosporine level. However, this study does not exclude the possibility that *in vivo* tissue hypoxia due to renal vasoconstriction might be responsible for tubular cell death during chronic Cyclosporine nephrotoxicity despite at the lower concentration than those in this study.

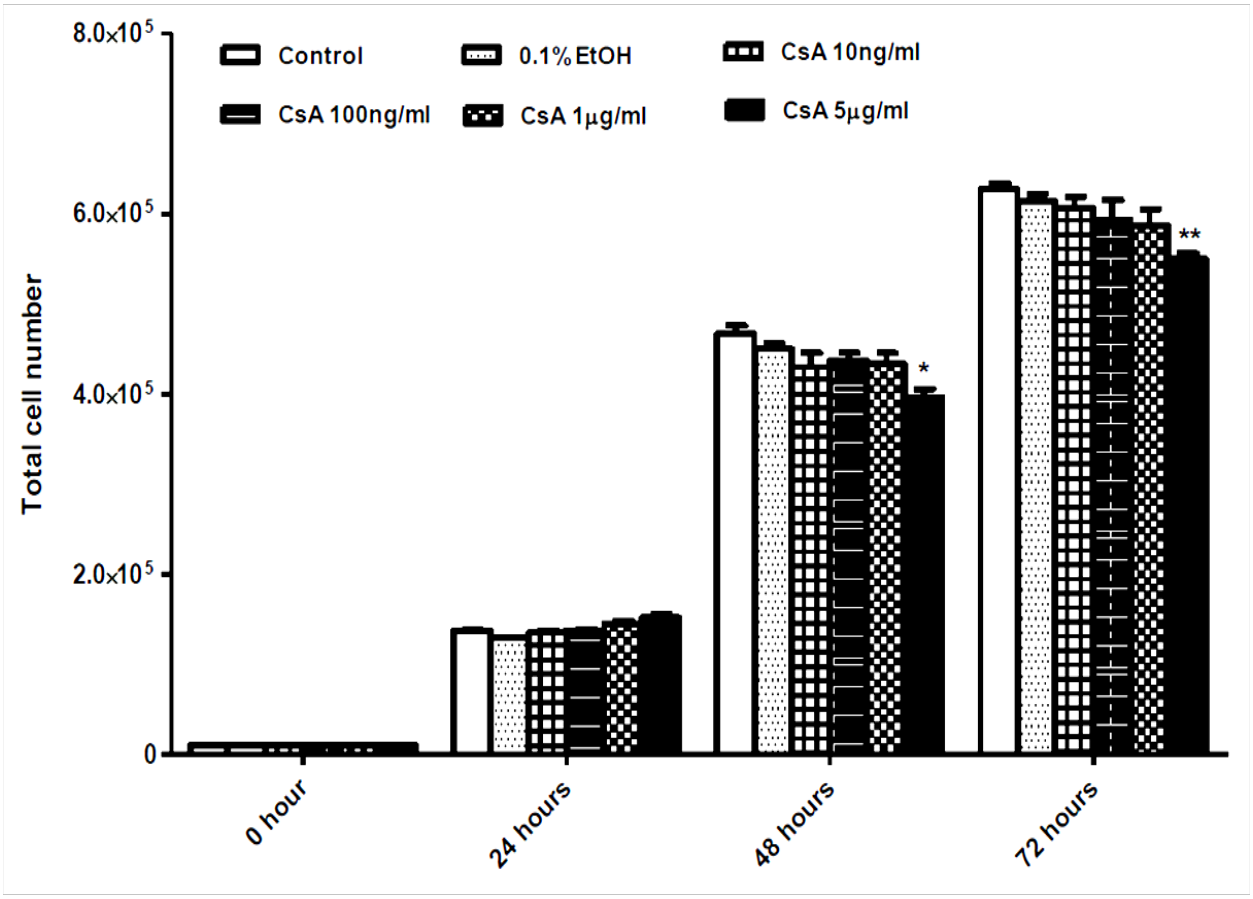

Figure 3.14 Bar graph illustrating the effect of Cyclosporine on renal tubular epithelial cells proliferation.

Semi-confluent HKC-8 cells were grown in complete medium or medium containing with 0.1% ethanol and Cyclosporine at the final concentration of 10ng/ml, 100ng/ml, 1ug/ml and 5ug/ml. Viable control and stimulated cells were counted using a haemocytometer after 0, 24, 48 and 72 hours. The maximum concentration of Cyclosporine significantly suppressed cells proliferation at 48 and 72 hours (* = $p < 0.05$, ** = $p < 0.01$). The bars show mean results and the error bars show the SEM. These results are representative of 2 similar experiments.

3.8.7 Effect of Cyclosporine on renal epithelial cells viability.

The cytotoxicity of Cyclosporine on renal tubular epithelial cells was assessed by propidium iodide (PI) staining using flow cytometric analysis. Confluent HKC-8 cells were incubated with 0.1% ethanol and Cyclosporine at a concentration of 10ng/ml, 100ng/ml, 1µg/ml and 5µg/ml for 72 hours. Control cells were grown in complete medium. The treated cells were harvested by a non-enzymatic method and stained with PI for 15 minutes. The stained cells were immediately verified by flow cytometry (FL-2 channel). The quadrants were set using unstained cell samples andwere then applied for all conditions.

Cells in left upper quadrant represented dead cells, most likely necrotic cells, while cells in the right lower quadrant were mainly viable cells. In normal condition, approximately 88% of HKC-8 cells were alive and 5% were dead after 72 hours culture. The proportion of dead cells was not different among normal, vehicle control and Cyclosporine-treated cells (Figure 3.15). However, some dead cells might have been lost during the centrifugation step of the cell harvesting process; results from this assay might be underestimated. The alternative studies such LDH cytotoxic assay and apoptosis assay probably are required to support this experiment.

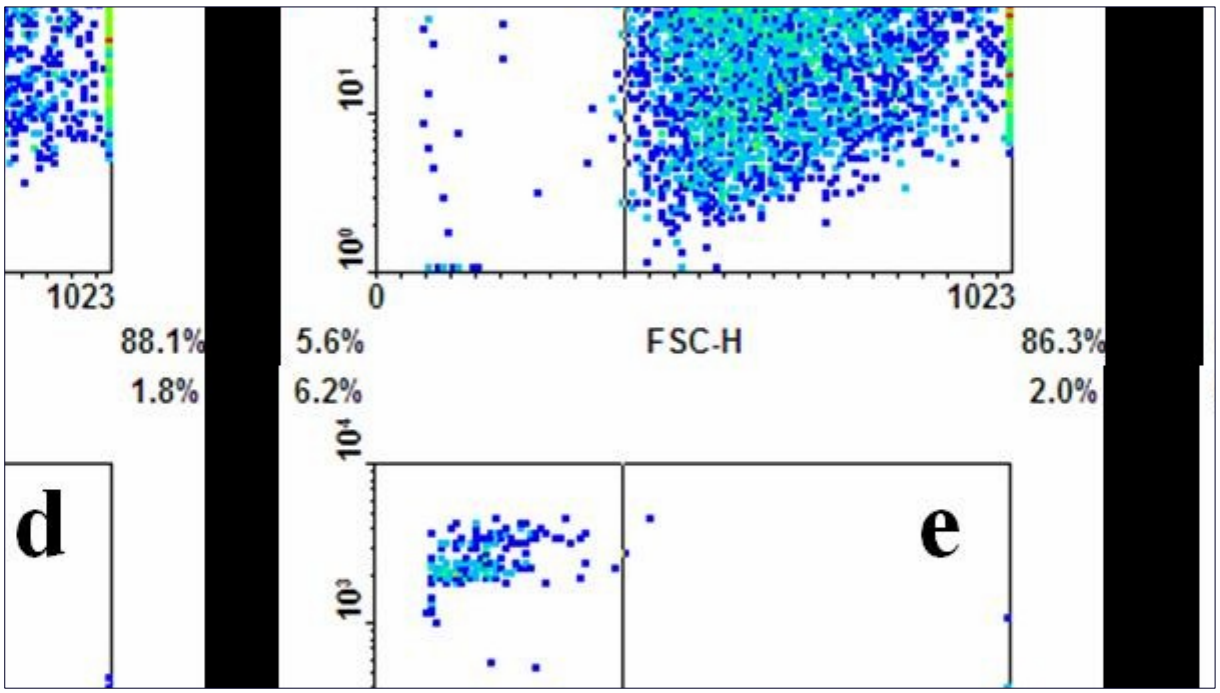

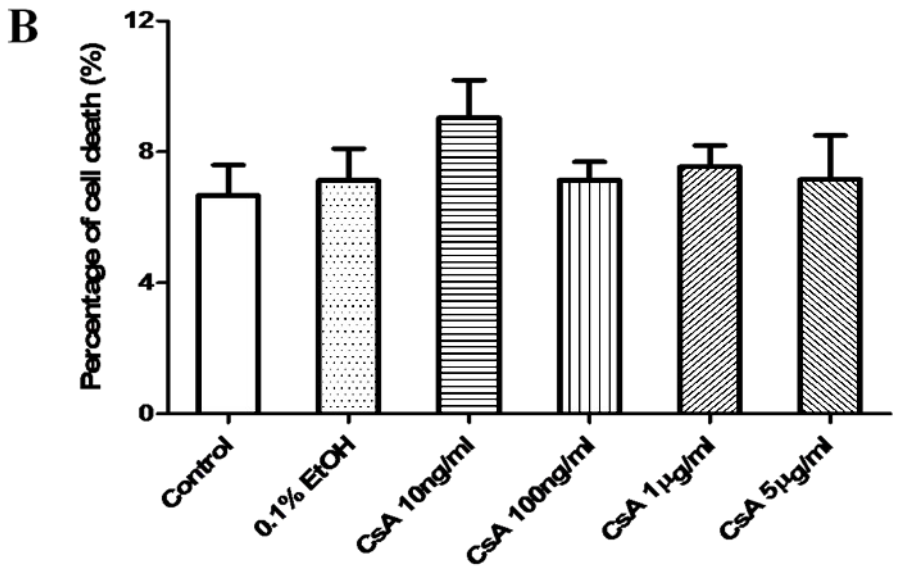

Figure 3.15 The effect of Cyclosporine on renal tubular epithelial cells viability.

HKC-8 cells were incubated with the medium (a) or medium in the presence of 0.1% ethanol (b) or Cyclosporine at the concentration of 10ng/ml (c), 100ng/ml (d), 1µg/ml (e) and 5µg/ml (f) for 72 hours. The stimulated cells were then incubated with PI before analyzing by flow cytometry. Panel A shows a density plot indicating the viability of HKC-8 in the FL2 channel. Panel B shows a bar graph illustrating the percentage of HKC-8 dead cells. The bars are the mean results and the error bars are the SEM. These results are from a single experiment.

3.8.8 Morphological changes following Cyclosporine treatment

A change in the morphology of epithelial cells is often used as a defining feature of EMT (Liu et al., 2004). This study (section 3.9.1) has already shown that HKC-8 cells adopt morphology typical of fibroblasts following TGF-β1 treatment. A further study was performed to examine any change in the morphology of these cells following treatment with Cyclosporine.

Semi-confluent HKC-8 cells were grown in medium or medium containing Cyclosporine at a concentration of 5µg/ml for 72 hours. The morphology of the HKC-8 cells was then examined under an inverted microscope.

Cells cultured in basal medium showed typical cobblestone morphology (Figure 3.16A). Cells cultured in medium containing Cyclosporine for 72 hours showed an elongated spindle-like morphology (Figure 3.16B). This suggests that, *in vitro*, a fibroblast-like morphology could be induced in renal tubular epithelial cells following Cyclosporine treatment. The morphological changes produced by Cyclosporine were similar to those induced by TGF-β1, indicating that Cyclosporine-induced morphological changes might be produced by TGF-β1.

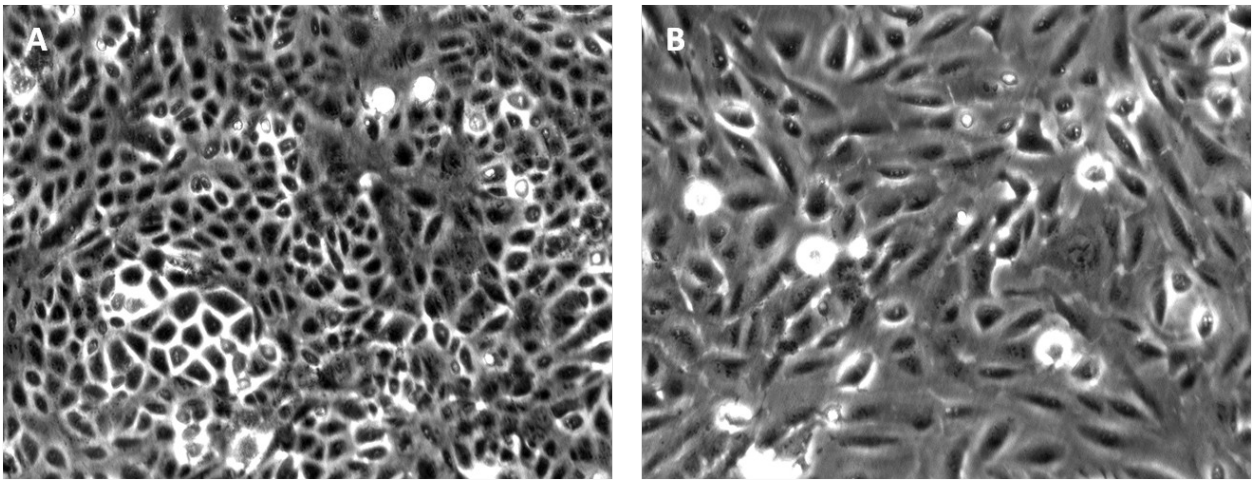

Figure 3.16 Morphology of renal tubular epithelial cells following Cyclosporine treatment.

The light microscopic analysis of the morphology of HKC-8 incubated in complete medium or medium containing Cyclosporine at a final concentration 5µg/ml for 72 hours. The normal cells (A) exhibited the cobblestone-like appearance, whereas the cells with Cyclosporine treatment adopted an elongated spindle-shaped morphology (B). The images were taken at x 200 magnification. The results are representative of 2 similar experiments.

3.8.9 Effect of Cyclosporine on adherent molecule expression in renal epithelial cells

It has already been demonstrated that E-cadherin, one of the main components constituting an adherent junction in epithelial cells, was disrupted by treatment with TGF-β1. Cyclosporine might have a similar effect on epithelial cells as TGF-β1. Therefore, the effect of Cyclosporine on E-cadherin expression was determined using microscopic immunofluorescence techniques.

Semi-confluent HKC-8 cells were incubated with Cyclosporine at concentrations of 10ng/ml, 100ng/ml, 1µg/ml and 5µg/ml for 72 hours in chamber slides. Control and vehicle-treated control cells were grown in medium or medium containing 0.1% ethanol respectively. Then, cells were stained with monoclonal mouse anti-E-cadherin antibody, followed by anti-mouse IgG FITC conjugated antibody (for detail of method see 2.5.1.4). E-cadherin expression (green fluorescence) was detected by confocal microscopy at 63 times magnification.

In normal HKC-8 cells, the typical linear pattern of E-cadherin was present at cell-cell junctions within confluent islands of epithelial cells (Figure 3.17A). In the presence of ethanol and Cyclosporine concentration less than 1µg/ml, the expression of E-cadherin was not different compared to control cells. However, treatment HKC-8 cells with Cyclosporine at concentrations of 1 and 5µg/ml clearly reduced E-cadherin expression (Figure 3.17 E-F). In addition, the immunofluorescence intensity was quantitatively measured using Leica confocal software and showed a significant reduction of E-cadherin expression by cells treated with 1 and 5µg/ml of Cyclosporine (Figure 3.17G). Although loss of E-cadherin is an important characteristic of EMT, it has been suggested that this is not necessarily followed by a change to a fibroblast phenotype (Veerasamy et al., 2009). Therefore, further experiments were performed to identify fibroblast marker expression by Cyclosporine-treated cells.

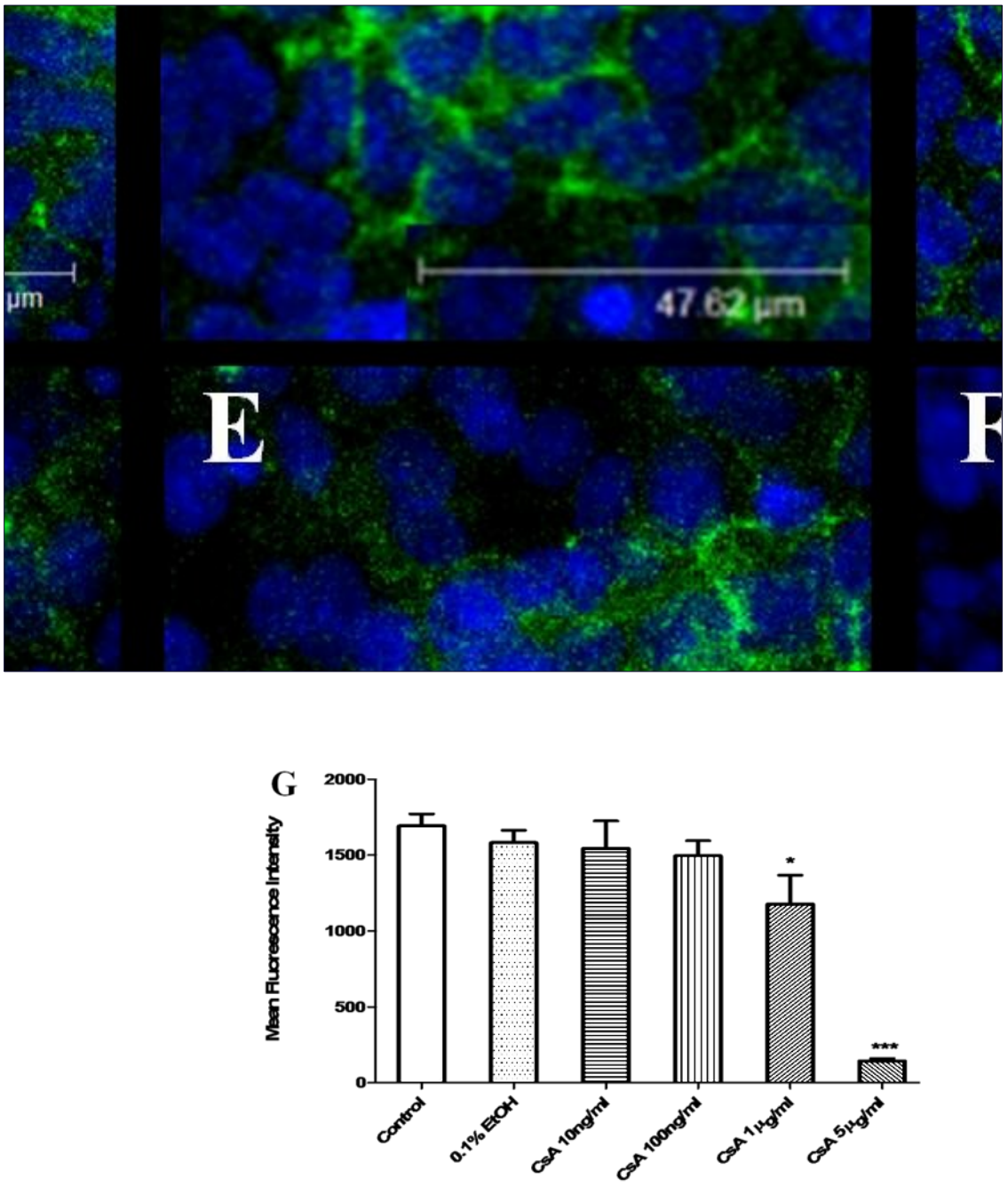

Figure 3.17 The expression of E-cadherin in renal tubular epithelial cells after Cyclosporine treatment.

The representative micrographic immunofluorescence analysis of E-caherin (Green) expression in HKC-8 cells incubated in normal medium (A) with 0.1% ethanol (B) or Cyclosporinet the concentration of 10ng/ml (C), 100ng/ml (D), 1µg/ml (E) and 5µg/ml (F) for 72 hours. The images were taken at x63 magnification. A bar graph (G) illustrating the immunofluorescence intensity of E-cadherin which was highly expressed in normal cells and significantly declined in the presence of Cyclosporinet 5µg/ml. The bars are the mean results and the error bars are the SEM. These results are representative of 2 similar experiments.

3.8.10 Effect of Cyclosporine on *de novo* mesenchymal marker expression.

Acquisition of fibroblast phenotypes is one of the characteristics of EMT. The next experiment was performed to determine whether Cyclosporine could change the phenotype of epithelial cells. Confluent HKC-8 cells were incubated with Cyclosporine at a concentration of 10ng/ml, 100ng/ml, 1μg/ml and 5μg/ml for 72 hours. Further cells were incubated with control and vehicle control media. Cells then were stained with rabbit monoclonal anti-S100A4, followed by anti-rabbit IgG FITC conjugated antibodies. The expression of S100A4 was visualised by confocal microscopy at x63 magnification.

Untreated HKC-8 cells showed slightly increased expression of cytoplasmic S100A4 similar to cells in the vehicle control (Figure 3.18A-B). The diffuse cytoplasmic expression of S100A4 increased when cells were treated with Cyclosporine. The level of S100A4 expression was dose-dependent and reached a maximum level at a Cyclosporine concentration of 1μg/ml. Surprisingly, however, S100A4 expression was reduced when cells were treated with 5μg/ml Cyclosporine.

It was not clear why the expression of S100A4 markedly reduced at Cyclosporine concentration 5μg/ml. However, this might be involved with the time-course of protein expression, post-translation processing, intra-individual/ inter-culture variability and the inhibition of cell proliferation.

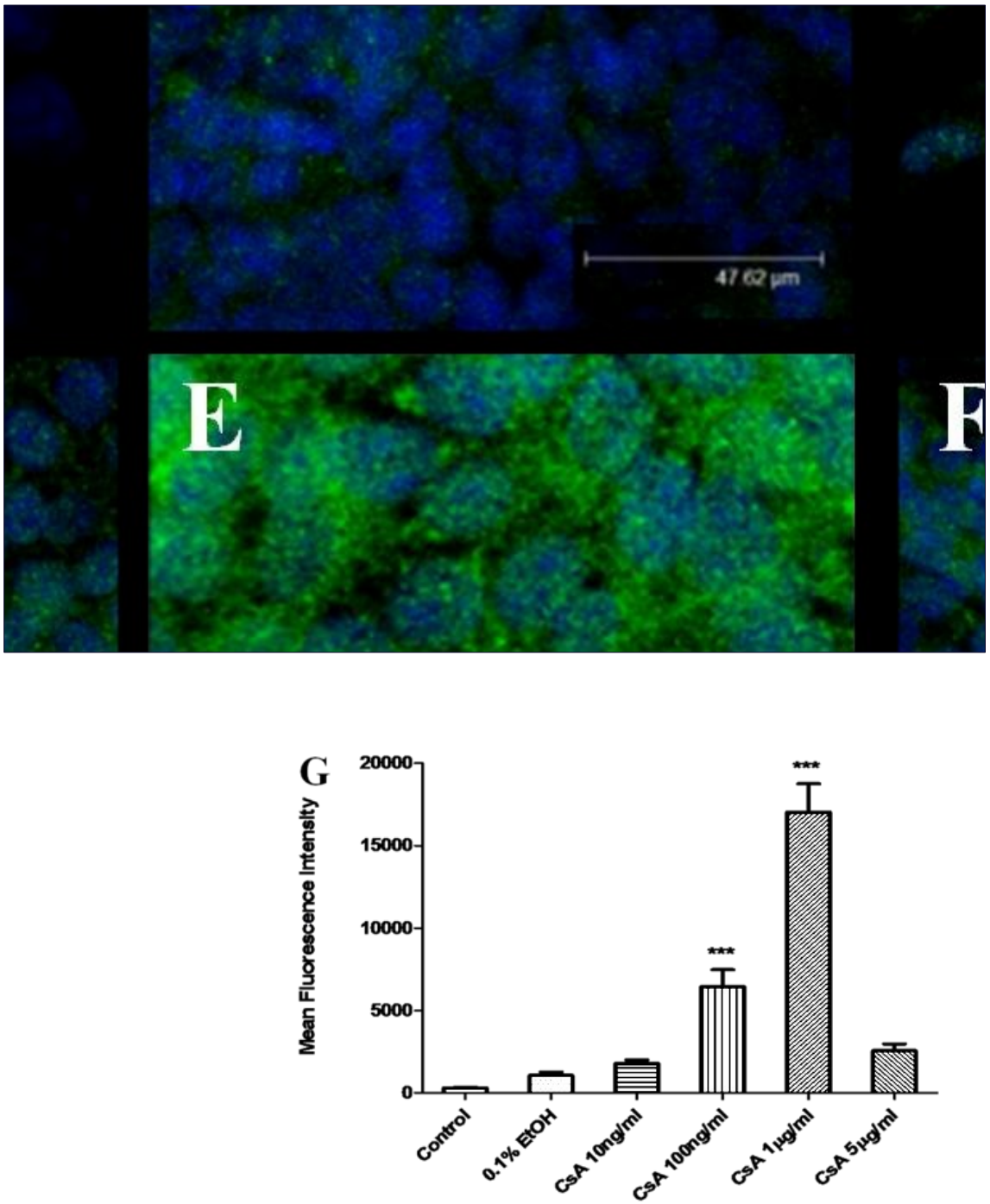

Figure 3.18 The expression of S100A4 in renal tubular epithelial cells after Cyclosporine treatment.

The representative micrographic immunofluorescence analysis of S100A4 (Green) expression in HKC-8 cells incubated in normal medium (A) with 0.1% ethanol (B) or Cyclosporine at a concentration of 10ng/ml (C), 100ng/ml (D), 1µg/ml (E) and 5µg/ml (F) for 72 hours. The images were taken at x63 magnification. (G) is a bar graph illustrating the immunofluorescence intensity of S100A4. The bars show the mean results and the error bars are the SEM. (*** = $p < 0.001$). The results are representative of 3 similar experiments.

3.8.11 SB-505124 partially prevented the loss of E-cadherin expression after Cyclosporine treatment

Cyclosporine was able to induce loss of E-cadherin expression. A similar result was observed for TGF-β1-treated cells. Therefore, it might be possible that Cyclosporine reduces E-cadherin expression as a consequence of activation of the TGF-β1 receptor. Functions of TGF-β require activation of TGF-β receptors including TGFβRI and TGFβRII (Section 1.9.2). In order to determine an association between Cyclosporine and TGF-β1, a selective inhibitor of the TGF-β type I receptor (SB-505124; ALK5 inhibitor), was added together with Cyclosporine. Confluent HKC-8 cells were incubated with 5μg/ml of Cyclosporine with or without 1-hour pre-treatment with 1μM of SB-505124 (see section 2.7.2) for 72 hours. E-cadherin expression was assessed by microscopic immunofluorescence staining and visualised by confocal microscopy at x63 magnification.

E-cadherin expression almost completely disappeared following 72 hours of Cyclosporine treatment; this loss was partially prevented by SB-505124 treatment (Figure 3.19C). Quantitative analysis of E-cadherin expression in the presence of SB-505124 also showed significantly greater expression compared to drug-treated cells without the TGF-β type I receptor inhibitor (Figure 3.19D).

It is clear that pre-treatment with the TGF-β type I receptor inhibitor partially attenuated the loss of E-cadherin expression, suggesting that Cyclosporine-induced loss of E-cadherin expression might be mediated by the TGF-β signalling pathway.

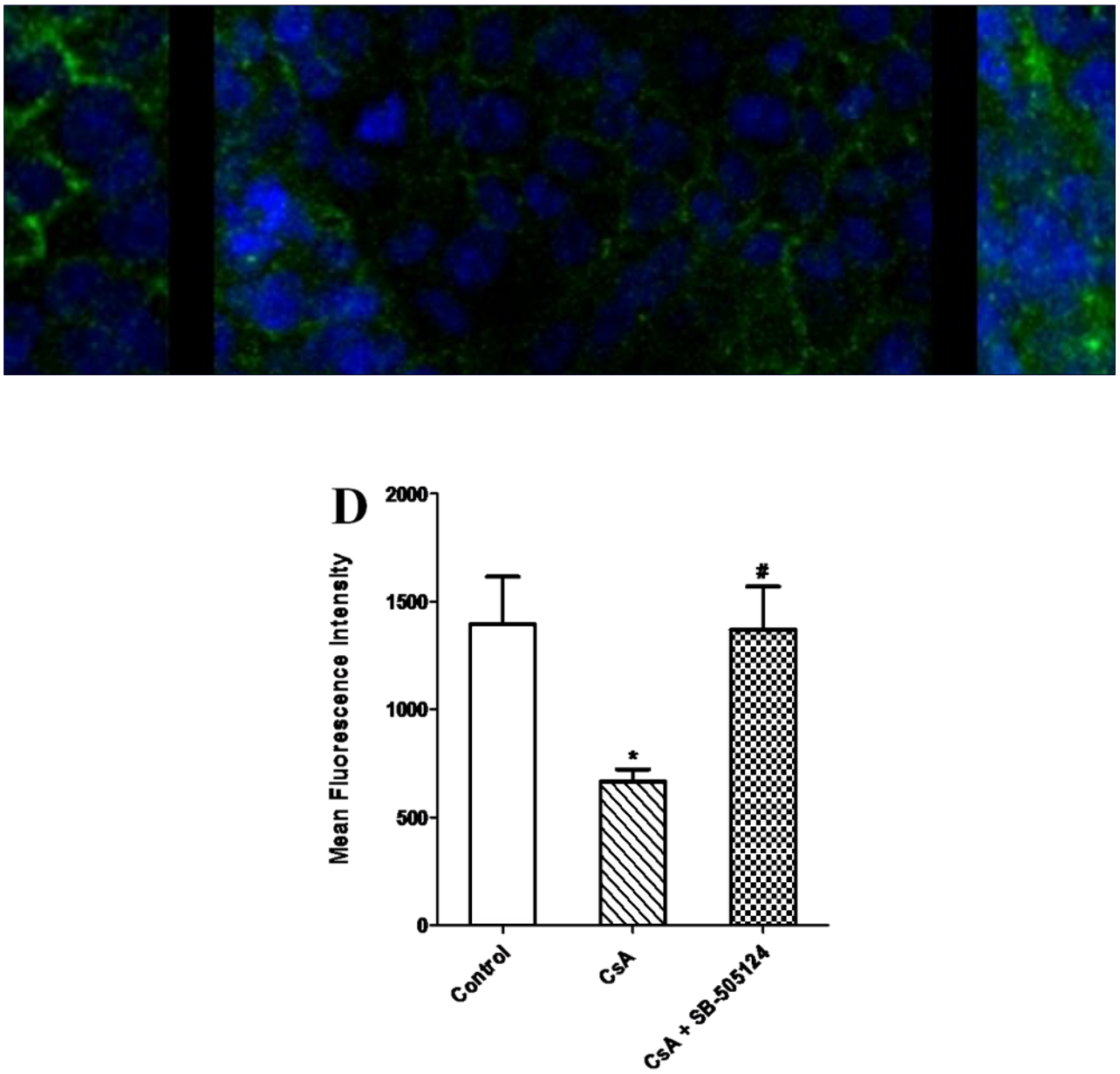

Figure 3.19 The preventive effect of ALK5 inhibitor (SB-505124) on E-cadherin expression after Cyclosporine treatment

The representative micrographic immunofluorescence analysis of E-cadherin expression (Green) in HKC-8 cells incubated with medium (A) or medium containing Cyclosporine 5µg/ml in the absence (B) or presence of SB-505124 pre-treatment (C). The images were taken at x63 magnification. (D) The bar graph illustrating the mean fluorescence intensity of E-cadherin which was significantly reduced after Cyclosporine treatment. However this effect could be significantly prevented by pre-treatment with SB-505124. The bars show mean results and the error bars are the SEM. The results are representative of 3 similar experiments. (* = $p < 0.05$ compared to control and # = $p < 0.05$ compared to Cyclosporine, ANOVA).

3.8.12 Pre-treatment with SB-505124 failed to reduce S100A4 expression after Cyclosporine treatment.

This study has been shown that S100A4 expression was induced by both Cyclosporine and TGF-β1 treatment. In this experiment confluent HKC-8 cells were treated with Cyclosporine 5μg/ml for 72 hours with or without 1 hour of pre-treatment with 1μM of SB-505124. S100A4 expression was detected by immunofluorescence staining and visualised by confocal microscopy at x63 magnification.

Cyclosporine-treated cells obviously up-regulated S100A4 expression compared to untreated cells (Figure 3.20A-B). However, pre-treatment with ALK5 inhibitor before adding Cyclosporine had no effect on this S100A4 induction (Figure 3.20C). In addition, the quantitative measurement of mean fluorescence intensity showed a significantly increased expression of S100A4 in both the Cyclosporine and ALK5 inhibitor pre-treatment group (Figure 3.20D).

Although the ALK5 inhibitor was able to partially prevent the loss of E-cadherin produced by Cyclosporine, a similar effect on S100A4 expression was not observed. This suggests that induction of S100A4 expression does not require the activation of TGFβRI.

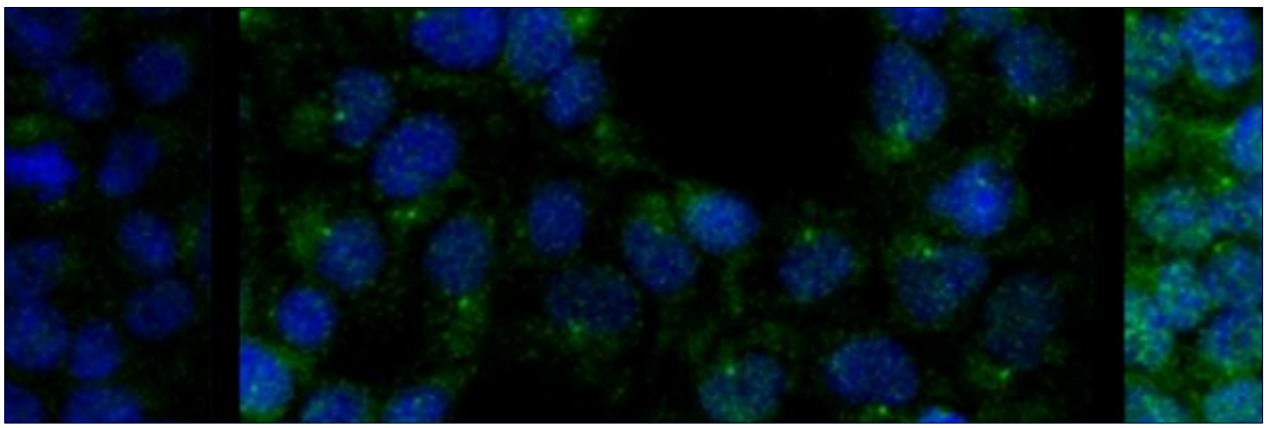

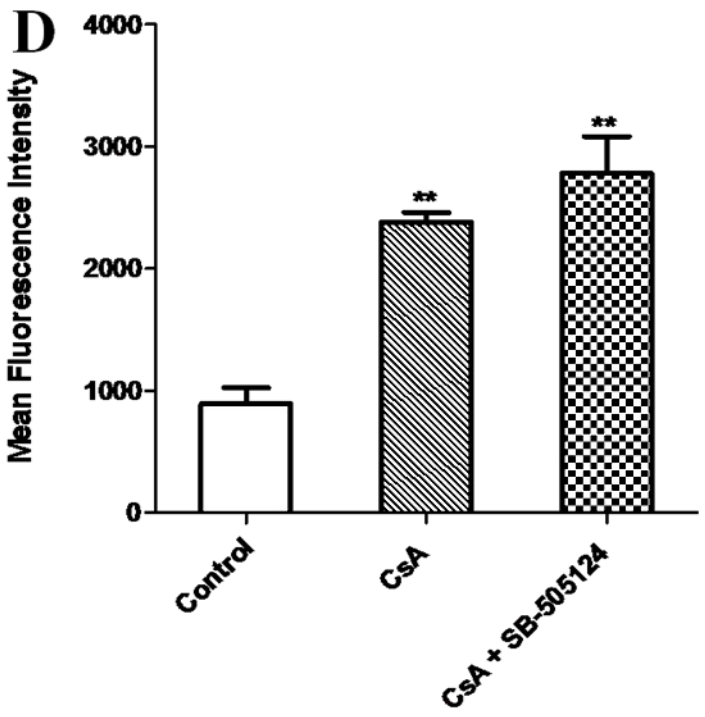

Figure 3.20 The preventive effect of SB-505124 on S100A4 expression after Cyclosporine treatment

The representative immunofluorescence analysis of S100A4 expression (Green) in HKC-8 cells incubated with medium (A) or medium containing Cyclosporine 5μg/ml in the absence (B) or presence of 1μM of SB-505124 pretreatment (C). The images were taken at x60 magnification. (D) shows the bar graph illustrating the mean fluorescence intensity of S100A4 which was significantly increased after Cyclosporine treatment. There was no protective effect of SB-505124 on S100A4 expression. The bars are mean results and the error bars are the SEM. The results are representative of 2 similar experiments. (** = $p < 0.01$ compared to control, ANOVA).

3.8.13 The expression of S100A4 gene in HKC-8 cells following Cyclosporine and TGF-β1 treatment

This study demonstrated the expression of S100A4 protein by HKC-8 following both TGF-β1 and Cyclosporine treatment. This experiment was performed to investigate the expression of S100A4 in molecular level by the quantitative real-time PCR.

Semi-confluent HKC-8 cells were incubated with 5μg/ml of Cyclosporine. The control samples were non-treated HKC-8 cells, while the positive control were cells treated with 5ng/ml of TGF-β1. The treatment period was 24 hours in all groups. GAPDH was used as an endogenous housekeeping gene to normalise mRNA levels between samples (Section 2.4.4).

Real-time PCR showed that TGF-β1 treated cells significantly up-regulated S100A4 mRNA level. However, treatment HKC-8 cells with Cyclosporine did not show any difference of S100A4 mRNA expression compared to the untreated HKC-8 cells (Figure 3.21).

This study showed that the high level expression of S100A4 protein produced by treatment with Cyclosporin A did not correlate well with changes in at the mRNA level. This suggests the involvement of post translational regulation.

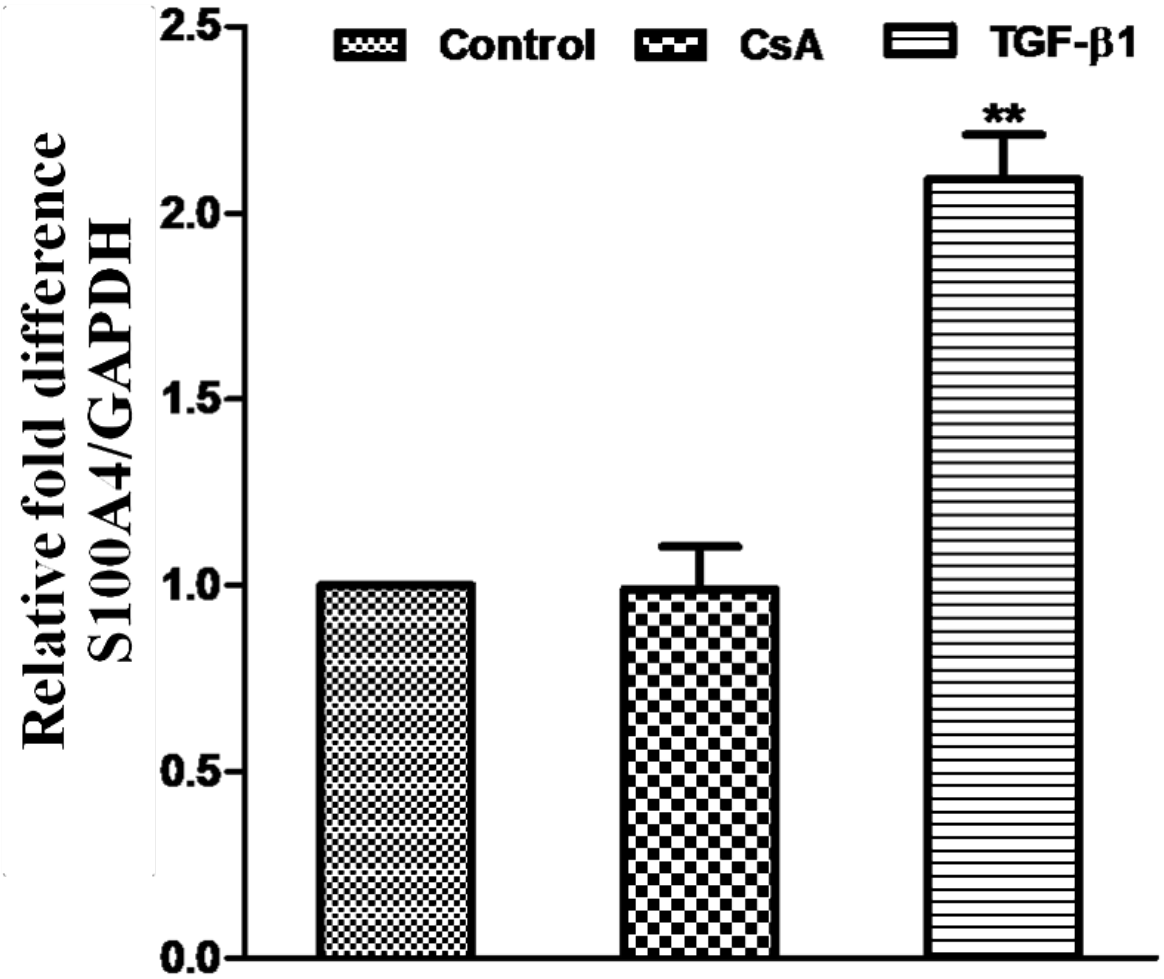

Figure 3.21 The expression of S100A4 mRNA after Cyclosporine and TGF-β1 treatment. Confluent HKC-8 cells were grown in medium or medium containing 5μg/ml of Cyclosporine or 5ng/ml of TGF-β1 for 24 hours. The S100A4 mRNA level was normalized to GAPDH mRNA and was presented as mean ± SEM (n=3). The S100A4 mRNA was significantly up- regulated in TGF-β1 treatment group, in contrast to the Cyclosporine treatment group which showed similar S100A4 gene level compared to control. The results are representative of 3 similar experiments. (** = $p < 0.01$ compared to control, ANOVA)

3.8.14 TGF-β1 expression by three different renal tubular epithelial cell lines following Cyclosporine and TGF-β1 treatment

This study was performed to determine whether treatment of 3 renal cell lines with Cyclosporine increases expression of the TGF-β1 gene.

Semi-confluent HKC-8, HK-2 and HRCE (section 2.2.3) were incubated in medium alone or medium containing 5μg/ml of Cyclosporine or 5ng/ml of TGF-β1 for 24 hours. RNA was extracted from stimulated renal epithelial cells and DNA was synthesised. GAPDH was used as a control housekeeping gene.

The TGF-β1 gene was significantly up-regulated in all TGF-β1 treated cells. However none of the Cyclosporine treated cells increased TGF-β1mRNA expression compared to the untreated cells (Figure 3.22). These results probably suggested that TGF-β1 did not mediate the transformation of epithelial cells but either other TGF-β subtype or other mediators might play a role in Cyclosporine-induced EMT in this cell model.

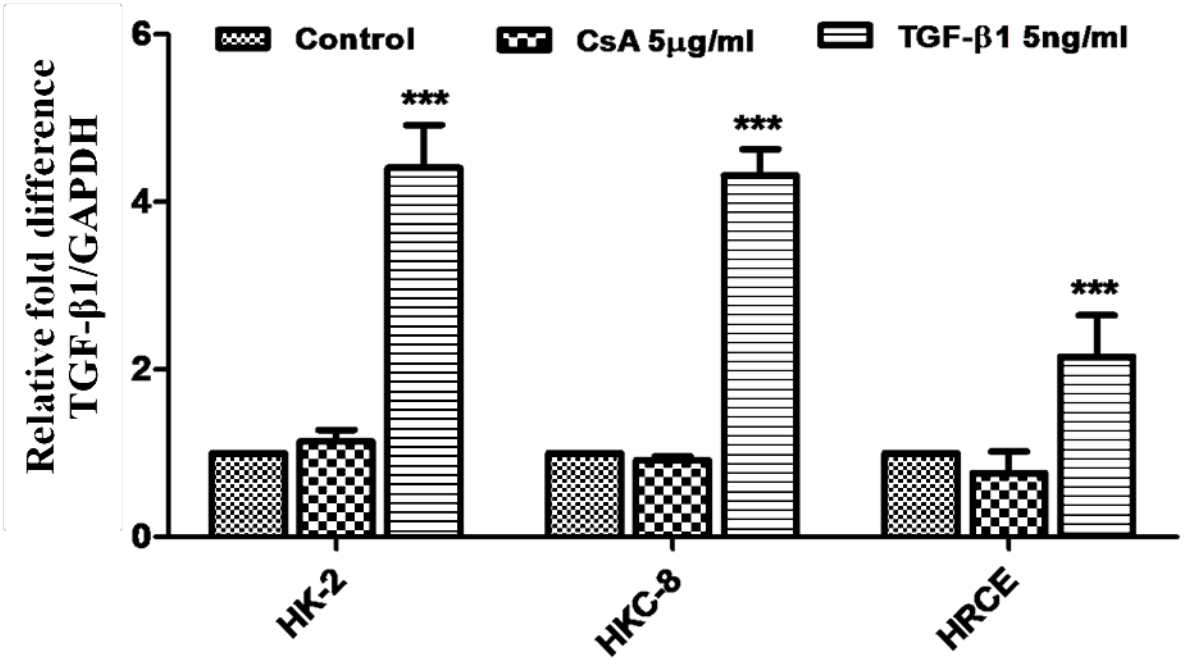

Figure 3.22 The comparison of real-time PCR analysis of the TGF-β1 mRNA expression among three different renal epithelial cell lines.

The semi-confluent HK-2, HKC-8 and HRCE cells were incubated in medium and medium containing 5μg/ml of Cyclosporine or 5ng/ml of TGF-β1 for 24 hours. The TGF-β1 mRNA was normalized to GAPDH mRNA and was presented as mean ± SEM (n=3). The TGF-β1 gene was significantly up-regulated after TGF-β1 treatment in all 3 cell lines. In contrast, there was no change of TGF-β1 mRNA level in Cyclosporine treatment group compared to control. The results are representative f 3 similar experiments. (*** = $p < 0.001$ compared to control)

3.8.15 The effect of Cyclosporine on active TGF-β1 protein production by renal epithelial cells

This study has shown that Cyclosporine is able to induce the loss of E-cadherin and increase S100A4 expression by renal epithelial cell lines; similar results were also obtained following TGF-β1 treatment. Therefore, it seems that Cyclosporine has a direct effect on renal tubular epithelial cells which might be mediated by TGF-β1. However, the generation of mRNA encoding TGF-β1 could not be demonstrated by real-time PCR. It is possible that Cyclosporine can alter the expression of other isoforms of TGF-β or the response to preformed TGF-β1 by activating the latent protein.

The cell-based MFB-F11 assay is a TGF-β bioassay which has ability to measure all forms of active TGF-β. Normally, TGF-β is secreted in a latent form and needs to be activated before binding to a receptor. This study selected heat as a latent TGF-β activator (section 1.10.1.2). Therefore, results from all experiments were shown as a comparison between non-activated and activated samples of each medium.

Initially, the basic TGF-β level was observed in complete medium, serum-free medium, 0.1% ethanol and 5μg/ml of Cyclosporine as a baseline control. Only complete medium contained any TGF-β activity, which was probably derived from foetal bovine serum (Figure 3.23). After that, the measurement of TGF-β in supernatant from Cyclosporine treated HKC-8 cells was performed. Confluent HKC-8 cells were incubated with serum-free medium containing 0.1% ethanol and 5μg/ml of Cyclosporine for 72 hours, and then supernatant was collected and processed following protocol, by being activated and further incubated with confluent MFB-F11 cells for 48 hours. These reporter cells produced alkaline phosphatase which was detected by using a luminometer measured at 405 nm.

After activating by heat, all groups showed high level of TGF-β and there was no difference between the groups (Figure 3.24). This experiment showed that HKC-8 cells could produce TGF-β and, interestingly, Cyclosporine did not enhance TGF-β secretion by renal tubular epithelial cells compared to the control.

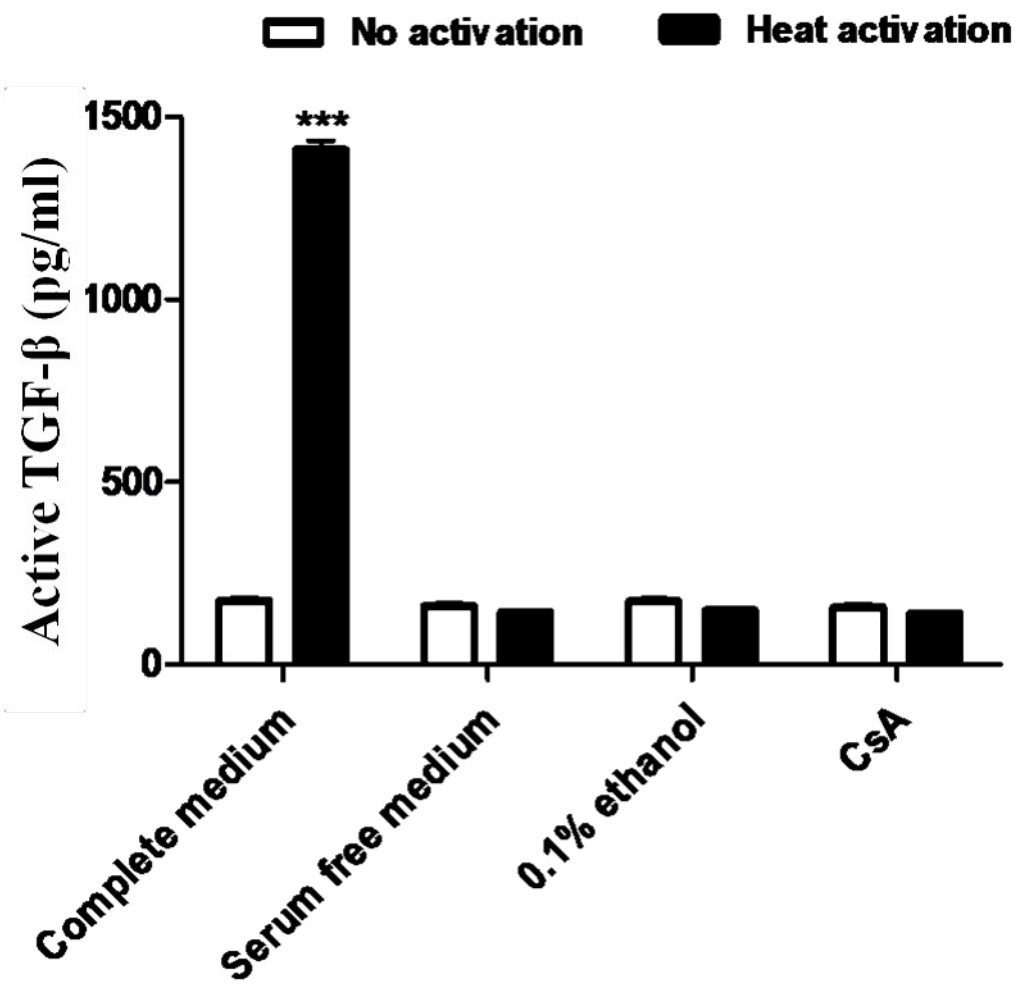

Figure 3.23 Bioassay analysis of active TGF-β level of reagents in a cell free experiment. Semi-confluent MFB-F11 cells were incubated in complete medium or serum free medium with or without 0.1% ethanol or Cyclosporine 5μg/ml for 48 hours. Medium containing serum showed significant higher level of TGF-β1 after activated at 80°C for 10 minutes. In contrast, there was no increase of active TGF-β1 in serum free medium, the vehicle and Cyclosporine after activation. The bars represent mean results (n=3) and the error bars means SEM. The results are representative of 3 similar experiments. (*** = $p < 0.001$)

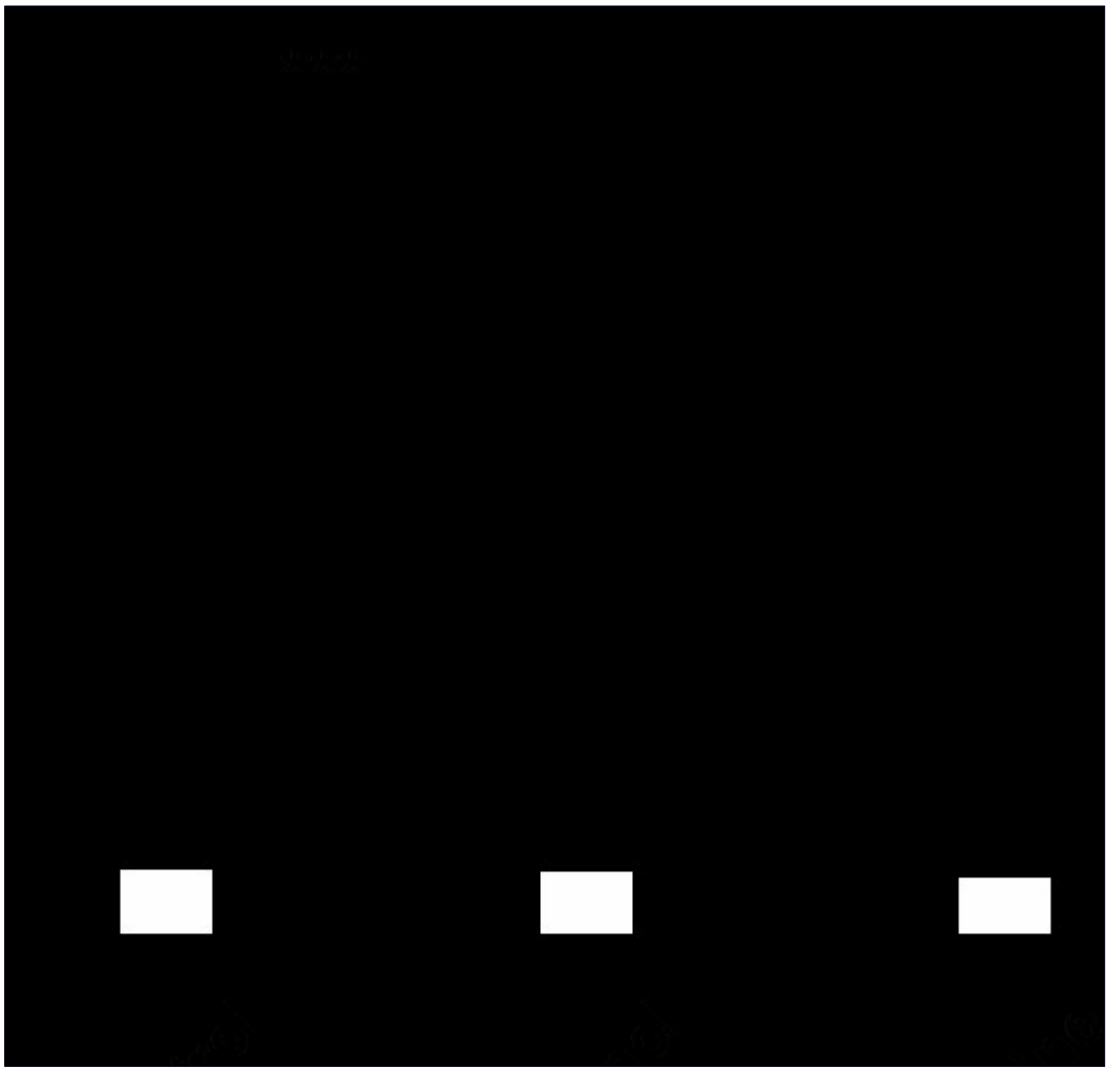

Figure 3.24 Bioassay analysis of the bioactive TGF-β level in culture medium of renal tubular epithelial cells after Cyclosporine treatment.

Semi-confluent HKC-8 cells were incubated in serum free medium with or without 0.1% ethanol and Cyclosporine 5μg/ml for 72 hours. The supernatants were collected and an aliquot was activated by heat before incubating with MFBF-11 cells for 48 hours. The TGF-β1 level was significantly increased in all 3 groups of HKC-8 cells (B). However, there was no difference among them. The bars are mean results (n=3) and error bars are SEM. These results are representative of 3 similar experiments. (*** = $p < 0.001$)

3.8.16 Active TGF-β1 detection from the culture medium of Cyclosporine treated HKC-8 cells by ELISA

In order to support the findings from the TGF-β bioassay, the measurement of the TGF-β level was repeated by using an ELISA kit (R&D system). The ELISA kit activates latent form of TGF-β by acidification method and detects all TGF-β isoforms including TGF-β1, TGF-β2 and TGF-β3.

Semi-confluent HKC-8 cells were incubated with serum free medium with or without 0.1% ethanol or 5μg/ml of Cyclosporine for 72 hours. The supernatant from treated cells was collected and processed following the instructions provided with the kit. The results showed no difference of active TGF-β level in the control, vehicle control and Cyclosporine (Figure 3.25). The findings from this study suggested that Cyclosporine could not induce HKC-8 to increase TGF-β production.

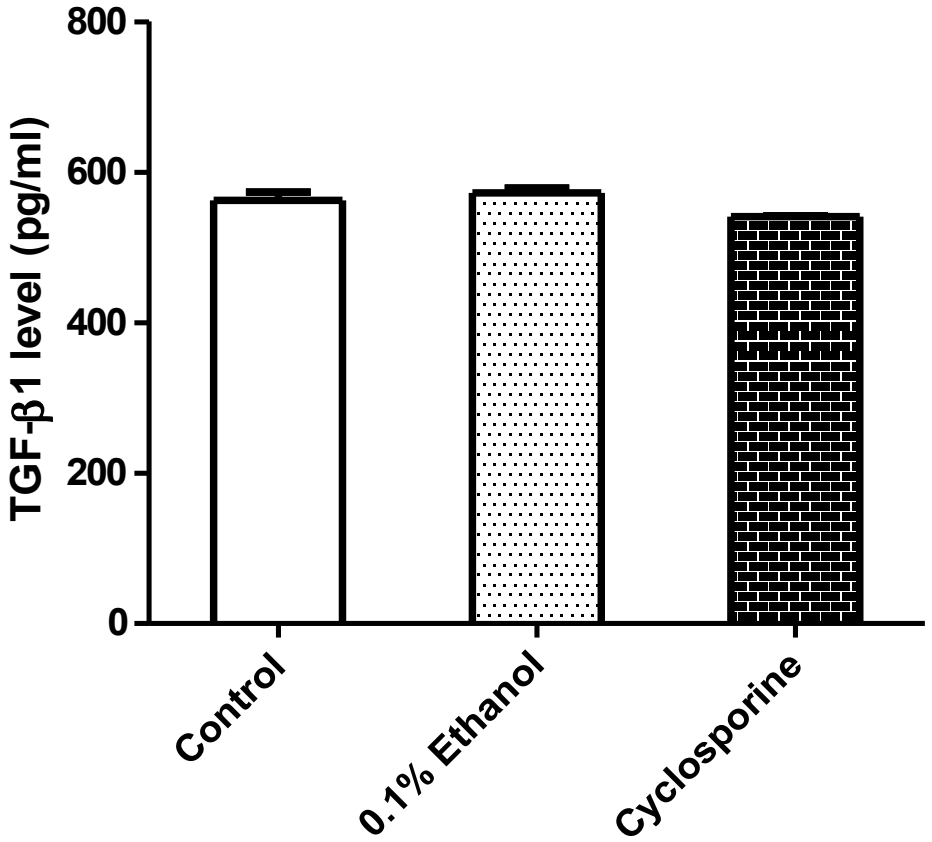

Figure 3.25 ELISA assay analysis of active TGF-β1 level from supernatant of HKC-8 cells.

Confluent HKC-8 cells were incubated in serum free medium and medium containing 0.1% ethanol or Cyclosporine 5μg/ml for 72 hours. The supernatants were collected and processed for ELISA. The ELISA showed no difference in TGF-β1 production in the presence of medium, 0.1%ethanol and CsA. The bars are mean results (n=3) and error bars are SEM. The results are from a single experiment.

3.9 Summary and discussion

3.9.1 Results summary

EMT was induced in renal tubular epithelial cell lines by TGF-β1, leading to morphological change, loss of the cell-cell adhesion molecule, E-cadherin, and *de novo* expression of mesenchymal phenotypes, S100A4 and α-SMA.

- An immunosuppressive concentration of Cyclosporine had no effect on the viability of renal tubular epithelial cells.
- A high concentration of Cyclosporine (5μg/ml) significantly suppressed renal tubular epithelial cell proliferation at 48 and 72 hours.
- Cyclosporine induced EMT-like changes in renal tubular epithelial cells, including the loss of E-cadherin expression and up-regulation of S100A4.
- The TGF-β1 receptor type I inhibitor, SB-505124 partially prevented E-cadherin disruption by Cyclosporine. However, this protective effect did not affect the expression of S100A4.
- S100A4 mRNA was significantly up-regulated after treatment with TGF-β1 while Cyclosporine did not change S100A4 mRNA expression compared to the control cells.
- Cyclosporine-treated cells did not up-regulate TGF-β1 mRNA expression in contrast to TGF-β1-treated cells which showed a significant up-regulation of the TGF-β1 gene.
- The MFB-F11 bioassay demonstrated that active TGF-β level was not strikingly increased in the supernatant from Cyclosporine treated renal tubular epithelial cells compared to untreated cells.
- An ELISA assay showed no significant increase of active TGF-β level in HKC-8 culture medium following Cyclosporine treatment compare to untreated cells.

3.9.2 Discussion

Cyclosporine is a potent immunosuppressive drug which is widely used in organ transplantation, producing greatly enhanced kidney allograft survival (Krönke et al., 1984). In addition, it is increasingly being introduced for the treatment of autoimmune diseases such a psoriasis (Maza et al., 2011) and rheumatoid arthritis (Migliore et al., 2010). However, the major limiting factor in the use of Cyclosporine is chronic nephrotoxicity which leads to irreversible renal failure, characterised by extensive tubulointerstitial fibrosis (Myers et al., 1988).

It has been demonstrated that EMT plays a significant role in TGF-β-mediated fibrosis (Iwano et al., 2002). Chronic cyclosporine nephrotoxicity induces a similar pathology (Slattery et al., 2005). In this study, it was demonstrated that exposure to Cyclosporine

induced an EMT-like event in human proximal tubular cell lines. This study showed that the characteristics of EMT were present after treating HKC-8 cells with TGF-β1. These included (i) morphological change from cuboidal epithelial cells to elongated spindle-shaped cells, (ii) decreased E-cadherin expression and (iii) up-regulation of S100A4 expression by immunofluorescence staining. This is consistent with findings of previous studies (Yang and Liu, 2001).

The immunosuppressive potential of Cyclosporine was demonstrated using a ^{3}H-Thymidine incorporation assay. The IC50 of Cyclosporine was approximately 0.05ng/ml. However, this might not reflect the optimal concentration to use in this study since it has been shown that renal fibrosis often associated with high blood level of Cyclosporine. Although the therapeutic level of Cyclosporine is approximately 200ng/ml, which is very low compared to the concentration used in this study, the metabolism of this drug in the human body and *in vitro* are different. This study followed previous studies which suggested that Cyclosporine at concentration 5µg/ml could induce EMT in the proximal renal tubular cell line, HK-2 (McMorrow et al., 2005; Slattery et al., 2005). Therefore, most of the experiments in this study used Cyclosporine at 5µg/ml for determining the role of Cyclosporine in the induction of EMT in HKC-8 cells.

The effects of cyclosporine on the proliferation and viability of HKC-8 cells were also evaluated. It was shown that 5µg/ml of Cyclosporine suppressed cell proliferation after 48 hours, whereas there was no effect on cell viability. This was in contrast to the previous study which showed no effect of 5µg/ml Cyclosporine to both proliferation and vitality on HK-2 cells (McMorrow et al., 2005). This probably resulted from the different cell lines, although they were both derived from human proximal renal tubular cells. In addition, it has been reported that *trans*-activation of p21 mediates the arrest of the cell cycle following Cyclosporine-induced p53 accumulation (Lally et al., 1999). A previous study in human proximal tubular epithelial cells (PTEC) suggested that cell death was observed using Cyclosporine at a concentration higher than 10µg/ml (Bakker et al., 2002). Since the highest concentration used in this study was 5µg/ml, this might explain why significant cell death was not observed.

E-cadherin is an epithelial cell specific intercellular adhesion molecule. Several studies have demonstrated that E-cadherin is an important determinant for maintenance of the epithelial phenotype (Zeisberg et al., 2003; Arias, 2001). Furthermore, the transition of an epithelial cell into a mesenchymal phenotype is shown by changes in the reciprocal expression of E-

cadherin and S100A4. E-cadherin expression gradually decreases while S100A4 expression increases (Zeisberg et al., 2003). The current study showed decreased expression of E-cadherin protein following Cyclosporine treatment; this was similar to the results produced by TGF-β1 treatment. However, it has been demonstrated that loss of E-cadherin does not always lead to an acquisition of mesenchymal-like phenotypes (Veerasamy et al., 2009). Thus, demonstration of mesenchymal marker expression was essential to identify EMT.

S100A4 has been reported to be a marker for fibroblasts (Strutz et al., 1995) though it also can be expressed by several types of immune cells including monocytes, lymphocytes and macrophages. However, renal tubular epithelial cells normally do not express S100A4, thus S100A4 was used in this study model. In the HKC-8 cell line, the S100A4 protein was up-regulated following Cyclosporine treatment for 72 hours. However, this up-regulation was not seen at the mRNA level, whereas TGF-β1-treated cells showed significantly increased S100A4 mRNA. In addition, this study showed that a different concentration of Cyclosporine showed different effect on S100A4 expression, for example Cyclosporine at 1μg/ml strongly induced S100A4 expression while Cyclosporine at 5μg/ml induced less intensity of S100A4 expression. This might be explained by several mechanisms including (i) the variability of post-translational process of S100A4 protein; (ii) the non-specificity of S100A4 as a fibroblast marker (Le Hir et al., 2005); (iii) the high concentration of Cyclosporine might have effect on proliferation of HKC-8 cells; and (iv) the time-course expression of low and high concentration of Cyclosporine might be different.

S100A4 belongs to a family of EF-hand calcium-binding proteins, which are well known to be multifunctional proteins. However the main function of S100A4 is enhanced cell migration and invasion (Schneider et al., 2008). The wide range of functions is due in part to the formation of various complexes both within and outside the cell. One such mechanism is heterodimerisation. Examples include the interaction between S100A4 and S100A1 from mouse mammary adenocarcinoma cell lines (Tarabykina et al., 2000), the heterodimer formation between S100B and S100A6 in human melanoma cell lines (Yang et al., 1999), and the association between S100A8 and S100A9, which regulate the adhesion of neutrophil (Newton and Hogg, 1998). In addition, a recent study of rheumatoid arthritis patients found the up-regulation of S100A4 in synovial fluid. Interestingly, this S100A4 was present in different conformational forms; however, the majority was a high molecular weight form (tetramer or higher) (Klingelhöfer et al., 2007). Therefore, it is possible that a huge amount of S100A4 expression from immunofluorescence staining was a complex form of S100A4 protein which is processed through various post-translational modifications such as phosphorylation,

deamidation, glutathionylation or cysteinylation (Haugen et al., 2008). Furthermore, the S100A4 may be associated with other proteins such as tropomyosin, p37, p53, methionine aminopeptidase, liprinβ1, CCN3 and myosin heavy chain (Haugen et al., 2008). Analysis of the expression of mRNA encoding S100A4 by quantitative RT-PCR demonstrated constitutive high level expression of this sequence (with Ct of 25), but this did not change following treatment of the cells with Cyclosporine. By contrast, immunohistochemistry showed a clear increase in the expression of S100A4 in the cytoplasm of cells. This discontinuity between mRNA and protein levels is consistent with post-transcriptional regulation of the expression of S100A4 which may be related to the increased stability of this protein after complex formation within the cell. A previous study has shown that a significant reduction in the mRNA encoding S100A4 mediated by transfection with shRNA, resulted in no significant change in the expression of macromolecular S100A4 complexes (although the expression of monomeric S100A4 was reduced) (Rygiel et al., 2010).

TGF-β is a major inducer of EMT during development, carcinogenesis and fibrosis. TGF-β1 was first reported as an inducer of EMT in normal mammary epithelial cells (Miettinen et al., 1994). Since then, TGF-β1 has been shown to mediate EMT *in vitro* in a number of different epithelial cells, including renal proximal tubular cells (Fan et al., 1999). This study demonstrated that Cyclosporine treatment led to changes in cell morphology and E-cadherin and S100A4 protein expression similar to those produced by TGF-β1 treatment. However, in the current study, when the TGFβRI was blocked with SB-505124, no change in S100A4 protein expression was observed, though the reduction of expression of E-cadherin protein was partially inhibited. This study did not demonstrate the effect of SB-505124 on the expression of E-cadherin, S100A4 and α-SMA. This limitation made the results of the SB-505124 experiment hard to interpret.

In real-time PCR, the Cyclosporine treated PTEC did not express TGF-β1 mRNA, whereas TGF-β1 was significantly up-regulated in TGF-β1 treated cells. Furthermore, the level of active TGF-β was determined by both MFB-F11 bioassay and the ELISA method. These assays showed no significant level of active TGF-β in culture medium Cyclosporine-treated PTEC. Although the effects of Cyclosporine were mediated in large parts via induction of TGF-β1, other studies could not confirm the mediation by TGF-β1 (Strutz personal communication). It is possible that other mediators such as ILK (Integrin-link kinase) (Li et al., 2003) and IGF-2 (Insulin growth factor-2) (Arciniegas et al., 2006) may be involved in EMT induction.

There are other studies investigating the association between Cyclosporine and EMT in renal epithelial cells. However these studies typically use HK-2 proximal renal tubular cells which show similar characteristics to the HKC-8 cells used in the current study (Slattery et al., 2005; McMorrow et al., 2005). These previous studies showed that Cyclosporine at a concentration of 5μg/ml was not toxic to HK-2 cells. In addition, treatment with this concentration of Cyclosporine led to a change in epithelial morphology which was supported by the rearrangement of F-actin and β-catenin. Furthermore, Cyclosporine induced a reduction in E-cadherin expression and the up-regulation of α- SMA, TGF-β and CTGF mRNA expression. These changes were inhibited by pre-treatment with a TGF-β neutralising antibody (McMorrow et al., 2005), suggesting not only an important role for TGF-β, but also the existence of TGF-β during Cyclosporine-induced epithelial transformation. However, an isotype-matched antibody control was not described in the paper; thus, the inhibitory effect of TGF-β neutralising antibody might be compromised. In contrast, TGF-β expression at mRNA and protein levels was not observed in the current study despite using a similar Cyclosporine concentration and treatment time. However, the current study does support a role for Cyclosporine-induced renal tubular epithelial transformation *in vitro*.

Chapter 4: A potential role for EMT in T cell-induced renal allograft fibrosis

4.1 Introduction

The two most common causes of long-term renal allograft loss are death with functioning graft and chronic allograft dysfunction (CAD) (Cornell and Colvin, 2005). CAD is defined as a functional and morphological deterioration of renal allograft function starting at least 3 months after transplantation (Safinia et al., 2010). The causes of CAD can be classified into immune dependent and non-immune dependent factors. An example of the latter is chronic CsA nephrotoxicity, which was discussed in chapter 3. This chapter will focus on the impact of immune dependent factors, in particular the role of T cell-mediated CAD.

4.2 Fibrosis: a final common pathway for chronic renal allograft dysfunction

The pathology of CAD is associated with fibrotic changes in the renal allograft, which include global or segmental glomerulosclerosis, hyaline material deposition in small arteries or arterioles or interstitial fibrosis and tubular atrophy (IF/TA) (Solez et al., 2007). Graft fibrosis is a final common pathway which results from both immune and non-immune mediated graft injury. Previously, renal graft fibrosis was described as chronic allograft nephropathy (CAN). However, this term was misused as a diagnosis for graft fibrosis from all causes instead of defining the specific causes, and the term IF/TA is now used to describe fibrosis with unidentified causes (Solez et al., 2007).

4.2.1 The relationship between cellular rejection and graft fibrosis

It is clear that the incidence of acute rejection has progressively been reduced, in contrast to long-term graft survival which remains unchanged. Interestingly, several papers have reported the potential impact of acute rejection on CAD, despite the low rate of acute rejection (Nankivell et al., 2001; Meier-Kriesche et al., 2004; Khalkhali et al., 2010). This might be explained by the observation that renal function after rejection episodes does not return to baseline after treatment (Meier-Kriesche et al., 2004). Additionally, in an era of protocol biopsies, the histology of subclinical rejection (SCR), which is characterized by tubulointerstitial mononuclear cell infiltration without concurrent functional deterioration (Sis et al., 2010), has been observed in the first

three weeks after transplantation in 31% of normal function grafts (Krejčí et al., 2011). Moreover, several papers have reported an association between the presence of SCR and chronic tubulointerstitial damage and development of IF/TA (Nankivell et al., 2001; Nankivell et al., 2004; Shishido et al., 2003). Graft survival rates with SCR were 88.4% and 62.3% at 1 year and 10 years respectively, whereas 1-year and 10-year normal graft survival rates were 97.9% and 96.2% (Choi et al., 2005). Interestingly, true chronic rejection, defined by persistent SCR for 2 or more years, appeared in only 5.8% of patients (Nankivell et al., 2004). Therefore, it remains possible that T cells are involved in renal allograft fibrosis.

4.2.1.1 Alloreactive $CD8^+$T lymphocytes target renal tubular epithelial cells during acute T cell-mediated rejection

T cell-mediated rejection is characterised by interstitial infiltration by T cells (Sis et al., 2010). According to the Banff classification, diagnosis of T cell-mediated rejection (TCMR) is based on histological assessment of the infiltrate, including the presence of lymphocytes in renal tubules (tubulitis), the interstitial area or the subendothelial arteries or arterioles (endothelialitis) (Solez et al., 2007). The extent of inflammatory cell infiltration is used in the Banff system for diagnosing and grading the severity of rejection and, additionally, also correlates with graft function (Racusen et al., 1999).

In situ hybridisation has shown that $CD8^+$ cytotoxic T lymphocytes (CTL) are the predominant infiltrating T cells in renal tubules during acute TCMR (Robertson et al., 1996). A subsequent study has shown CD103 (the αEβ7 integrin) expression by approximately 60-70% of intratubular $CD8^+$T cells (Hadley et al., 1997); the αEβ7 integrin is known to promote interactions between lymphocytes with epithelial cells (Hadley et al., 1997). This integrin was first identified in human intraepithelial lymphocytes (IEL) in the gut (Cerf-Bensussan et al., 1987), but it is expressed by only about 2% of circulating T cells (Cerf-Bensussan et al., 1987).

It has been suggested that the αEβ7 integrin mediates adhesion of IEL to epithelial cells through the specific ligand, E-cadherin (Cepek et al., 1994). E-Cadherin is a tissue-restricted adhesion protein expressed specifically by many epithelial cells (Corps et al., 2003); see section 1.3.2. The engagement of CD103 on CTL with E-cadherin promotes cell lysis via cytotoxic granule release. Cytotoxic granules released

from CTL contain perforin and granzymes. Perforin forms pores in the cell membrane of the epithelium in order to allow granzymes entry into the cell, resulting in cell lysis (Halloran, 2010). A study of mouse kidney allografts has demonstrated the association between severe tubular deterioration and $CD103^+$CTL. However this was not mediated by αEβ7 integrin/E-cadherin adhesion or granzyme-perforin cytotoxic mechanisms but by a cell contact-independent mechanism related to delayed-type hypersensitivity and tubulitis (Einecke et al., 2006).

4.2.1.2 Interleukin (IL)-15 supports long-lived $CD103^+$ $CD8^+$ T cells

As described in section 4.1.2, a longitudinal study has observed that 5.8% of subclinical rejection persisted in kidney grafts for 2 or more years (Nankivell et al., 2004). A study of human kidney graft biopsy tissue has also shown that renal tubular epithelial cells up-regulate IL-15 expression from 10% at baseline to 35% during acute rejection, as well as during the post rejection period (Wong et al., 2003). Furthermore, intratubular T cells co-expressed both CD8 and the α-chain of the IL-15 receptor during acute rejection (Wong et al., 2003). The basic functions of IL-15 are to activate and promote clonal T cell expansion and to suppress apoptotic T cell deletion (Robertson et al., 2003). However, IL-15 alone cannot induce $CD103^+CD8^+$T cell differentiation, which requires TGF-β that is produced locally by renal tubular epithelial cells (Wong et al., 2003). Therefore, synergy between IL-15 and TGF-β maintains the population of intratubular $CD103^+CD8^+$ T cells after acute rejection. These cells might induce chronic IF/TA.

4.2.1.3 TGF-β links intraepithelial $CD8^+$T cells and renal graft fibrosis

It is known that stressed renal tubular epithelial cells produce a range of cytokines, such as IL-6 and IL-1β, and chemokines including CCL-2, CCL-3, CCL-4, CCL-5, and in particular TGF-β (Robertson et al., 2004). This locally produced TGF-β has an ability to induce CD103 expression by intratubular $CD8^+$T cells during acute rejection. Data from our group also support TGF-β-induced CD103 expression *in vitro* (Figure 4.1). Furthermore, once acute rejection has subsided, synergy between TGF-β and IL-15 supports the long-term survival of a relatively quiescent memory $CD8^+$T-cell population. A study of renal allograft tissue sections has shown that the

presence of intratubular $CD8^+$T cells is commonly associated with S100A4-expressing renal tubular epithelial cells (Figure 4.2) (Robertson et al., 2004). Further *in vitro* experiments have shown that a model intraepithelial T cell line can directly induce tubular epithelial cells to undergo transformation to fibroblasts and myofibroblasts (Robertson et al., 2004). Currently, EMT is recognized as a potential mechanism for the pathogenesis of fibrogenesis in the kidney. It is clear that TGF-β is essential for the development of both $CD103^+$T cells and EMT.

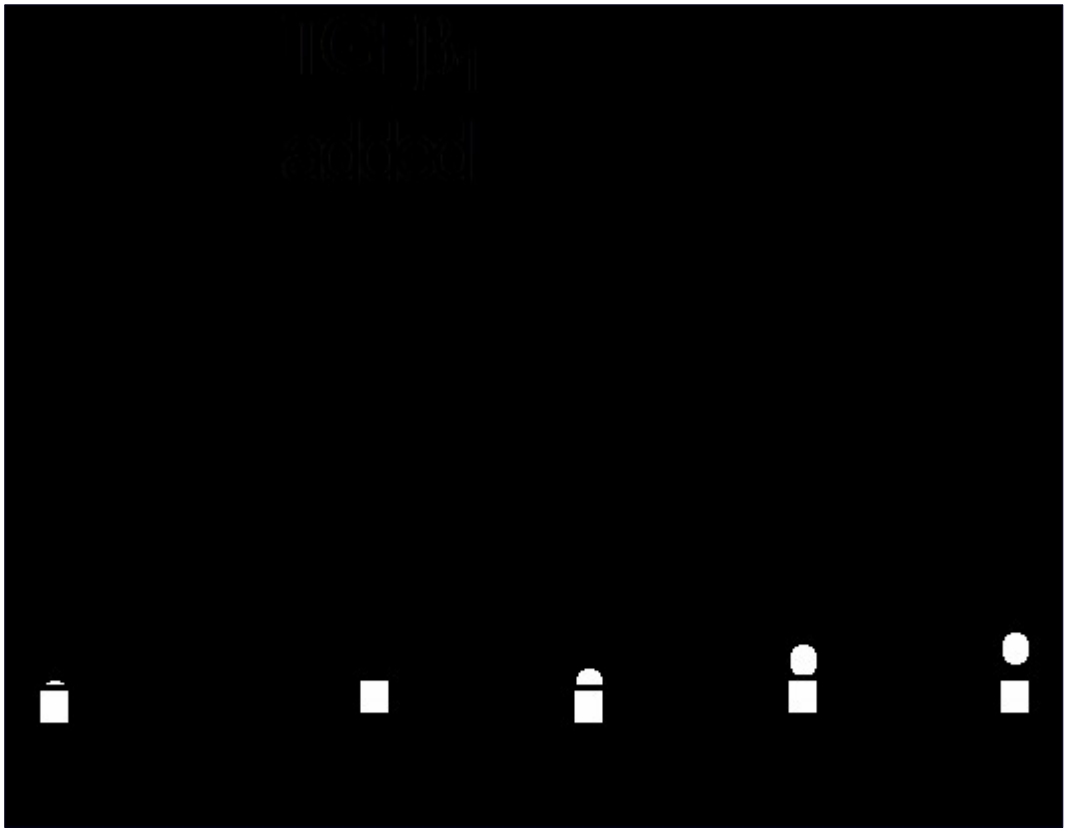

Figure 4.1 Graph demonstrating the percentage of CD103-expressing T cells.
During allogenic MLR, fewer than 8% of $CD8^+$T cells and 2.5% of $CD4^+$T cells expressed CD103. However, after TGF-β1 treatment, the proportion of CD103 expressing cells increased, with 52% of $CD8^+$T cells expressing CD103; the proportion of $CD4^+$ T cells expressing CD103 had also increased to 22%. This image is taken from Wong et al, 2003.

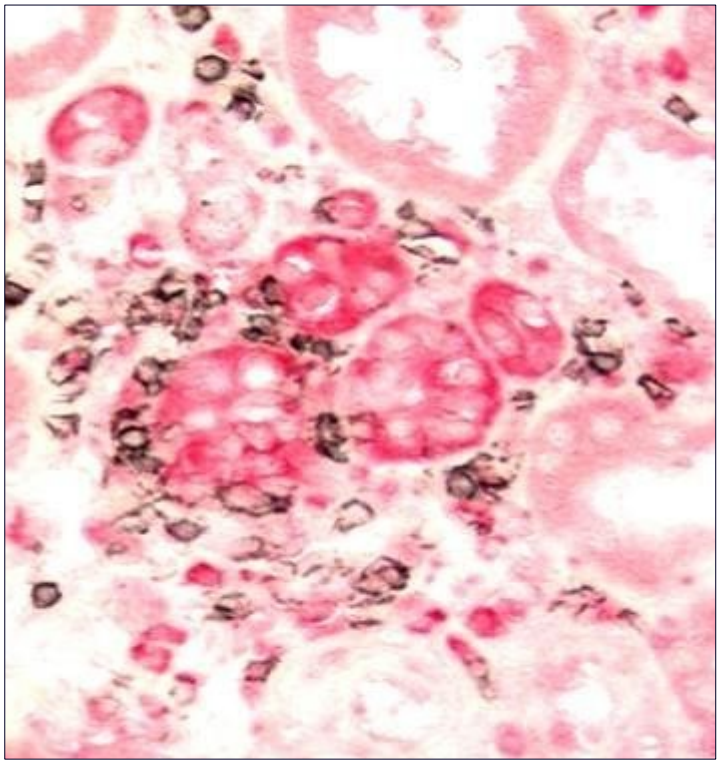

Figure 4.2 Co-localization of $CD8^+$T cells (black) and S100A4-expressing (red) tubular epithelial cells during acute renal allograft rejection. The image is obtained from Robertson et al., 2004.

4.3 The co-expression of CD103 and LAP on the surface of T cells

$CD103^+CD8^+$T cells have been implicated in renal allograft destruction during acute rejection. However, in a rat liver transplantation study, $CD103^+CD8^+$ T cells shared functions and mechanisms with regulatory T cells (Treg) (Lu et al., 2009). It has been demonstrated that the αEβ7 integrin was upregulated on $CD8^+$ T cells after liver transplantation and these cells remained in the graft recipient for a long time (Lu et al., 2009). Moreover, an *in vitro* study has shown that TGF-β or alloantigen induce $CD103^+CD8^+$ Treg. In addition, the immunoregulatory activity of Treg was shown to be cell-cell contact dependent manner (Lu et al., 2009).

LAP (latency associated peptide) is cleaved from the N-terminal sequence of the precursor TGF-β protein by the action of furin proteases during protein maturation (section 1.7.1). An i*n vitro* study has shown that activated $CD4^+CD25^+$ T cells to produce both surface-bound and secreted TGF-β (Nakamura et al., 2001). It has been observed that regulatory T cells function by a cell-to-cell contact dependent mechanism

(Thornton and Shevach, 1998). The surface TGF-β may be activated by molecules on the T cell surface or target cell surface, then the active TGF-β binds to its receptor for signal transduction and the induction of phenotypic differentiation.

A recent study of SLE (systemic lupus erythematosus) patients with haematopoietic stem cell transplantation has reported an increase of $CD8^+Foxp3^+$Treg post transplantation. This $CD8^+$ Treg showed more suppressive effects than $CD4^+CD25^+$ T cells and highly expressed both CD103 and LAP (Zhang et al., 2009).

Chapter 4: A potential role for EMT in T cell-induced renal allograft fibrosis

4.4 Aim

Chronic cellular infiltration is one of the key factors in kidney allograft fibrosis. The origin of these fibroblasts remains unclear. However, EMT is one of the potential mechanisms for the fibrosis.

This study will define the potential of T cells to induce de-differentiation (EMT) of human renal tubular epithelial cells by:

- Demonstration that EMT can be induced in renal epithelial cell lines by human T cells.
- Demonstration that TGF-β signalling is associated with T cell-mediated EMT.
- Demonstration of the expression of CD103 and LAP on the MOLT-16 T cell line and human primary T cells.

4.5 Material and Methods

4.5.1Cell lines

4.5.1.1 MOLT-4 cell line

The MOLT-4 T cell line was established from cells taken from a 19-year old male patient with a relapse of acute lymphoblastic leukaemia, following multidrug chemotherapy (Minowada and Moore, 1975). This cell line does not produce immunoglobulin or Epstein-Barr virus, but has tumorigenic capacity (Minowada et al., 1972). MOLT-4 T cell line belongs to the intermediate thymocyte category based on expression of CD1, CD2, CD5 and CD6 on more than 50% of the cells. Minority of MOLT-4 T cells express CD4 and CD8 but CD3 is negative (Minowada et al., 1985). MOLT-4 T cells were grown in RPMI 1640 complete medium (section 2.2) in a vertical 75 cm^2 tissue culture flask. They were passaged as described in section 2.1.1.2 at a ratio of 1:4 when the cell density reached over $2x10^6$cells/ml. The culture medium was changed every 2-3 days. These cells were used as a $CD103^-$ control T cell line.

4.5.1.2 MOLT-16 T cell line

The MOLT-16 T cell line is a human leukemic T cell line which was established from the peripheral blood of a 5-year-old girl with T cell acute lymphoblastic leukaemia (T-ALL) (Drexler and Minowada, 1989). MOLT-16 T cells are round or elongated with single cells growing in suspension. MOLT-16 T cell line appears to have an immature thymocyte phenotype which includes the absence of CD1, CD4 and CD8, and the presence of CD2, CD3, CD5 and CD7 (Minowada et al., 1985. In addition, it has been demonstrated that MOLT-16 T cells also expressed CD103 and LAP on their cell surface (Rygiel et al., 2008). MOLT-16 T cells were cultured in RPMI 1640 complete medium in 75cm^2 tissue culture flasks in a vertical position and split at a ratio of 1:3 when the cell density reached $2x10^6$cells/ml.

4.5.2 Immunocytochemistry

4.5.2.1 Immunofluorescence staining for cell co-culture system

In order to examine the induction of EMT by T cells, HKC-8 cells were seeded in 4-well plastic chamber slides. When the HKC-8 cells reached a semi-confluent stage, $1x10^5$ MOLT-16 T cells were added to each well. After 72 hours' co-culture, the slides were washed in PBS three times. Cells were then fixed in pre-cooled acetone at -20°C for 10 minutes, and then air-dried. The fixed cells were processed as described in section 2.5.2.4.

4.5.2.2 Addition of SB-505124 to the cell co-culture system

TGF-β signaling and its role in T cell-mediated EMT was investigated by applying the ALK5 inhibitor SB-505124 (section 2.7.2). Briefly, HKC-8 cells were cultured in chamber slides until they reached a semi-confluent stage. An optimal 1 μM of SB-505124 was added and incubated with the HKC-8 cells at 37°C for 1 hour. After the pre-treatment, MOLT-16 T cells were then added and co-cultured with HKC-8 cells for 72 hours. The cells were washed in PBS three times and then fixed and stained as described in section 2.5.2.

4.5.3 Compensation for two-colour flow cytometry

The emission spectra of fluorescent dyes are broad. While the peak emission is clearly separated for each dye, there is considerable overlap between dyes. In this study, fluorescein (FITC) and phycoerythrin (PE) dyes were used to detect two different antigens on the same cell. It has been shown that some of the light emitted by FITC passes through the filter used for PE; this is called spectrum overlap (Figure 4.3). The result of this spectrum overlap is that cells labelled with FITC will appear to have some PE fluorescence. In order to obtain a correct representation of the data, a correction (colour compensation) is required. The compensation was established by running unstained cells and cells stained with each antibody-fluorochrome conjugate individually (single stain) and analyzing the data using 2-colour dot plots (Figure 4.4A). The compensation settings were adjusted by keeping the stained cells in line with the unstained background cells and parallel to the appropriate axis. For FITC-conjugated, antibody stained cells, the FL2-%FL1 setting was adjusted so that the FL1 cells were horizontally aligned with the FL1 negative (Figure 4.3B). Then, with the PE-conjugated antibody stained cells, the FL1-%FL2 setting was adjusted until the FL2 cells were vertically aligned with the FL2 negative cells (Figure 4.4C). The compensation was then fine-tuned by running 2-colour control samples stained with FITC and PE monoclonal antibodies (Figure 4.4D).

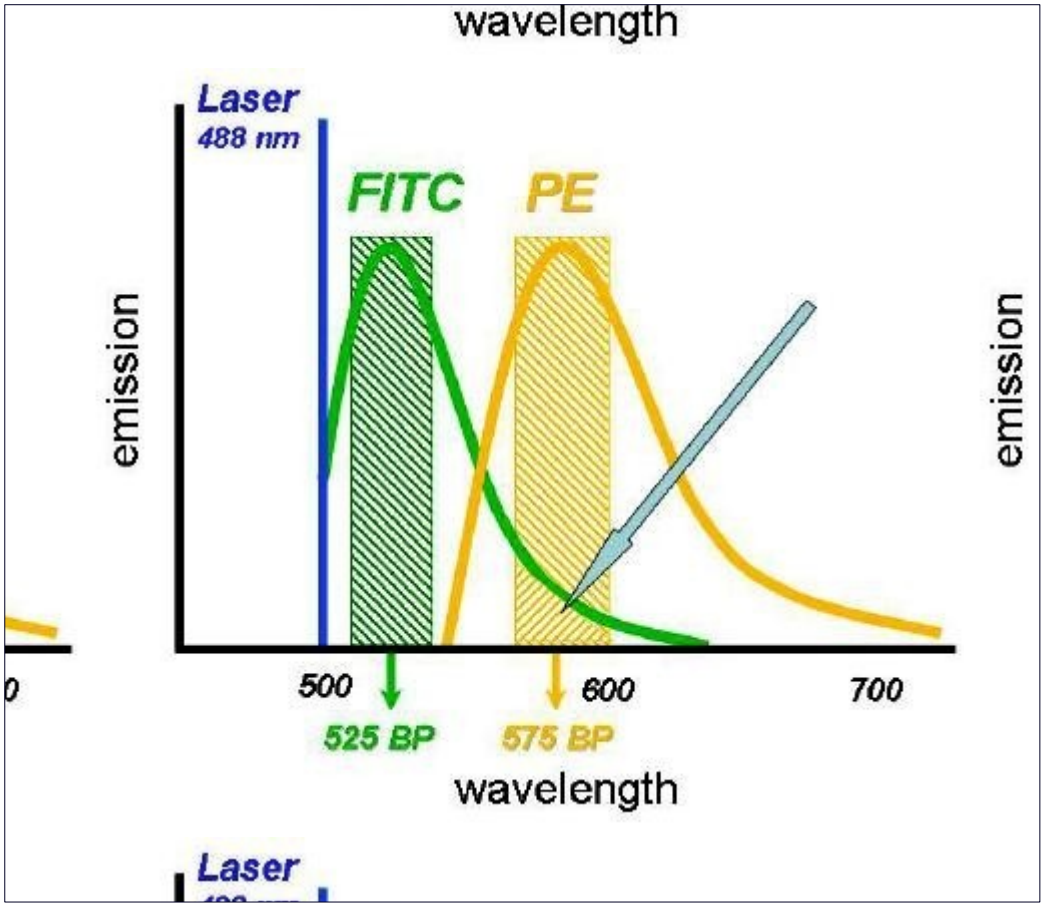

Figure 4.3 The emission spectra of fluorescein (FITC) and phycoerythrin (PE) fluorescent overlap.

The image is obtained from flow cytometry-A basic introduction book, Michael G Ormerod (http://flowbook.denovosoftware.com/).

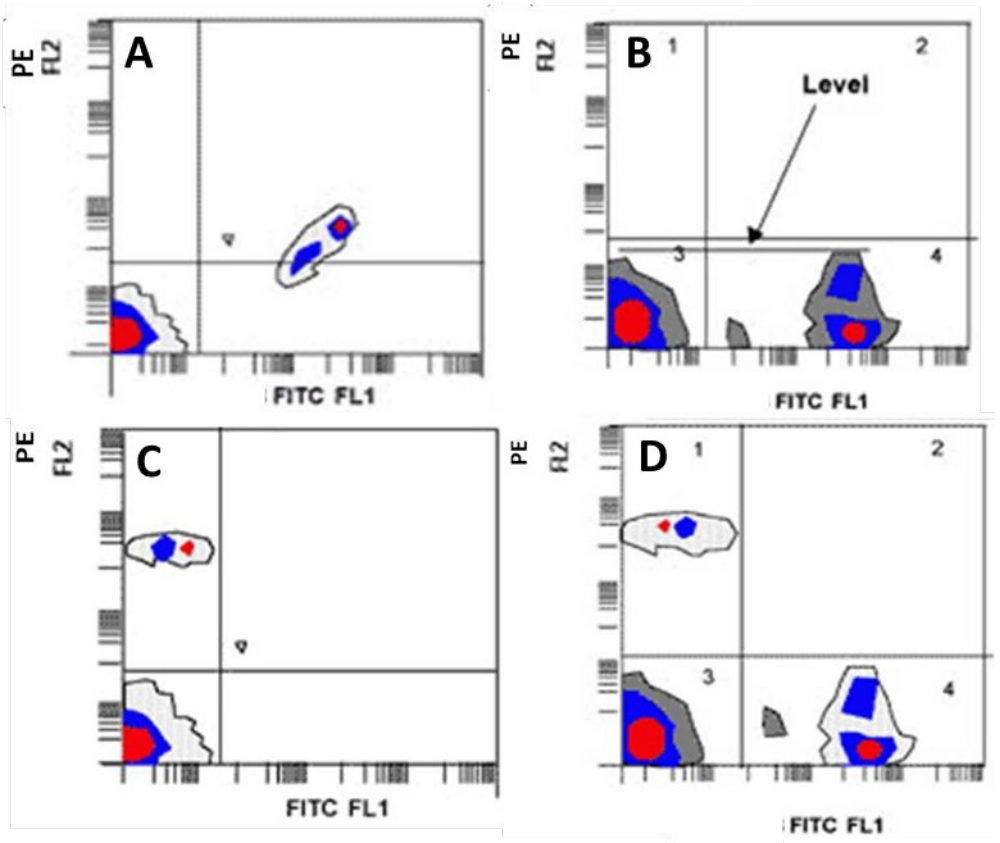

Figure 4.4 Two colour compensation for flow cytometry.

The compensation settings were adjusted by running individually stained samples to adjust the compensation (A). For FITC-conjugated antibody stained cells, the FL2-%FL1 setting was adjusted so that the FL1 cells were horizontally aligned with the FL1 negative (B). Then, with the PE-conjugated antibody stained cells, the FL1-%FL2 setting was adjusted until the FL2 cells were vertically aligned with the FL2 negative cells (C). The setting was again adjusted with the dual colour stained samples (D). (From basic information on fluorescence compensation, the UC Berkeley Campus, US)

4.5.4 Fluorescence-activated cell sorting (FACS)

FACS is a specialised type of flow cytometry, which can separate and isolate cells that are phenotypically different from each other, based on the specific light scattering and/or fluorescent characteristics of each cell.

The process begins by placing the cell suspension into a tube and forcing the cells to enter a narrow flowing stream of liquid. The cells travel down the nozzle which is vibrated at an optimal frequency to produce drops at a fixed distance from the nozzle. As the cells flow down the stream of liquid, they are scanned by a laser. Some of the laser light is scattered by the cells and detected by a number of

photomultiplier tubes; this signal is used to count the cells. This scattered light can also be used to measure cell size.

If the separation of a subpopulation of cells is required, the cells of interest are typically defined using an antibody linked to a fluorescent dye, which binds to an antigen on the surface of the cells of interest. The laser light excites the dye which emits a colour of light that is detected by the photomultiplier tube, or light detector. By collecting the information from the light (scatter and fluorescence) a computer can determine which cells are to be separated and collected. As the drop forms, an electrical charge is applied to the stream and the new drop will form with that charge. The charged drops are then deflected left or right by charged electrodes for collection in sample tubes (Figure 4.5).

This study focused on separating TGF-β treated T cells into $CD103^-$ and $CD103^+$ sub-populations. Briefly, T cells were isolated from the blood of healthy volunteers (section 2.2.5). Resting T cells were then activated with CD3/CD28 Dynabeads® for 72 hours. After the activation, activated T cells were incubated with 10ng/ml of TGF-β for 72 hours. After the incubation, the cells were incubated with anti-CD103 FITC-conjugated antibody (1:10) for 30 minutes on ice. The cells were washed in PBS and resuspended in 2%FBS/PBS. The cell suspension was sorted by FACSAria II sorter (BD Biosciences) (Figure 4.6).

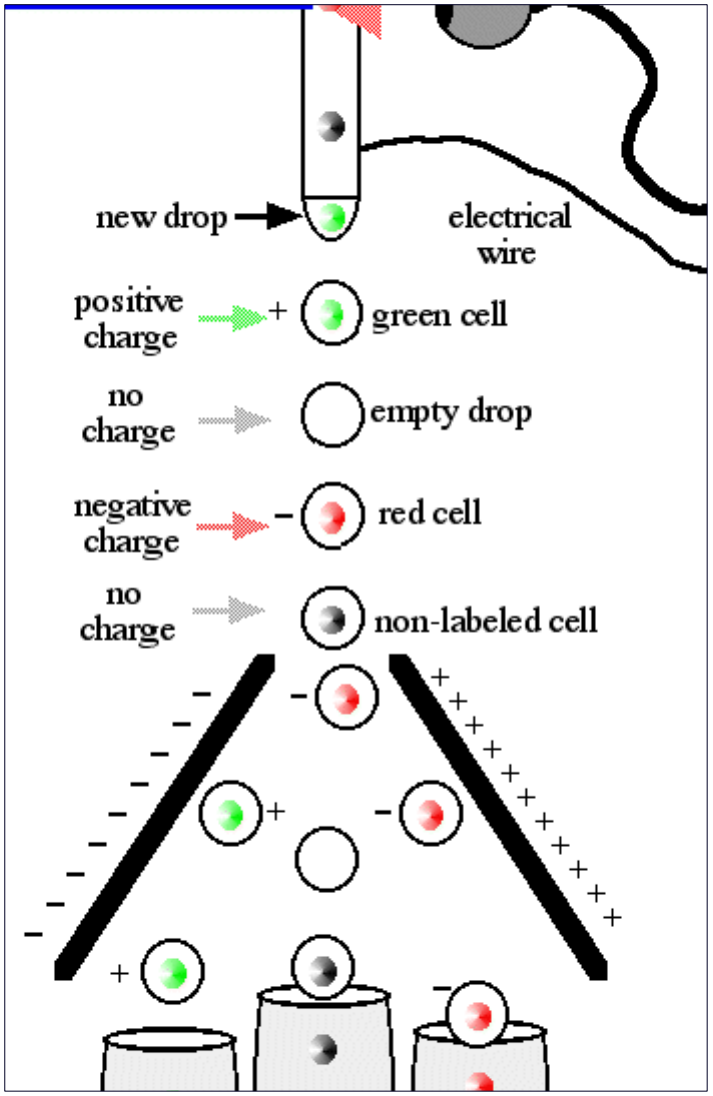

Figure 4.5 Diagram of fluorescence-activated cell sorting.

Specific cells are detected using fluorochrome-conjugated antibodies and deflected left or right on the basis of electrical charges applied appropriately to the cell-containing liquid droplets. (Image obtained from Department of Biology, Davidson College, NC)

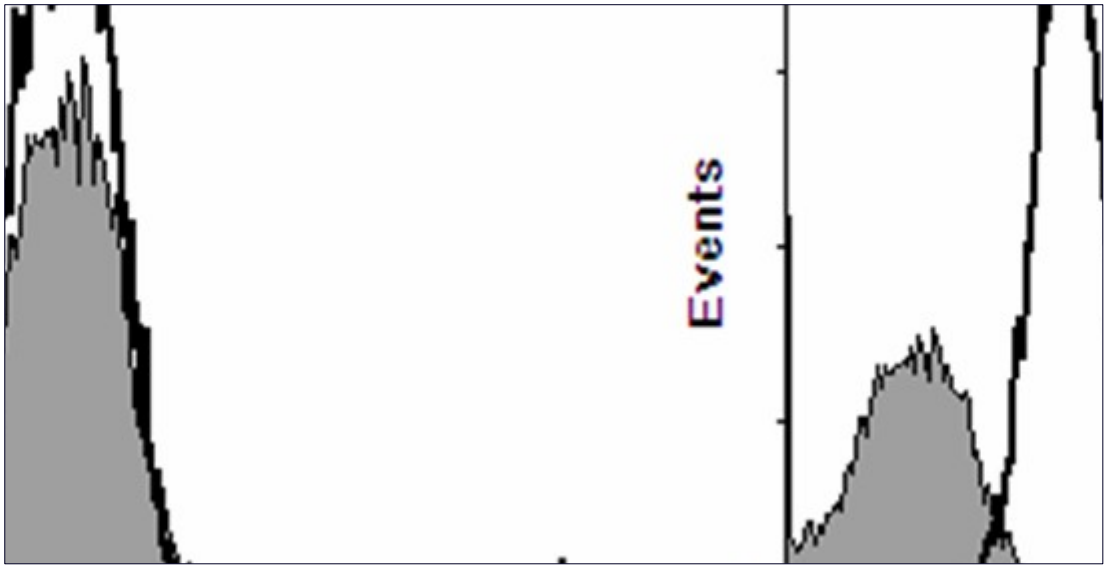

Figure 4.6 Histograms analysing the expression of CD103 after T cell sorting.
Activated T cells were treated with 10ng/ml of TGF-β for 72 hours. After the incubation, the cells were stained with anti-CD103 FITC-conjugated antibody, and then sorted for $CD103^-$ (A) and $CD103^+$ T cells (B) with the FACSAria II sorter. Each shaded histogram shows the result of labelling with isotype-matched control antibodies; the open histograms show CD103 labelling.

4.6 Results

4.6.1 MOLT-16 T cells express the αEβ7 integrin (CD103) on their cell surface

In order to investigate the biological function of $CD103^{+}$T cells, a series of experiments was performed using the MOLT-16 T cell line which constitutively expresses this integrin (Rygiel et al., 2008); a CD103-ve T cell line, MOLT-4, was used for control. The phenotype of both of these cell lines was validated prior to use by immunofluorescence flow cytometry.

Briefly, cells were washed in 2%FBS/PBS and the cell density adjusted to $1x10^{6}$ cells per ml. 100µl of cell suspension were incubated with mouse monoclonal anti-CD103 FITC conjugated antibody (1:10) (clone 2G5, Eurobiosciences) and mouse IgG_{2A} isotype control antibody (1:10) on ice for 30 minutes. After washing in 2%FBS/PBS two times, CD103 expression was measured by flow cytometry (BD FACSCalibur).

The flow cytometric analysis suggested that MOLT-16 T cells expressed CD103 uniformly while no CD103 was present on MOLT-4 T cells (Figure 4.7).

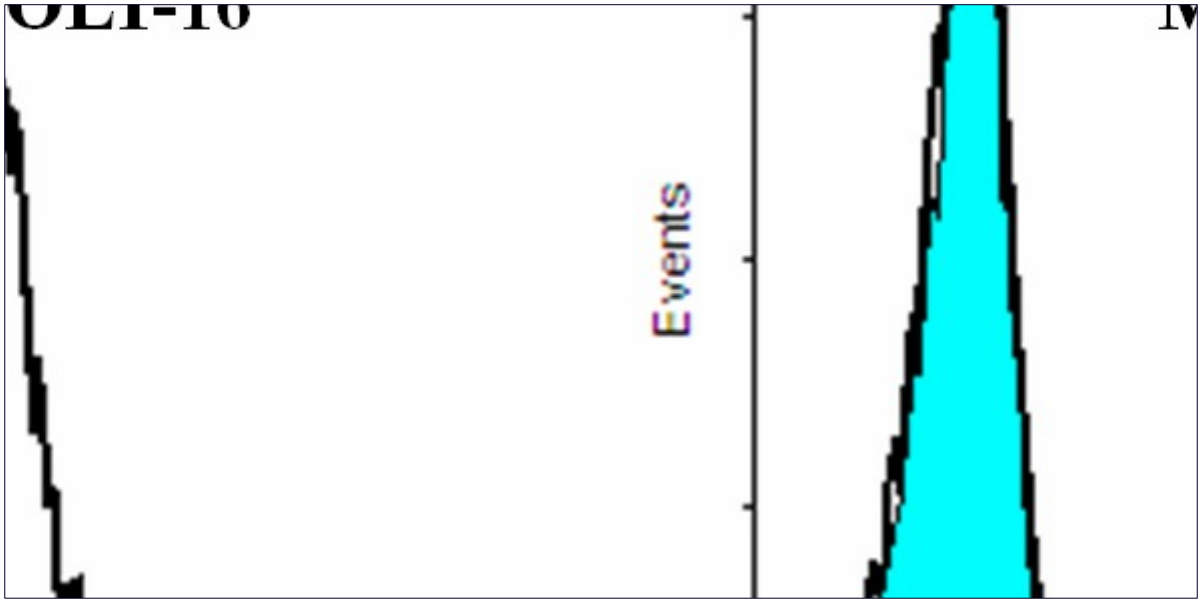

Figure 4.7 Histograms demonstrating the expression of the αEβ7 integrin (CD103) T cell lines.

MOLT-16 (A) and MOLT-4 (B) T cells were incubated with CD103 antibody and analysed by flow cytometry. The CD103 was highly expressed in MOLT-16 T cells, whereas CD103 was not expressed by MOLT-4 T cells. The results were representative of 3 similar experiments. The shaded histogram shows fluorescence produced by labelling with an isotype-matched control antibody; the open histogram shows experimental labelling.

4.6.2 Loss of E-cadherin expression by renal epithelial cells co-cultured with MOLT-16 T cells

One of the main characteristics of EMT is a decrease in the expression of the epithelial marker, E-cadherin (section 1.8.1). Therefore, a series of experiments was conducted to examine the effect of MOLT-16 T cells on the expression of E-cadherin by HKC-8 cells.

Semi-confluent HKC-8 cells were co-cultured with $1x10^5$ MOLT-16 T cells in chamber slides for 72 hours. For the positive control, HKC-8 cells were incubated in medium containing TGF-β 5ng/ml. Cells were washed and then fixed in pre-cooled acetone at -20°C for 10 minutes. The fixed cells were incubated with mouse monoclonal anti-E-cadherin antibody (1:50) at 4°C overnight. After washing three times in PBS, cells were incubated with mouse polyclonal IgG FITC-conjugated antibody (1:100) for 1 hour at room temperature. The slides were then viewed by laser scanning confocal microscopy (section 2.5.2).

E-cadherin was expressed along the boundary between epithelial cells in fully-developed epithelial monolayers (Figure 4.8A). This cell-surface expression of E-cadherin by HKC-8 cells was reduced by both co-cultured with MOLT-16 T cells and treatment with TGF-β1 (Figure 4.8B-C). Quantitative analysis of fluorescence intensity also showed a significant reduction of E-cadherin expression after co-culture with T cells and TGF-β1 treatment (Figure 4.8D). However, following the co-culture with MOLT-16 T cells, E-cadherin was still expressed by some HKC-8 cells. This probably suggested that MOLT-16 T cells did not contact some HKC-8 cells.

The similar down-regulation of E-cadherin produced by MOLT-16 co-culture and TGF-β1 treatment suggests a common mechanism, with the T cells potentially presenting TGF-β to the renal cell line.

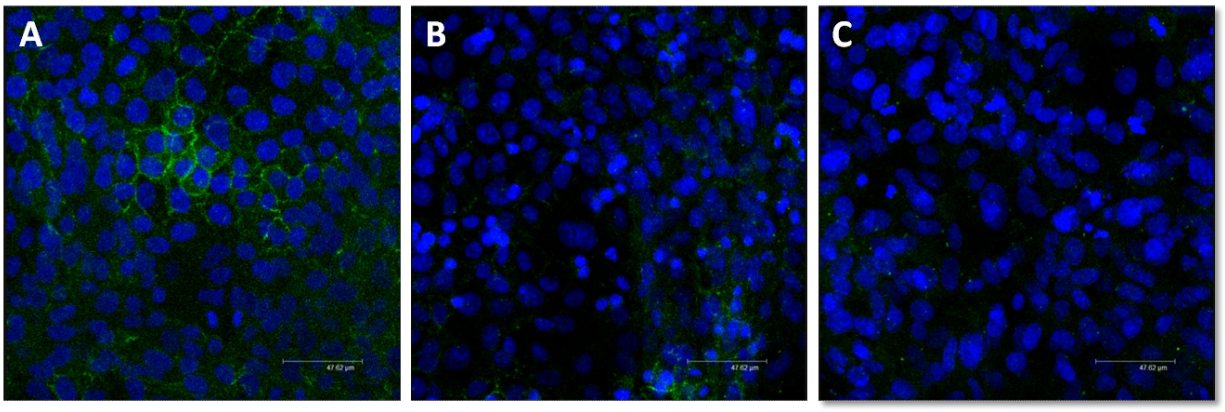

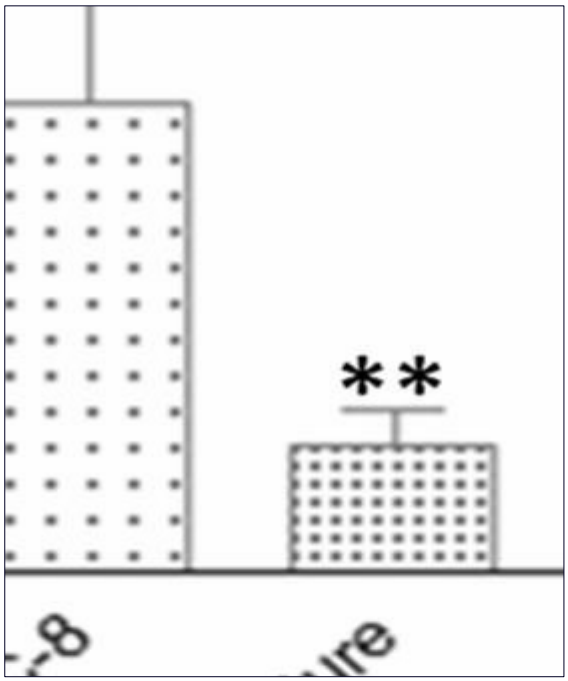

Figure 4.8 Micrographic immunofluorescence staining analysis of E-cadherin expression in a cell co-culture experiment.

Semi-confluent HKC-8 cells were incubated in medium with or without TGF-β1 5ng/ml ad co-cultured with MOLT-16 T cells for 72 hours. The immunofluorescence staining showed the expression of E-cadherin at cell junction of control cells (A). Its expression was reduced and internalized after co-culture with MOLT-16 T cells (B) and TGF-β1 treatment (C). The microscopic pictures were taken from the confocal microscope at x 63 magnification. The bar graph (D) shows the quantitative measurement of mean fluorescence intensity which significantly declined in co- culture and treatment groups. The bars are means (n=4) and the error bars are SEM. These results are representative of 3 similar experiments. (** = $p < 0.01$)

4.6.3 MOLT-16 T cell line-induced S100A4 expression in renal epithelial cells

This study has already shown that MOLT-16 T cells might induce EMT by reducing E-cadherin expression by confluent HKC-8 cells. A further series of experiments was performed to determine whether MOLT-16 T cells can induce expression of the mesenchymal marker, S100A4.

The expression of S100A4 was measured in HKC-8 cells co-cultured with MOLT-16 T cells. Semi-confluent HKC-8 cells were co-cultured with MOLT-16 T cells and were then processed as described in section 4.4.3. The fixed cells were incubated with rabbit polyclonal anti-S100A4 antibody (1:100) (DAKO) at 4°C overnight. After washing the cells were incubated with FITC-conjugated anti-rabbit IgG (1:150) at room temperature for 1 hour.

There was an absence of S100A4 expression in normal HKC-8 cells (Figure 4.9A). However, the expression of S100A4 by HKC-8 cells was up-regulated during co-culture with MOLT-16 T cells or by treatment with TGF-β1 (Figure 4.9B-C). In addition, quantitative measurement of fluorescent intensity showed a significant increase of S100A4 expression in HKC-8 cells following either MOLT-16 T cells co-culture or TGF-β1 treatment (Figure 4.9C-D). However, MOLT-16 T cells did not induce S100A4 in all cells, probably suggested that S100A4-negative HKC-8 cells did not interact with MOLT-16 T cells.

These results are consistent with a model in which MOLT-16 T cells can induce S100A4 by a mechanism involving presentation of TGF-β.

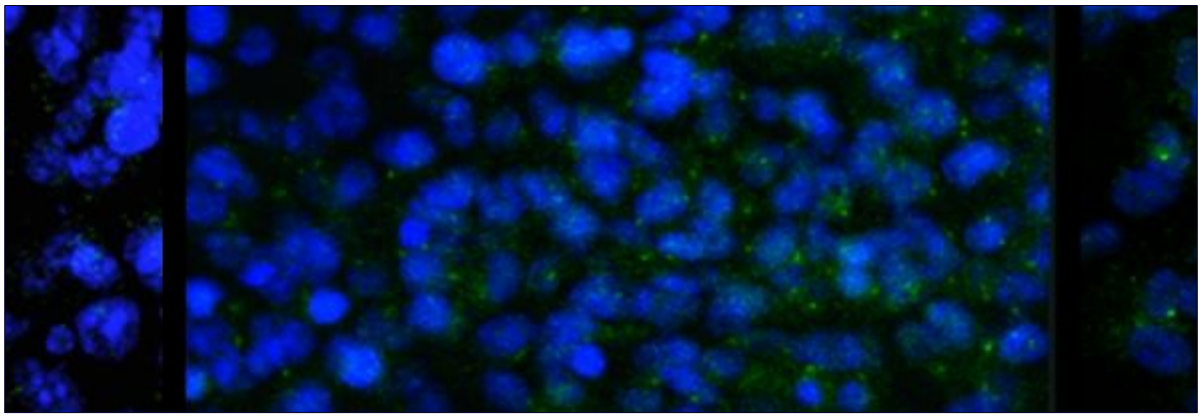

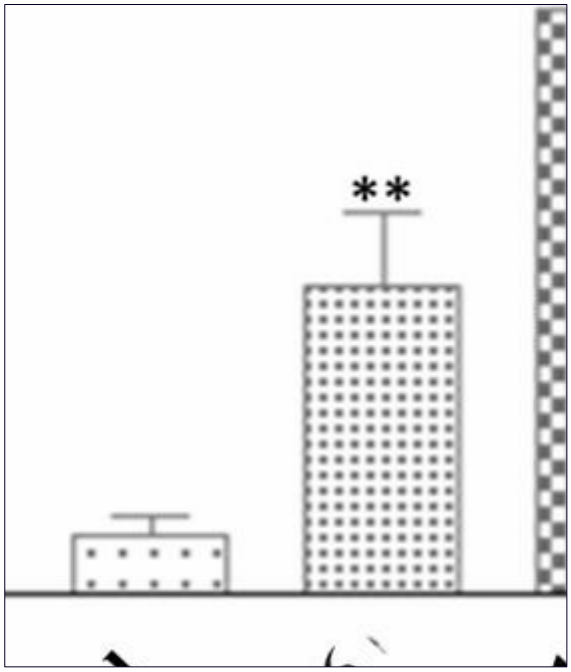

Figure 4.9 Micrographic immunofluorescence staining analysis of S100A4 expression in co-culture experiment.

The semi-confluent HKC-8 cells were incubated in medium with or without TGF-β1 5ng/ml for 72 hours. The S100A4 expression (Green) was nearly absent in control cells (A). However, its expression was increased by co-culture with MOLT-16 cells (B) or TGF-β1 treatment (C). The microscopic pictures were taken from the confocal microscope at x 63 magnification. The bar graph (D) shows the quantitative measurement of mean fluorescence intensity which significantly increased in co-culture and treatment groups. The bars are means (n=4) and the error bars are SEM. These results are representative of 3 similar experiments. (** = $p < 0.01$, *** = $p < 0.001$)

4.6.4 α-SMA was expressed by HKC-8 cells co-cultured with MOLT-16 T cells

Since lymphoma cells such as MOLT-16 T cells are known to express S100A4 (Tulchinsky et al., 1995), another mesenchymal marker was required to confirm that addition of T cells can induce EMT *in vitro*. The expression of α-SMA is frequently used to define myofibroblast; the induction of this marker was also examined by immunofluorescence staining.

Semi-confluent HKC-8 cells were co-cultured with MOLT-16 for 72 hours. Cells were fixed (section 4.3.1) and incubated with mouse monoclonal anti-α-SMA antibody (1:100) at 4°C overnight. Following this incubation, the cells were washed and incubated with mouse polyclonal IgG FITC-conjugated antibody (1:100) at room temperature for 1 hour.

α-SMA expression was not present in any normal HKC-8 cells (Figure 4.10A). However, some of the HKC-8 cells expressed α-SMA following co-culture with MOLT-16 T cells or TGF-β1 (Figure 4.10B-C).

Although α-SMA was not expressed by all HKC-8 in the presence of MOLT-16 T cells, the induction of this marker in some cells provides further evidence that culture with T cells can induce EMT leading to myofibroblast formation. The heterogeneity of α-SMA induction by culture with both TGF-β1 and T cells is consistent with the observation *in vivo* that not all epithelial cells express this marker during the induction of EMT (Okada et al., 2000).

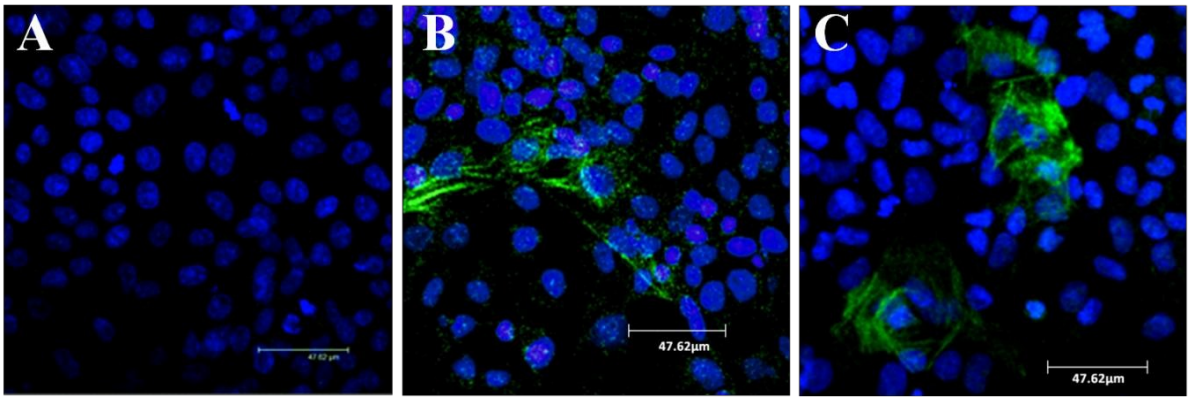

Figure 4.10 Micrographic immunofluorescence staining analysis of α-SMA expression in co-culture experiment.

The semi-confluent HKC-8 cells were incubated in medium with or without TGF-β1 5ng/ml for 72 hours. The α-SMA expression (Green) was absent in control cells (A). However, it appeared in as the microfilament-like structure in the presence of MOLT-16 cells (B) and TGF-β1 (C). The microscopic pictures were taken from the confocal microscope at x 63 magnification. The results are representative from 3 similar experiments.

4.6.5 MOLT-16 induced EMT via the TGF-β signalling pathway

Currently, TGF-β has been reported as a major inducer of the EMT during renal allograft fibrosis (Liu et al., 2010). According to the above results, co-culture of MOLT-16 T cells and HKC-8 cells resulted in loss of the epithelial marker E-cadherin and acquisition of the mesenchymal markers S100A4 and α-SMA. Similar phenotypic changes were produced by treatment of HKC-8 cells with TGF-β1, suggesting that this growth factor may also be involved in the phenotypic transition produced by T cells.

In order to determine the contribution of TGF-β signalling in the T cell co-culture model, HKC-8 cells were pre-treated with the TGFβR1 (ALK5) antagonist, SB-505124 at a concentration of 0.1, 0.5 and 1μM at 37°C for 1 hour. After this pre-treatment, HKC-8 cells were co-cultured with MOLT-16 T cells for 72 hours. The cells were then fixed and incubated with anti-E-cadherin (1:50), anti-S100A4 (1:100) and anti-α-SMA (1:100) antibodies at 4°C overnight. After washing, the cells were incubated with appropriate secondary antibodies at room temperature for 1 hour. The expression of E-cadherin, S100A4 and α-SMA were examined by confocal microscopy at time 63 magnification.

Normal HKC-8 cells expressed E-cadherin at the point of cell-cell contact (Figure 4.11A) but neither S100A4 (Figure 4.12A) nor α-SMA (Figure 4.13A) were expressed. Following co-culture with MOLT-16 T cells, there was a loss of E-cadherin expression at the cell borders (Figure 4.11B) and an increase in the expression of S100A4 (Figure 4.12B) and α-SMA (Figure 4.13B). However, addition of SB-505124 at a concentration of 1μM partially prevented the loss of E-cadherin (Figure 4.11E), and also reduced the induction of S100A4 (Figure 4.12E) and α-SMA (Figure 4.13E).

Inhibition of the phenotypic transition produced by treatment of HKC-8 cells with MOLT-16 T cells by blockade of TGF-β signalling suggests that these T cells at least partially induce EMT by a TGF-β dependent mechanism.

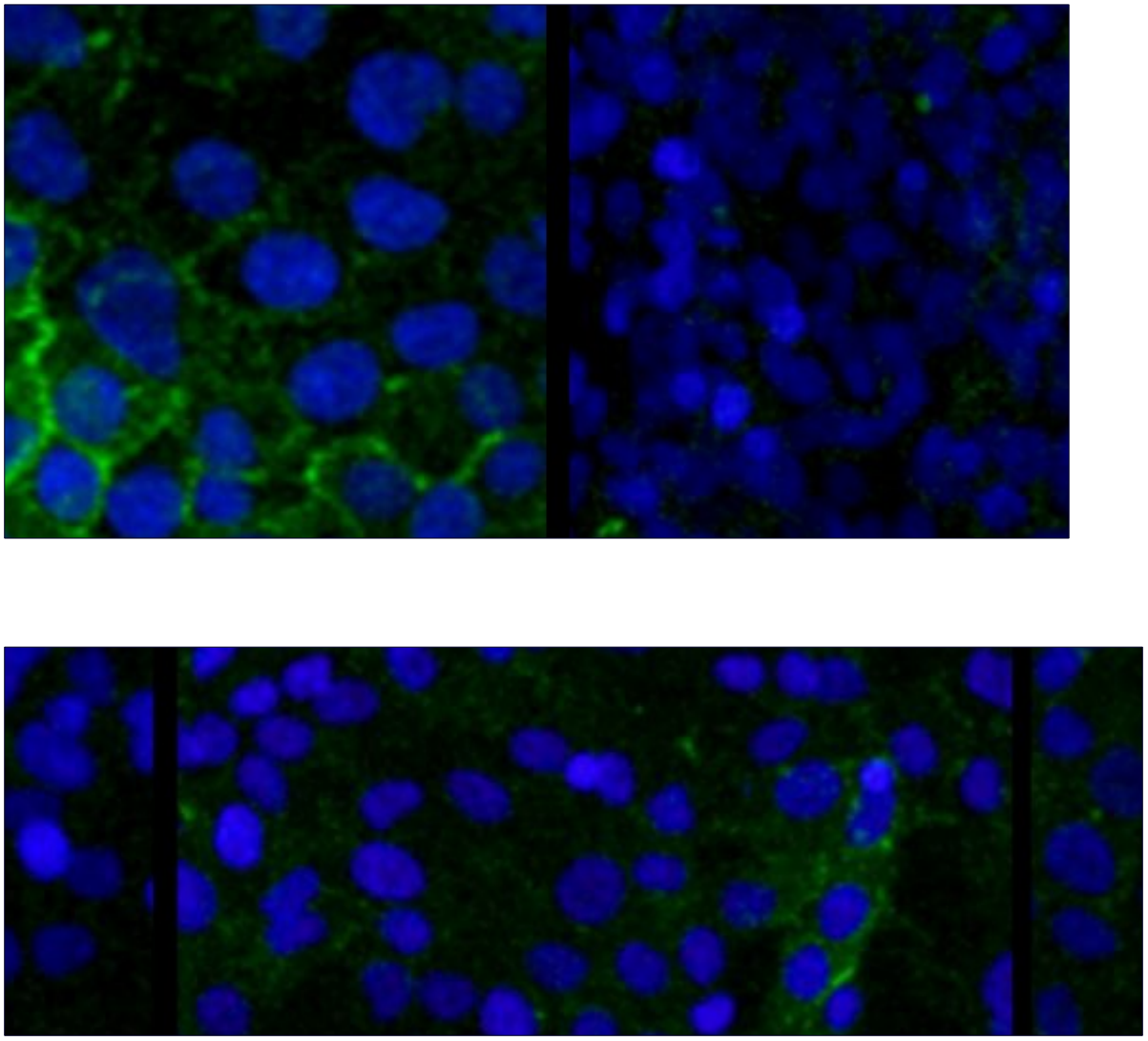

Figure 4.11 Microscopic immunofluorescence images demonstrating the effect of ALK5 inhibitor on E-cadherin expression.

Semi-confluent HKC-8 cells were co-cultured with MOLT-16 cells in the absence or presence of ALK-5 inhibitor at concentration 0.1, 0.5 and 1uM. The control was HKC-8 cells grown in normal medium. The images were taken from confocal microscope at x63 magnification. The control (A) showed linear expression of E- cadherin at the cell borders which then changed to punctuated expression following MOLT-16 co-culture (B). The ALK-5 inhibitor at 0.1μM (C) and 0.5μM (D) did not recover the cell border staining of E-cadherin in the presence of MOLT-16 cells. However, some staining at cell borders was shown with ALK-5 inhibitor 1μM E). The images were taken by the confocal microscopy at x63 magnification. The results are representative of 3 similar experiments.

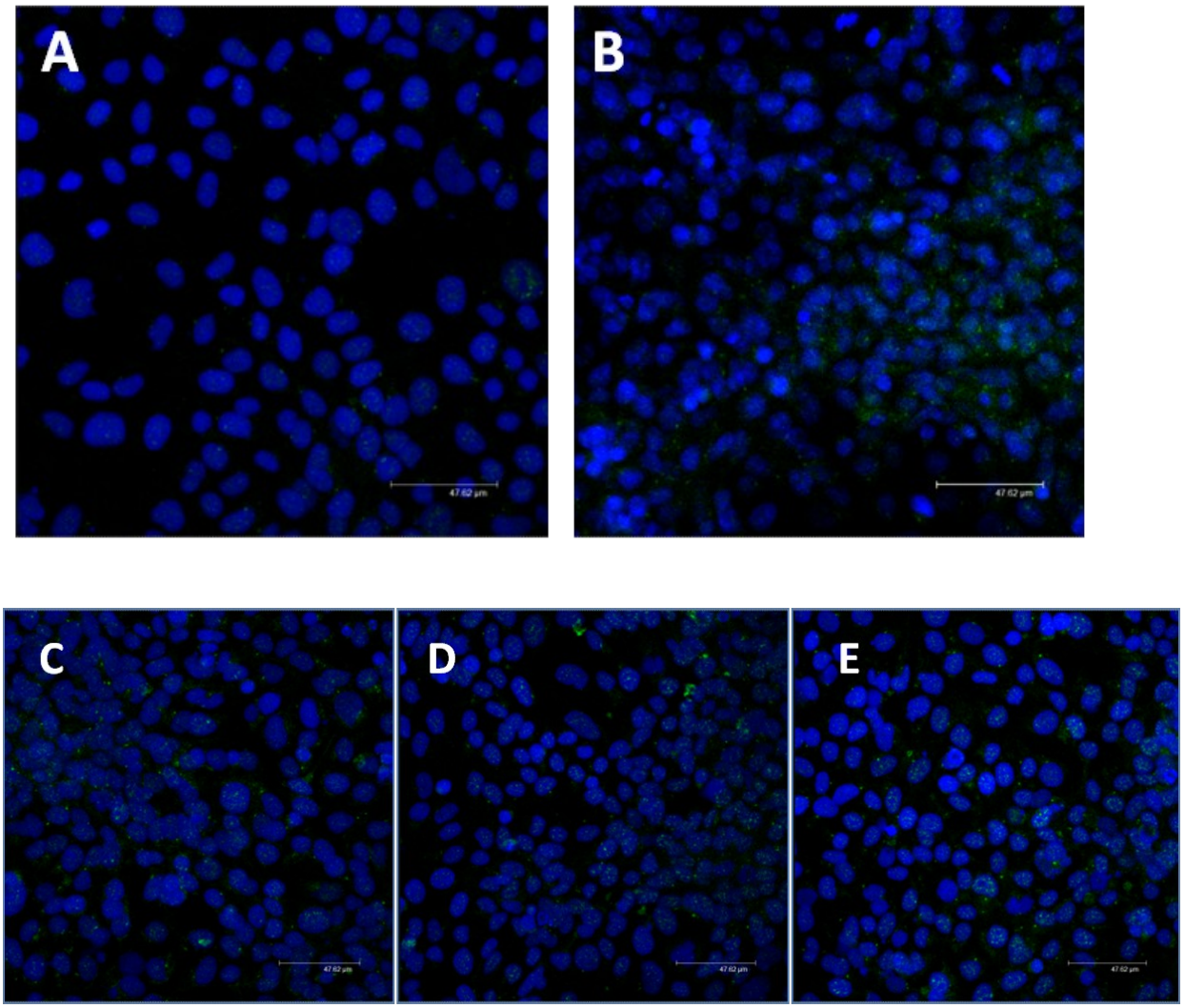

Figure 4.12 Immunofluorescence micrographic images demonstrating the effect of ALK5 inhibitor on S100A4 expression.

Semi-confluent HKC-8 cells were co-cultured with MOLT-16 cells in the absence or presence of ALK-5 inhibitor at concentration 0.1, 0.5 and 1μM. The control (A) showed no staining of S100A4. This antigen was induced in the cytoplasm after MOLT-16 co-culture (B). In the presence of ALK-5 inhibitor at 0.1 (C), 0.5 (D) and 1μM (E), S100A4 expression was reduced and appeared punctuate. The images were taken by the confocal microscopy at x63 magnification. The results are representative of 3 similar experiments.

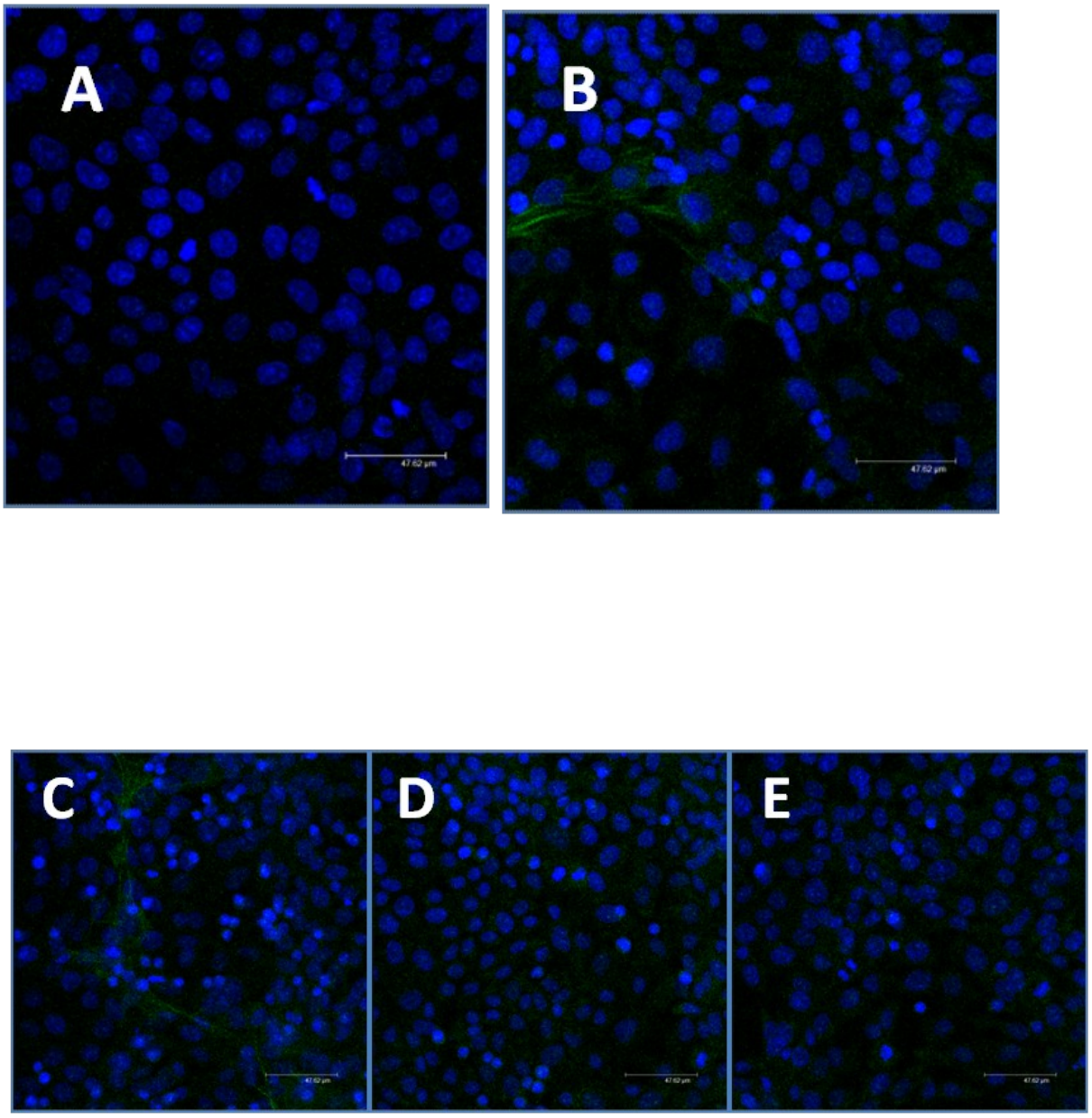

Figure 4.13 Immunofluorescence micrographic images demonstrating the effect of ALK5 inhibitor on α-SMA expression.

Semi-confluent HKC-8 cells were co-cultured with MOLT-16 cells in the absence or presence of ALK5 inhibitor at concentration 0.1, 0.5 and 1μM. The control (A) showed no staining of α-SMA. However, α-SMA was present in microfilament bundles in the presence of MOLT-16 (B). The ALK5 inhibitor did not inhibit the induction of α-SMA expression at 0.1μM (C), but the increase in α-SMA expression produced by co-culture with MOLT-16 T cells was inhibited when the ALK5 inhibitor was present at 0.5uM (D) and 1μM (E). The images were taken by the confocal microscopy at x63 magnification. The results are representative of 3 similar experiments.

4.6.6 LAP was expressed by MOLT-16 T cell line

From the above results, MOLT-16 T cells partially induced EMT by activation of the TGF-β signalling pathway. It has been observed that TGF-β is predominantly produced from renal epithelial cells during rejection (Robertson et al., 2001), and is normally secreted in an inactive form complexed with LAP (Section 1.9.1). However, it has also been observed that MOLT-16 T cells express LAP (Rygiel et al., 2010), suggesting that these cells present TGF-β to renal epithelial cells (Oida et al., 2003).

In order to determine the expression of latent TGF-β, MOLT-16 and MOLT-4 T cells were grown in serum-free medium for 72 hours. These cells were then incubated with mouse monoclonal anti-LAP FITC-conjugated antibody (1:10) for 30 minutes on ice. After the washing step, the cells were examined by flow cytometry.

There was minimal expression of LAP on the surface of MOLT-4 T cells (Figure 4.14A). However, the MOLT-16 T cell line expressed this antigen (Figure 4.14B). Since this study did not use MOLT-4 as a negative control in co-culture studies, the suggestion that LAP on surface of MOLT-16 T cells played a role in MOLT-16 T cell-induce EMT remains inconclusive.

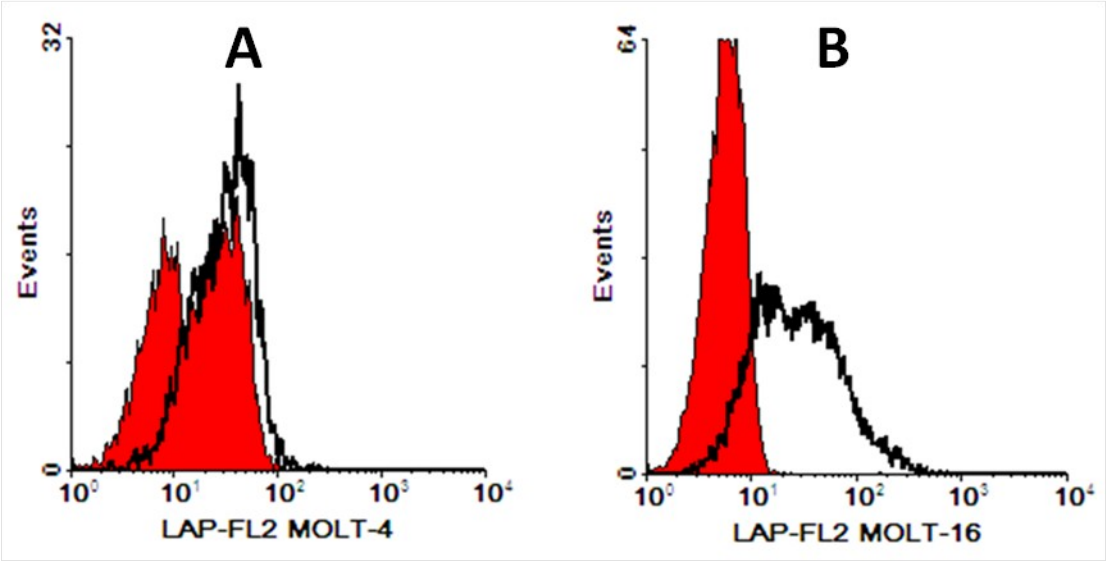

Figure 4.14 Flow cytometric analysis of LAP expression on lymphoma T cell lines.

MOLT-4 and MOLT-16 cells were cultured in serum free RPMI 1640 for 72 hours. Cells were stained with anti-LAP PE-conjugated antibody for 30 minutes on ice. Very few of MOLT-4 T cells expressed LAP (A) whereas the majority of MOLT-16 T cells expressed LAP on their cell surface (B). The shaded histogram shows fluorescence produced by labelling with an isotype-matched control antibody; the open histogram shows experimental labelling. These results are representative of 2 similar independent experiments.

4.6.7 TGF-β1 induced CD103 expression on primary T cells

This study has already shown that the MOLT-16 T cell line expresses CD103 at a high level. In this study a series of experiments was performed to examine antigen expression by primary human T cell lines..

In order to determine the conditions in which human T cells express CD103, T cells were isolated from healthy volunteer blood and processed as described in section 2.2.5. The resting T cells were activated with CD3/CD28 Dynabead® for 72 hours. After the activation, some of the activated T cells were incubated in medium containing 10ng/ml TGF-β1 for 72 hours. These T cells were then incubated with monoclonal anti-CD103 FITC-conjugated antibody (1:10) for 30 minutes on ice. Cells were examined for CD103 expression by flow cytometry.

Approximately 7.6 ± 1.3% (mean ± SEM, n=4) of CD3/CD28 activated T cells expressed CD103 in the absence of TGF-β1 (Figure 4.15A). However, following TGF-β1 stimulation, 45.7 ± 6.6% (mean ± SEM, n=4) of the activated T cells expressed CD103 expression on their cell surface (Figure 4.15B). Quantification of CD103 expression is shown in and demonstrates significant induction of CD103 expression by TGF-β1 (Figure 4.15C).

These results are consistent with previous data from our group and others (Hadley et al., 2001; Wong et al., 2003) suggest that the induction of CD103 observed on T cells which have penetrated renal tubules during rejection is dependent on local expression of TGF-β1.

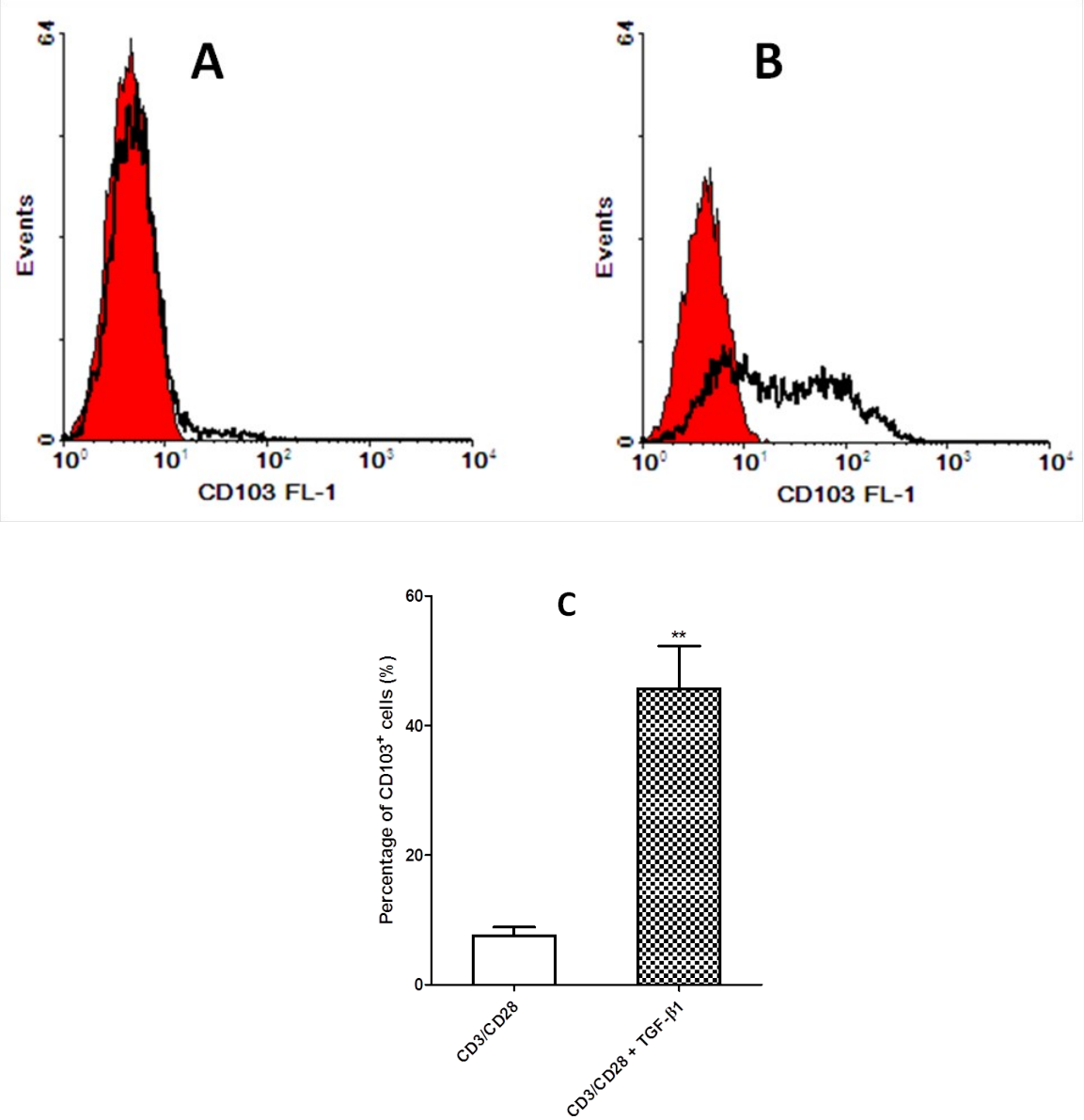

Figure 4.15 Flow cytometric analysis of the expression of CD103 by human primary T cells.

The isolated human T cells were activated with CD3/CD28 for 72 hours and then incubated in medium or medium containing TGF-β1 10ng/ml for 72 hours before analyzing by flow cytometry. A small number of activated T cells expressed CD103 on their cell surface (A). In contrast, TGF-β1 treated T cells increased the expression of CD103 (B). The bars (C) show mean and the error bars are SEM. The shaded histogram shows fluorescence produced by labelling with an isotype-matched control antibody; the open histogram shows experimental labelling. The quadrants were set from the isotype control. (** = $p<0.01$). These results are representative of 4 similar experiments.

4.6.8 The expression of LAP by primary human T cells

Results in section 4.4.6 demonstrated that MOLT-16 T cells express cell surface LAP which might be involved TGF-β-mediated induction of EMT. A further series of experiments was performed to measure the expression of LAP by primary human T cells.

To determine whether primary T cells express LAP or not, T cells were isolated from the blood of healthy volunteers. After the isolation, the T cells were activated with CD3/CD28 Dynabeads® for 72 hours, followed by incubation with TGF-β1 at 10ng/ml for 72 hours. These cells were then incubated with anti-LAP monoclonal antibody conjugated with PE (R&D system) for 30 minutes on ice. LAP expression was detected by flow cytometry.

A small proportion of both activated T cells [16.43% ± 1.03 (mean ± SEM, n = 4 and activated T cells which had been cultured with TGF-β1 [10.43 ± 1.05% (mean ± SEM, n = 4) expressed LAP on the cell surface (Figure 4.16A-B). In addition, comparison of LAP expression between these two groups showed no statistical difference using the paired t-test method (Figure 4.16C). The data from this experiment provided 98.3% power (alpha = 0.05, two-tail).This suggests that TGF-β1 is not required for LAP expression by activated human T cells.

The statistical power was calculated by using a calculator from DSS research web site. (http://www.dssresearch.com/KnowledgeCenter/toolkitcalculators/statisticalpowercalculators.aspx)

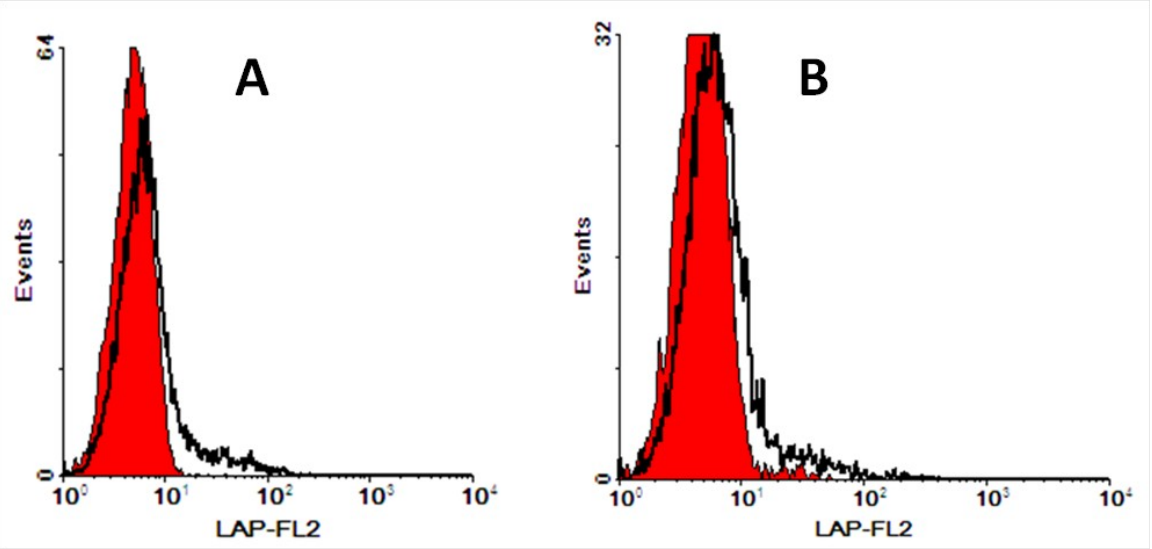

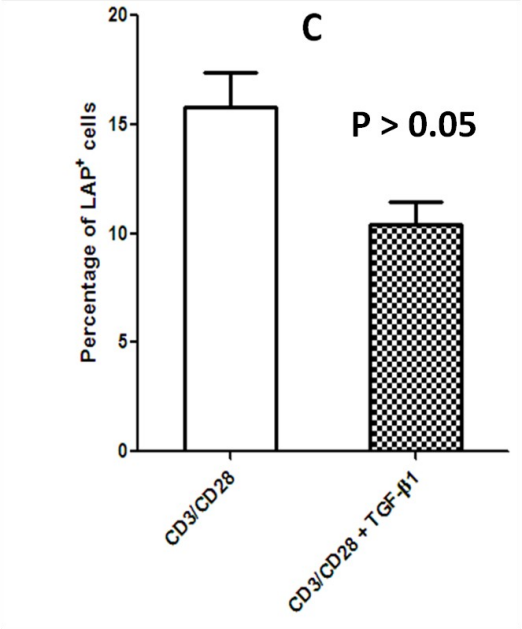

Figure 4.16 Flow cytometry analysis of the expression of LAP compared between CD3/CD28 activation and TGF-β1 treatment.

CD3/CD28 activated T cells were incubated in medium with absence or presence of TGF-β1 10ng/ml for 72 hours of activated T cells. A small population of activated T cells (A) and activated T cells with TGF-β1 stimulation (B) expressed LAP. There was no difference between control and treatment groups (C). The bars show mean results and error bars are SEM. The shaded histogram shows fluorescence produced by labelling with an isotype-matched control antibody; the open histogram shows experimental labelling. The quadrants were determined from the appropriate isotype antibody control samples. The results are representative of 4 similar experiments with different blood donors (Paired t-test, alpha = 0.05, 98.9% power).

4.6.9 The co-existence of CD103 and LAP on primary T cells

CD103 and LAP are potentially associated with T cell-induced EMT. Interestingly, a study of SLE patients concluded that there was an increase of $CD103^+LAP^+CD8^+$ Treg after Hematopoietic stem cell transplantation (HSCT) (Zhang et al., 2009). However, no data has been reported for $CD103^+LAP^+$ T cells *in vitro*. This series of experiments was performed to explore the potential relationship between CD103 and LAP on the surface of human T cells.

The co-expression of surface molecules on both activated and TGF-β treated T cells were measured by flow cytometry. Human T cells were isolated, activated with Dynabeads® and then stimulated with TGF-β1, as described in section 4.3.8. Cells were then incubated with both FITC conjugated anti-CD103 and PE-conjugated anti-LAP antibodies for 30 minutes on ice, followed by flow cytometric analysis.

Appropriately conjugated isotype control antibodies were used to set the analysis quadrants.

Two-colour flow cytometric analysis demonstrated that a small proportion of activated T cells expressed LAP (Figure 4.17); as in section 4.6.8, the proportion of LAP expressing T cells was not altered by treatment of the cells with TGF-β1. A majority of the small population of $CD103^+$ T cells observed in non-TGF-β1 induced cultures expressed LAP. However, a similar small proportion of $CD103^+$ and $CD103^-$ T cells in TGF-β1 treated cultures expressed LAP. This experiment provides no evidence that the CD103 induced on activated T cells by TGF-β treatment is associated with a similar induction of LAP.

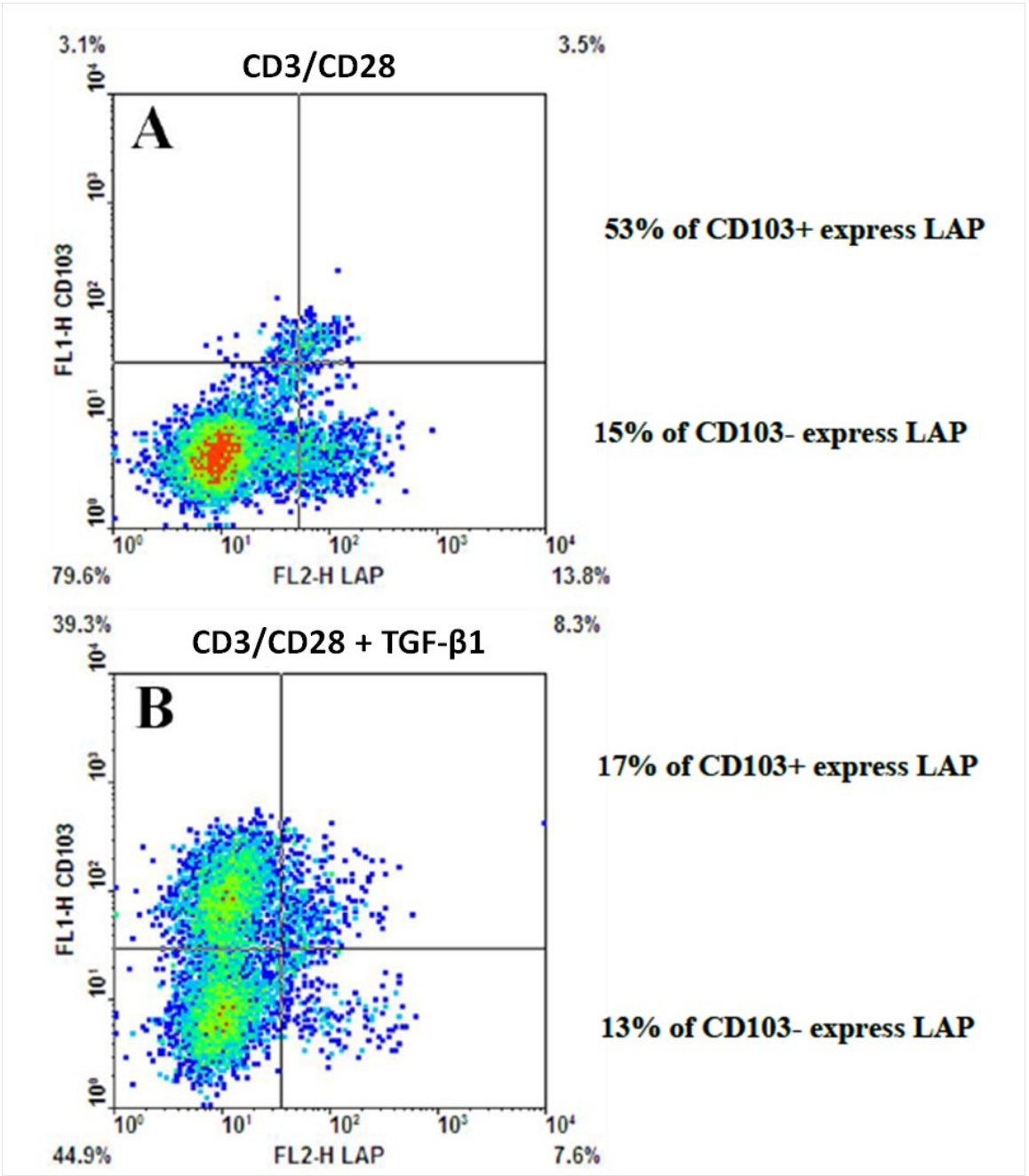

Figure 4.17 Flow cytometric analysis of the co-expression of CD103 and LAP in activated T cells and TGF-β1 treated T cells.

CD3/CD28 activated T cells were incubated in medium with or without 10ng/ml of TGF-β1 for 72 hours. In activated T cells, 13.8% of $CD103^-$ T cells expressed LAP (A). After TGF-β1 treatment, LAP was expressed in 17% of $CD103^+$Tcells (B). The results are representative of 2 similar experiments. The quadrants were set by analysing of samples after labelling with isotype control antibodies.

4.6.10 Examination of LAP expression by T cells sorted into $CD103^+$ and $CD103^-$ fractions

In order to examine further the expression of LAP by $CD103^+$ and $CD103^-$ T cells, these T cell subsets were separated after TGF-β treatment by FACS as described in section 4.3.4. The sorted cells were then stained with anti-LAP PE-conjugated antibody (1:10) and analysed using a FACSCalibur flow cytometer.

As in Figure 4.17, it was found that only a small sub-population of the separated $CD103^+$ and $CD103^-$ T cells expressed LAP (Figure 4.18). In the case of $CD103^-$ T cells (Figure 4.18A) 14.9 ± 0.4% (mean ± SEM) of the cells expressed LAP, whilst 11 ± 1.8% (mean ± SEM) of $CD103^+$T cells expressed this antigen (Figure 4.18B). These data were not significantly different (Figure 4.18C; $P>0.05$; n=3 separated experiment; analysed by paired t-test).

On the basis of this data it can be concluded that a small proportion of activated T cells does express LAP. However, this LAP is not induced by treatment with TGF-β1 and is not preferentially expressed by CD103 expressing T cells following treatment with TGF-β1.

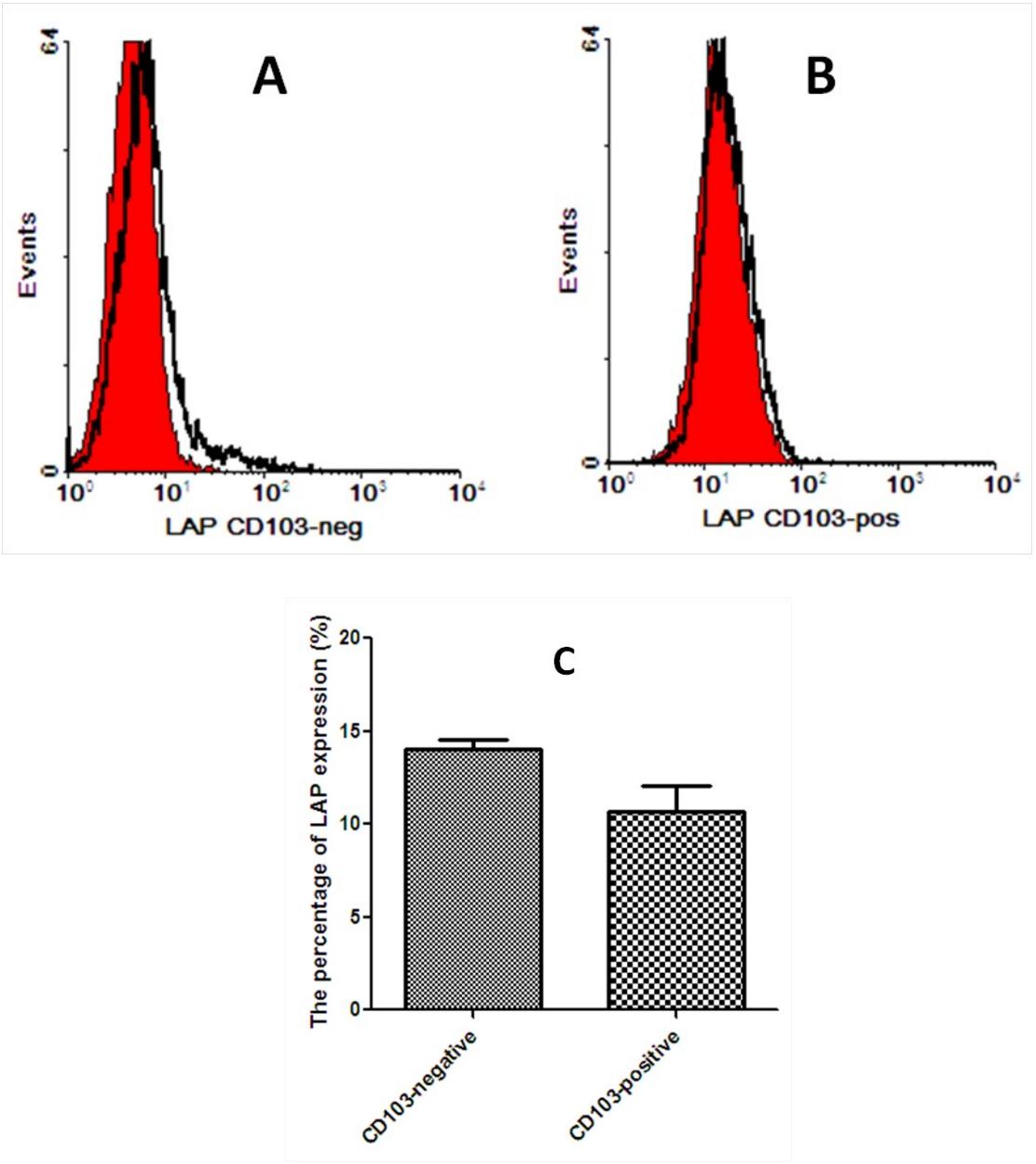

Figure 4.18 Flow cytometry analysis of LAP expression in CD103 sorting T cells. CD3/CD28 activated T cells were incubated with TGF-β1 10ng/ml for 72 hours and then sorted for $CD103^-$ and $CD103^+$T cells. The sorted T cells were examined for LAP expression by flow cytometry. The percentage of LAP positive T cells in $CD103^-$ T cells (A) and $CD103^+$ T cells (B) were minimal in both groups. There was no significant difference of LAP expression between these two groups (C). The quadrants were set using isotype-matched control labelling. The results are presented in mean ± SEM (n=3) and are representative of 3 independent experiments.

4.7 Summary and discussion

4.7.1 Results summary

- The MOLT-16 T cell line expressed cell surface CD103, providing a good model for the CD103 expressing T cells found within renal tubules during renal allograft rejection. Immortalised proximal renal tubular cells showed changes consistent with EMT as a consequence of incubation with the MOLT-16 T cell line.
- Inhibition of the TGF-β receptor partially blocked the EMT induced by MOLT-16 T cells. Treatment of activated T cells with TGF-β1 induced the expression of CD103.
- A small proportion of primary human T cell lines expressed latent TGF-β following CD3/CD28 activation. .

  The expression of latent TGF-β by activated T cells was not increased by incubation with TGF-β1. The expression of latent TGF-β1 by TGF-β1 treated T cells was similar in the $CD103^+$ and $CD103^-$ subpopulations.

4.7.2 Discussion

Tubulitis is defined as the accumulation of mononuclear leukocytes within the renal tubular compartment (Racusen et al., 1999). This feature is now one of the major criteria for diagnosing acute T cell-mediated rejection following allogeneic human renal transplantation (Section 1.6) (Sis et al., 2010). It has been reported that many activated T cells within the tubules during rejection express the αE(CD103)β7 integrin (Robertson et al., 2003). Since T cell-mediated rejection is associated with chronic allograft fibrosis and leads to approximately 6% of renal allograft loss (El-Zoghby et al., 2009), it was hypothesised that $CD103^+$ T cells mediate fibrosis by the induction of EMT.

The MOLT-16 T cell line was established as one of six cell lines from patients with acute leukaemia (Minowada and Moore, 1975). MOLT-16 T cells have been shown to strongly express αEβ7 integrin (CD103) and efficiently bind to primary renal epithelial cells in culture (Robertson et al., 2004). Furthermore, MOLT-16 T cells have been demonstrated to express latent TGF-β on their cell surface (Oida et al., 2003; Rygiel et al., 2008). For these reasons, MOLT-16 T cells were used as a robust and reproducible model of intratubular T cells during co-culture experiments with HKC-8 immortalised renal tubular epithelial cells.

Previous studies by our group have shown up-regulation of the mesenchymal marker S100A4 following co-culture of MOLT-16 T cells with primary renal epithelial cells. In addition, treatment with the TGF-β neutralising antibody down-regulated this S100A4 induction, suggesting that active TGF-β on the cell surface of MOLT-16 T cells plays a role in the induction of epithelial cell transformation (Robertson et al., 2004). In the current study, MOLT-16 T cells were co-cultured with the immortalised proximal renal tubular epithelial cell line, HKC-8 (Racusen et al., 1997). In order to examine the possible induction of EMT during these co-cultures, the expression of a range of antigens was examined. Although S100A4 was induced, this antigen has a limitation for examination of EMT in the presence of T cell lines. Specifically, it is known that S100A4 is expressed by MOLT-16 T cells. This might complicate quantification of this antigen in mixed renal cell-T cell co-cultures (Inoue et al., 2005; Osterreicher et al., 2011). Thus, α-SMA, which is a mesenchymal marker commonly used to identify myofibroblast, was used in conjunction with S100A4 to identify myofibroblast differentiation in the co-culture system. However, this study found that

MOLT-16 lymphocytes induce typical changes of EMT in HKC-8 cells following 72 hours' co-culture. The immunofluorescence labelling for E-cadherin showed a reduced, punctate expression pattern at the cell borders, whereas α-SMA labelling showed the appearance of microfilament bundles. In addition, S100A4 expression was up-regulated in renal epithelial cells but was also observed in the MOLT-16 T cell line. This de-differentiation of co-cultured renal epithelial cells was similar to the features of these cells following TGF-β1 treatment, supporting a key role of TGF-β1 in T cell-induced EMT.

In order to specify the role of TGF-β in this co-culture experiment, SB-505124, a selective ALK5 inhibitor (DaCosta et al., 2004), was pre-incubated with renal epithelial cells before the co-culture. Pre-treatment with the TGFβRI inhibitor showed a protective effect against T cell-mediated loss of E-cadherin expression and the expression of S100A4 and α-SMA on renal epithelial cells. This indicated that MOLT-16 T cells induced EMT through a TGF-β-dependent mechanism. However, further studies are necessary to confirm the role of CD103 expression in T cell-induced EMT. For example, by using the appropriate negative control cells ($CD103^-$T cells) such as MOLT-4 T cell line and CD3/CD28 activated T cells. In addition, blocking CD103 with the anti-CD103 antibody may also provide useful information on contact-dependent mechanism of T cell-induced EMT.

This study has indicated an important role for TGF-β in T cell-induced EMT. Potential sources of this profibrotic cytokine include secretion from parenchymal cells following tissue injury or from infiltrating T cells. It has been shown that renal tubular epithelial cells express TGF-β in kidney diseases, including diabetic nephropathy (Ziyadeh, 2004) and IgA nephropathy (Wu et al., 2009), as well as in experimental models of chronic kidney disease such as UUO (Fukuda et al., 2001). In addition, several factors have been shown to induce TGF-β production by renal epithelial cells *in vitro*, including Cyclosporine (Slattery et al., 2005; McMorrow et al., 2005) and high glucose (Park et al., 2001).

Infiltrating T cells are another potential source of TGF-β during acute rejection. The role of TGF-β produced by T cells has been shown in a model of experimental autoimmune encephalitis (EAE), which is induced by Th17 T cells The inhibition of TGF-β prevents EAE (Veldhoen et al., 2006) whilst overexpression promotes the disease (Bettelli et al., 2006). Furthermore, T cell-specific TGF-β knockout mice developed mild EAE and less IL-17 compared to the control, suggesting that TGF-β produced by T cells is required for Th17 differentiation. It has been shown that murine T cell culture supernatants do not contain active TGF-β when measured by ELISA (Oida and Weiner, 2011), suggesting that this factor remains bound to the T cell surface. This finding is consistent with our observation in which MOLT-16 T cells did not secrete active TGF-β in the culture medium when measured by MFB-F11 bioassay.

Evidence of membrane-bound TGF-β on the T cell surface was first reported by Nakamura *et al* in 2001. This study demonstrated the expression of LAP-TGF-β on the surface of murine $CD4^+CD25^+$Treg) and led to the proposal of a cell contact-dependent immunosupression mechanism. Further study has also shown the expression of LAP on the surface of human $Foxp3^+$ Treg (Tran et al., 2009). As described above, surface LAP is expressed on MOLT-16 T cells (but not by MOLT-4 T cells). Thus, it is possible that TGF-β signalling in HKC-8 cells can be induced by MOLT-16 T cells via a cell-cell contact mechanism dependent on the expression of surface LAP-TGF-β on the T cells.

A previous study has shown that a small population (1.3%) of circulating $CD4^+$ T cells express LAP (Gandhi et al., 2010). Gandhi *et al* also showed a significant induction of LAP expression after T cell activation by stimulation of CD3 and CD8 or by addition of IL-2 (2.8%) and IL-8 (3.6%). The current study demonstrated a small

proportion of LAP^+ T cells following CD3/CD28 activation for 72 hours (15%); the addition of TGF-β1 made no significant difference to the proportion of LAP-expressing T cells. More study is required to define any immunoregulatory activity of LAP^+ T cells and the role of these cells in kidney transplantation.

CD103 is predominantly expressed on allograft infiltrating T cells during renal allograft rejection. The main function of CD103 appears to be targeting $CD8^+$T cells to their ligand, E-cadherin on epithelial cells. This is shown by the failure of $CD8^+$T cells from CD103 knockout mice to accumulate within islet allografts (Feng et al., 2002). Recently, immunoregulatory activity has been observed in $CD103^+CD8^+$ T cells (Uss et al., 2006). However, the regulatory function of this subset of T cells during renal allograft rejection remains controversial. Renal and liver biopsies in patients with early acute rejection reported the absence of CD103 expression on infiltrating lymphocytes (Leteurtre et al., 2000). In contrast, $CD103^+CD8^+$ T cells are commonly associated with late allograft rejection (Hadley et al., 2001) and subclinical rejection (Rowshani et al., 2004).

This study also focused on the potential for co-expression of CD103 and LAP by TGF-β1-induced T cells. Clearly such co-expression would provide a potential mechanism for stabilisation of T cell-epithelial cell conjugates allowing the bound T cells to present cell-surface TGF-β to adjacent renal cells. It was found that some 17% of $CD103^+$T cells did express LAP which might allow such a mechanism to function. However a similar proportion of $CD103^-$T cells also expressed LAP, suggesting that these two antigens are regulated separately. The relatively small proportion of activated primary T cells that expresses LAP is consistent with results from previous reports (Gandhi et al., 2010) and indicates that the potential for LAP presentation by MOLT-16 T cells may be greater than that of activated primary T cells. Clearly, an unresolved issue is the mechanism by which LAP-associated TGF-β becomes activated in order to stimulate the TGF-β receptor system. This problem is addressed in the next chapter.

Chapter 5: Mechanism of TGF-β activation by infiltrating T Cells: potential role of thrombospondin-1 and neuropilin-1

5.1 Introduction

As detailed earlier, TGF-β plays a critical role in kidney allograft fibrosis (section 1.9). Normally, TGF-β is secreted as a latent TGF-β complex. Since the activity of TGF-β requires cognate interaction between active TGF-β and its receptor, the activation of latent TGF-β is a vital step in the response to TGF-β. Several mechanisms have been proposed for latent TGF-β activation. These include the activity of protease enzymes (Jenkins, 2008), integrins (Sheppard, 2005), thrombospondin-1 (TSP-1) (Hugo and Daniel, 2009) and neuropilin-1 (NRP1) Glinka and Prud'homme, 2008). Analysis of the literature suggests that the TGF-β-mediated immune regulation may depend less on proteolytic pathways than on the cell-surface, LAP-binding receptors and conformational activation of TGF-β (Lawler et al., 1998). Spontaneous lung inflammation was observed in mice with TSP-1 knocked out (Lawler et al., 1998). In addition, αVβ6 knockout mice showed exaggerated skin and lung inflammation after irritation (Huang et al., 1996). Furthermore, double TSP-1/β6 knockout mice showed severe inflammation in the lungs and other tissues (Ludlow et al., 2005).

Unpublished data from our group has shown that CD103 expression is induced equally by co-culture with normal proximal tubular epithelial cells (PTEC) or αVβ6 transfected PTECs. Interestingly, blockade of the β6 integrin with a specific peptide did not inhibit the induction of CD103 expression during co-culture with activated T cells (Figure 5.1). Thus, other factors such as TSP-1 or NRP-1 may play a role in TGF-β activation in this system. This chapter will focus on the mechanism of latent TGF-β activation by the non-protease molecules, TSP-1 and NRP-1.

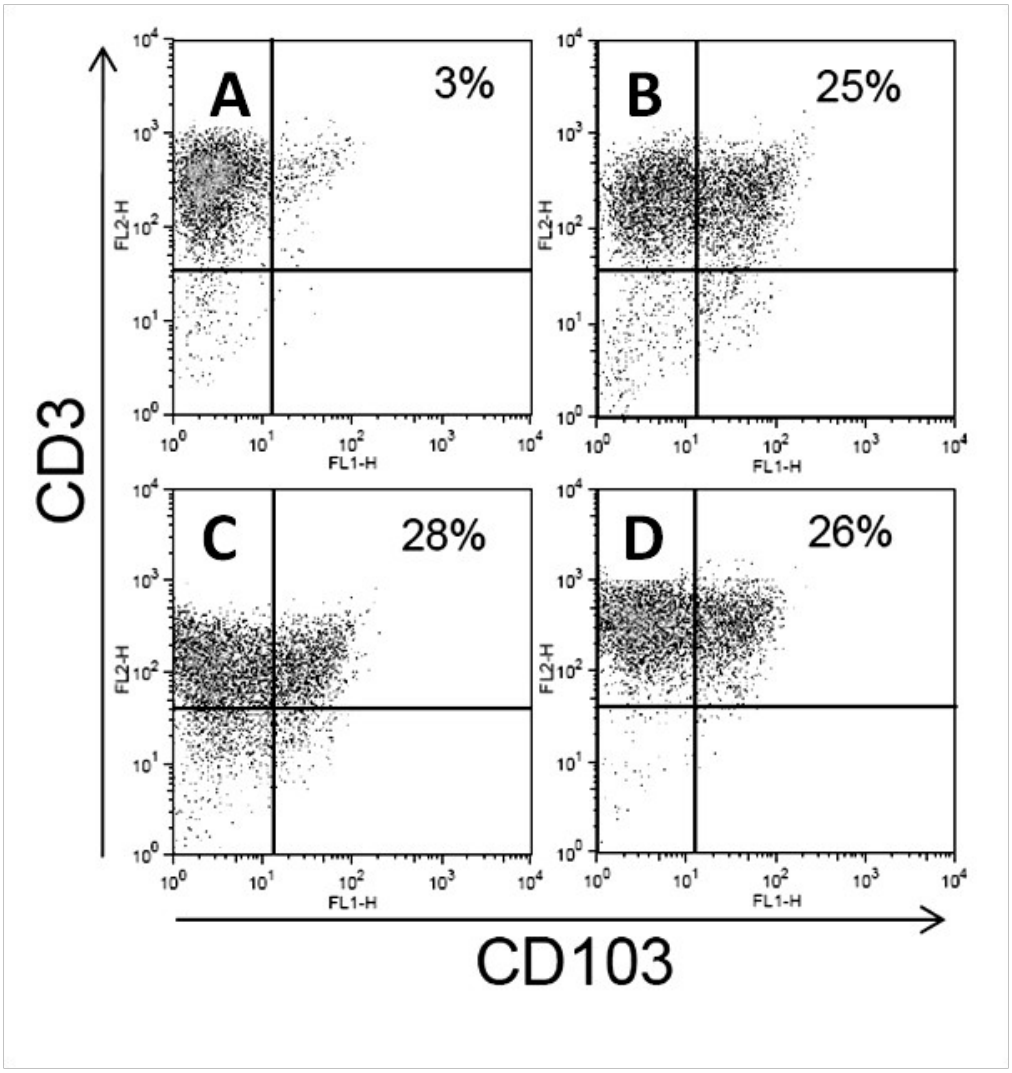

Figure 5.1 TGF-β induces the differentiation of activated T cells

(A) A flow cytometric dot plot showing that few (3%) activated T cells express CD103 in the absence of exogenous TGF-β1. (B) Significant induction of CD103 is observed on activated T cells following co-culture with PTEC. **(C**) The level of induction of CD103 expression by activated T cells is not increased further by co-culture with PTEC which have been transfected to express high levels of the β6 integrin. **(D**) Blockade of the β6 integrin with a specific peptide did not inhibit the induction of CD103 expression during co-culture with activated T cells. (This image shows unpublished data provided by Prof John A Kirby).

5.2 Thrombospondin-1 (TSP-1)

The thrombospondins (TSP) are a family of multifunctional proteins that exist as both secreted proteins and insoluble extracellular matrix molecules (Adams and Lawler, 1993; Bornstein, 2001). This family consists of 5 isoforms which can be divided into 2 subgroups, A and B, according to their oligomerisation status and molecular architecture (Adam and Lawler, 1993). Subgroup A contains TSP-1 and TSP-2, whereas subgroup B contains TSP-3, TSP-4 and TSP-5. TSP-1 and TSP-2 are highly homologous trimers with a chain molecular mass of

approximately 145 kDa, consisting of three identical subunits, whereas TSP-3, TSP-4 and TSP-5 are homopentamers with chain molecular masses of approximately 100 kDa. TSP-1 is a homotrimeric matricellular glycoprotein. It is expressed by a variety of cell types such as platelets, vascular smooth muscle cells and renal cells, including mesangial cells, podocytes, endothelial cells, tubular epithelial cells and interstitial cells (Hugo et al., 1995; Hugo et al., 1998). In adults, TSP-1 is regulated by cytokines including platelet derived growth factor (PDGF), fibroblast growth factor (FGF)-2 and TGF-β; thus, it is commonly expressed in inflamed areas and during wound healing and tissue remodelling (Bornstein, 2001).

5.2.1 Structure of thrombospondin-1

TSP-1 is comprised of multiple domains of repeating subunits. These include (i) an amino-terminal heparin binding region, (ii) a procollagen-like region containing the intermolecular disulfide bonds, three properdin-like type 1 repeats, three EGF-like type 2 repeats, calcium-sensitive EF-hand-like type 3 repeats, and (iii) a C- terminal globular domain (Adams and Lawler, 1993; Bornstein, 2001) (Figure 5.2). The various biological activities of TSP-1 relate to specific domains of the complex molecule.

Figure 5.2 Structure of thrombospondin-1.

The homotrimer TSP-1 comprised of three major domains including an N-terminal heparin binding domain (HBD), a procollagen domain (PC) containing three properdin-like type 1 repeats (1), three EGF-like type 2 repeats (2) and seven calcium sensitive EF-hand-like type 3 repeats (3), and a C-terminal domain. The figure is from Murphy-Ullrich and Poczatek, 2000.

5.2.2 The mechanism of TGF-β activation by TSP-1

It has been suggested that TSP-1 is an activator of TGF-β *in vitro* in different cell systems, as well as a cell-free system (Ribeiro et al., 1999; Daniel et al., 2007). TSP-1 forms a tri-molecular complex with the TGF-β procytokine complex by interacting with both mature TGF-β and LAP. Recent data has defined the two major binding sites which play an important role in TGF-β activation by TSP-1.

I. The hexapeptides GGWXXW present in each of the three type 1 repeats: GGWSPW, GGWSHW and GGWGPW respectively. These hexapeptides bind to the VLAL sequence of mature TGF-β (Figure 5.3) (Young and Murphy-Ullrich, 2004). This allows the molecular interaction of the KRFK amino acid sequence of the TSP-1 molecule with the N-terminal LSKL (Leucine-Serine-Lysine-Leucine) sequence of the LAP by hydropathic bonding (Schultz- Cherry et al., 1995).

II. The KRFK (Lysine-Arginine-Phenylalanine-Lysine) amino acid sequence is located between the first and second type I properdin-like repeats (Schultz-Cherry et al., 1995). With the contribution of the GGWXXW, the KRFK of TSP-1 binds to the LSKL sequence at N-terminal of the LAP (Figure 5.3) (Ribeiro et al., 1999; Schultz-Cherry and Murphy-Ullrich, 1993). KRFK peptide has been shown to activate latent TGF-β by disrupting interactions between LAP and mature TGF-β; additionally, it can competitively inhibit complex formation between the LAP and TSP-1 (Ribeiro et al., 1999). Furthermore, the hexapeptide GGWSXW and LSKL peptide are able to block the activation of TGF-β by TSP-1 (Ribeiro et al., 1999; Schultz-Cherry and Murphy-Ullrich, 1993).

Studies using an anti-Thy1 model have shown that renal arterial transfer of anti-sense phosphorothioate oligodeoxynucleotide against TSP-1 and continuous intravenous infusion of GGWSXW or LSKL peptides, interfere with the activation of TGF-β (Daniel et al., 2003; Daniel et al., 2004). The treated mice in these studies showed decreased TGF-β activity and TGF-β receptor signalling, as assessed by trichrome collagen I&IV and fibronectin staining. Activation of latent TGF-β is a property unique to TSP-1. The TSP-2 family member lacks the KRFK sequence and does not activate TGF-β. This finding is consistent with the observation that the corresponding peptide from TSP-2 (RIR) does not activate TGF-β (Schultz-Cherry et al., 1995).

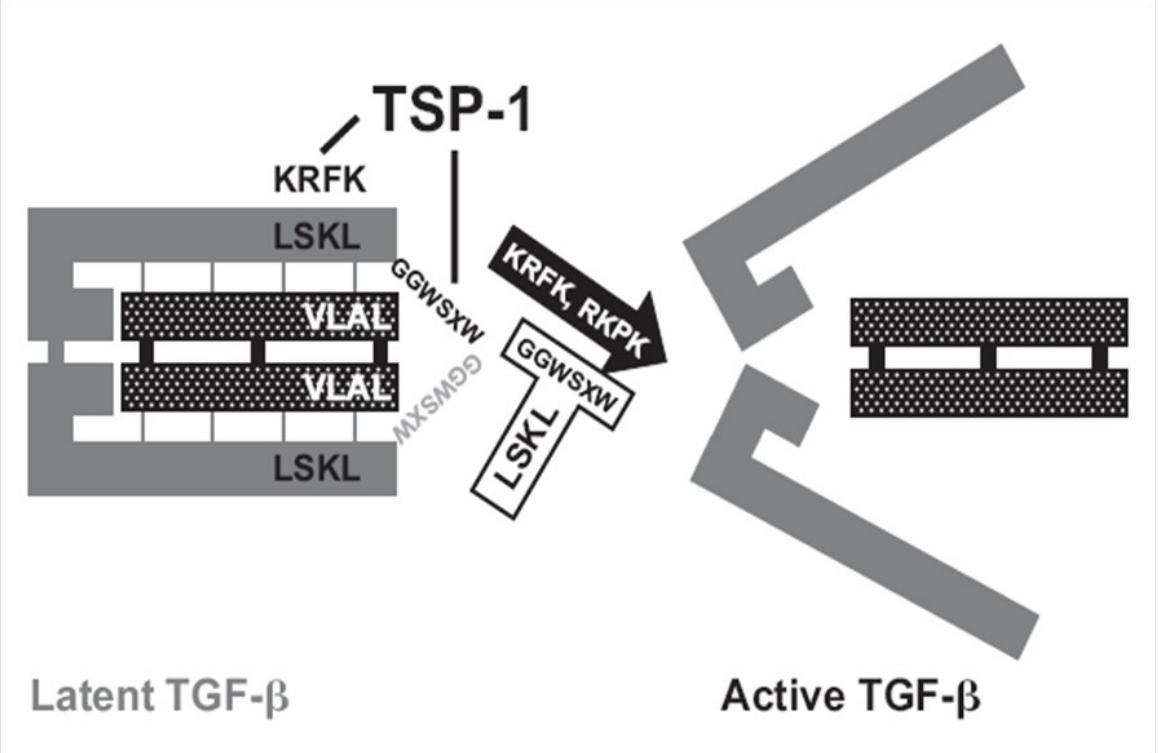

Figure 5.3 The mechanism of latent TGF-β activation by TSP-1.

There are two major sites in properdin-like type I repeat of TSP-1 which bind to the latent TGF-β. Initially, GGWSXW sequence of TSP-1 binds to VLAL sequence of mature TGF-β. This interaction facilitates the association between KRFK sequence of TSP-1 and LSKL sequence of LAP which results to the conformational change of latent TGF-β and exposes the mature TGF-β to the receptor. This image is obtained from Hugo and Daniel, 2009.

5.3 Neuropilin-1

Neuropilin-1 (NRP-1) is a multifunctional protein expressed by several cell types, including endothelial cells, dendritic cells, regulatory T cells (Treg), malignant cells (Romeo et al., 2002; Beilenberg et al., 2006) and epithelial cells of the breast, uterus, endometrium, kidney and lung (Gagnon et al., 2000). The well known functions of NRP-1 are axonal guidance via the binding with chemorepulsive class 3 semaphorin (SEMA3) proteins (Kolodkin et al., 1997) and angiogenesis through its interaction with vascular endothelial growth factor (VEGF) family members and their receptors (VEGFR1 and VEGFR2) (Pellet-Many et al., 2008).

Neuropilin-2 (NRP-2), which shares 45% homology with NRP-1, is mostly expressed by malignant cells (Gray et al., 2008). Interestingly, a recent study reported that TGF-β1, IL-1 and OSM (oncostatin M) were able to stimulate NRP-2 expression in renal proximal tubular cells (Schramek et al., 2009).

5.3.1 Structure of Neuropilin-1

The molecular weight of NRPs is 120kDa. The basic structure of NRPs consists of four domains (Figure 5.4):

1. A short cytoplasmic domain which binds to the PDZ protein. PDZ results from the first letters of three proteins: Post-synaptic density 95, Drosophila disc large tumour suppressor and zonula occludens-1 protein (Wang et al., 2007).
2. The three extracellular domains:
   a. The CUB (a1/a2) domain (named for its identification in complement components C1r and C1s, Uegf, and bmp1). This domain is commonly found in developmentally regulated proteins (Bork and Beckmann, 1993), and is involved in SEMA3 binding (Miao et al., 1999).
   b. The FV/FVIII (b1/b2) domain, which is involved in both SEMA3 and VEGF binding (Miao et al., 1999).
   c. The MAM domain which is derived from Meprin, A-5 protein and protein-tyrosine phosphatase mu.

Recent studies have reported NRP-1 can bind several growth factors, including hepatocyte growth factor (HGF), the HGF receptor (c-Met), fibroblast growth factors (FGFs) and platelet derived growth factor (PDGF) (Matsushita et al., 2007; West et al., 2005; Dhar et al., 2010). It also has affinity for the β1 integrin (Fukasawa et al., 2007).

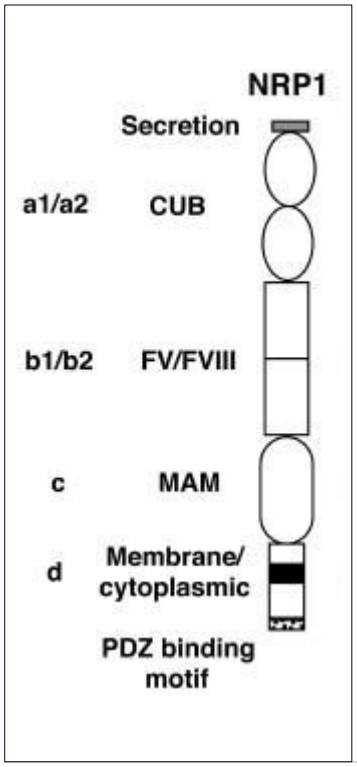

Figure 5.4 The structure of Neuropilin-1.

NRP-1 consists of four domains, (i) CUB domain contains two repeats of complement (a1/a2, (ii) FV/FVIII domain contains two repeats of coagulation factor (b1/b2), (iii) MAM domain, and (iv) a transmembrane or cytoplasmic region (d) which possess a PDZ binding motif at the carboxyl termini. This image is obtained from Nakamura *et al*. 2002.

5.3.2 The mechanism of latent TGF-β activation by NRP-1.

A study of human T cells has shown that the proliferation of activated T cells is suppressed when soluble LAP-TGF-β1 is added (Glinka and Prud'homme, 2008). This suppression is restored by addition of a blocking anti-TGF-β1 monoclonal antibody (Glinka and Prud'homme, 2008). Glinka *et al* suggest that NRP-1-Fc activates LAP-TGF-β1 via a sequence RKFK in the b2 domain, which is closely similar to the KRFK sequence of TSP-1 (Glinka and Prud'homme, 2008). Furthermore, both the RKFK and KRFK peptides are equally effective at activating TGF-β1 by binding LSKL within the N-terminal region of LAP, leading to a conformational change which exposes the active growth factor (Figure 5.5) (Schultz-Cherry et al., 1995; Ribeiro et al., 1999; Crawford et al., 1998).

NRP-1 expression has been observed in 3-4% of splenic T cells, with $CD4^+$T cells expressing this antigen (Glinka and Prud'homme, 2008). In addition, 60% of murine $CD4^+CD25^+$ T cells co-express NRP-1 and LAP; however, 10-12% of $CD4^+CD25^+NRP^-$ T cells also express LAP. Thus, NRP-1 is not the only LAP receptor on the surface of T cells. Furthermore, it has been reported that NRP-1 expression correlates with high FOXP3 expression in mice and humans (Battaglia et al., 2008).

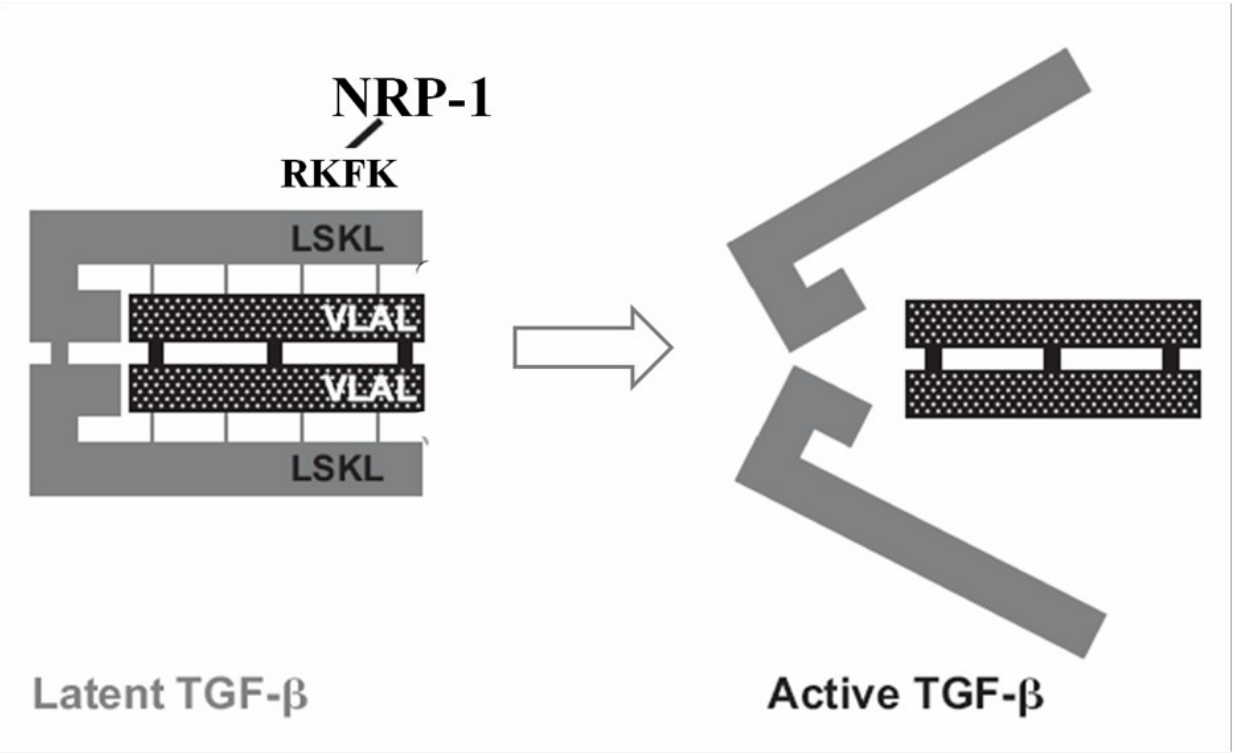

Figure 5.5 Mechanism of latent TGF-β activation by NRP-1.

The RKFK sequence in the b2 domain of NRP-1 binds to LSKL sequence of LAP producing the conformational change in latent TGF-β. This image is adapted from Hugo and Daniel, 2009.

5.4 Aim and objectives

TGF-β plays a central role in the induction of fibrosis in many organs. In addition, it is increasingly recognised that TGF-β-induced EMT is a potential inducer of renal fibrosis. Since TGF-β activation is a key step in TGF-β regulation, a series of experiment was designed to determine whether activated T cells can activate latent TGF-β by mechanisms involving TSP-1 and NRP-1.

The objectives of this study are to:

- Detect and quantify the expression of TSP-1 and NRP-1 at both protein and mRNA levels in human T cells.
- Examine the expression of NRP-1 in human kidney allograft biopsies.
- Demonstrate that cytoplasmic Smad3 is phosphorylated by treatment of NRP-1 expressing MDA231 cancer cells with latent TGF-β1 and determine whether this can be inhibited by addition of the LSKL inhibitory peptide.
- Demonstrate that activated T cells are responsive to latent TGF-β1 and that this response can be inhibited by addition of the LSKL peptide inhibitor of TSP-1 and NRP-1.

5.5 Materials and Methods

5.5.1 MFB-11 Bioassay

As described in section 2.7.1, the MFB-F11 assay can be developed using either P-Nitrophenyl Phosphate (pNPP) or the Tropix® Phospha-Light™ system. The latter assay will be described in this chapter. The Tropix® Phospha-Light™ system is a chemiluminescent system designed for the detection of secreted placental alkaline phosphatase (SEAP), which is a truncated form of human placental alkaline phosphatase, in cell culture medium. Technically, cell culture medium is first heated to 65°C to inactivate endogenous alkaline phosphatase. The heated sample is then incubated with assay buffer solution, which contains a proprietary mixture of non-placental alkaline phosphatase inhibitors. CSPD (chemiluminescent substrate for alkaline phosphatase)-containing reaction buffer is then added and incubated until maximum light emission is reached. The chemiluminescent signal is then measured using a luminometer. This assay allows detection of less than 10 femtogram of SEAP (Chemiluminescent product guide, Applied Biosystem), which is more sensitive than colorimetric detection of SEAP.

5.5.1.1 Detection of secreted placental alkaline phosphatase by Phospha-Light Assay

MFB-F11 $4x10^4$ cells were seeded in each well of a 96-well plate and cultured overnight. These cells were then washed and incubated in serum free medium for 2 hours. The cells were then incubated with 50µl of a serial TGF-β1 dilution (concentration 0-1nM) to make a standard curve (Figure 5.6) or with test samples for 24 hours. The Phospha-Light assay kit was prepared in accordance with the manufacturer's instructions.

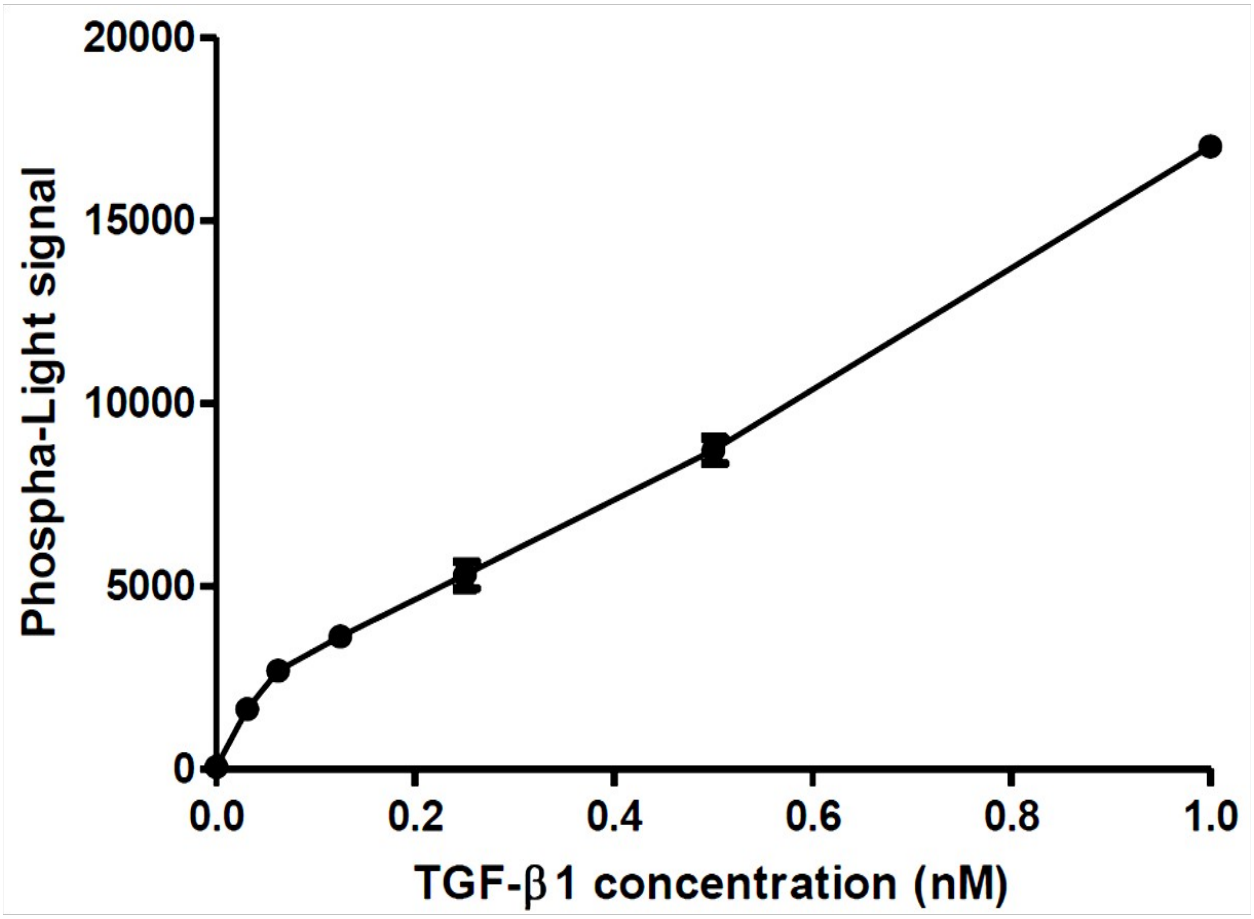

Figure 5.6 TGF-β1 standard curve for detecting secreted placental alkaline phosphatase using the Tropix Phospha-Light system. The results are presented as mean values (n = 6) ± SEM.

5.5.2 Intracellular staining for flow cytometry

In order to detect antigens within the cytoplasm of cells, it is necessary to permeabilise the plasma membrane to allow large antibody molecules to penetrate the cell. As this process can disrupt cellular architecture, it is normally necessary to first fix the cell structure by chemical treatment.

5.5.2.1 Fixative agents

Fixative agents can be divided into 5 main groups, including (i) cross-linking agents which are the most popular fixatives, (ii) precipitating agents or alcohols, (iii) oxidising agents, (iv) mercurials and (v) picrates.

Paraformaldehyde (PFA) is a cross-linking fixative and was used in this study. PFA fixes cells or tissues by forming covalent chemical bonds in the proteins, particularly between lysine residues. This anchors and stabilises most antigens and prevents antigen loss or migration. Although PFA provides a beneficial effect in the preservation of intracellular

structure and plasma membrane integrity, adverse effects such as autofluorescence or cell shrinkage can be a problem.

5.5.2.2 Permeabilising agents

Following fixation, antibody fluorescence dyes must access the intracellular compartment. This can be achieved by treatment with detergents or organic solvents. Saponin (Sigma), which was used in this study, is a plant-derived glycoside detergent which acts mainly by solubilising cholesterol. Saponin is widely used to permeabilise the plasma membrane and intracellular membranes, depending on the concentration (Wassler et al., 1987).

5.5.2.3 Intracellular staining for flow cytometry procedure

Cells were harvested and washed two times in 2% FBS/PBS. The cells were fixed in 2% paraformaldehyde at room temperature for 15 minutes and then washed in 0.1% saponin in 2%FBS/PBS by spinning at 500g for 5 minutes. After washing, the fixed cells were incubated with a biotin conjugated anti-TSP-1 antibody (1:10), which was diluted in 0.1% saponin/2% FBS/PBS, on ice for 30 minutes. The wash step was repeated three times, followed by incubation with streptavidin conjugated anti-mouse IgG antibody (1:50) on ice for 30 minutes. The cells were washed three times before analysis using a FACSCalibur machine (BD Biosciences).

5.5.3 Cytocentrifugation

Centrifugation in a Cytospin (Shandon) is a method used to prepare suspension cells for microscopic viewing. Human T cells were activated with CD3/CD28 beads for 48 hours. The activated T cells were washed and diluted in 2% FBS/PBS at a concentration of $1x10^5$cells/ml. Microscope slides were mounted with a paper pad and cuvette in the metal holder. 200µl of cell suspension was loaded into each cuvette before centrifugation at 1000rpm for 3 minutes. The slides were carefully detached from the paper pads and allowed to dry before being fixed in methanol at -20°C for 1 hour. The fixed cells were dried again in air before processing for immunofluorescence staining as described in section 2.5.2.4.

5.5.4 CFSE staining protocol

Carboxyfluorescein succinimidyl ester (CFSE) is a fluorescent cell staining dye which is commonly used for proliferation analysis. Initially, the dye enters cells in a diacetylated form, carboxyfluorescein diacetate succinimidyl ester (CFDA, SE). Then, intracellular esterases remove the acetate groups and convert the molecules into the fluorescent ester (CFSE), which is retained within the cells after covalently coupling, via the succinimidyl group, to intracellular proteins (Figure 5.7). Since CFSE is membrane impermeable, it can be retained within cells for

extremely long periods without being transferred to adjacent cells. When cells divide, the CFSE is equally split between the daughter cells, leading to CFSE signal reduction. The cells may then be analysed by flow cytometry to quantify CFSE within individual cells and dilution of the label produced by cell division (Quah et al., 2010).

5.5.4.1 CFSE labelling procedure

After isolating human T cells, as described in section 2.2.5.1, $6x10^6$cells were resuspended in 300µl of 0.1% FBS/PBS. The cell suspension was split equally into 2 tubes. The T cells were incubated with 150µl of 2µM CFSE at 37°C for 5 minutes. After incubation, 5ml of cold complete medium was added to both tubes, which were then placed on ice for 5 minutes. The T cells were washed by adding 10ml of complete medium and centrifuged twice at 800G for 10 min. Prior to activation the cells were incubated with medium overnight to allow early loss of CFSE. The cells were washed again before activation by CD3/CD28 beads.

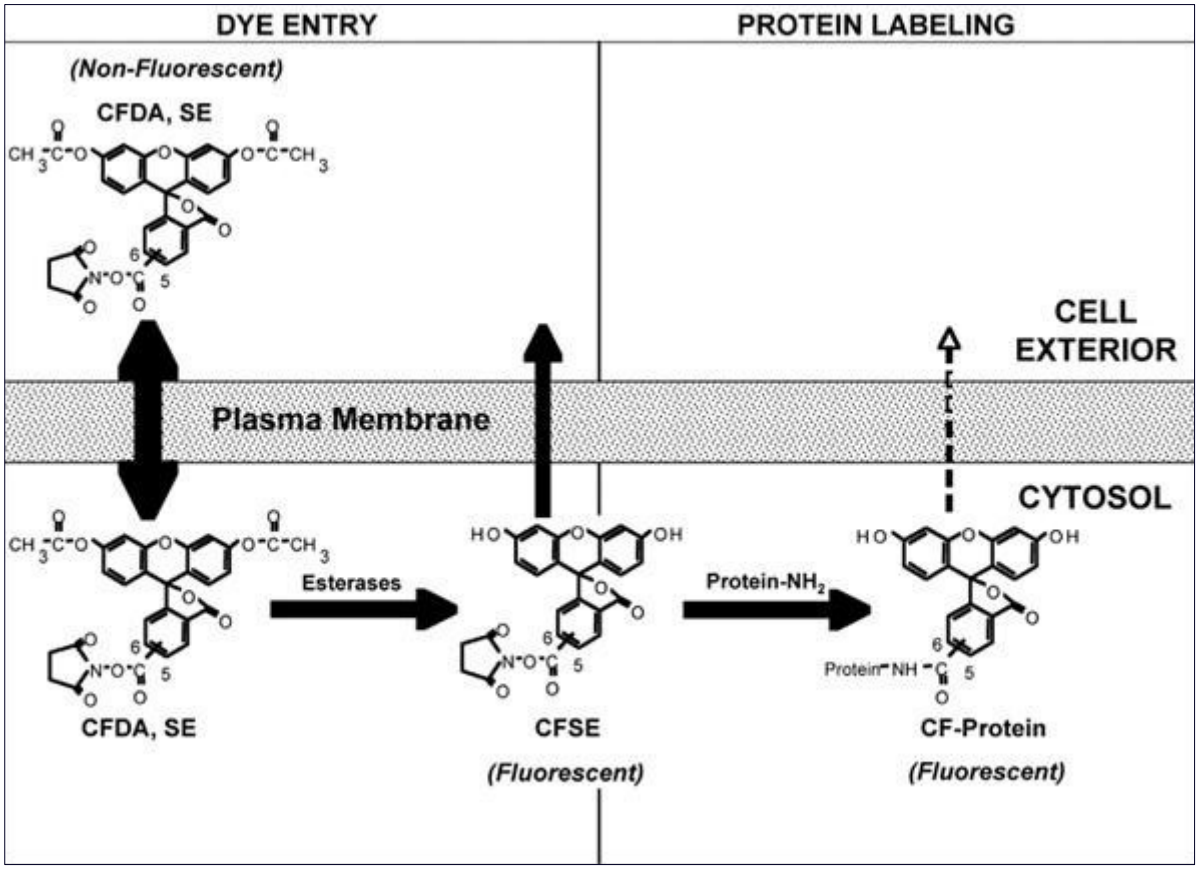

Figure 5.7 Illustration of the chemical changes that fix CFSE within a cell during the labelling process. The image is obtained from Quah et al. 2010.

5.5.5 Immunohistochemistry staining for paraffin section

Immunohistochemistry is a method for demonstrating the presence and location of proteins in tissue sections. Immunohistochemical staining is accomplished using antibodies specific for target antigens. The antibody-antigen interaction is then visualised using either chromogenic detection, in which an enzyme conjugated to the antibody cleaves a substrate to produce a coloured precipitate, or fluorescent detection, in which a fluorophore is conjugated to the antibody and can be visualised directly by fluorescence microscopy.

IHC-P refers to immunohistochemical staining of tissues that have been fixed and then embedded in paraffin before being sectioned. The basic steps of the IHC-P protocol are as follows.

5.5.5.1 Deparaffinisation

Before proceeding with the staining protocol, the slides must be deparaffinised and rehydrated. Incomplete removal of paraffin can cause poor staining of the section. The slides were placed in a rack and washed in a xylene tank for 10 minutes. The slides were then washed for 1 minute in 100% and 95% ethanol tanks respectively, before being held in tap water until antigen retrieval.

5.5.5.2 Endogenous peroxidase blocking

Endogenous peroxidase activity is found in many tissues and can be detected by reacting fixed tissue sections with DAB substrate. Endogenous peroxidase activity is inhibited by pre-treatment of the tissue section with hydrogen peroxide prior to antigen retrieval or incubation with primary antibody.

5.5.5.3 Antigen retrieval

During the formalin fixation process, a methylene bridge is formed, which cross-links proteins and masks antigenic sites. Antigen retrieval is required to break the methylene bridges and expose antigenic sites in order to allow antibodies to bind. There are two methods of antigen retrieval: heat-induced and enzyme-mediated. This study used heat-induced epitope retrieval.

1000ml of sodium citrate buffer (2.94g Tri-sodium citrate in 1000ml distilled water at pH6.0; 0.5ml Tween-20 was added before use) was added to a pressure cooker and heated to 100C. Once boiling, the slides in a metal rack were transferred from tap water to the pressure cooker. The lid of the pressure cooker was secured following the manufacturer's instructions, and the samples were heated at full pressure for 60 seconds. After cooling in water, the lid was removed and the slides were washed in tap water for 5 minutes.

5.5.5.4 Immunohistochemical staining

A. Control

Negative controls were performed to test for the specificity of each primary antibody involved. First, no staining must be shown when omitting the primary antibody or replacing a specific primary antibody with normal serum (of the same species as the primary antibody). This control is easy to achieve and can be used routinely in immunohistochemical staining.

B. Blocking

The main cause of non-specific background staining is non-immunological binding of the specific immune sera by hydrophobic and electrostatic forces to certain sites within tissue sections. This form of background staining is usually uniform and can be reduced by blocking non-specific sites with normal serum. Some tissues, including the kidney, contain endogenous biotin. To avoid unwanted avidin binding to endogenous biotin, if using a biotin-avidin detection system, it is necessary to pre-treat these tissues with unconjugated avidin.

C. Indirect staining: Avidin-Biotin Complex (ABC) method

The ABC method is one of the most widely used techniques for immunhistochemical staining. Avidin, a large glycoprotein, can be labelled with peroxidase or fluorescein and has a very high affinity for biotin. Biotin, a low molecular weight vitamin, can be conjugated to a variety of biological molecules, including antibodies. The technique involves three layers. The first layer is unlabelled primary antibody. The second layer is biotinylated secondary antibody. The third layer is a complex of avidin-biotin peroxidase. The peroxidase is then developed by reaction with3, 3'-diaminobenzidine (DAB), which is oxidised to give a brown colour.

Briefly, endogenous biotin was blocked by incubating kidney sections with avidin at room temperature for 15 minutes, followed by biotin for 15 minutes (Avidin/Biotin Blocking kit, Vector). The slides were then washed in TBS twice for 5 minutes. The sections were then incubated in 20% swine serum at 4°C for 1 hour to block non-specific binding. After blocking, the sections were incubated with primary antibody, rabbit monoclonal anti-NRP-1 (1:100) diluted in 20% swine serum at 4°C overnight. The next day, the slides were washed in TBS before incubating with biotinylated goat anti-rabbit IgG (1:200) at room temperature for 1 hour. The slides were washed twice in TBS for 5 minutes. The sections were then incubated with avidin-biotin peroxidase at room temperature for 30 minutes, followed by the washing step. The slides were then incubated with a solution containing DAB and H_2O_2 at room temperature for 2 minutes, or until the colour changed to brown, then rinsed in running tap water.

5.5.5.5 Counterstain

A counterstain is a stain with colour which contrasts with the principal stain, making the stained structures more easily visible. The slides were placed in a haematoxylin tank for 30 seconds, and then rinsed in running water before being incubated in Scott's tap water for 30 seconds and washed again.

5.5.5.6 Dehydration

Dehydration was performed by placing the rack of slides for 1 minute each in 50% ethanol, 70% ethanol, 95% ethanol, 100% ethanol and xylene, respectively.

5.5.5.7 Mounting the slide

The slides were mounted with DPX, which is a mixture of distyrene (a polystyrene), a plasticiser (tricresyl phosphate), and xylene.

5.5.6 Two colour immunofluorescence staining

This method was used to assess the co-expression of NRP-1 and CD3 in the transplant kidney biopsy sections. The sections were passed through the following processes: deparaffinisation, rehydration and antigen retrieval as described in section 5.2. The sections were then incubated with normal serum at room temperature for 1 hour, followed by incubation overnight with primary rabbit monoclonal anti-NRP-1 (1:100) and mouse monoclonal anti-CD3 (1:100) at 4°C. The following day, the sections were washed in TBS for 5 minutes 3 times before incubation with polyclonal anti-rabbit IgG FITC conjugated (1:150) at room temperature for 1 hour. The slides were washed in TBS three times. After washing, the sections were incubated with polyclonal anti-mouse IgG TRITC conjugated (1:100) for 1 hour. After washing, the nuclei were stained with DAPI for 2 minutes, followed by one wash. Auto-fluorescence was reduced by placing the slides in a Sudan Black solution for 10 minutes. After washing, the slides were mounted with fluorescence mounting medium. The slides were stored in the dark at 4°C until they were viewed by confocal microscopy.

5.6 Results

5.6.1 NRP-1 expression by normal renal tubular epithelial cells and graft infiltrating inflammatory cells

It has been suggested that NRP-1 is expressed by many cell types including endothelial cells, malignant cells, epithelial cells, and regulatory T cells (Kragbrun et al., 2002). However, the data of NRP-1 expression in transplanted kidney has rarely been reported. This experiment was performed in order to examine the expression of NRP-1 in transplanted kidney biopsy sections by using the immunoperoxidase technique. Normal and rejected kidney graft sections were processed as described in section 5.5.5, and, following the staining, the slides were viewed by light microscope at time 20 magnification.

In normal transplant kidney sections, NRP-1 was present along the luminal surface of some renal tubules (Figure 5.8A) while there was absence of NRP-1-positive interstitial cells. However, the expression of NRP-1 was reduced in the damaged tubules of kidney grafts with cell-mediated rejection, but some infiltrating inflammatory cells did express NRP-1 in the interstitium (Figure 5.8B).

Several immune cell types, including macrophages and lymphocytes, have been reported to express NRP-1 (Ji et al., 2009). The potential association between CD3 and NRP-1 in kidney allograft sections was determined by performing 2-colour immunofluorescence to localise these antigens.

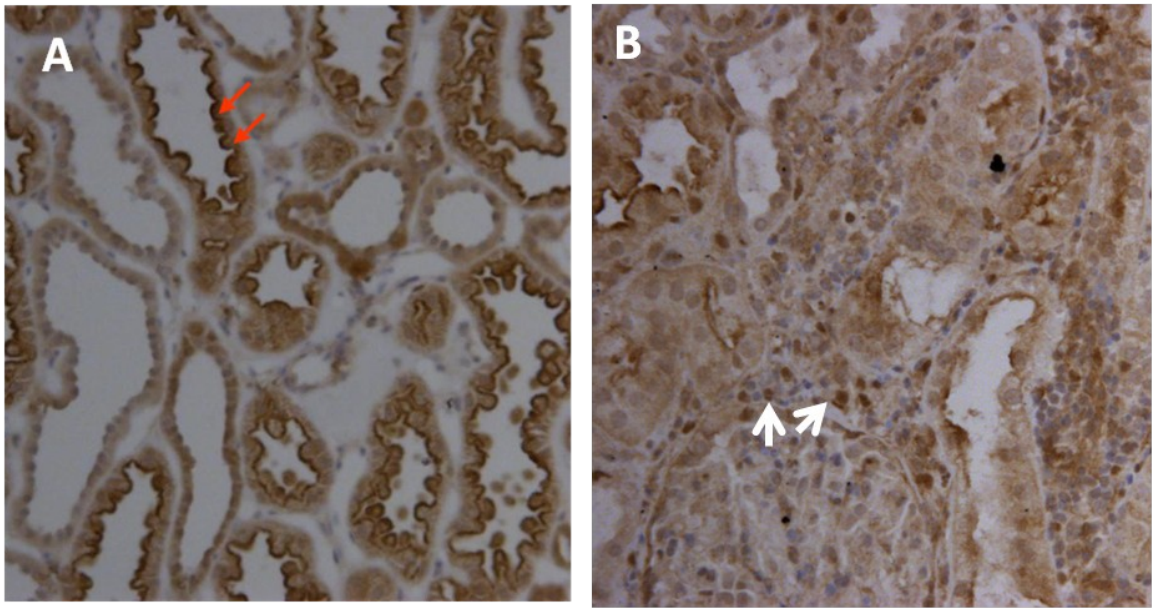

Figure 5.8 Microscopic analysis of NRP-1 expression in human kidney graft biopsies.
In a normal kidney allograft (A), NRP-1 was predominantly localized at the luminal surface of renal tubules (red arrows). However, NRP-1 preferentially appeared in inflammatory cells in the interstitial areas during rejection (white arrows) whereas the appearance in luminal areas seemed to decrease. The images were captured at x200 magnification. The results are representative of 2 similar experiments.

5.6.2 NRP-1 was expressed on infiltrating CD3-expressing cells during graft rejection

In order to determine what type of inflammatory cells expressed NRP-1, sections showing renal allograft rejection were examined by 2-colour immunofluorescence staining (section 5.5.6). Transplanted kidney biopsies including normal and rejecting grafts were stained with anti-NRP-1 and anti-CD3 monoclonal antibodies. The expression of NRP-1 and CD3 was localised intracytoplasmic by confocal microscopy. Interestingly, some infiltrating inflammatory cells expressed both CD3 and NRP-1 (Figure 5.9) during an acute rejection episode. This suggested that NRP-1 was expressed by activated T cells during graft rejection.

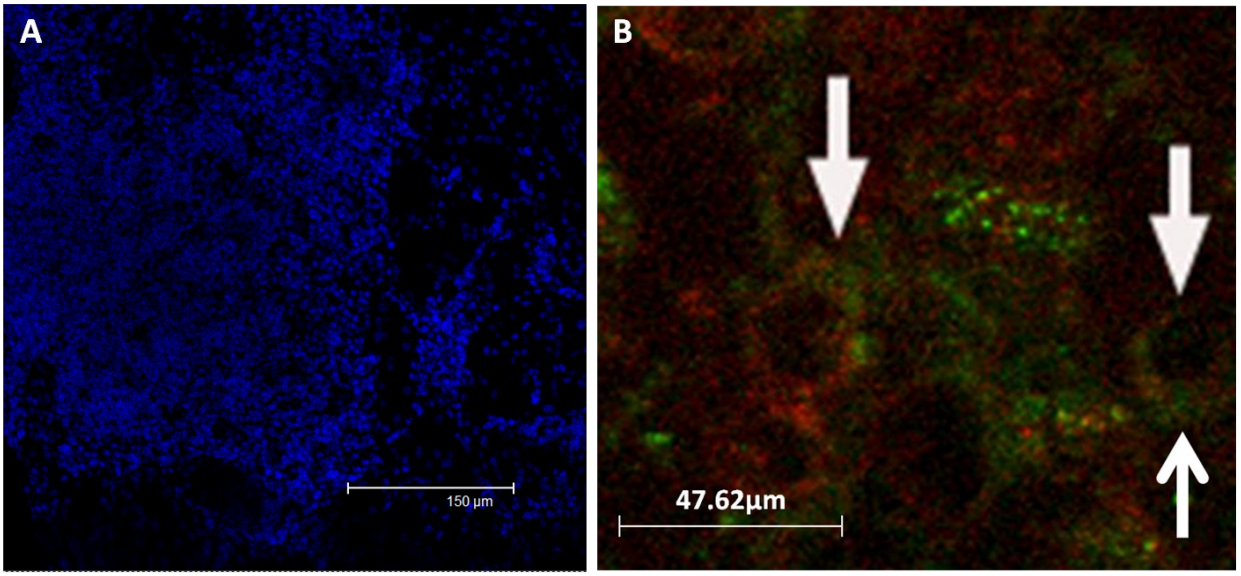

Figure 5.9 Immunofluorescence analysis of NRP-1 co-expression with CD3 in a kidney allograft biopsy showing acute rejection.

Two colour immunofluorescence staining of CD3 (Red) and NRP-1 (Green) in cell-mediated rejection showing some $CD3^{+}$cells co-expressed NRP-1 (white arrows) (B) compared to a negative control section (A). The images were taken at x 20 (A) and x 63 (B) magnification. The results are representative of 2 similar labelling experiments.

5.6.3 NRP-1 was highly expressed by human T cells after activation for 48 hours

A previous study has shown that 3-4% of mouse splenic T cells express NRP-1 (Glinka and Prud'homme, 2008). However, results for human T cells have been inconclusive (Milpied et al., 2009). To determine the exact number of NRP-1^+ T cells, human T cells were isolated from the blood of healthy volunteers as described in section 2.2.5. Some of the resting T cells were then activated with CD3/CD28 beads (section 2.2.5.1). The time course of NRP-1 expression was determined by staining resting T cells and activated T cells after 24, 48 and 72 hours with an APC conjugated anti-NRP-1 monoclonal antibody. In addition, the T cells were co-stained with a FITC conjugated anti-CD4 antibody in order to identify the specific subtype of T cells which expressed NRP-1. Following the staining process, the phenotype of the T cells was examined by flow cytometry.

Approximately 1-2% of circulating human T cells expressed NRP-1. Interestingly, the population of NRP-1^+ T cells increased after activation, and reached a maximum of 17.52 ± 3% (mean ± SEM; n=8) after 48 hours (Figure 5.10C). After 48 hours, the expression of NRP-1 gradually declined (Figure 5.10D). Two parameter immunophenotyping showed that 80% of the cells expressing NRP-1 were $CD4^+$ T cells (Figure 5.10A-D). Normally, T cells are activated during antigen-specific immune processes such as acute rejection. The results from this experiment suggest that NRP-1 may be up-regulated on the surface of $CD4^+$ T cells after activation by allogantigen-expressing cells within a renal allograft This is consistent with the finding of NRP-1 expressing T cells in kidney graft biopsies from patients with acute cell-mediated rejection.

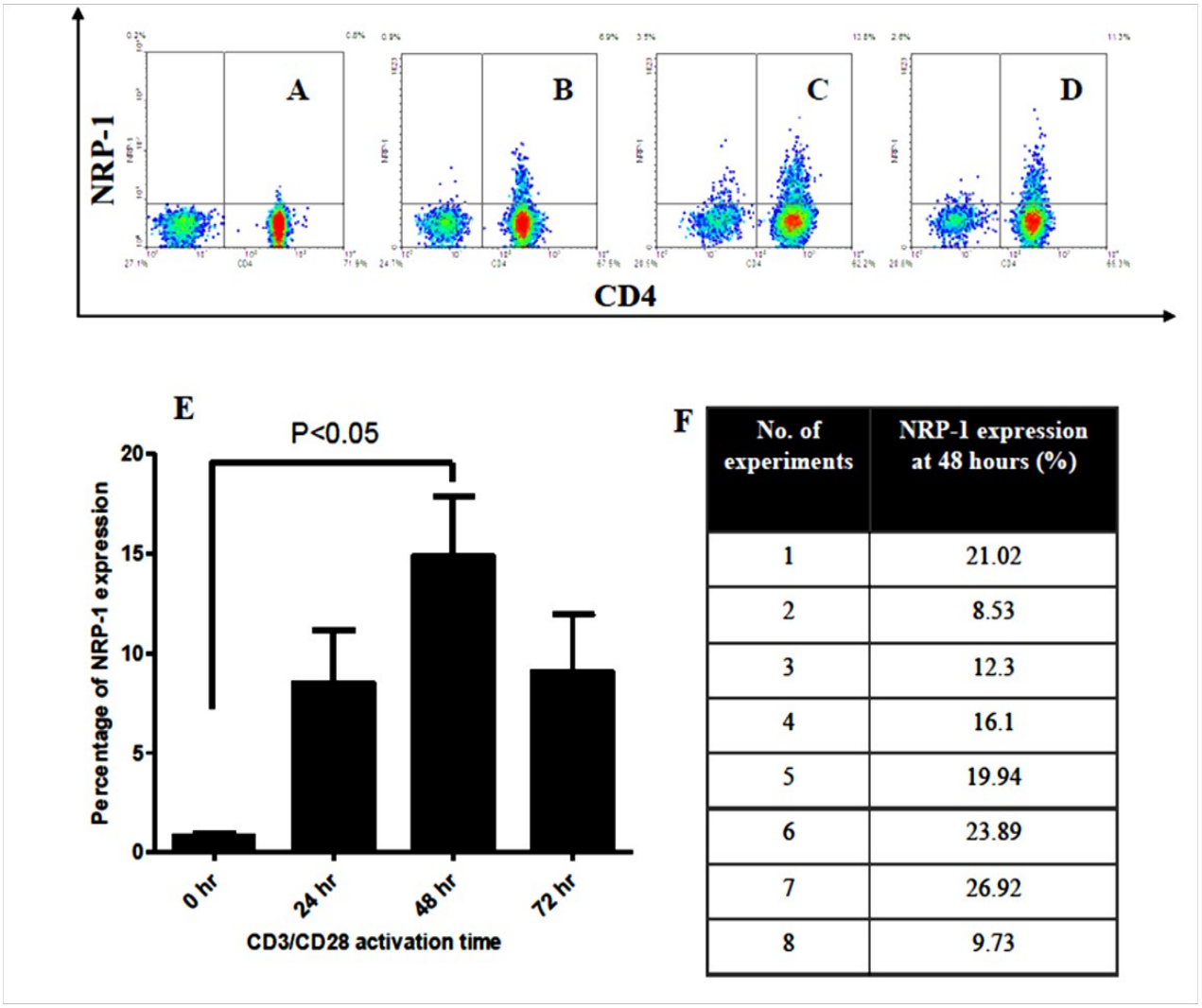

F

No. of experiments	NRP-1 expression at 48 hours (%)
1	21.02
2	8.53
3	12.3
4	16.1
5	19.94
6	23.89
7	26.92
8	9.73

Figure 5.10 Time course expression of NRP-1 by activated human T cells.

CD3/CD28 activated T cells were analyzed for NRP-1 expression at 0, 24, 48 and 72 hours by flow cytometry. The percentage of NRP-1 positive resting $CD4^+$T cells (%) was 1.2 ± 0.13 (A), this increased to 8.5 ± 2.7 after 24 hours (B). Expression reached the highest value of 17.52 ± 3 at 48 hours (C) and then gradually declined to 9.82 ± 2.6 at 72 hours (D). All data are presented as mean ± SEM; NRP-1 preferentially appeared in the $CD4^+$ T cell sub-population. The dot-plot results are representative of 4 similar experiments. The bar graph (E) summarizes the percentage of NRP-1 expression by all T cells. The bars show mean value (n=4) and error bars are SEM. The quadrants were set by analysing of samples after labelling with isotype control antibodies. The table shows the percentage of NRP-1 expression by activated T cells after 48 hours (data from 8 independent experiments using different T cell donors).

5.6.4 Cytosmear showing the presence of NRP-1 in activated T cells.

Flow cytometric data showed the expression of NRP-1 on the surface of activated T cells. This was confirmed by cytocentrifugation followed by immunofluorescence staining to determine the distribution of NRP-1 in activated T cells (see section 2.5.2.4). Fluorescence microscopy was used to examine the presence of NRP-1(Figure 5.11).

Results of this study showed the expression of cytoplasmic NRP-1 in T cells after activation with CD3/CD28 beads for 24 hours. Interestingly, nearly all the cells expressed NRP-1 by cytosmear staining. However, at this time the flow cytometer showed cell surface expression of this antigen on a minority of the cells. This might suggest that NRP-1 is stored in the cytoplasm of all activated T cells but is driven to the surface of only some cells after activation. A further experiment was designed to test whether cell-surface expression of NRP-1 is dependent on cell proliferation.

5.6.5 Cell division and NRP-1 expression

To ascertain whether the expression of NRP-1 is associated with the cell cycle, flow cytometric analysis was performed. Resting T cells were incubated with 2μM CFSE at 37°C for 5 minutes, and then the excess CFSE was removed by washing in medium. The stained cells were left overnight in medium before activation by CD3/CD28. The activated T cells were collected at 24, 48 and 72 hours and stained with APC conjugated anti-NRP-1 antibody. The presence of both CFSE and NRP-1 was determined by 2-colour flow cytometry collecting data o fluorescence channels 1 and 4 respectively.

After activation for 48 hours, the fluorescence results showed clear CFSE peaks corresponding to undivided cells (M1) and cells which had undergone 1 (M2), 2 (M3) and 3 (M4) cycles of proliferation; a few cells had undergone 4 cycles of division (M5) (Figure 5.12A, B, C); the greatest proportion of T cells was in peak M4 at this time. Examination of NRP-1 expression in each cell cycle showed that 20% of the cells in each cycle (including undivided cells) expressed cell-surface NRP-1. Hence, the expression of cell surface NRP-1 is not dependent on T cell proliferation or the number of cycles of cells division.

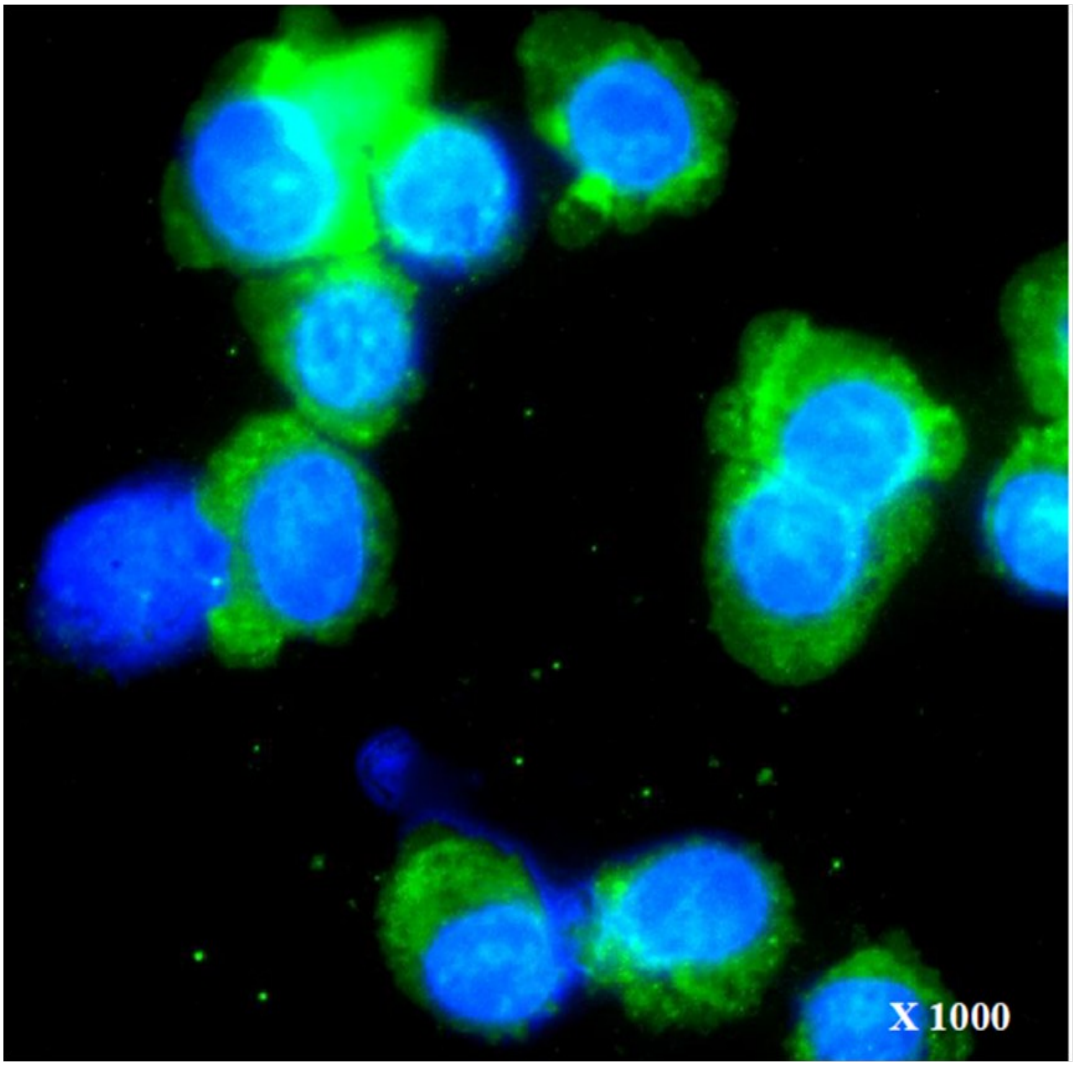

Figure 5.11 Localization of NRP-1 in CD3/CD28 activated T cells

The isolated T cells were activated with CD3/CD28 for 48 hours. Then the activated T cells were attached to slides by cytocentrifugation, and stained with anti-NRP-1 mAb (Green). Nuclei were visualized by DAPI stain (Blue). The images were taken at x 100 magnification. The result is representative of 2 similar experiments.

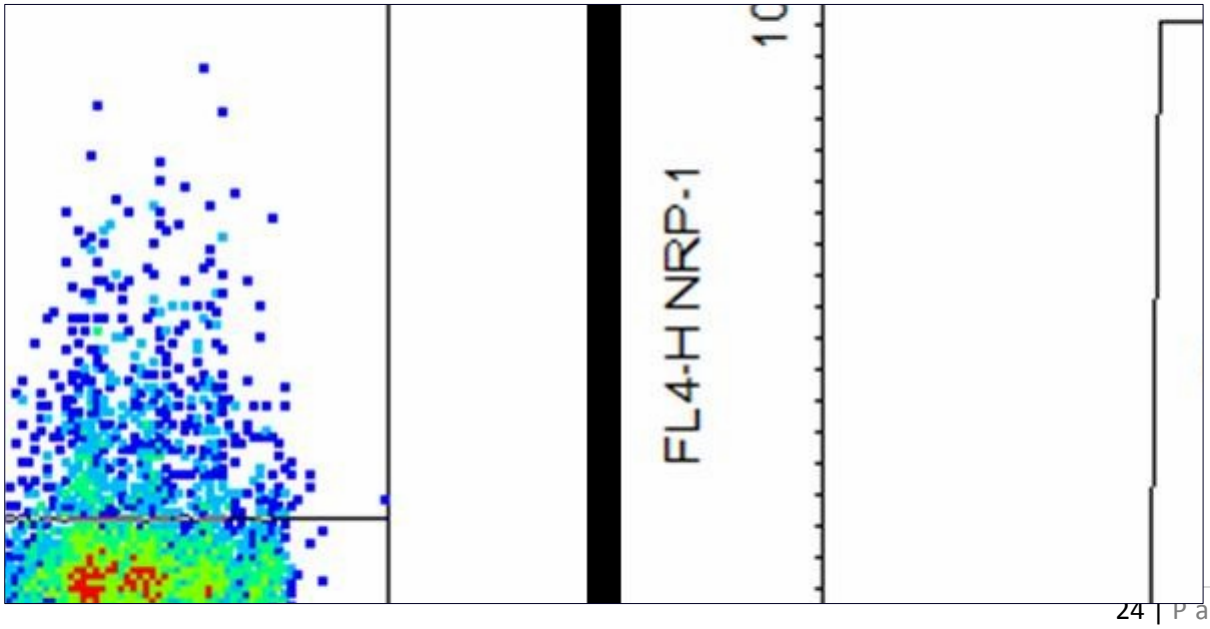

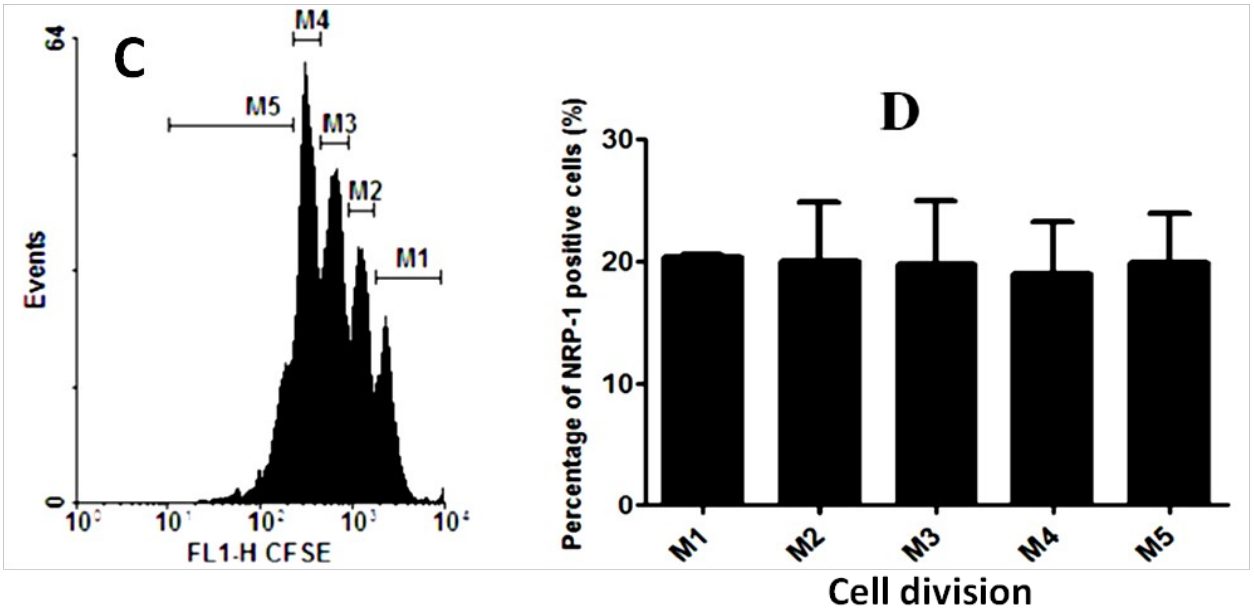

Figure 5.12 Flow cytometric analysis of NRP-1 expression after 48 hours of T cell division.

Isolated human T cells were incubated in medium containing 2μM of CFSE overnight, followed by activating T cells with CD3/CD28 beads for 48 hours before flow cytometry analysis. (A and B) Dotplot and (C) histogram show T cells division at 48 hours. (D) The bar graph shows the percentage of NRP-1 expressing cells in each cell cycle (mean ± SEM, n = 3). The results are representative of 2 similar experiments. The quadrants were set by analysing samples after labelling with appropriate isotype control antibodies.

5.6.6 Cytoplasmic thrombospondin-1 was mobilised to the surface of activated T cells after co-culture with renal epithelial cells

It has been demonstrated that TSP-1 plays an important role in the activation of latent TGF-β *in vivo (*Ludlow et al., 2005). The following series of experiments was designed to examine the expression of TSP-1 by human T cells.

Initially, flow cytometry was performed to quantify the expression of TSP-1 by activated T cells. The human T cells were activated with CD3/CD28 for 72 hours. The activated T cells were then incubated with a biotin-conjugated anti-TSP-1 antibody (Abcam) for 30 minutes, followed by incubation with FITC-conjugated streptavidin for 30 minutes. The cells were examined by immunofluorescence flow cytometry using a FACSCalibur machine.

After activation, TSP-1 was expressed on the surface of fewer than 10% of activated T cells (Figure 5.13A). A previous study has suggested that T cells cultured with fibronectin and collagen strongly express TSP-1, with a possibility that this antigen is moved from cytoplasmic stores to the cell surface in response to cell contact with these matrix proteins (Li et al., 2002). To examine this possibility, activated T cells were either permeabilised with saponin or co-cultured with HK-2 before labelling with an anti-TSP-1 monoclonal antibody. Interestingly, the proportion of TSP-1 expressing cells increased to 36.6% following permeabilisation (Figure 5.13B). Furthermore, 21.7% of the T cells expressed TSP-1 after co-culture with HK-2 cells for 30 minutes (Figure 5.13C). These results suggest that TSP-1 is expressed in the cytoplasm of a greater proportion of T cells than expresses this antigen on the cell surface. Furthermore, brief exposure of the t cells to HK-2 cells was sufficient to markedly increase T cell surface expression of TSP-1. It is possible that this induction of cell-surface TSP-1 expression is due to contact with matrix proteins produced by the immortalised kidney cells. This possibility will require further investigation.

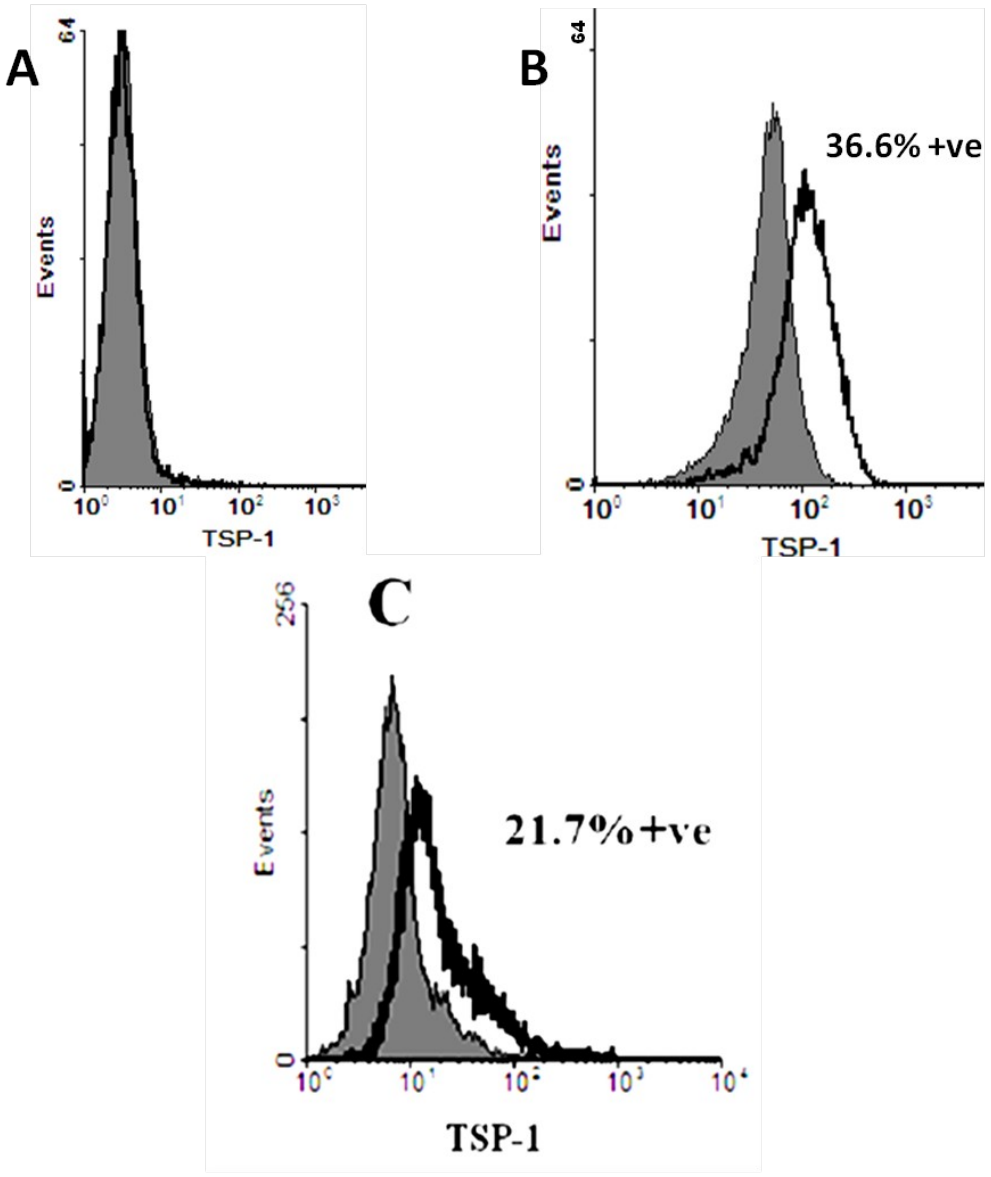

Figure 5.13 Activated T cells co-cultured with renal tubular epithelial cells increased cell surface expression of TSP-1.

(A) A flow cytometric histogram shows TSP-1 on surface of <10% of activated T cells. (B) When activated T cells were permeabilized by saponin, 36.6% ± 1.3 (mean ± SEM, n = 4) of the cells expressed TSP-1. (C) Activated T cells co-cultured with HK-2 increased TSP-1 expression to 21.7%. In all cases, the shaded histogram shows fluorescence produced by labelling with an isotype-matched control antibody. The open histogram shows experimental labelling. Results are shown from 1 of 4 similar experiments.

5.6.7 Changes in gene expression following T cell activation

This study has shown that NRP-1 protein was maximally expressed after T cell activation for 48 hours. In order to determine whether this resulted from significant induction of the NRP-1 gene, a series of quantitative real-time PCR analyses was performed.

T cells were activated for 24 hours by stimulation with CD3/CD28 beads (section 2.2.5), followed by 24 hours incubation with no further stimulation or with 10ng/ml TGF-β1 or an equimolar 30ng/ml of latent TGF-β1. After the stimulation, RNA was prepared for cDNA synthesis (section 2.3.4). Real-time PCR was performed to quantify changes in the basal expression of RNA encoding CD103, FoxP3, TGF-β, TSP-1 and NRP-1; 18s rRNA was used as an internal standard (section 2.4.3).

After CD3/CD28 activation for 48 hours the expression of FOXP3 mRNA was significantly increased, but none of the other assayed mRNA sequences showed a change in expression (Figure 5.14). T cells treated with TGF-β1 significantly increased their expression of the CD103, FOXP3, TSP-1 and TGF-β1 genes. Treatment with latent TGF-β1 also increased the expression of CD103, FOXP3 and TSP-1 (albeit to a lesser extent that the induction caused by TGF-β1); latent TGF-β1 did not significantly increase TGF-β1 mRNA expression. The expression of mRNA encoding NRP-1 was not increased by T cell activation, suggesting that the increase in protein expression observed is produced by post-transcriptional regulation. However, the gene expression study did not have positive control for NRP-1 expression. Further study is required to explore this issue.

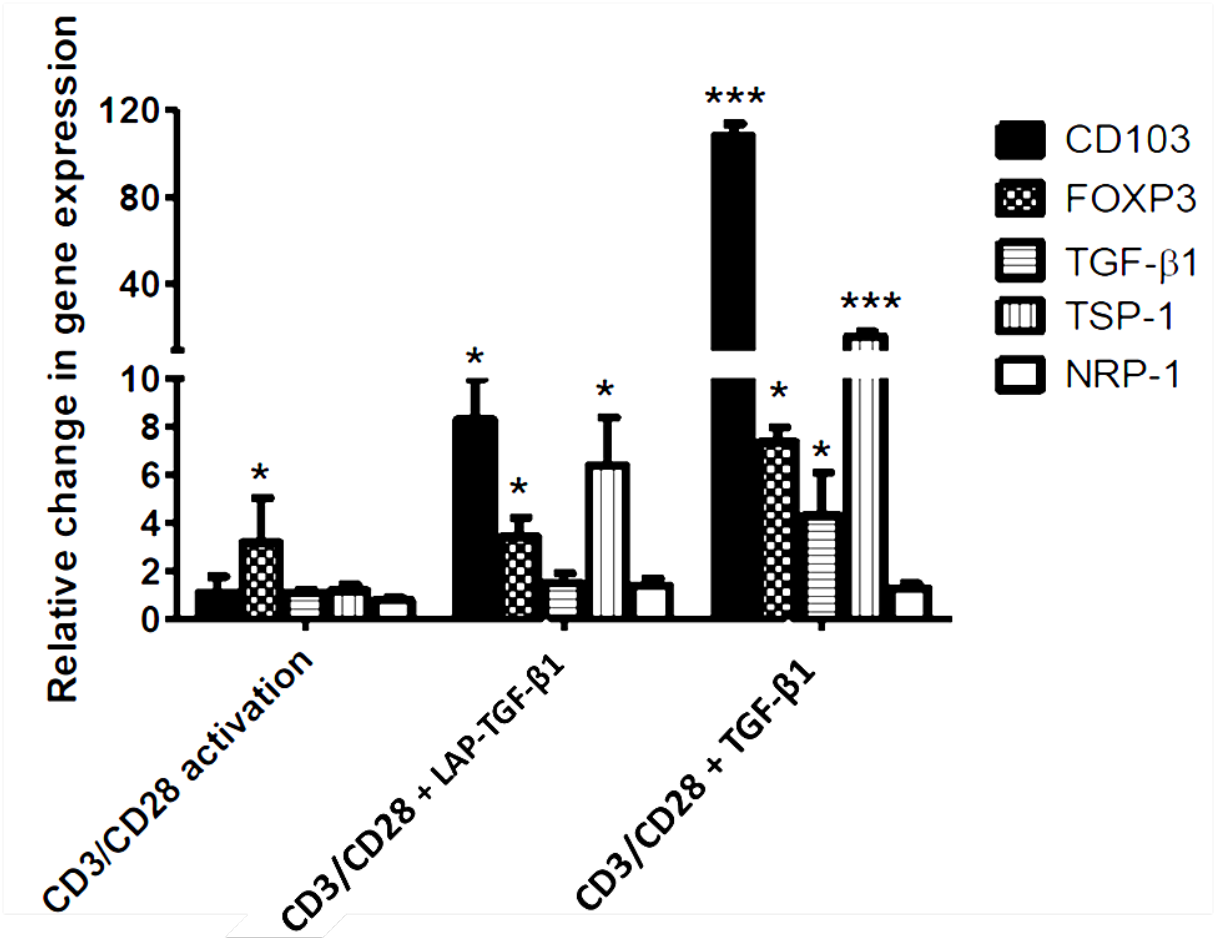

Figure 5.14 Comparison of CD103, FOXP3, TGF-β1, TSP-1 and NRP-1 gene expression in activated T cells, TGF-β1 treated cells and latent TGF-β1 treated cells.

The isolated human T cells were activated by CD3/CD28 Beads for 24 hours followed by 24-hours of 10ng/ml TGF-β1 or equimolar (30ng/ml) latent TGF-β incubation. All genes were normalized to 18S rRNA and are presented as mean values ± SEM (n=3). FOXP3 mRNA was significantly expressed in all treatment groups relative to resting T cells. CD103 and TSP-1 mRNA were significantly up-regulated in latent TGF-β1 and TGF-β1 treated T cells, whereas TGF-β1 mRNA was significantly expressed in T cells with TGF-β1 treatment. However, none of treated T cells up-regulated NRP-1 mRNA. These results are representative of 3 similar experiments. (* = $p < 0.05$, *** = $p<0.001$; ANOVA).

5.6.8 LAP is necessary and sufficient to confer the latency to TGF-β

Latent TGF-β usually consists of active TGF-β and LAP. Thus, if active TGF-β is added to LAP, the activity of TGF-β should be inhibited by the formation of the latent complex. This hypothesis was tested by incubating MFB-F11 cells with 1nM TGF-β1 with or without LAP at concentrations between 0.001-100nM for 24 hours. The culture medium was collected and response to active TGF-β1 was detected using the Phospha™-Light assay.

No significant response to TGF-β was observed in control wells which contained serum-free medium; LAP alone also produced no positive response in the assay. In contrast, TGF-β1 samples showed the highest levels SEAP production indicating the response to active TGF-β1; this activity was significantly reduced in the presence of increasing concentrations of LAP(Figure 5.15) with complete blockade observed after addition of 100nM LAP.

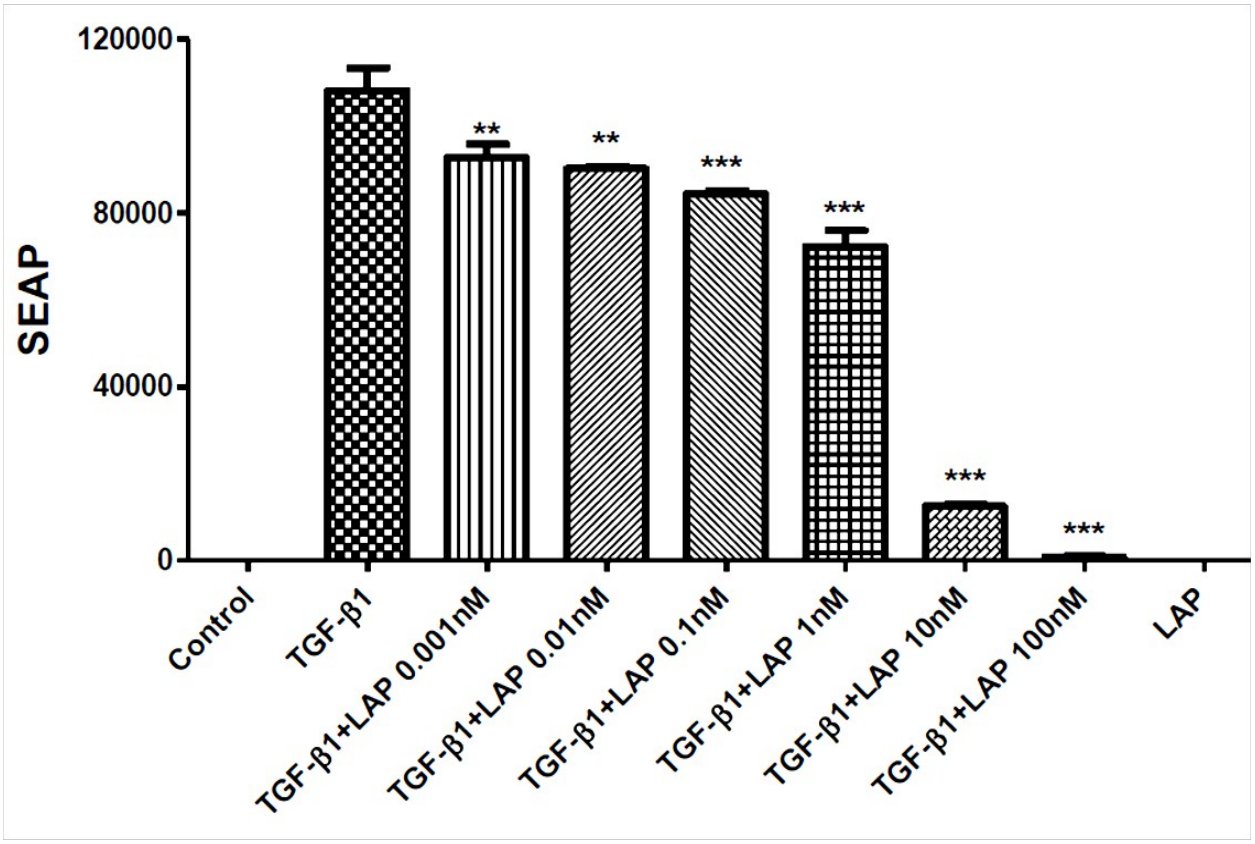

Figure 5.15 Bioassay analysis of active TGF-β activity of TGF-β1 in the presence of LAP.

Semi-confluent MFB F-11 cells were incubated in medium or medium containing 1nM of TGF-β1 or TGF-β1 with LAP at concentrations between 0.001 – 100 nM for 24 hours. In the presence of LAP, the level of TGF-β1 significantly decreased with complete blockade at a LAP concentration of 100nM. The bars shows mean and the error bars are SEM. The results are representative of 3 similar experiments. (** = $p < 0.01$, *** = $p < 0.001$; ANOVA).

5.6.9 NRP-1 was expressed by the MDA231 human breast cancer cell line

MDA231 is a breast carcinoma cell line which strongly expresses NRP-1 (Ginkla et al., 2008). These cells were used in this study as a positive control for NRP-1 expression. This cell line was first validated for both NRP-1 and TSP-1 expression by flow cytometry. Confluent MDA231 cells were harvested and incubated with APC conjugated anti-NRP-1 and biotin conjugated anti-TSP-1 for 30 minutes. To examine the expression of TSP-1, the cells were incubated with FITC conjugated streptavidin before analysis.

The flow cytometric results demonstrated that MDA231specifically expressed NRP-1 but did not express TSP-1 (Figure 5.18). The following experiments used this cell line to demonstrate a role for NRP-1 in the activation of latent TGF-β and also to validate the inhibitory effect of the LSKL peptide.

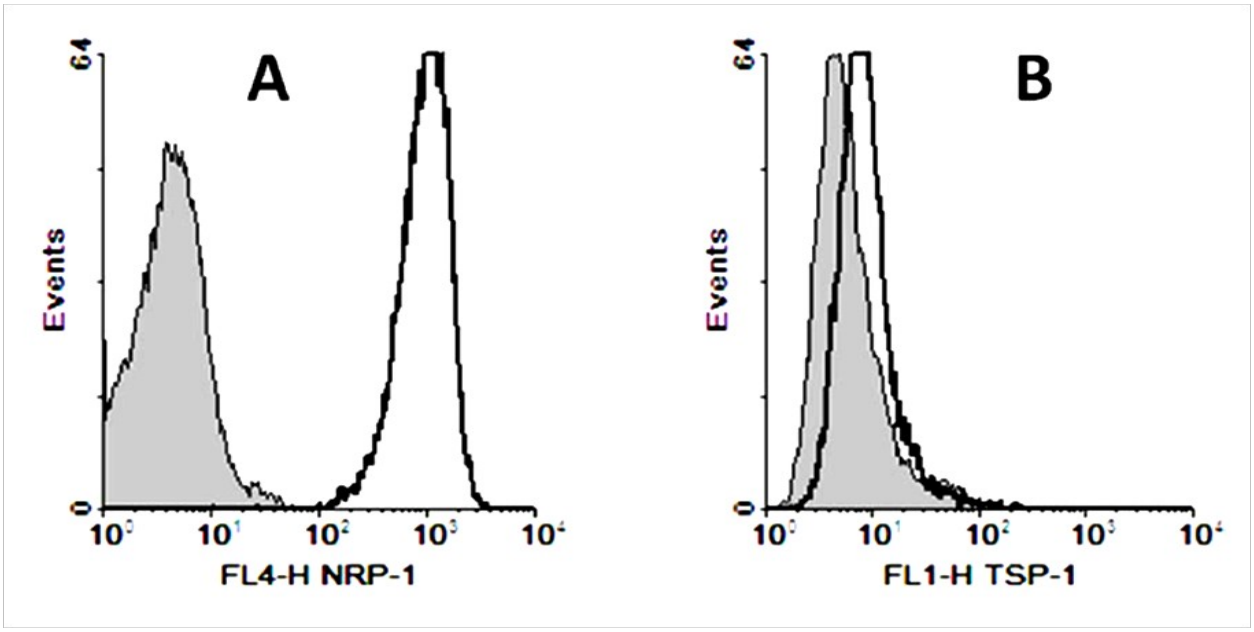

Figure 5.16 Histogram demonstrating the expression of NRP-1 and TSP-1 by MDA231 cells.

Confluent MDA231 cells were incubated with anti-NRP-1 (A) and anti-TSP-1 (B) antibodies before analysis by flow cytometry. In all cases, the shaded histogram shows fluorescence produced by labelling with an isotype-matched control antibody. The open histogram shows experimental labelling. The results are a representative of 2 independent experiments and show that all the cells express NRP-1 at a high level but TSP-1 was not expressed.

5.6.10 The LSKL peptide inhibited pSmad2/3 expression by MDA231 cells.

Members of the TGF-β superfamily predominantly signal via activation of the intracellular Smad signalling pathway; in particular, the functions of TGF-β1, TGF-β2 and TGF-β3, are generally mediated by the Smad2 and Smad3 signalling molecules (Feng et al., 2005). The LSKL peptide sequence of LAP is the binding site for KRFK and RKFK of TSP-1 and NRP-1 respectively (section 5.2.2 and 5.3.2). Therefore, addition of LSKL peptide could competitive bind to KRFK or RKFK sequence leading to inhibition of latent TGF-β activation, which subsequently phosphorylate intracellular Smad molecules. Although it is well known that the LSKL peptide can inhibit the activity of TSP-1 (Ribeiro et al., 1999), the potential of this peptide to inhibit the activation of latent TGF-β1 by NRP-1 has not been previously demonstrated. In this study a series of experiments was performed to validate this inhibition of NRP-1.

MDA231 cells which express NRP-1 but no TSP-1 (section 5.6.9) were incubated with 1nM TGF-β1 and an equimolar concentration of latent TGF-β1 with or without 50μM LSKL or SLLK peptides for 24 hours. After incubation, the cells were fixed with 4% paraformaldehyde at room temperature for 20 minutes. The fixed cells were then permeabilised with Tween 20 for 30 minutes. Non-specific antibody binding was blocked by incubation with 1%BSA/PBS at room temperature for 1 hour. The cells were then incubated with anti-phosphoSmad 2/3 antibody (1:100) at 4°C overnight. After washing in TBS three times for 5 minutes, the cells were incubated with FITC-conjugated anti-rabbit IgG at room temperature for 1 hour, followed by staining the nuclei with DAPI. The slides were visualised by confocal microscopy at 63 times magnification.

Resting cells showed no expression of pSmad 2/3. However, when the cells were treated with TGF-β1, pSmad 2/3 expression was clearly visible (Figure 5.20). The latent TGF-β1 treated cells also expressed pSmad 2/3, though at a reduced intensity, suggesting that latent TGF-β1 was activated in the culture system. Importantly, the LSKL peptide inhibited the potential of latent TGF-β1 to induce the expression of pSmad 2/3; this inhibition was not observed when the control SLLK peptide sequence was present (Figure 5.17). This study provides evidence that the LSKL can inhibit NRP-1 dependent activation of latent TGF-β1. However, the inhibition observed in this assay was incomplete, suggesting the additional activity of non-inhibitable mechanisms of TGF-β1 activation during the prolonged culture period. For this reason a second experiment was conducted across a shorter time period using a sensitive western blot system to detect phosphorylated Smad 3.

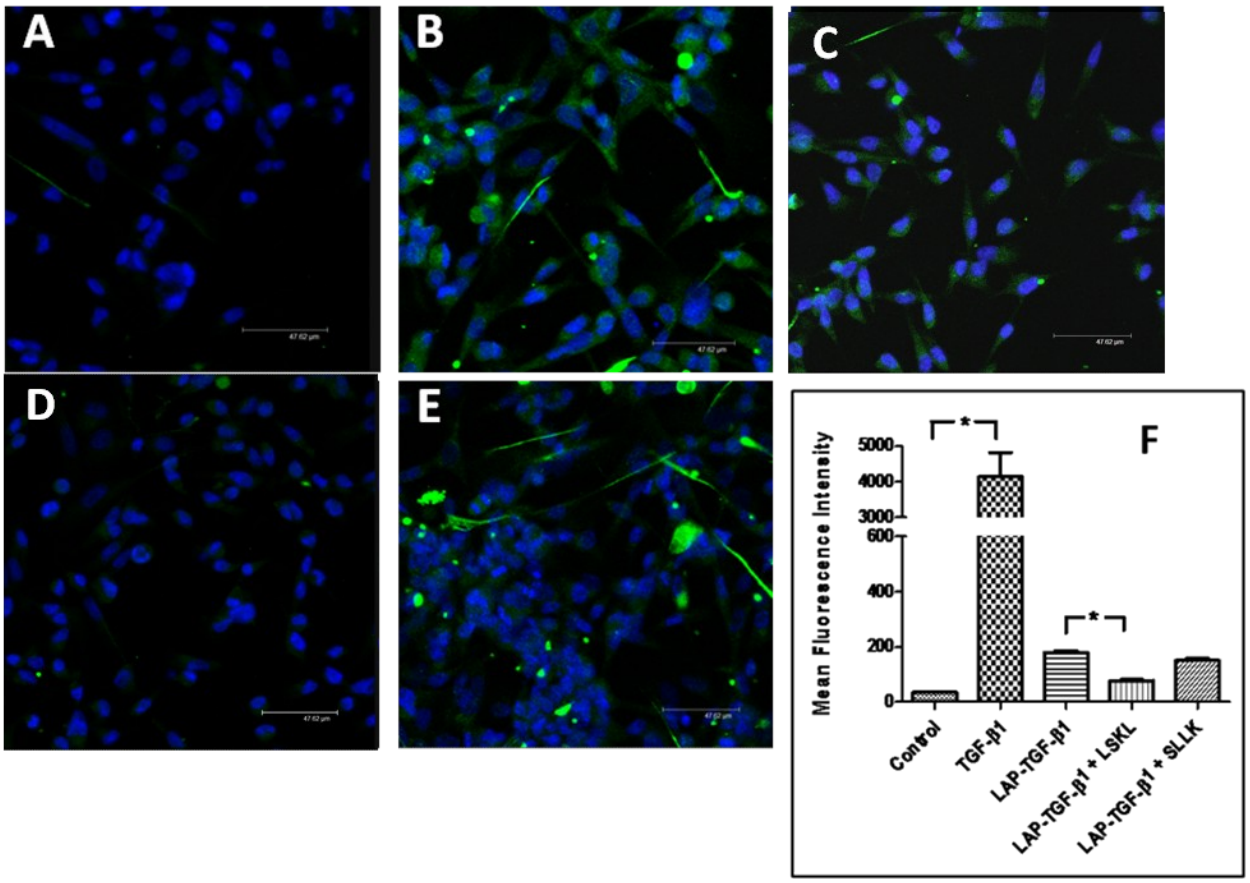

Figure 5.17 The expression of pSmad2/3 in the MDA231 cell line.

Confluent MDA231 cells were incubated in medium (A) or medium containing 10ng/ml of TGF-β1 (B) or equimolar (30ng/ml) LAP-TGF-β1 (C) with 50μM LSKL (D) or SLLK (E) peptide for 72 hours. pSmad2/3 was demonstrated by microscopic immunofluorescence staining (Green). Nuclei were visualized by DAPI staining (Blue). The images were recorded at x60 magnification. The quantitative analysis of fluorescence intensity showed that pSmad2/3 was significantly increased in the TGF-β1-treated group. LAP-TGF-β1 also induced pSmad2/3 expression, but this was significantly decreased after incubating with the LSKL peptide. The bars show mean (n=5 areas of fluorescent measurement) and error bars are SEM. The results are representative of 2 similar experiments. (* = $p < 0.05$, student's t-test).

5.6.11 Phospho (p)Smad3 expression by MDA231 cells was inhibited by the LSKL peptide.

The inhibitory effect of the LSKL peptide was confirmed using the Western Blot method. MDA231 cells were treated with 1nM TGF-β1 or equimolar latent TGF-β1 with or without 50μM LSKL or SLLK for 30 minutes. After the treatment, the cells were lysed in a buffer containing mixed phosphatase inhibitors. After the reduction of disulphide bonds with SDS solubilisation (see section 2.6.3), an equal concentration of protein in each sample was loaded and run in 10%SDS-PAGE at 100V for 2 hours. The separated proteins were then transferred to a PVDF membrane at 100mA overnight. The membrane was incubated with monoclonal mouse anti-pSmad3, diluted in 3%BSA/TBS (1:2000) at 4°C overnight. After washing in TBS three times, the membrane was incubated with anti-rabbit HRP for 1 hour at room temperature. After further washing, the films were developed using the ECL method (section 2.6.5). Equal protein loading was monitored by probing with an anti-α tubulin antibody (1:5000).

Resting MDA231 cells did not express pSmad3; however, following 30 minutes with TGF-β1 and latent TGF-β1, pSmad3 was up-regulated. The appearance of pSmad3 after treatment with latent TGF-β1 was inhibited by the LSKL inhibitor peptide (Figure 5.18); the control peptide was not active in this assay.

In the absence of TGF-β1 there was no evidence of activation of the TGF-β signalling pathway in MDA231 cells. However, in the presence of both active and latent TGF-β1, the TGF-β receptors were stimulated and Smad3 was phosphorylated, suggesting that the NRP-1 expressed by the cells was activating latent TGF-β1. This was supported by the observation that the LSKL inhibitor almost completely inhibited the phosphorylation of Smad3 in response to latent TGF-β1. Since MDA231 cells specifically express NRP-1, this effect most likely was mediated by inhibition of the NRP-1 cell-surface protein.

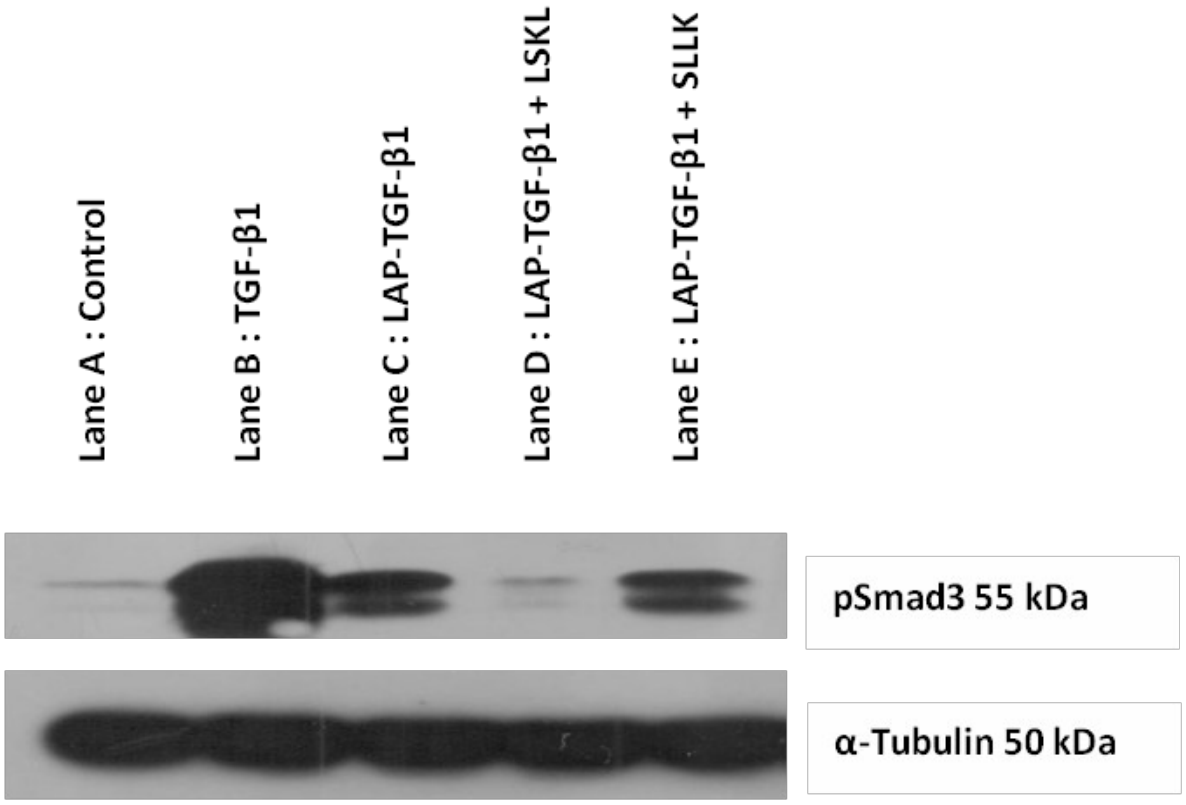

Figure 5.18 The expression of pSmad3 protein in MDA231 cells by Western Blotting.
Confluent MDA 231 cells were grown in medium (A) or medium containing 10ng/ml of TGF-β1 (B) and 30ng/ml of LAP-TGF-β1 (C) with or without 50μM of LSKL (C) or SLLK (D) peptides for 72 hours. The expression of pSmad3 was analyzed by western blot experiment. α-Tubulin was used as control between groups. pSmad3 was strikingly expressed in TGF-β1 (B) as well as in the LAP-TGF-β1 (C) groups, though the latter appeared in lower amount. The expression of pSmad3 was markedly decreased in LAP-TGF-β1 with LSKL peptide (D) but the SLLK control peptide was inactive (E). The results are representative of 3 separate experiments.

5.6.12 LSKL peptide can inhibit the activation of latent TGF-β1 by T cells.

It has been reported that CD103 expression is induced in activated T cells by the action of active TGF-β1 (Wong et al., 2003). Interestingly, the results from real-time PCR (Figure 5.14) showed an up-regulation of CD103 in T cells which had been treated with latent TGF-β1. This study has already shown that activated T cells can express both TSP-1 (section 5.6.3) and NRP-1 (section 5.6.6) on their cell surface, providing a candidate mechanism for the activation of latent TGF-β1. It has also been shown that the LSKL peptide sequence can inhibit the potential of NRP-1 to interact with and activate latent TGF-β1 (section 5.6.10). In this study a series of experiments was performed to determine whether inhibition of both TSP-1 and NRP-1 can block the response of activated human T cells to the latent, LAP-TGF-β1 complex.

Activated T cells were incubated with 30ng/ml LAP-TGF-β1 in the presence of 50μM LSKL peptides and 50μM SLLK control peptides. After 6 hours the treated T cells were processed for RNA extraction followed by cDNA synthesis. The expression of CD103, Foxp3 and TGF-β1 genes were quantified relative to 18S rRNA expression by real-time PCR.

As expected, CD103mRNA and FoxP3 mRNA were up-regulated following stimulation with latent TGF-β1; TGF-β1 mRNA also showed a small increase in this experiment. The expression of each of these genes was reduced significantly in cultures containing both latent TGF-β1 and the LSKL peptide in comparison with matched cultures containing the scrambled control peptide, SLLK (Figure 5.19). However, in was also apparent that the LSKL peptide did not completely inhibit the response to latent TGF-β1, suggesting that another mechanism might contribute to the activation of TGF-β1 in this system

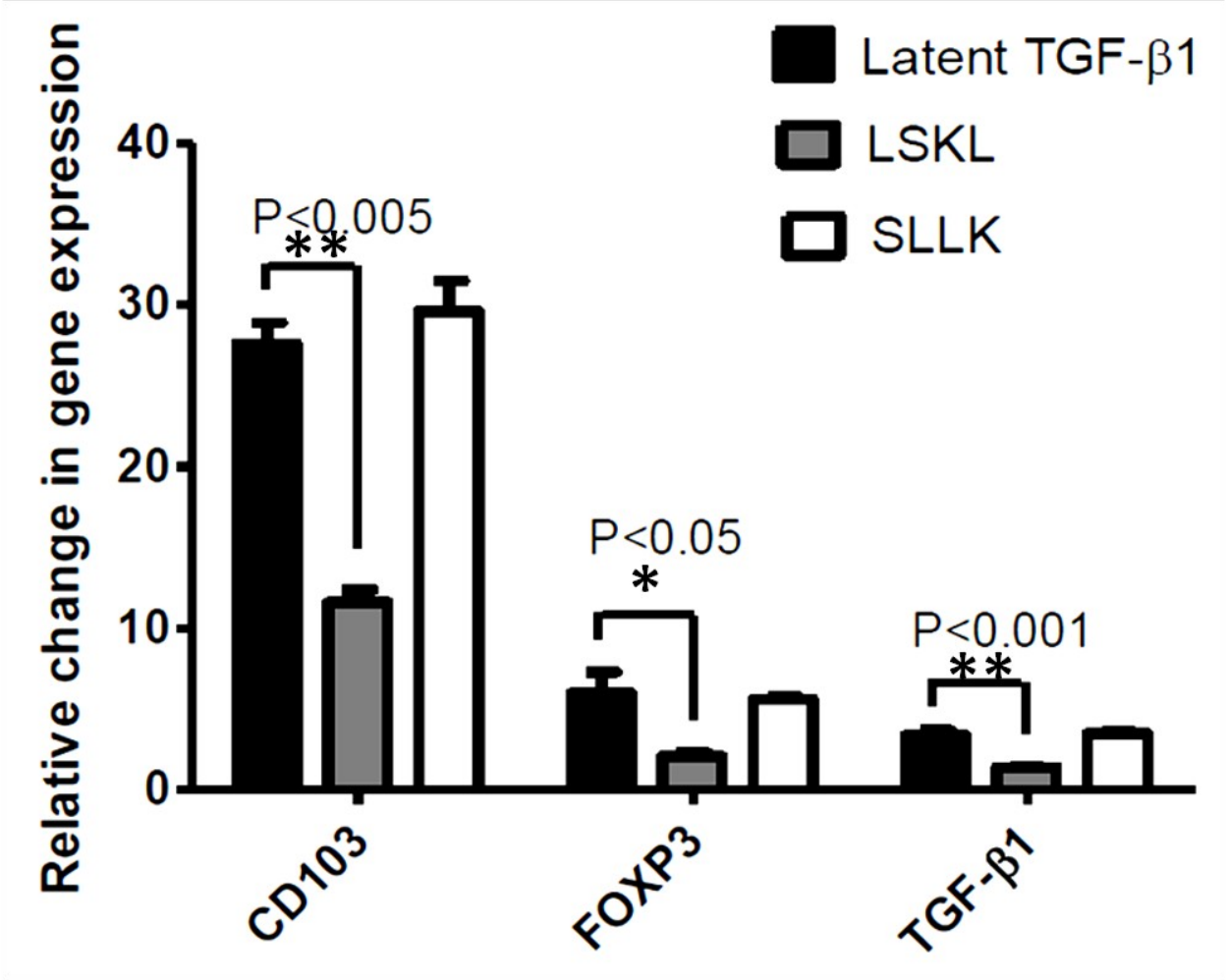

Figure 5.19 The comparison of CD103, FOXP3 and TGF-β1 genes expression in LAP-TGF-β1 stimulated human T cells in the presence of LSKL and SLLK peptides.

Isolated human T cells were activated by CD3/CD28 Beads for 24 hours followed by 6-hour of 30ng/ml LAP-TGF-β1 stimulation in the presence of LSKL or SLLK peptide 50μM. The quantitative measurement of mRNA was analyzed by real time PCR. The CD103, Foxp3 and TGF-β1 mRNA levels were normalized to 18s rRNA and are presented as the means ± SEM (n=3). LSKL peptide significantly reduced CD103, Foxp3 and TGF-β1 mRNA expression compared to latent TGF-β treated group. These results are representative from 3 similar experiments. (** = $p < 0.001$, * = $p < 0.05$; student's t test).

5.6.13 The induction of CD103 protein in response to treatment of activated human T cells with latent TGF-β1 was reduced by the LSKL peptide.

It has been shown that the induction of CD103 protein expression on activated human T cells is a consequence of stimulation of the TGF-β receptor (Wong et al., 2003). The following series of experiments was performed to test whether latent TGF-β1 had a similar effect on CD103 induction as active TGF-β1 and to determine whether the response to latent TGF-β was sensitive to inhibition by addition of the LSKL peptide.

Activated T cells were incubated with 1nM TGF-β1 with or without 50μM LSKL and SLLK peptides, and equimolar (3nM) latent TGF-β1 with or without 50μM LSKL and SLLK peptides for 72 hours. After this incubation, the cells were labelled with FITC conjugated anti-CD103 and examined using the FACSCalibur flow cytometer.

TGF-β1 treated T cells expressed a high level of CD103 (Figure 5.20B); as expected, this was not altered by addition of either the LSKL or SLLK peptides (Figure 5.20F, G). Neither the LSKL nor the SLLK peptides alone induced CD103 expression (Figure 5.20D, E). Stimulation of the cells with latent TGF-β1 also increased the expression of cell surface CD103 (Figure 5.20C). Interestingly, addition of LSKL to latent TGF-β1 treated T cells significantly reduced CD103 expression (Figure 5.20I) compared to latent TGF-β1 alone or latent TGF-β1 with SLLK (Figure 5.20H).

These results are consistent with the mRNA data (section 5.6.12) and support a model in which activated T cells can use cell-surface TSP-1 and NRP-1 to activate latent TGF-β1. However, as in the mRNA data, the flow cytometry experiment also shows that T cells can show a partial response to latent TGF-β1 in the presence of blockade of both TSP-1 and NRP-1 with the LSKL peptide sequence.

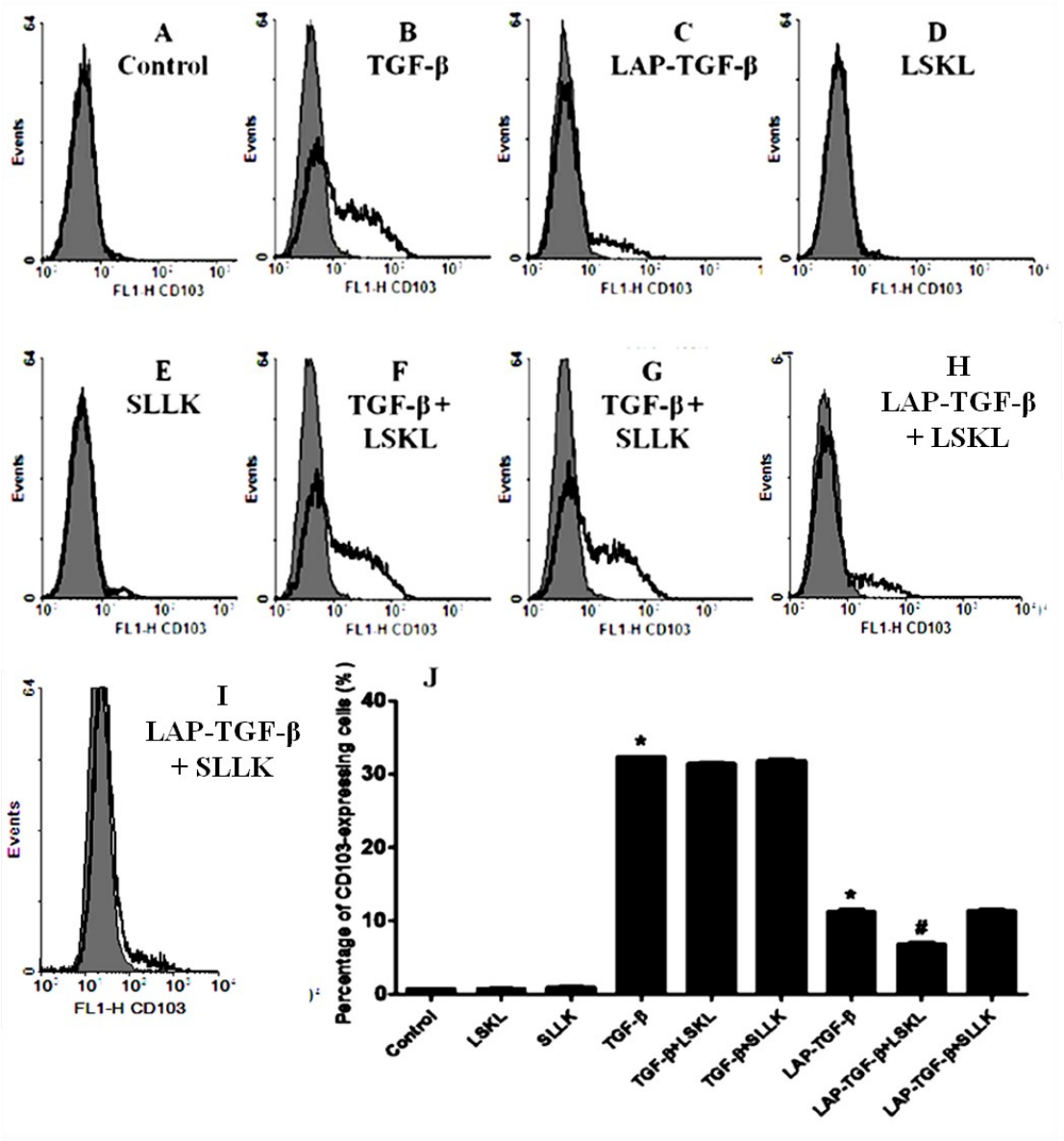

Figure 5.20 Induction of CD103 on activated T cells by latent TGF-β1 in the presence of LSKL or control peptides

Activated T cells were incubated in medium (A) or medium containing 1nM of TGF-β1 (B) or 3nM LAP-TGF-β1 (C) or 50μM LSKL (D) or 50μM SLLK (E) or 1nM of TGF-β1 with LSKL (F) or SLLK (G) or LAP-TGF-β1 with LSKL (H) or SLLK (I) for 72 hours. CD103 expression was analyzed by flow cytometry. The bar graph (J) shows the percentage of $CD103^+$ T cells was significantly increased after TGF-β1 and LAP-TGF-β1 stimulation. The expression on this integrin was reduced significantly in the presence of LSKL compared to LAP-TGF-β1 alone or LAP-TGF-β1 with SLLK. The bars shows mean (n=3) and error bars are SEM. The results are representative of 3 similar experiments. (* = $p < 0.05$ compared to control and # = $p < 0.05$ compared to the LAP-TGF-β1 group).

5.7 Summary and discussion

5.7.1 Results summary

- In human kidney allograft biopsy tissue, NRP-1 was co-expressed with some CD3-expressing infiltrating cells during cellular rejection.
- Only 1% of resting $CD4^+$ T cells expressed NRP-1; however, NRP-1 expression increased to 18% following CD3/CD28 activation for 48 hours. The expression of NRP-1 was not regulated by cell division.
- TSP-1 was predominantly stored in the cytoplasm of both resting and activated T cells. However, after co-culture with renal epithelial cells, surface TSP-1 expression was up-regulated.
- At the mRNA level, TSP-1 was significantly up-regulated following latent TGF-β1 and TGF-β1 treatment, whereas NRP-1 expression was not significantly increased in T cells following CD3/CD28 activation and latent TGF-β1 and TGF-β1 treatment.
- FoxP3 mRNA was significantly expressed in activated T cells, latent TGF-β1-treated and TGF-β1-treated T cells. CD103 mRNA was also up-regulated in latent TGF-β1-treated and TGF-β1-treated T cells, and TGF-β1 mRNA was significantly increased after TGF-β1 treatment.
- LAP had a capacity to confer latency to TGF-β, as demonstrated by the TGF-β bioassay.
- The MDA231 breast cancer cell line strongly expressed NRP-1 on the cell surface. In contrast, TSP-1 expression was absent on the surface of MDA231 cells.
- Both TGF-β1 and latent TGF-β1-treated MDA231 cells increased pSmad2/3 expression. This was inhibited by the addition of the LSKL peptide demonstrating for the first time the sensitivity of NRP-1 mediated activation of latent TGF-β to blockade with the LSKL peptide sequence.
- Addition of the LSKL peptide significantly inhibited latent TGF-β1-induced CD103, FoxP3 and TGF-β1 mRNA expression, compared to the latent TGF-β1- treated T cells and latent TGF-β1- treated T cells in the presence of the SLLK control peptide.
- CD103 induction on latent TGF-β1-treated T cells was significantly decreased following addition of the LSKL peptide; in contrast, the LSKL peptide had no effect on CD103 expression by TGF-β1-treated T cells.

5.7.2 Discussion

Fibrosis is one of the leading causes of late allograft loss in many organs, including the kidney. It is clear that TGF-β plays a central role in the development of fibrosis. Normally, TGF-β is produced and secreted in an inactive or latent form, which is complexed with LAP. This latent TGF-β must be activated before binding to its receptors to induce intracellular signal transduction. Several mechanisms have been proposed for latent TGF-β

activation (Taylor, 2009). However, the epithelial αVβ6 integrin and TSP-1 are both thought to play a dominant role in the activation of latent TGF-β *in vivo* (Lawler et al., 1998; Huang et al., 1996; Ludlow et al., 2005). Data from our group have already shown that inhibition of the αVβ6 integrin cannot inhibit CD103 induction by T cells during co-culture with HK-2 kidney cells (Figure 5.1). On this basis it is reasonable to propose the hypothesis that T cells can activate latent TGF-β by a different mechanism involving T cell surface molecules such as TSP-1. A recent study has also suggested that NRP-1 also binds to both the latent and active forms of TGF-β1 leading to activation through a molecular mechanism similar to that of TSP-1 (Glinka and Prud'homme, 2008).

5.7.2.1 The Expression of NRP-1 and TSP-1 on the surface of human T cells.

NRP-1 is associated with axonal guidance and angiogenesis via interaction with class III semaphorin and VEGF respectively (Neufeld et al., 2002). Furthermore, NRP-1 has been shown to promote interactions between human dendritic cells and T cells (Tordjman et al., 2002). Previous studies have reported that 3-4% of mouse splenic $CD4^+$ T cells express NRP-1 (Glinka and Prud'homme, 2008). In addition, the majority of these NRP-1 expressing cells are $CD4^+CD25^+$ regulatory T cells (Bruder et al., 2004). However, recent data from humans have shown only very low expression of NRP-1 (0.5%) on peripheral blood T cells, but increased expression in lymph nodes (2.61%) and tonsils (5.43%) (Milpied et al., 2009). Milpied *et al* also demonstrated that NRP-1 expression can be induced *in vitro* by CD3/CD28 activation to reach a maximum level after between 48 and 72 hours. These data are consistent with the results from this study, which found 1-2% of resting $CD4^+$ T cells expressed NRP-1, with this number increasing to approximately 18% after CD3/CD28 activation for 48 hours. After this time, the expression of NRP-1 gradually decreased. In addition, the association between NRP-1 and T cell division was examined by quantification of CFSE dilution. This study suggested that NRP-1 expression by activated T cells was cell cycle independent.

The current study also demonstrated the presence of the NRP-1 expressing cells in human kidney allograft biopsies from normal and acute cellular rejection patients. Renal tubular epithelial cells normally expressed NRP-1 on the luminal surface. However, during acute rejection, this NRP-1 was reduced but the expression of NRP-1 was increased on some infiltrating cells within the renal interstitium. A previous study has reported that the apical expression of NRP-1 by renal tubular epithelial cells is reduced by TGF-β (Schramek et al., 2009). Two-colour immunofluorescence staining showed some evidence of co-expression of CD3 (T cells) and NRP-1 within renal tissues. This is also supported by a previous study which

demonstrated the expression of NRP-1 by human T cells *in vivo* (Tordjman et al., 2002). However, further detailed morphometric study will be required to determine whether NRP-1 is preferentially expressed by T cells or other inflammatory cells such as macrophages during acute rejection.

TSP-1 is a trimeric functional glycoprotein. It was originally identified with alpha granules of human platelets (see section 5.2). It has been reported that lymphocytes can produce TSP-1 (Li et al., 2002). This study found that TSP-1 was predominantly stored in the cytoplasm of activated T cells, although some T cell-surface expression was observed. When activated T cells were co-cultured with renal tubular epithelial cells, TSP-1 expression on the T cell surface was increased. This finding is consistent with a previous study which showed that T cells in suspension express very low levels of TSP-1, in contrast to T cells cultured with fibronectin and collagen which strongly expressed surface TSP-1 (Li et al., 2002). This suggests that surface TSP-1 expression is associated with a cell adhesion-dependent mechanism. It has been reported that TSP-1 connects to ECM through an interaction with fibronectin (Sottile e al., 2002). Fibronectin is an important component of the interstitial ECM in several forms of experimentally-induced renal fibrosis and chronic kidney disease (Sady et al., 1995). It has also been shown that human renal tubular epithelial cells produce fibronectin *in vitro* (Niculescu-Duvaz et al., 2007). In addition, TGF-β and PDGF have an ability to up-regulate fibronectin production by renal tubular epithelial cells (Bürger et al., 1998). Thus, it is possible that during co-culture, activated renal epithelial cells express fibronectin, allowing increased TSP-1 expression on the T cell surface.

5.7.2.2 The expression of NRP-1 and TSP-1 mRNA in human T cells.

At the mRNA level, TSP-1 expression by T cells was significantly up-regulated following TGF-β1 and LAP-TGF-β1 treatment; the level of NRP-1mRNA was not changed in this study. A previous study of human T cells demonstrated that $CD4^{+}CD25^{+}$T cells up-regulated NRP-1 mRNA expression, whereas NRP-1 expression in non-Treg cells was down-regulated following CD3/CD28 activation (Bruder et al., 2004). In addition, it has been reported that TGF-β suppressed NRP-1 expression by human proximal renal tubular cells (Schramek et al., 2009). The inconsistent expression of NRP-1 protein and mRNA in this study may result from post-transcriptional control. Moreover, a limitation of the current study was lack of a positive control for real-time PCR; the MDA231 cell line would provide suitable RNA samples. Further studies need to be undertaken to clarify this issue.

5.7.2.3 The LSKL peptide inhibits the activation of latent TGF-β by human T cells.

MDA231 is a breast cancer cell line reported to strongly express NRP-1 (Glinka and Prud'homme, 2008). This is consistent with the finding in this study that MDA231 cells expressed a high level of NRP-1, whereas TSP-1 expression was absent. It is known that activation of the TGF-β receptor system results in phosphorylation and nuclear translocation of Smad 2 and 3. The current study demonstrated increased expression of pSmad 2/3 in MDA231 cells following stimulation with latent TGF-β. Furthermore, addition of the LSKL peptide to latent TGF-β1 significantly inhibited the expression of pSmad2/3 by MDA231 cells. This is the first practical demonstration that the LSKL peptide can inhibit activation of latent TGF-β1 by NRP-1.

Besides its role in TGF-β activation, a recent study demonstrated that NRP-1 can regulate the balance between activation of the Smad2/3 and the Smad1/5/8 signalling pathways. Specifically, it was shown that knockdown of NRP-1 expression enhanced the phosphorylation of Smad1/5 and decreased phosphorylation of Smad2/3 following TGF-β stimulation, suggesting a new role for NRP-1 in the regulation of Smad protein function and intracellular signalling (Cao et al., 2010). The current study also demonstrated that the association with LAP is sufficient to confer the latency of otherwise active TGF-β, supporting data from a previous study (Young et al., 2004). Thus, induction of the dissociation of LAP from active TGF-β can be seen as a key part of the activation of latent TGF-β.

CD103 expression by T cells is specifically induced by TGF-β1 *in vitro* (Wong et al., 2003). This allows the induction of CD103 to be used as a bioassay of the activation of latent TGF-β1 by activated T cells. It was found that latent TGF-β1 increased CD103 expression at both mRNA and protein levels in activated T cells in a similar way to the induction observed after TGF-β1 treatment. This indicates that latent TGF-β was activated by T cells through a mechanism which might include cell surface TSP-1 and/or NRP-1 molecules. Addition of the LSKL peptide produced a significant reduction inCD103 induction by latent TGF-β1 at both protein and mRNA levels, compared to treatment with the SLLK negative control peptide. However, this suppressive effect did not affect TGF-β1-induced CD103 expression. These results demonstrate that specific interaction between T cell surface TSP-1 and/or NRP-1 and the LSKL peptide motif in the LAP sequence contributes to the activation of latent TGF-β1 by human T cells.

It is becoming clear that this mechanism for T cell-mediated activation of TGF-β is biologically important for regulation of the immune response. For example, a recent paper has

shown that a specific deficiency of NRP-1 in $CD4^+$ T cells can potentiate central nervous system inflammation in experimental autoimmune encephalomyelitis (Solomon et al., 2011). Work from the current study extends this concept by raising the possibility that graft infiltrating T cells can activate latent TGF-β1 leading to the induction of fibrosis via the EMT pathway.

This study demonstrated the potential role of surface TSP-1 and NRP-1 in activated T cells to activate latent TGF-β. Although TSP-1 and/or NRP-1 inhibition might provide an alternative strategy for fibrosis treatment, it is also possible that blocking these molecules on the surface of T cells impairs the physiological immune response of T cells, including their migratory ability and regulatory function. Therefore, blocking latent TGF-β activation through αVβ6 integrin on activated renal epithelial cells seems to be a promising potential approach for renal allograft fibrosis treatment, since it would not interfere with the homeostasis of TGF-β.

Chapter 6: Concluding discussion

6.1 EMT: a potential role in renal allograft fibrosis

Regardless of the primary cause, chronic renal allograft graft dysfunction is often characterized by the development of progressive interstitial fibrosis and tubular atrophy (IF/TA) leading to the deterioration of graft function (Racusen and Regele, 2010). Tubular interstitial fibrosis is caused by an excessive production and deposition of extracellular matrix in the tubular interstitium by fibroblasts and myofibroblasts, which express S100A4 and α-SMA respectively. Both myofibroblasts and fibroblasts are highly active in synthesizing extracellular matrix proteins such as fibrillary collagens and fibronectin. The origin of these cells has been a topic of increasing interest over the last decade. To date, it has been reported that myofibroblasts are derived from the activation of renal interstitial fibroblasts (Strutz and Zeisberg, 2006), perivascular fibroblasts and pericytes (Lin et al., 2008), from the differentiation of bone marrow-derived stem cells (Broekema et al., 2007), and by direct phenotypic transition from endothelial (Zeisberg et al., 2008) and tubular epithelial cells (Strutz et al., 1995; Iwano et al., 2002) to mesenchymal cells. The mechanism of epithelial to mesenchymal transition has been studied intensively *in vitro* and *in vivo.*

6.1.1 HKC-8 cells undergo EMT following stimulation with profibrotic cytokines

It has been shown previously that both primary and immortalised human renal epithelial cells have the capacity to become fibroblast-like cells following stimulation with the profibrotic cytokine, TGF-β1 (Robertson et al., 2004). Epithelial to mesenchymal transition (EMT) of these cells has been demonstrated by both morphological and proteomic changes (Zeisberg et al., 2003; Robertson et al., 2004).

The current study also demonstrated clearly that cultured human renal proximal tubular epithelial cell lines can transform into fibroblasts. In the resting state, renal tubular epithelial cells show typical features of a polarized epithelium, such as cobblestone morphology and the presence of intercellular tight junctions. Stimulation of these cells with recombinant TGF-β1 resulted in the acquisition of elongated cells with a fibroblast-like morphology. In addition, TGFβ-1 treatment of the immortalised HKC-8 cell line produced a loss of cell-surface expression together with a decrease in the overall expression of the epithelial marker E-cadherin and up-regulated the expression of the

mesenchymal proteins S100A4 and α-SMA. These changes are entirely consistent with the induction of EMT *in vitro*.

6.1.2 A potential role for EMT in chronic Cyclosporine nephrotoxicity

Cyclosporine is a potent immunosuppressive drug which greatly improves the survival of kidney allografts (Krönke et al., 1984). However, a major limiting factor in the use of Cyclosporine is chronic nephrotoxicity, which leads to irreversible renal failure characterized by extensive tubulointerstitial fibrosis (Myers et al., 1984) (section 3.4.2). Several factors have previously been implicated as playing a role in the development of renal fibrosis associated with Cyclosporine treatment. These include angiotensin II (Shang et al., 2008), aldosterone (Bobadilla and Gamba, 2007), endothelin-1 and reactive oxygen species (Jennings et al., 2007), and nitric oxide insufficiency (Shihab et al., 2000). A further process which may be relevant is the potential of Cyclosporine to stabilise the mitochondrial permeability transition pore by binding the cyclophilin D component of this pore (Crompton, 1999). By this mechanism, Cyclosporine can prevent or reduce the induction of apoptosis in some cells by inhibiting the release of cytochrome C from mitochondria (Kowaltowski et al., 2000). This might contribute to the Cyclosporine-induced cellular overgrowth observed in some tissues (Seymour et al., 1996). Although the exact mechanisms of Cyclosporine-induced tubulointerstitial fibrosis remain unclear, it has been hypothesized that EMT may play a role (Slattery et al., 2005; McMorrow et al., 2005).

In this study, it has been demonstrated that Cyclosporine induced the de-differentiation of cultured renal epithelial cells through induction of a decrease in expression of the epithelial adhesion molecule E-cadherin together with increased expression of the mesenchymal marker S100A4. Although S100A4 protein expression has been demonstrated in some monocytes, macrophages, polymorphonuclear granulocytes and lymphocytes (Takenaga et al., 1994), it has not been detected in normal tissues obtained from the breast, colon, thyroid, lung, kidney, and pancreas (Ilg et al., 1996). Increased S100A4 expression following Cyclosporine treatment suggested the acquisition of a mesenchymal phenotype by transformed renal epithelial cells. However, the increased expression of S100A4 protein occurred without an apparent increase in expression of the S100A4 gene. Previous studies suggest that the S100A4 protein is commonly present in a high molecular weight form (typically a tetramer) which can associate with other proteins (Klingelhöfer et al., 2007). It is considered most likely that

the poor relationship between the expression of S100A4 protein and mRNA results from a post-translational process which may alter S100A4 distribution and/or stability.

Besides de novo expression of mesenchymal markers, a reduction in the expression of epithelial markers is also one of the main features of the EMT process. This study focused on the expression of E-cadherin as an epithelial marker. E-cadherin is an important determinant for maintenance of the epithelial phenotype (Zeisberg et al., 2003). The loss of this adherens junction protein is commonly used to demonstrate the presence of EMT. However, loss of E-cadherin expression is not always associated with EMT (Veerasamy et al., 2009). In addition, TGF-β may not always lead to a loss of E-cadherin expression. A study using a model TGF-β1-containing adenoviral vector-induced peritoneal fibrosis showed a slightly increased E-cadherin expression in experimental animals (Margetts et al., 2005). Hypotonic stretch-induced E-cadherin expression has also been observed in a mouse model of UUO (Docherty et al., 2009). This raises some questions about the reliability of E-cadherin expression when used alone as a marker of EMT for *in vivo* studies.

It has been reported that TGF-β1 is a crucial driver of renal tubular epithelial to mesenchymal transition *in vitro* (Liu et al., 2004). Results in the current study are consistent with this observation. However, this study also provided three pieces of evidence suggesting that the phenotypic changes produced in renal tubular epithelial cells by culture with a high concentration of Cyclosporine are not associated with TGFβ.

- Blocking the TGF-β receptor type I (ALK5) with the effective inhibitor SB-505124 failed to prevent de novo expression of S100A4 following Cyclosporine treatment. However, this ALK5 inhibitor was able partially to inhibit the reduction of E-cadherin expression. This might suggest that Cyclosporine-induced expression of S100A4 by HKC-8 cells was not dependent on the TGF-β signalling pathway, whilst the Cyclosporine-induced loss of E-cadherin was partly regulated through this receptor. The limitation of this study is the lack of a proper negative and positive control. Further studies should quantify the expression of both S100A4 and E-cadherin in HKC-8 cells incubated with SB-505124 alone and SB-505124 together with TGF-β.
- Real-time PCR showed no up-regulation of TGF-β1 mRNA following Cyclosporine treatment of three different renal epithelial cell lines including HKC-8, HK-2 and primary renal cells. Although the TGF-β1 gene was induced in these cells by treatment with TGF-β1 as a positive control, further work should include examination of changes in the expression of the other isoforms of TGF-β.

- The concentration of active TGF-β was measured in medium conditioned by culture of renal epithelial cells in the presence of a high concentration of Cyclosporine. Two fundamentally different assays were used, but each was sensitive to all TGF-β isoforms. Firstly the MFB-F11 bioassay was used to quantify TGF-β following activation by heat and secondly an ELISA was used to measure active TGF-β following acidification of the medium. Neither assay provided evidence that the presence of Cyclosporine increased the secretion of any isoform of TGF-β above levels produced by resting cells or present in fresh medium alone.

It has been observed that other growth factors have a capacity to induce or augment EMT. These include FGF-2 (Strutz et al., 2002), PDGF-B (Patel et al., 2010), IGF-II (Morali et al., 2001), EGF (Lo et al., 2007) and CTGF (Burns et al., 2006). This variety of relevant growth factors suggests that one or more of a multitude of additional mechanisms may induce the development of an EMT-like phenotype following treatment of renal tubular epithelial cells with Cyclosporine. These could be explored by additional gene-profiling experiments using an appropriate cytokine-targeted PCR-array after treatment with Cyclosporine. Previous studies have also demonstrated up-regulation of E2A mRNA expression in tubular epithelial cells following Cyclosporine exposure (Slattery et al., 2005). The E2A gene encodes two basic helix-loop-helix (bHLH) proteins, E12 and E47 (Massari and Murre, 2000). Both E12 and E47 have effects on cell morphology and phenotypes, including a reduction in E-cadherin and induction of α-SMA expression after Cyclosporine treatment (Slattery et al., 2006). This provides further evidence for the existence of additional mechanisms to explain the apparent absence of a direct role for TGF-β in the induction of EMT following treatment of renal tubular epithelial cells with Cyclosporine.

Overall this study supported a role for EMT during Cyclosporine-induced renal fibrosis *in vitro*. However, the possibility that this action is mediated by an increase in the activity of TGF-β remains controversial.

6.1.3 Examination of the role of TGF-β in T cell-mediated EMT

Chronic graft dysfunction is associated with T cell–mediated rejection, suggesting a mechanism that involves immunological damage of renal epithelial cells (Gourishankar and Halloran, 2002; Robertson et al., 2003). A previous study has demonstrated that the expression of S100A4 in tubular cells during renal allograft rejection is associated with infiltration of the tubules by $CD8^+$ T cells, potentially indicating the induction of EMT by these T cells (Robertson et al., 2004). It has also

been suggested that infiltrating T cells might present membrane bound active TGF-β during adhesive contact with renal epithelial cells, leading to the induction of EMT (Robertson et al., 2004). However, unpublished work from our group failed to show active TGF-β when T cells were co-cultured with MFB-F11 reporter cells *in vitro*. As a consequence of this work a series of experiments was performed to re-examine the potential of activated T cells to induce EMT by a TGF-β dependent mechanism.

It has been widely reported that $CD8^+CD103^+$ T cells constitute the majority of intratubular T cells during renal allograft rejection (Robertson et al., 2004). This phenotype is characteristic of intraepithelial T cells, which are commonly modelled using the human $CD103^+$ MOLT-16 T cell line. In addition to a range of T cell markers, these cells are known to express both the LAP component of TGF-β and thrombospondin-1 (Oida et al., 2003).

The MOLT-16 T cell line was used in co-culture experiments with HKC-8 renal epithelial cells to model the cell contacts that occur during renal tubulitis. The epithelial marker for this experiment was E-cadherin, whilst S100A4 and α-SMA were selected as mesenchymal markers. It is known that S100A4 is expressed by some leukocytes (Le Hir et al., 2005), including MOLT-16 and other lymphoma cell lines (Rygiel et al., 2010). This study showed that following addition of MOLT-16 T cells, the expression of E-cadherin by HKC-8 cells was reduced. By contrast, the expression of S100A4 and α-SMA showed an increase; with S100A4 showing general expression whilst α-SMA was restricted to a small number of cells. This might suggest that during EMT *in vitro*, the epithelial cells were transformed into different fibroblastic cell types, since α-SMA is specific for myofibroblasts (Desmouliére et al., 1992). Interestingly, it has been reported that some activated intra-renal fibroblasts also fail to make the change to a myofibroblast phenotype *in vivo* (Okada et al., 2000).

The role played by TGF-β during T cell-induced EMT was explored by blocking the TGF-β receptor using the selective inhibitor SB-505124. Use of this inhibitor is superior to the application of TGF-β blocking antibodies which can sometimes fail to inhibit signal transduction (Ganapathy et al., 2010). The ALK5 inhibitor reduced the expression of both S100A4 and α-SMA, and also reduced the loss of E-cadherin expression during co-culture of MOLT-16 T cells and HKC-8 renal cells. This suggests a role for TGF-β in the epithelial phenotypic transition induced by MOLT-16 T cells. One limitation with this study is the failure to determine the role played by CD103-mediated adhesion during the induction of EMT *in vitro*. Further experiments should

include a $CD103^-$ T cell line; MOLT-4 T cells which lack both cell-surface CD103 and LAP might provide such a negative control. However, use of allospecific $CD8^+CD103^+$ activated primary T cells would provide the most robust model for further study.

The expression of LAP by activated $CD103^+$ and $CD103^-$ human T cells was examined *in vitro* by immunofluorescence flow cytometry. Approximately 15-16% of activated T cells expressed surface LAP. Stimulation of these cells with TGF-β1 did not induce additional LAP expression, although CD103 was induced by this treatment.

Besides their potential role in the induction of EMT, CD103 and LAP have been proposed as cell-surface markers of efficient Treg. Indeed, it has been shown that up to 20% of murine Treg express CD103 (Zelenika et al., 2002). In addition, a previous study has shown that TGF-β can induce cell surface LAP expression by murine T cells (Oida et al., 2011). In humans, $CD103^+LAP^+$ T cells have been classified as a newly differentiated population of Tregs (Zhang et al., 2009). However the role of these Treg in clinical organ transplantation remains unknown.

6.2 Potential role of Thrombospondin-1 and Neuropilin-1 in TGF-β activation

Previous studies have demonstrated that T cells attach to the renal epithelial cell membrane at least partially by adhesive interaction between the αEβ7 integrin and E-cadherin (Benmerah et al., 1994). The affinity of this interaction is enhanced by the presence of local inflammatory chemokines (Al-Hamidi et al., 2008). This cell–cell interaction may play an important role in regulating the EMT process as renal cells do not undergo this phenotypic transition in response to supplementation of the culture with T-cell conditioned medium (Robertson et al., 2004).

Although TGF-β plays an essential role in immune homeostasis (Shi and Massagué, 2003), the over-expression of TGF-β results in excessive deposition of ECM leading to organ fibrosis. TGF-β is normally produced and secreted in an inactive form, the latent TGF-β complex. Thus, a key step in regulation of TGF-β function is the activation of latent TGF-β. It has been suggested that the T cell-associated molecules TSP-1 and NRP-1 may play an important role in the activation of latent TGF-β (Li et al., 2002; Glinka and Prud'homme, 2008); hence, these molecules may be relevant to the induction of T cell-mediated EMT. The final part of this study focused on examination of the function of these two molecules.

6.2.1 Expression of NRP-1 and TSP-1 on the human T cell surface

NRP-1 is well known as a receptor for both VEGF and SEMA3A (Pellet-Many et al., 2008; Kolodkin et al., 1997). However, recent data has been demonstrated a new role of NRP-1 in latent TGF-β activation *in vitro* (Glinka and Prud'homme, 2008). TSP-1 is a matrix and cellular glycoprotein which has been long been recognised as a mediator of latent TGF-β activation both *in vitro* and *in vivo* (Hugo and Daniel, 2009). It has been suggested that the KRFK sequence of TSP-1 and the RKFK sequence of NRP-1 can both interact with the LSKL sequence of LAP leading to a conformational change in the structure of latent TGF-β which exposes the active form of TGF-β (Glinka and Prud'homme, 2008; Ribeiro et al., 1999).

This study demonstrated that human T cells express TSP-1, but this is normally stored within the cytoplasm. When activated T cells were co-cultured with PTEC, TSP-1 was mobilized and expressed on the T cell-surface. A previous study demonstrated similar mobilization of intracellular TSP-1 following stimulation with fibronectin, suggesting a role for endogenous TSP-1 in maintaining T cell interactions with fibronectin in the ECM (Li et al., 2002).

It has been reported that 0.01% of human circulating T cells express NRP-1 (Battaglia et al., 2008). However, sensitive flow cytometry in the current study demonstrated that 1.3% of resting human T cells expressed NRP-1. In addition, the number of NRP-1 expressing $CD4^+$ T cells increased to a mean of 18% after CD3/CD28 activation for 48 hours. Interestingly, a parallel CFSE-labelling study demonstrated that this induction was independent of T cell division.

The expression of mRNA encoding both TSP-1 and NRP-1 was measured by real-time PCR. TSP-1 mRNA was not changed when T cells were activated but was significantly up-regulated following treatment with either latent TGF-β1 or active TGF-β1. In contrast, the expression of NRP-1 mRNA was similar between resting T cells, activated T cells, and latent or active TGF-β1-treated T cells. When considered the C_T value, resting T cells showed a C_T of 34 suggesting very low level expression of NRP-1 in these cells. However, following CD3/CD28 activation and/or latent TGF-β1 and TGF-β1 stimulation, the C_T value was decreased to 32-33 indicting a trend towards increased NRP-1 mRNA expression; this was not statistically significant. It is possible that the apparently low level NRP-1 mRNA expression might result from poor quality PCR templates, primers or reagents. A further study should be performed to investigate this possibility using RNA from an appropriate control such as the NRP-1 positive MDA231 cell line.

6.2.2 The LSKL peptide inhibits the induction of CD103 and phosphorylation of Smad2/3 expression by latent TGF-β1

This study demonstrated the expression of both TSP-1 and NRP-1 by activated T cells at the protein level. In order to identify a role for these two molecules in latent TGF-β activation, a peptide sequence specific inhibitor was applied. Hydropathic binding (Ribeiro et al., 1999) of the KRFK amino acid sequence of TSP-1 (Murphy-Ullrich et al., 2000) and, potentially, the similar RKFK sequence of NRP-1 (Glinka and Prud'homme, 2008) to the LSKL sequence of LAP is thought to induce a conformational rearrangement of LAP leading to exposure of the functional domain of TGF-β (section 5.2.2 and 5.3.2). Therefore, exogenous application of the LSKL peptide should inhibit the activation of latent TGF-β by competitive binding to RKFK or KRFK on NRP-1 and TSP-1 respectively. In this study, the potential of this blocking peptide to inhibit NRP-1 was validated for the first time using the positive control NRP-1-expressing cell line, MDA231.

TGF-β1 signalling occurs through the phosphorylation of Smad2 and Smad3 (Nakao et al., 1997). The current study demonstrated increased phosphorylation of Smad2 and/or Smad3 following latent TGF-β1 treatment of MDA231 cells. Importantly, addition of the LSKL peptide decreased this phosphorylation of Smad2/3 indicating inhibition of the activation of latent TGF-β. This represents the first clear demonstration that the activation of latent TGF-β by NRP-1 can be inhibited using the LSKL peptide sequence. Addition of the LSKL peptide to latent TGF-β-treated T cells significantly reduced CD103 expression at both protein and mRNA levels compared to latent TGF-β alone, whereas the non-binding SLLK scrambled peptide control had no such inhibitory effect. This suggested that TSP-1 and/or NRP-1 on T cells played a role in the activation of latent TGF-β.

These data are significant as they indicate that activated human T cells have the potential to activate latent TGF-β. This activation can be mediated by NRP-1, which is expressed, albeit transiently, by a significant sub-population of activated T cells. However, activated T cells can also be induced to express cell-surface TSP-1 following interaction with renal epithelial cells or fibronectin, providing a microenvironment-sensitive second mechanism for the activation of latent TGF-β.

Both NRP-1 and TSP-1 activate latent TGF-β in a way that retains immobilized TGF-β within the LAP complex; this provides an explanation for the requirement for T cell contact with renal epithelial cells before phenotypic transition can be induced.

6.3 A model of renal allograft fibrosis

Results from the current study are consistent with the following model of renal allograft fibrosis (Figure 6.1). Renal tubular epithelial cells exposed to a high but not directly toxic concentration of Cyclosporine can undergo a phenotypic transition consistent with EMT. However, this drug-induced change does not appear to involve an increased production of TGF-β at mRNA, protein or functional levels. It is now clear that drug-stressed cells can undergo a range of life-preserving changes which includes the induction of replicative senescence (Jennings et al., 2007) and autophagy (Pallet et al., 2008) as well as the epithelial de-differentiation associated with EMT. States such as senescence are associated with specific cytokine secretomes (Kuilman and Peeper, 2009) which might influence epithelial de-differentiation by modification of factors including ILK, IGF-II, CTGF and E12/E47.

A large number of T cells are recruited to activated renal tubules during periods of allograft rejection in response to locally produced chemokines (Robertson et al., 2000). It is known that many of these lymphocytes start to express CD103 within the tubular microenvironment. It is also known that renal tubular epithelial cells can undergo EMT. Both of these processes are induced by a response to active TGF-β. Importantly, both T cells and renal epithelial cells can also produce TGF-β, although this cytokine is always produced and sequestered in a latent form.

Stressed epithelial cells can activate latent TGF-β through a mechanism which involves local expression of the αvβ6 integrin. However, the mechanism by which T cells activate latent TGF-β has been less clear. The current study has focused specifically on this problem and demonstrated that both NRP-1 and TSP-1 can be expressed by activated human T cells and can activate latent TGF-β. Importantly, the cell surface expression of TSP-1 by T cells is increased by culture with RTEC or fibronectin.

Following activation, TGF-β can have diverse actions. Firstly, T cells are stimulated to differentiate. This can limit the potential of activated $CD8^+$ T cells to lyse specific target cells (Robertson et al., 1996), can induce the development of FOXP3-expressing regulatory T cells (Singh et al., 2007) and can promote the formation of pro-inflammatory Th17 cells if further pro-inflammatory cytokines are present (Morishima et al., 2009). Secondly, epithelial cells can be stimulated to undergo EMT, resulting in

the formation of a de-differentiated mesenchymal phenotype which will limit renal function.

To date, it remains uncertain whether the de-differentiated epithelial cells produced by EMT can fully transform to fibroblast or myofibroblasts in vivo. It has been shown in this study that complete de-differentiation and EMT of renal epithelial cells occurs *in vitro*. However, the renal microenvironment is more complex, providing a range of cytokines and other stimuli which can signal epithelial cells. These include BMP-7 (Zeisberg et al., 2005) and hepatocyte growth factor (Shukla et al., 2009) which can both antagonize development of the EMT phenotype. For this reason, the *in vitro* system may provide an incomplete model of the changes in epithelial phenotype that are observed in vivo.

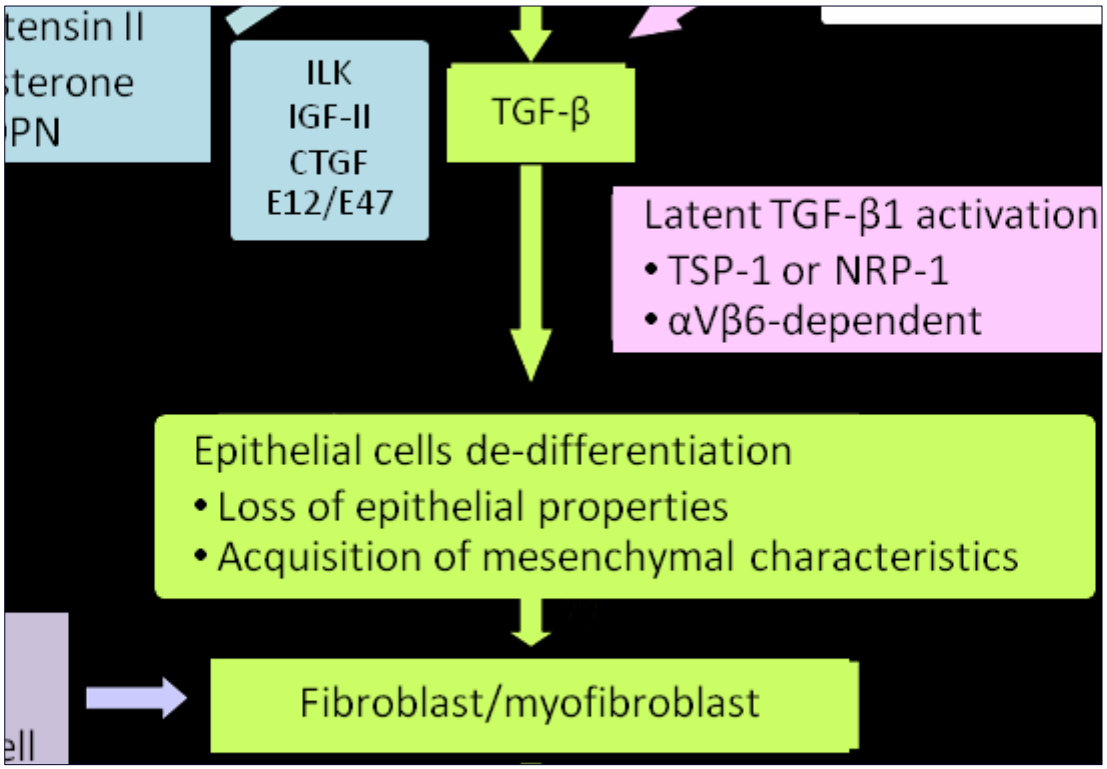

Figure 6.1 Diagram illustrating a putative model of renal fibrosis.

(i) Cyclosporine can activate renal epithelial directly or in combinationwith factors such as angiotensin II, aldosterone and macrophage infiltration (section 3.5.7). Activated renal epithelial cells produce TGF-β or other factors such as ILK, IGF-II, CTGF and E12E47 leading to epithelial de-differentiation. (ii) After transplantation, recipient T cells recognize alloantigen resulting to the accumulation of activated intraepithelial T cells. These T cells can induce latent TGF-β production. (iii) Latent TGF-β is then activated by

two different mechanisms: TSP-1 and NRP-1 on the T cell surface and the αvβ6 integrin on activated renal epithelial cells. This active TGF-β causes the de-differentiation of epithelial cells including loss of epithelial properties and acquisition of mesenchymal characteristics. Although these cells may not be transformed to myofibroblasts or fibroblast *in vivo*, they have capacity to induce fibrosis *in vitro*.

6.4 Conclusion

In summary, this in vitro study provides some evidence suggesting that both Cyclosporine and intratubular T cells contribute to chronic renal allograft failure by the activation of epithelial to mesenchymal transition. However, the mechanisms for induction of this phenotypic transition appear to differ, with TGF-β playing little apparent role in mediating Cyclosporine nephropathy but playing a more central role in T cell-mediated induction of EMT.

It was also shown that activated T cells can respond directly to latent TGF-β, leading to T cell differentiation and the induction of markers including FOXP3 and CD103. This process was substantially inhibited using an LSKL peptide well known to block TSP-1 but shown for the first time in this study to also inhibit the activation of latent TGF-β by NRP-1. Demonstration of the potential of activated T cells to express both NRP-1 and TSP-1 on their cell surface suggests an important mechanism by which these cells can activate latent TGF-β encountered within the kidney, leading both to local T cell differentiation and T cell-mediated induction of graft-damaging EMT.

6.5 Further work

6.5.1 Cyclosporine-induced EMT

Further studies are required to completely define the role of Cyclosporine-induced EMT and the underlying pathways leading to this transition. These include:

- Use of a more clinically relevant concentration of Cyclosporine to model drug effects on renal epithelial cells

6.5.2 T cell-induced EMT

Further studies to define the role of infiltrating T cell-induced epithelial cell de-differentiation include:

- Determining the role of the CD103 integrin for adhesion of T cells to renal epithelial cells during T cell-induced epithelial cell de-differentiation.

- Investigating the role of surface LAP on T cells during the induction of epithelial transformation during T cell-mediated rejection.
- Studying the immunosuppressive activity of $CD103^{+}LAP^{+}$ T cells and the potential role of this subset of T lymphocytes during renal allograft rejection.
- Further defining the possibility that T cells can activate latent TGF-β produced by renal epithelial cells.

6.5.3 Defining the roles of TSP-1 and NRP-1 in the activation of latent TGF-β

Further studies should include:

- Examination of the regulation of NRP-1 expression, since NRP-1 was found in the T cell cytoplasm and might be driven to surface under some conditions.
- Use an appropriate positive control cell line to optimize RT-PCR for NRP-1.
- Definition of the contribution of TSP-1 and NRP-1 on activated T cells and the αvβ6 integrin on activated epithelial cells to the activation of latent TGF-β using siRNA or blocking antibodies.
- Determining the relative expression of NRP-1 and TSP-1 by T cells, macrophages and other inflammatory cells during acute rejection.

References

ABE, M., HARPEL, J. G., METZ, C. N., NUNES, I., LOSKUTOFF, D. J. & RIFKIN, D. B. 1994. An assay for transforming growth factor-beta using cells transfected with a plasminogen activator inhibitor-1 promoter-luciferase construct. Anal Biochem, 216, 276-84.

ADAMS, J. & LAWLER, J. 1993. Extracellular matrix: the thrombospondin family. Curr Biol, 3, 188-90.

AFZALI, B., LECHLER, R. I. & HERNANDEZ-FUENTES, M. P. 2007. Allorecognition and the alloresponse: clinical implications. Tissue Antigens, 69, 545-56.

AL-HAMIDI, A., PEKALSKI, M., ROBERTSON, H., ALI, S. & KIRBY, J. A. 2008. Renal allograft rejection: the contribution of chemokines to the adhesion and retention of alphaE(CD103)beta7 integrin-expressing intratubular T cells. Mol Immunol, 45, 4000-7.

AMOS, W. B. & WHITE, J. G. 2003. How the confocal laser scanning microscope entered biological research. Biol Cell, 95, 335-42.

ANDREONI, K. A., BRAYMAN, K. L., GUIDINGER, M. K., SOMMERS, C. M. & SUNG, R. S. 2007. Kidney and pancreas transplantation in the United States, 1996-2005. Am J Transplant, 7, 1359-75.

ANGST, B. D., MARCOZZI, C. & MAGEE, A. I. 2001. The cadherin superfamily: diversity in form and function. J Cell Sci, 114, 629-41.

ANNES, J. P., MUNGER, J. S. & RIFKIN, D. B. 2003. Making sense of latent TGFbeta activation. J Cell Sci, 116, 217-24.

APOSTOLOPOULOS, V., YURIEV, E., LAZOURA, E., YU, M. & RAMSLAND, P. A. 2008. MHC and MHC-like molecules: structural perspectives on the design of molecular vaccines. Hum Vaccin, 4, 400-9.

ARAYA, J., CAMBIER, S., MARKOVICS, J. A., WOLTERS, P., JABLONS, D., HILL, A., FINKBEINER, W., JONES, K., BROADDUS, V. C., SHEPPARD, D., BARZCAK, A., XIAO, Y., ERLE, D. J. & NISHIMURA, S. L. 2007. Squamous metaplasia amplifies pathologic epithelial-mesenchymal interactions in COPD patients. J Clin Invest, 117, 3551-62.

ARAYA, J., CAMBIER, S., MORRIS, A., FINKBEINER, W. & NISHIMURA, S. L. 2006. Integrin-mediated transforming growth factor-beta activation regulates homeostasis of the pulmonary epithelial-mesenchymal trophic unit. Am J Pathol, 169, 405-15.

ARCINIEGAS, E., NEVES, Y. C. & CARRILLO, L. M. 2006. Potential role for insulin-like growth factor II and vitronectin in the endothelial-mesenchymal transition process. Differentiation, 74, 277-92.

References

AREND, L. J., SMART, A. M. & BRIGGS, J. P. 2000. Mouse beta(6) integrin sequence, pattern of expression, and role in kidney development. J Am Soc Nephrol, 11, 2297-305.

ARESU, L., RASTALDI, M. P., PREGEL, P., VALENZA, F., RADAELLI, E., SCANZIANI, E. & CASTAGNARO, M. 2008. Dog as model for down-expression of E-cadherin and beta-catenin in tubular epithelial cells in renal fibrosis. Virchows Arch, 453, 617-25.

ARIAS, A. M. 2001. Epithelial mesenchymal interactions in cancer and development. Cell, 105, 425-31.

ASANO, Y., IHN, H., YAMANE, K., JINNIN, M., MIMURA, Y. & TAMAKI, K. 2005. Increased expression of integrin alpha(v)beta3 contributes to the establishment of autocrine TGF-beta signaling in scleroderma fibroblasts. J Immunol, 175, 7708-18.

ASANO, Y., IHN, H., YAMANE, K., JINNIN, M. & TAMAKI, K. 2006. Increased expression of integrin alphavbeta5 induces the myofibroblastic differentiation of dermal fibroblasts. Am J Pathol, 168, 499-510.

ATABAI, K., JAME, S., AZHAR, N., KUO, A., LAM, M., MCKLEROY, W., DEHART, G., RAHMAN, S., XIA, D. D., MELTON, A. C., WOLTERS, P., EMSON, C. L., TURNER, S. M., WERB, Z. & SHEPPARD, D. 2009. Mfge8 diminishes the severity of tissue fibrosis in mice by binding and targeting collagen for uptake by macrophages. J Clin Invest, 119, 3713-22.

AUCHINCLOSS, H., JR., LEE, R., SHEA, S., MARKOWITZ, J. S., GRUSBY, M. J. & GLIMCHER, L. H. 1993. The role of "indirect" recognition in initiating rejection of skin grafts from major histocompatibility complex class II-deficient mice. Proc Natl Acad Sci U S A, 90, 3373-7.

BAGNIS, C., DERAY, G., DUBOIS, M., ADABRA, Y., JACQUIAUD, C., JAUDON, M. C. & JACOBS, C. 1997. Comparative acute nephrotoxicity of FK-506 and ciclosporin in an isolated in situ autoperfused rat kidney model. Am J Nephrol, 17, 17-24.

BAKKER, R. C., VAN KOOTEN, C., VAN DE LAGEMAAT-PAAPE, M. E., DAHA, M. R. & PAUL, L. C. 2002. Renal tubular epithelial cell death and cyclosporin A. Nephrol Dial Transplant, 17, 1181-8.

BARCELLOS-HOFF, M. H. & DIX, T. A. 1996. Redox-mediated activation of latent transforming growth factor-beta 1. Mol Endocrinol, 10, 1077-83.

BARRIENTOS, S., STOJADINOVIC, O., GOLINKO, M. S., BREM, H. & TOMIC-CANIC, M. 2008. Growth factors and cytokines in wound healing. Wound Repair Regen, 16, 585-601.

BARTH, R., COUNCE, S., SMITH, P. & SNELL, G. D. 1956. Strong and weak histocompatibility gene differences in mice and their role in the rejection of homografts of tumors and skin. Ann Surg, 144, 198-204.

References

BATTAGLIA, A., BUZZONETTI, A., MONEGO, G., PERI, L., FERRANDINA, G., FANFANI, F., SCAMBIA, G. & FATTOROSSI, A. 2008. Neuropilin-1 expression identifies a subset of regulatory T cells in human lymph nodes that is modulated by preoperative chemoradiation therapy in cervical cancer. Immunology, 123, 129-38.

BAUM, B. & GEORGIOU, M. 2011. Dynamics of adherens junctions in epithelial establishment, maintenance, and remodeling. J Cell Biol, 192, 907-17.

BECKER, G. J., PERKOVIC, V. & HEWITSON, T. D. 2001. Pharmacological intervention in renal fibrosis and vascular sclerosis. J Nephrol, 14, 332-9.

BELOT, N., POCHET, R., HEIZMANN, C. W., KISS, R. & DECAESTECKER, C. 2002. Extracellular S100A4 stimulates the migration rate of astrocytic tumor cells by modifying the organization of their actin cytoskeleton. Biochim Biophys Acta, 1600, 74-83.

BENMERAH, A., BADRICHANI, A., NGOHOU, K., MEGARBANE, B., BEGUE, B. & CERF-BENSUSSAN, N. 1994. Homotypic aggregation of CD103 (alpha E beta 7)+ lymphocytes by an anti-CD103 antibody, HML-4. Eur J Immunol, 24, 2243-9.

BENSON, M. J., ERICKSON, L. D., GLEESON, M. W. & NOELLE, R. J. 2007. Affinity of antigen encounter and other early B-cell signals determine B-cell fate. Curr Opin Immunol, 19, 275-80.

BETTELLI, E., CARRIER, Y., GAO, W., KORN, T., STROM, T. B., OUKKA, M., WEINER, H. L. & KUCHROO, V. K. 2006. Reciprocal developmental pathways for the generation of pathogenic effector TH17 and regulatory T cells. Nature, 441, 235-8.

BIELENBERG, D. R., PETTAWAY, C. A., TAKASHIMA, S. & KLAGSBRUN, M. 2006. Neuropilins in neoplasms: expression, regulation, and function. Exp Cell Res, 312, 584-93.

BLAND, R., WALKER, E. A., HUGHES, S. V., STEWART, P. M. & HEWISON, M. 1999. Constitutive expression of 25-hydroxyvitamin D3-1alpha-hydroxylase in a transformed human proximal tubule cell line: evidence for direct regulation of vitamin D metabolism by calcium. Endocrinology, 140, 2027-34.

BOBADILLA, N. A. & GAMBA, G. 2007. New insights into the pathophysiology of cyclosporine nephrotoxicity: a role of aldosterone. Am J Physiol Renal Physiol, 293, F2-9.

BOREL, J. F. & BAUMANN, G. 1994. Molecular mechanisms of immunosuppressive agents. Bull Mem Acad R Med Belg, 149, 97-101; discussion 101-3.

BORK, P. & BECKMANN, G. 1993. The CUB domain. A widespread module in developmentally regulated proteins. J Mol Biol, 231, 539-45.

BORNSTEIN, P. 2001. Thrombospondins as matricellular modulators of cell function. J Clin Invest, 107, 929-34.

References

BOTTINGER, E. P. & BITZER, M. 2002. TGF-beta signaling in renal disease. J Am Soc Nephrol, 13, 2600-10.

BRADHAM, D. M., IGARASHI, A., POTTER, R. L. & GROTENDORST, G. R. 1991. Connective tissue growth factor: a cysteine-rich mitogen secreted by human vascular endothelial cells is related to the SRC-induced immediate early gene product CEF-10. J Cell Biol, 114, 1285-94.

BRINKLEY, B. R., BEALL, P. T., WIBLE, L. J., MACE, M. L., TURNER, D. S. & CAILLEAU, R. M. 1980. Variations in cell form and cytoskeleton in human breast carcinoma cells in vitro. Cancer Res, 40, 3118-29.

BROEKEMA, M., HARMSEN, M. C., VAN LUYN, M. J., KOERTS, J. A., PETERSEN, A. H., VAN KOOTEN, T. G., VAN GOOR, H., NAVIS, G. & POPA, E. R. 2007. Bone marrow-derived myofibroblasts contribute to the renal interstitial myofibroblast population and produce procollagen I after ischemia/reperfusion in rats. J Am Soc Nephrol, 18, 165-75.

BROWN, P. D., WAKEFIELD, L. M., LEVINSON, A. D. & SPORN, M. B. 1990. Physicochemical activation of recombinant latent transforming growth factor-beta's 1, 2, and 3. Growth Factors, 3, 35-43.

BRUDER, D., PROBST-KEPPER, M., WESTENDORF, A. M., GEFFERS, R., BEISSERT, S., LOSER, K., VON BOEHMER, H., BUER, J. & HANSEN, W. 2004. Neuropilin-1: a surface marker of regulatory T cells. Eur J Immunol, 34, 623-30.

BURNS, W. C., KANTHARIDIS, P. & THOMAS, M. C. 2007. The role of tubular epithelial-mesenchymal transition in progressive kidney disease. Cells Tissues Organs, 185, 222-31.

BURNS, W. C., TWIGG, S. M., FORBES, J. M., PETE, J., TIKELLIS, C., THALLAS-BONKE, V., THOMAS, M. C., COOPER, M. E. & KANTHARIDIS, P. 2006. Connective tissue growth factor plays an important role in advanced glycation end product-induced tubular epithelial-to-mesenchymal transition: implications for diabetic renal disease. J Am Soc Nephrol, 17, 2484-94.

CABALLERO, A., FERNANDEZ, N., LAVADO, R., BRAVO, M. J., MIRANDA, J. M. & ALONSO, A. 2006. Tolerogenic response: allorecognition pathways. Transpl Immunol, 17, 3-6.

CABEZON, T., CELIS, J. E., SKIBSHOJ, I., KLINGELHOFER, J., GRIGORIAN, M., GROMOV, P., RANK, F., MYKLEBUST, J. H., MAELANDSMO, G. M., LUKANIDIN, E. & AMBARTSUMIAN, N. 2007. Expression of S100A4 by a variety of cell types present in the tumor microenvironment of human breast cancer. Int J Cancer, 121, 1433-44.

CAMBIER, S., GLINE, S., MU, D., COLLINS, R., ARAYA, J., DOLGANOV, G., EINHEBER, S., BOUDREAU, N. & NISHIMURA, S. L. 2005. Integrin alpha(v)beta8-mediated activation of transforming growth factor-beta by perivascular astrocytes: an angiogenic control switch. Am J Pathol, 166, 1883-94.

CAMBIER, S., MU, D. Z., O'CONNELL, D., BOYLEN, K., TRAVIS, W., LIU, W. H., BROADDUS, V. C. & NISHIMURA, S. L. 2000. A role for the integrin alphavbeta8 in the negative regulation of epithelial cell growth. Cancer Res, 60, 7084-93.

CANTAROVICH, D., RENOU, M., MEGNIGBETO, A., GIRAL-CLASSE, M., HOURMANT, M., DANTAL, J., BLANCHO, G., KARAM, G. & SOULILLOU, J. P. 2005. Switching from cyclosporine to tacrolimus in patients with chronic transplant dysfunction or cyclosporine-induced adverse events. Transplantation, 79, 72-8.

CAO, G., LU, Y., GAO, R., XIN, Y., TENG, D., WANG, J., WANG, L. & LI, Y. 2006. Comparison of cyclosporine versus mycophenolate mofetil on expression of Fractalkine and CX3CR1 in chronic allograft nephropathy. Transplant Proc, 38, 2234-6.

CAO, Y., SZABOLCS, A., DUTTA, S. K., YAQOOB, U., JAGAVELU, K., WANG, L., LEOF, E. B., URRUTIA, R. A., SHAH, V. H. & MUKHOPADHYAY, D. 2010. Neuropilin-1 mediates divergent R-Smad signaling and the myofibroblast phenotype. J Biol Chem, 285, 31840-8.

CARLOS, C. P., MENDES, G. E., MIQUELIN, A. R., LUZ, M. A., DA SILVA, C. G., VAN ROOIJEN, N., COIMBRA, T. M. & BURDMANN, E. A. 2010. Macrophage depletion attenuates chronic cyclosporine A nephrotoxicity. Transplantation, 89, 1362-70.

CARMAN, C. V. 2009. Mechanisms for transcellular diapedesis: probing and pathfinding by 'invadosome-like protrusions'. J Cell Sci, 122, 3025-35.

CEPEK, K. L., SHAW, S. K., PARKER, C. M., RUSSELL, G. J., MORROW, J. S., RIMM, D. L. & BRENNER, M. B. 1994. Adhesion between epithelial cells and T lymphocytes mediated by E-cadherin and the alpha E beta 7 integrin. Nature, 372, 190-3.

CERF-BENSUSSAN, N., JARRY, A., BROUSSE, N., LISOWSKA-GROSPIERRE, B., GUY-GRAND, D. & GRISCELLI, C. 1987. A monoclonal antibody (HML-1) defining a novel membrane molecule present on human intestinal lymphocytes. Eur J Immunol, 17, 1279-85.

CHAKRAVORTY, S. J., HOWIE, A. J., GIRDLESTONE, J., GENTLE, D. & SAVAGE, C. O. 2001. Potential role for monocyte chemotactic protein-4 (MCP-4) in monocyte/macrophage recruitment in acute renal inflammation. J Pathol, 194, 239-46.

CHEIFETZ, S. & MASSAGUE, J. 1991. Isoform-specific transforming growth factor-beta binding proteins with membrane attachments sensitive to phosphatidylinositol-specific phospholipase C. J Biol Chem, 266, 20767-72.

CHEN, G., LIN, S. C., CHEN, J., HE, L., DONG, F., XU, J., HAN, S., DU, J., ENTMAN, M. L. & WANG, Y. 2011. CXCL16 recruits bone marrow-derived fibroblast precursors in renal fibrosis. J Am Soc Nephrol, 22, 1876-86.

CHEN, Q., SIVAKUMAR, P., BARLEY, C., PETERS, D. M., GOMES, R. R., FARACH-CARSON, M. C. & DALLAS, S. L. 2007. Potential role for heparan sulfate proteoglycans in

regulation of transforming growth factor-beta (TGF-beta) by modulating assembly of latent TGF-beta-binding protein-1. J Biol Chem, 282, 26418-30.

CHEN, Z., LING, J. & GALLIE, D. R. 2004. RNase activity requires formation of disulfide bonds and is regulated by the redox state. Plant Mol Biol, 55, 83-96.

CHENG, S. & LOVETT, D. H. 2003. Gelatinase A (MMP-2) is necessary and sufficient for renal tubular cell epithelial-mesenchymal transformation. Am J Pathol, 162, 1937-49.

CHENG, S., POLLOCK, A. S., MAHIMKAR, R., OLSON, J. L. & LOVETT, D. H. 2006. Matrix metalloproteinase 2 and basement membrane integrity: a unifying mechanism for progressive renal injury. FASEB J, 20, 1898-900.

CHOI, B. S., SHIN, M. J., SHIN, S. J., KIM, Y. S., CHOI, Y. J., KIM, Y. S., MOON, I. S., KIM, S. Y., KOH, Y. B., BANG, B. K. & YANG, C. W. 2005. Clinical significance of an early protocol biopsy in living-donor renal transplantation: ten-year experience at a single center. Am J Transplant, 5, 1354-60.

CORNELL, L. D. & COLVIN, R. B. 2005. Chronic allograft nephropathy. Curr Opin Nephrol Hypertens, 14, 229-34.

CORPS, E. M., ROBERTSON, A., DAUNCEY, M. J. & KILSHAW, P. J. 2003. Role of the alphaI domain in ligand binding by integrin alphaEbeta7. Eur J Immunol, 33, 2599-608.

CRAWFORD, S. E., STELLMACH, V., MURPHY-ULLRICH, J. E., RIBEIRO, S. M., LAWLER, J., HYNES, R. O., BOIVIN, G. P. & BOUCK, N. 1998. Thrombospondin-1 is a major activator of TGF-beta1 in vivo. Cell, 93, 1159-70.

CROMPTON, M. 1999. The mitochondrial permeability transition pore and its role in cell death. Biochem J, 341 (Pt 2), 233-49.

CUI, X., ZHOU, J., QIU, J., JOHNSON, M. R. & MRUG, M. 2009. Validation of endogenous internal real-time PCR controls in renal tissues. Am J Nephrol, 30, 413-7.

DACOSTA BYFIELD, S., MAJOR, C., LAPING, N. J. & ROBERTS, A. B. 2004. SB-505124 is a selective inhibitor of transforming growth factor-beta type I receptors ALK4, ALK5, and ALK7. Mol Pharmacol, 65, 744-52.

DALLAS, S. L., SIVAKUMAR, P., JONES, C. J., CHEN, Q., PETERS, D. M., MOSHER, D. F., HUMPHRIES, M. J. & KIELTY, C. M. 2005. Fibronectin regulates latent transforming growth factor-beta (TGF beta) by controlling matrix assembly of latent TGF beta-binding protein-1. J Biol Chem, 280, 18871-80.

DANIEL, C., SCHAUB, K., AMANN, K., LAWLER, J. & HUGO, C. 2007. Thrombospondin-1 is an endogenous activator of TGF-beta in experimental diabetic nephropathy in vivo. Diabetes, 56, 2982-9.

References

DANIEL, C., TAKABATAKE, Y., MIZUI, M., ISAKA, Y., KAWASHI, H., RUPPRECHT, H., IMAI, E. & HUGO, C. 2003. Antisense oligonucleotides against thrombospondin-1 inhibit activation of tgf-beta in fibrotic renal disease in the rat in vivo. Am J Pathol, 163, 1185-92.

DANIEL, C., WIEDE, J., KRUTZSCH, H. C., RIBEIRO, S. M., ROBERTS, D. D., MURPHY-ULLRICH, J. E. & HUGO, C. 2004. Thrombospondin-1 is a major activator of TGF-beta in fibrotic renal disease in the rat in vivo. Kidney Int, 65, 459-68.

DELVA, E., TUCKER, D. K. & KOWALCZYK, A. P. 2009. The desmosome. Cold Spring Harb Perspect Biol, 1, a002543.

DERYNCK, R. & ZHANG, Y. E. 2003. Smad-dependent and Smad-independent pathways in TGF-beta family signalling. Nature, 425, 577-84.

DESMOULIERE, A., RUBBIA-BRANDT, L., ABDIU, A., WALZ, T., MACIEIRA-COELHO, A. & GABBIANI, G. 1992. Alpha-smooth muscle actin is expressed in a subpopulation of cultured and cloned fibroblasts and is modulated by gamma-interferon. Exp Cell Res, 201, 64-73.

DHAR, K., DHAR, G., MAJUMDER, M., HAQUE, I., MEHTA, S., VAN VELDHUIZEN, P. J., BANERJEE, S. K. & BANERJEE, S. 2010. Tumor cell-derived PDGF-B potentiates mouse mesenchymal stem cells-pericytes transition and recruitment through an interaction with NRP-1. Mol Cancer, 9, 209.

DICKSON, M. C., MARTIN, J. S., COUSINS, F. M., KULKARNI, A. B., KARLSSON, S. & AKHURST, R. J. 1995. Defective haematopoiesis and vasculogenesis in transforming growth factor-beta 1 knock out mice. Development, 121, 1845-54.

DOCHERTY, N. G., CALVO, I. F., QUINLAN, M. R., PEREZ-BARRIOCANAL, F., MCGUIRE, B. B., FITZPATRICK, J. M. & WATSON, R. W. 2009. Increased E-cadherin expression in the ligated kidney following unilateral ureteric obstruction. Kidney Int, 75, 205-13.

DREXLER, H. G. & MINOWADA, J. 1989. Morphological, immunophenotypical and isoenzymatic profiles of human leukemia cells and derived T-cell lines. Hematol Oncol, 7, 115-25.

DRUML, W. 2002. The beginning of organ transplantation: Emerich Ullmann (1861-1937). Wien Klin Wochenschr, 114, 128-37.

DUBOIS, C. M., LAPRISE, M. H., BLANCHETTE, F., GENTRY, L. E. & LEDUC, R. 1995. Processing of transforming growth factor beta 1 precursor by human furin convertase. J Biol Chem, 270, 10618-24.

EEDY, D. J. 2005. Summary of inaugural meeting of the Skin Care in Organ Recipients Group, UK, held at the Royal Society of Medicine, 7 October 2004. Br J Dermatol, 153, 6-10.

References

EINECKE, G., BRODERICK, G., SIS, B. & HALLORAN, P. F. 2007. Early loss of renal transcripts in kidney allografts: relationship to the development of histologic lesions and alloimmune effector mechanisms. Am J Transplant, 7, 1121-30.

EINECKE, G., FAIRHEAD, T., HIDALGO, L. G., SIS, B., TURNER, P., ZHU, L. F., BLEACKLEY, R. C., HADLEY, G. A., FAMULSKI, K. S. & HALLORAN, P. F. 2006. Tubulitis and epithelial cell alterations in mouse kidney transplant rejection are independent of CD103, perforin or granzymes A/B. Am J Transplant, 6, 2109-20.

EINECKE, G., SIS, B., REEVE, J., MENGEL, M., CAMPBELL, P. M., HIDALGO, L. G., KAPLAN, B. & HALLORAN, P. F. 2009. Antibody-mediated microcirculation injury is the major cause of late kidney transplant failure. Am J Transplant, 9, 2520-31.

EL-ZOGHBY, Z. M., STEGALL, M. D., LAGER, D. J., KREMERS, W. K., AMER, H., GLOOR, J. M. & COSIO, F. G. 2009. Identifying specific causes of kidney allograft loss. Am J Transplant, 9, 527-35.

ESPOSITO, C., FORNONI, A., CORNACCHIA, F., BELLOTTI, N., FASOLI, G., FOSCHI, A., MAZZUCCHELLI, I., MAZZULLO, T., SEMERARO, L. & DAL CANTON, A. 2000. Cyclosporine induces different responses in human epithelial, endothelial and fibroblast cell cultures. Kidney Int, 58, 123-30.

ESSAWY, M., SOYLEMEZOGLU, O., MUCHANETA-KUBARA, E. C., SHORTLAND, J., BROWN, C. B. & EL NAHAS, A. M. 1997. Myofibroblasts and the progression of diabetic nephropathy. Nephrol Dial Transplant, 12, 43-50.

FAN, J. M., NG, Y. Y., HILL, P. A., NIKOLIC-PATERSON, D. J., MU, W., ATKINS, R. C. & LAN, H. Y. 1999. Transforming growth factor-beta regulates tubular epithelial-myofibroblast transdifferentiation in vitro. Kidney Int, 56, 1455-67.

FANG, Z., FORSLUND, N., TAKENAGA, K., LUKANIDIN, E. & KOZLOVA, E. N. 2006. Sensory neurite outgrowth on white matter astrocytes is influenced by intracellular and extracellular S100A4 protein. J Neurosci Res, 83, 619-26.

FENG, X. H. & DERYNCK, R. 2005. Specificity and versatility in tgf-beta signaling through Smads. Annu Rev Cell Dev Biol, 21, 659-93.

FENG, Y., WANG, D., YUAN, R., PARKER, C. M., FARBER, D. L. & HADLEY, G. A. 2002. CD103 expression is required for destruction of pancreatic islet allografts by CD8(+) T cells. J Exp Med, 196, 877-86.

FISCHER, G., WITTMANN-LIEBOLD, B., LANG, K., KIEFHABER, T. & SCHMID, F. X. 1989. Cyclophilin and peptidyl-prolyl cis-trans isomerase are probably identical proteins. Nature, 337, 476-8.

FUKASAWA, M., MATSUSHITA, A. & KORC, M. 2007. Neuropilin-1 interacts with integrin beta1 and modulates pancreatic cancer cell growth, survival and invasion. Cancer Biol Ther, 6, 1173-80.

FUKUDA, K., YOSHITOMI, K., YANAGIDA, T., TOKUMOTO, M. & HIRAKATA, H. 2001. Quantification of TGF-beta1 mRNA along rat nephron in obstructive nephropathy. Am J Physiol Renal Physiol, 281, F513-21.

GABBIANI, G. 1981. The myofibroblast: a key cell for wound healing and fibrocontractive diseases. Prog Clin Biol Res, 54, 183-94.

GABBIANI, G. 2003. The myofibroblast in wound healing and fibrocontractive diseases. J Pathol, 200, 500-3.

GAFFEN, S. L. & LIU, K. D. 2004. Overview of interleukin-2 function, production and clinical applications. Cytokine, 28, 109-23.

GAGNON, M. L., BIELENBERG, D. R., GECHTMAN, Z., MIAO, H. Q., TAKASHIMA, S., SOKER, S. & KLAGSBRUN, M. 2000. Identification of a natural soluble neuropilin-1 that binds vascular endothelial growth factor: In vivo expression and antitumor activity. Proc Natl Acad Sci U S A, 97, 2573-8.

GAME, D. S. & LECHLER, R. I. 2002. Pathways of allorecognition: implications for transplantation tolerance. Transpl Immunol, 10, 101-8.

GANAPATHY, V., GE, R., GRAZIOLI, A., XIE, W., BANACH-PETROSKY, W., KANG, Y., LONNING, S., MCPHERSON, J., YINGLING, J. M., BISWAS, S., MUNDY, G. R. & REISS, M. 2010. Targeting the Transforming Growth Factor-beta pathway inhibits human basal-like breast cancer metastasis. Mol Cancer, 9, 122.

GANDHI, R., FAREZ, M. F., WANG, Y., KOZORIZ, D., QUINTANA, F. J. & WEINER, H. L. 2010. Cutting edge: human latency-associated peptide+ T cells: a novel regulatory T cell subset. J Immunol, 184, 4620-4.

GARRETT, S. C., VARNEY, K. M., WEBER, D. J. & BRESNICK, A. R. 2006. S100A4, a mediator of metastasis. J Biol Chem, 281, 677-80.

GHANNAD, F., NICA, D., FULLE, M. I., GRENIER, D., PUTNINS, E. E., JOHNSTON, S., ESLAMI, A., KOIVISTO, L., JIANG, G., MCKEE, M. D., HAKKINEN, L. & LARJAVA, H. 2008. Absence of alphavbeta6 integrin is linked to initiation and progression of periodontal disease. Am J Pathol, 172, 1271-86.

GLINKA, Y. & PRUD'HOMME, G. J. 2008. Neuropilin-1 is a receptor for transforming growth factor beta-1, activates its latent form, and promotes regulatory T cell activity. J Leukoc Biol, 84, 302-10.

GLINKA, Y., STOILOVA, S., MOHAMMED, N. & PRUD'HOMME, G. J. 2011. Neuropilin-1 exerts co-receptor function for TGF-beta-1 on the membrane of cancer cells and enhances responses to both latent and active TGF-beta. Carcinogenesis, 32, 613-21.

GOKMEN, M. R., LOMBARDI, G. & LECHLER, R. I. 2008. The importance of the indirect pathway of allorecognition in clinical transplantation. Curr Opin Immunol, 20, 568-74.

References

GOLDSCHMEDING, R., ATEN, J., ITO, Y., BLOM, I., RABELINK, T. & WEENING, J. J. 2000. Connective tissue growth factor: just another factor in renal fibrosis? Nephrol Dial Transplant, 15, 296-9.

GOOCH, J. L., BARNES, J. L., GARCIA, S. & ABBOUD, H. E. 2003. Calcineurin is activated in diabetes and is required for glomerular hypertrophy and ECM accumulation. Am J Physiol Renal Physiol, 284, F144-54.

GOOCH, J. L., GORIN, Y., ZHANG, B. X. & ABBOUD, H. E. 2004. Involvement of calcineurin in transforming growth factor-beta-mediated regulation of extracellular matrix accumulation. J Biol Chem, 279, 15561-70.

GORDON, K. J. & BLOBE, G. C. 2008. Role of transforming growth factor-beta superfamily signaling pathways in human disease. Biochim Biophys Acta, 1782, 197-228.

GOURISHANKAR, S. & HALLORAN, P. F. 2002. Late deterioration of organ transplants: a problem in injury and homeostasis. Curr Opin Immunol, 14, 576-83.

GRAEF, I. A., CHEN, F., CHEN, L., KUO, A. & CRABTREE, G. R. 2001. Signals transduced by Ca(2+)/calcineurin and NFATc3/c4 pattern the developing vasculature. Cell, 105, 863-75.

GRAY, M. J., VAN BUREN, G., DALLAS, N. A., XIA, L., WANG, X., YANG, A. D., SOMCIO, R. J., LIN, Y. G., LIM, S., FAN, F., MANGALA, L. S., ARUMUGAM, T., LOGSDON, C. D., LOPEZ-BERESTEIN, G., SOOD, A. K. & ELLIS, L. M. 2008. Therapeutic targeting of neuropilin-2 on colorectal carcinoma cells implanted in the murine liver. J Natl Cancer Inst, 100, 109-20.

GRIMM, P. C., NICKERSON, P., JEFFERY, J., SAVANI, R. C., GOUGH, J., MCKENNA, R. M., STERN, E. & RUSH, D. N. 2001. Neointimal and tubulointerstitial infiltration by recipient mesenchymal cells in chronic renal-allograft rejection. N Engl J Med, 345, 93-7.

GRONE, H. J., WEBER, K., GRONE, E., HELMCHEN, U. & OSBORN, M. 1987. Coexpression of keratin and vimentin in damaged and regenerating tubular epithelia of the kidney. Am J Pathol, 129, 1-8.

GROSCURTH, P. & FILGUEIRA, L. 1998. Killing Mechanisms of Cytotoxic T Lymphocytes. News Physiol Sci, 13, 17-21.

GROTENDORST, G. R. 1997. Connective tissue growth factor: a mediator of TGF-beta action on fibroblasts. Cytokine Growth Factor Rev, 8, 171-9.

HADLEY, G. A., BARTLETT, S. T., VIA, C. S., ROSTAPSHOVA, E. A. & MOAINIE, S. 1997. The epithelial cell-specific integrin, CD103 (alpha E integrin), defines a novel subset of alloreactive CD8+ CTL. J Immunol, 159, 3748-56.

References

HADLEY, G. A., CHARANDEE, C., WEIR, M. R., WANG, D., BARTLETT, S. T. & DRACHENBERG, C. B. 2001. CD103+ CTL accumulate within the graft epithelium during clinical renal allograft rejection. Transplantation, 72, 1548-55.

HAHM, K., LUKASHEV, M. E., LUO, Y., YANG, W. J., DOLINSKI, B. M., WEINREB, P. H., SIMON, K. J., CHUN WANG, L., LEONE, D. R., LOBB, R. R., MCCRANN, D. J., ALLAIRE, N. E., HORAN, G. S., FOGO, A., KALLURI, R., SHIELD, C. F., 3RD, SHEPPARD, D., GARDNER, H. A. & VIOLETTE, S. M. 2007. Alphav beta6 integrin regulates renal fibrosis and inflammation in Alport mouse. Am J Pathol, 170, 110-25.

HALLORAN, P. F. 2010. T cell-mediated rejection of kidney transplants: a personal viewpoint. Am J Transplant, 10, 1126-34.

HARIHARAN, S., JOHNSON, C. P., BRESNAHAN, B. A., TARANTO, S. E., MCINTOSH, M. J. & STABLEIN, D. 2000. Improved graft survival after renal transplantation in the United States, 1988 to 1996. N Engl J Med, 342, 605-12.

HAUGEN, M. H., FLATMARK, K., MIKALSEN, S. O. & MALANDSMO, G. M. 2008. The metastasis-associated protein S100A4 exists in several charged variants suggesting the presence of posttranslational modifications. BMC Cancer, 8, 172.

HELDIN, C. H., MIYAZONO, K. & TEN DIJKE, P. 1997. TGF-beta signalling from cell membrane to nucleus through SMAD proteins. Nature, 390, 465-71.

HERRERA, O. B., GOLSHAYAN, D., TIBBOTT, R., SALCIDO OCHOA, F., JAMES, M. J., MARELLI-BERG, F. M. & LECHLER, R. I. 2004. A novel pathway of alloantigen presentation by dendritic cells. J Immunol, 173, 4828-37.

HEWITSON, T. D. & BECKER, G. J. 1995. Interstitial myofibroblasts in IgA glomerulonephritis. Am J Nephrol, 15, 111-7.

HEWITSON, T. D., DARBY, I. A., BISUCCI, T., JONES, C. L. & BECKER, G. J. 1998. Evolution of tubulointerstitial fibrosis in experimental renal infection and scarring. J Am Soc Nephrol, 9, 632-42.

HINZ, B., GABBIANI, G. & CHAPONNIER, C. 2002. The NH2-terminal peptide of alpha-smooth muscle actin inhibits force generation by the myofibroblast in vitro and in vivo. J Cell Biol, 157, 657-63.

HO, S., CLIPSTONE, N., TIMMERMANN, L., NORTHROP, J., GRAEF, I., FIORENTINO, D., NOURSE, J. & CRABTREE, G. R. 1996. The mechanism of action of cyclosporin A and FK506. Clin Immunol Immunopathol, 80, S40-5.

HOLLAND, P. M., ABRAMSON, R. D., WATSON, R. & GELFAND, D. H. 1991. Detection of specific polymerase chain reaction product by utilizing the 5'----3' exonuclease activity of Thermus aquaticus DNA polymerase. Proc Natl Acad Sci U S A, 88, 7276-80.

HORNICK, P. I., MASON, P. D., YACOUB, M. H., ROSE, M. L., BATCHELOR, R. & LECHLER, R. I. 1998. Assessment of the contribution that direct allorecognition makes to the progression of chronic cardiac transplant rejection in humans. Circulation, 97, 1257-63.

HUANG, X., GRIFFITHS, M., WU, J., FARESE, R. V., JR. & SHEPPARD, D. 2000. Normal development, wound healing, and adenovirus susceptibility in beta5-deficient mice. Mol Cell Biol, 20, 755-9.

HUANG, X. Z., WU, J. F., CASS, D., ERLE, D. J., CORRY, D., YOUNG, S. G., FARESE, R. V., JR. & SHEPPARD, D. 1996. Inactivation of the integrin beta 6 subunit gene reveals a role of epithelial integrins in regulating inflammation in the lung and skin. J Cell Biol, 133, 921-8.

HUGO, C. & DANIEL, C. 2009. Thrombospondin in renal disease. Nephron Exp Nephrol, 111, e61-6.

HUGO, C., PICHLER, R., MEEK, R., GORDON, K., KYRIAKIDES, T., FLOEGE, J., BORNSTEIN, P., COUSER, W. G. & JOHNSON, R. J. 1995. Thrombospondin 1 is expressed by proliferating mesangial cells and is up-regulated by PDGF and bFGF in vivo. Kidney Int, 48, 1846-56.

HUGO, C., SHANKLAND, S. J., PICHLER, R. H., COUSER, W. G. & JOHNSON, R. J. 1998. Thrombospondin 1 precedes and predicts the development of tubulointerstitial fibrosis in glomerular disease in the rat. Kidney Int, 53, 302-11.

HUMPHREYS, B. D., LIN, S. L., KOBAYASHI, A., HUDSON, T. E., NOWLIN, B. T., BONVENTRE, J. V., VALERIUS, M. T., MCMAHON, A. P. & DUFFIELD, J. S. 2010. Fate tracing reveals the pericyte and not epithelial origin of myofibroblasts in kidney fibrosis. Am J Pathol, 176, 85-97.

HYNES, R. O. 2004. The emergence of integrins: a personal and historical perspective. Matrix Biol, 23, 333-40.

HYYTIAINEN, M., PENTTINEN, C. & KESKI-OJA, J. 2004. Latent TGF-beta binding proteins: extracellular matrix association and roles in TGF-beta activation. Crit Rev Clin Lab Sci, 41, 233-64.

ILG, E. C., SCHAFER, B. W. & HEIZMANN, C. W. 1996. Expression pattern of S100 calcium-binding proteins in human tumors. Int J Cancer, 68, 325-32.

INGULLI, E. 2010. Mechanism of cellular rejection in transplantation. Pediatr Nephrol, 25, 61-74.

INOUE, T., PLIETH, D., VENKOV, C. D., XU, C. & NEILSON, E. G. 2005. Antibodies against macrophages that overlap in specificity with fibroblasts. Kidney Int, 67, 2488-93.

IWANO, M., PLIETH, D., DANOFF, T. M., XUE, C., OKADA, H. & NEILSON, E. G. 2002. Evidence that fibroblasts derive from epithelium during tissue fibrosis. J Clin Invest, 110, 341-50.

JENKINS, G. 2008. The role of proteases in transforming growth factor-beta activation. Int J Biochem Cell Biol, 40, 1068-78.

JENKINS, R. G., SU, X., SU, G., SCOTTON, C. J., CAMERER, E., LAURENT, G. J., DAVIS, G. E., CHAMBERS, R. C., MATTHAY, M. A. & SHEPPARD, D. 2006. Ligation of protease-activated receptor 1 enhances alpha(v)beta6 integrin-dependent TGF-beta activation and promotes acute lung injury. J Clin Invest, 116, 1606-14.

JENNINGS, P., KOPPELSTAETTER, C., AYDIN, S., ABBERGER, T., WOLF, A. M., MAYER, G. & PFALLER, W. 2007. Cyclosporine A induces senescence in renal tubular epithelial cells. Am J Physiol Renal Physiol, 293, F831-8.

JI, J. D., PARK-MIN, K. H. & IVASHKIV, L. B. 2009. Expression and function of semaphorin 3A and its receptors in human monocyte-derived macrophages. Hum Immunol, 70, 211-7.

JIANG, S., HERRERA, O. & LECHLER, R. I. 2004. New spectrum of allorecognition pathways: implications for graft rejection and transplantation tolerance. Curr Opin Immunol, 16, 550-7.

KAARTINEN, V., VONCKEN, J. W., SHULER, C., WARBURTON, D., BU, D., HEISTERKAMP, N. & GROFFEN, J. 1995. Abnormal lung development and cleft palate in mice lacking TGF-beta 3 indicates defects of epithelial-mesenchymal interaction. Nat Genet, 11, 415-21.

KALLURI, R. & NEILSON, E. G. 2003. Epithelial-mesenchymal transition and its implications for fibrosis. J Clin Invest, 112, 1776-84.

KAPTURCZAK, M. H., MEIER-KRIESCHE, H. U. & KAPLAN, B. 2004. Pharmacology of calcineurin antagonists. Transplant Proc, 36, 25S-32S.

KELLY, M., HWANG, J. M. & KUBES, P. 2007. Modulating leukocyte recruitment in inflammation. J Allergy Clin Immunol, 120, 3-10.

KHALKHALI, H. R., GHAFARI, A., HAJIZADEH, E. & KAZEMNEJAD, A. 2010. Risk factors of long-term graft loss in renal transplant recipients with chronic allograft dysfunction. Exp Clin Transplant, 8, 277-82.

KHANNA, A., PLUMMER, M., BROMBEREK, C., BRESNAHAN, B. & HARIHARAN, S. 2002. Expression of TGF-beta and fibrogenic genes in transplant recipients with tacrolimus and cyclosporine nephrotoxicity. Kidney Int, 62, 2257-63.

KIM, S. J. & GILL, J. S. 2009. H-Y incompatibility predicts short-term outcomes for kidney transplant recipients. J Am Soc Nephrol, 20, 2025-33.

KIM, Y. J., PARK, Y. H. & MOON, H. K. 1997. Reduction of chronic ciclosporin nephrotoxicity by thromboxane synthase inhibition with OKY-046. Kidney Blood Press Res, 20, 38-43.

KIMMEL, P. L., COHEN, D. J., ABRAHAM, A. A., BODI, I., SCHWARTZ, A. M. & PHILLIPS, T. M. 2003. Upregulation of MHC class II, interferon-alpha and interferon-gamma receptor protein expression in HIV-associated nephropathy. Nephrol Dial Transplant, 18, 285-92.

KINO, T., HATANAKA, H., HASHIMOTO, M., NISHIYAMA, M., GOTO, T., OKUHARA, M., KOHSAKA, M., AOKI, H. & IMANAKA, H. 1987. FK-506, a novel immunosuppressant isolated from a Streptomyces. I. Fermentation, isolation, and physico-chemical and biological characteristics. J Antibiot (Tokyo), 40, 1249-55.

KLAGSBRUN, M., TAKASHIMA, S. & MAMLUK, R. 2002. The role of neuropilin in vascular and tumor biology. Adv Exp Med Biol, 515, 33-48.

KLINGELHOFER, J., SENOLT, L., BASLUND, B., NIELSEN, G. H., SKIBSHOJ, I., PAVELKA, K., NEIDHART, M., GAY, S., AMBARTSUMIAN, N., HANSEN, B. S., PETERSEN, J., LUKANIDIN, E. & GRIGORIAN, M. 2007. Up-regulation of metastasis-promoting S100A4 (Mts-1) in rheumatoid arthritis: putative involvement in the pathogenesis of rheumatoid arthritis. Arthritis Rheum, 56, 779-89.

KLINTMALM, G. B., IWATSUKI, S. & STARZL, T. E. 1981. Cyclosporin A hepatotoxicity in 66 renal allograft recipients. Transplantation, 32, 488-9.

KLINTMALM, G. B., IWATSUKI, S. & STARZL, T. E. 1981. Nephrotoxicity of cyclosporin A in liver and kidney transplant patients. Lancet, 1, 470-1.

KOBAYASHI, A., YAMAMOTO, I., ITO, S., AKIOKA, Y., YAMAMOTO, H., TERAOKA, S., HATTORI, M., TANABE, K., HOSOYA, T. & YAMAGUCHI, Y. 2010. Medullary ray injury in renal allografts. Pathol Int, 60, 744-9.

KOLI, K., SAHARINEN, J., HYYTIAINEN, M., PENTTINEN, C. & KESKI-OJA, J. 2001. Latency, activation, and binding proteins of TGF-beta. Microsc Res Tech, 52, 354-62.

KOLODKIN, A. L., LEVENGOOD, D. V., ROWE, E. G., TAI, Y. T., GIGER, R. J. & GINTY, D. D. 1997. Neuropilin is a semaphorin III receptor. Cell, 90, 753-62.

KOLODKIN, A. L., LEVENGOOD, D. V., ROWE, E. G., TAI, Y. T., GIGER, R. J. & GINTY, D. D. 1997. Neuropilin is a semaphorin III receptor. Cell, 90, 753-62.

KOSKI, C., SAHARINEN, J. & KESKI-OJA, J. 1999. Independent promoters regulate the expression of two amino terminally distinct forms of latent transforming growth factor-beta binding protein-1 (LTBP-1) in a cell type-specific manner. J Biol Chem, 274, 32619-30.

KOTH, L. L., ALEX, B., HAWGOOD, S., NEAD, M. A., SHEPPARD, D., ERLE, D. J. & MORRIS, D. G. 2007. Integrin beta6 mediates phospholipid and collectin homeostasis by activation of latent TGF-beta1. Am J Respir Cell Mol Biol, 37, 651-9.

KOWALTOWSKI, A. J., SMAILI, S. S., RUSSELL, J. T. & FISKUM, G. 2000. Elevation of resting mitochondrial membrane potential of neural cells by cyclosporin A, BAPTA-AM, and bcl-2. Am J Physiol Cell Physiol, 279, C852-9.

KREJCI, K., TICHY, T., AL-GABRI, S., HORAK, P., CIFERSKA, H., HRUBY, M., HORCICKA, V., JR., STREBL, P., ZAMBOCH, K., BACHLEDA, P. & ZADRAZIL, J. 2011. Protocol biopsy of a transplanted kidney as a tool for monitoring adequacy of immunosuppressive therapy: 10 years of experience from a single transplant center. Transplant Proc, 43, 1576-82.

KRONKE, M., LEONARD, W. J., DEPPER, J. M., ARYA, S. K., WONG-STAAL, F., GALLO, R. C., WALDMANN, T. A. & GREENE, W. C. 1984. Cyclosporin A inhibits T-cell growth factor gene expression at the level of mRNA transcription. Proc Natl Acad Sci U S A, 81, 5214-8.

KUILMAN, T. & PEEPER, D. S. 2009. Senescence-messaging secretome: SMS-ing cellular stress. Nat Rev Cancer, 9, 81-94.

KULKARNI, A. B. & KARLSSON, S. 1993. Transforming growth factor-beta 1 knockout mice. A mutation in one cytokine gene causes a dramatic inflammatory disease. Am J Pathol, 143, 3-9.

KURUS, M., ESREFOGLU, M., BAY, A. & OZTURK, F. 2005. Protective effect of oral L-arginine supplementation on cyclosporine induced nephropathy in rats. Int Urol Nephrol, 37, 587-94.

LAFFERTY, K. J., BOOTES, A., DART, G. & TALMAGE, D. W. 1976. Effect of organ culture on the survival of thyroid allografts in mice. Transplantation, 22, 138-49.

LALLY, C., HEALY, E. & RYAN, M. P. 1999. Cyclosporine A-induced cell cycle arrest and cell death in renal epithelial cells. Kidney Int, 56, 1254-7.

LAN, H. Y., YANG, N., BROWN, F. G., ISBEL, N. M., NIKOLIC-PATERSON, D. J., MU, W., METZ, C. N., BACHER, M., ATKINS, R. C. & BUCALA, R. 1998. Macrophage migration inhibitory factor expression in human renal allograft rejection. Transplantation, 66, 1465-71.

LAWLER, J., SUNDAY, M., THIBERT, V., DUQUETTE, M., GEORGE, E. L., RAYBURN, H. & HYNES, R. O. 1998. Thrombospondin-1 is required for normal murine pulmonary homeostasis and its absence causes pneumonia. J Clin Invest, 101, 982-92.

LAWRENCE, D. A. 2001. Latent-TGF-beta: an overview. Mol Cell Biochem, 219, 163-70.

LAZZERI, E., ROTONDI, M., MAZZINGHI, B., LASAGNI, L., BUONAMANO, A., ROSATI, A., PRADELLA, F., FOSSOMBRONI, V., LA VILLA, G., GACCI, M., BERTONI, E., SERIO, M., SALVADORI, M. & ROMAGNANI, P. 2005. High CXCL10 expression in rejected kidneys and predictive role of pretransplant serum CXCL10 for acute rejection and chronic allograft nephropathy. Transplantation, 79, 1215-20.

LE HIR, M., HEGYI, I., CUENI-LOFFING, D., LOFFING, J. & KAISSLING, B. 2005. Characterization of renal interstitial fibroblast-specific protein 1/S100A4-positive cells in healthy and inflamed rodent kidneys. Histochem Cell Biol, 123, 335-46.

LE MOINE, A., GOLDMAN, M. & ABRAMOWICZ, D. 2002. Multiple pathways to allograft rejection. Transplantation, 73, 1373-81.

LEE, D. A. & MOLINARO, G. A. 2003. Activated peripheral T lymphocytes undergo apoptosis when cultured with monocytes activated by HLA class II ligation. Cell Immunol, 225, 101-12.

LEE, R. S., GRUSBY, M. J., GLIMCHER, L. H., WINN, H. J. & AUCHINCLOSS, H., JR. 1994. Indirect recognition by helper cells can induce donor-specific cytotoxic T lymphocytes in vivo. J Exp Med, 179, 865-72.

LETEURTRE, E., COPIN, M. C., LABALETTE, M., NOEL, C., ROUMILHAC, D., PRUVOT, F. R., LECOMTE-HOUCKE, M., GOSSELIN, B. & DESSAINT, J. P. 2000. Negative immunohistochemical detection of CD103 (alphaEbeta7 integrin) in the infiltrates of acute rejection in liver and kidney transplantation. Transplantation, 70, 227-9.

LI, S. S., IVANOFF, A., BERGSTROM, S. E., SANDSTROM, A., CHRISTENSSON, B., VAN NERVEN, J., HOLGERSSON, J., HAUZENBERGER, D., ARENCIBIA, I. & SUNDQVIST, K. G. 2002. T lymphocyte expression of thrombospondin-1 and adhesion to extracellular matrix components. Eur J Immunol, 32, 1069-79.

LI, Y., YANG, J., DAI, C., WU, C. & LIU, Y. 2003. Role for integrin-linked kinase in mediating tubular epithelial to mesenchymal transition and renal interstitial fibrogenesis. J Clin Invest, 112, 503-16.

LIANG, H., ZHAO, Y., SAN, Z., LIAO, C., SHA, C., XIE, B., CHEN, J., XIA, J., WANG, Y. & QI, Z. 2010. The recall alloresponse following retransplantation is more intense compared with the T cell memory-transfer model. Immunol Invest, 39, 39-53.

LIM, B. J., KIM, P. K., HONG, S. W. & JEONG, H. J. 2004. Osteopontin expression and microvascular injury in cyclosporine nephrotoxicity. Pediatr Nephrol, 19, 288-94.

LIN, S. L., KISSELEVA, T., BRENNER, D. A. & DUFFIELD, J. S. 2008. Pericytes and perivascular fibroblasts are the primary source of collagen-producing cells in obstructive fibrosis of the kidney. Am J Pathol, 173, 1617-27.

LING, H., LI, X., JHA, S., WANG, W., KARETSKAYA, L., PRATT, B. & LEDBETTER, S. 2003. Therapeutic role of TGF-beta-neutralizing antibody in mouse cyclosporin A

nephropathy: morphologic improvement associated with functional preservation. J Am Soc Nephrol, 14, 377-88.

LIPTAK, P. & IVANYI, B. 2006. Primer: Histopathology of calcineurin-inhibitor toxicity in renal allografts. Nat Clin Pract Nephrol, 2, 398-404; quiz following 404.

LIU, B. C., LI, M. X., ZHANG, J. D., LIU, X. C., ZHANG, X. L. & PHILLIPS, A. O. 2008. Inhibition of integrin-linked kinase via a siRNA expression plasmid attenuates connective tissue growth factor-induced human proximal tubular epithelial cells to mesenchymal transition. Am J Nephrol, 28, 143-51.

LIU, E. H., SIEGEL, R. M., HARLAN, D. M. & O'SHEA, J. J. 2007. T cell-directed therapies: lessons learned and future prospects. Nat Immunol, 8, 25-30.

LIU, Y. 2004. Epithelial to mesenchymal transition in renal fibrogenesis: pathologic significance, molecular mechanism, and therapeutic intervention. J Am Soc Nephrol, 15, 1-12.

LIU, Y. 2010. New insights into epithelial-mesenchymal transition in kidney fibrosis. J Am Soc Nephrol, 21, 212-22.

LO, H. W., HSU, S. C., XIA, W., CAO, X., SHIH, J. Y., WEI, Y., ABBRUZZESE, J. L., HORTOBAGYI, G. N. & HUNG, M. C. 2007. Epidermal growth factor receptor cooperates with signal transducer and activator of transcription 3 to induce epithelial-mesenchymal transition in cancer cells via up-regulation of TWIST gene expression. Cancer Res, 67, 9066-76.

LOVETT, D. H., JOHNSON, R. J., MARTI, H. P., MARTIN, J., DAVIES, M. & COUSER, W. G. 1992. Structural characterization of the mesangial cell type IV collagenase and enhanced expression in a model of immune complex-mediated glomerulonephritis. Am J Pathol, 141, 85-98.

LU, L., YU, Y., LI, G., PU, L., ZHANG, F., ZHENG, S. & WANG, X. 2009. CD8(+)CD103(+) regulatory T cells in spontaneous tolerance of liver allografts. Int Immunopharmacol, 9, 546-8.

LUDLOW, A., YEE, K. O., LIPMAN, R., BRONSON, R., WEINREB, P., HUANG, X., SHEPPARD, D. & LAWLER, J. 2005. Characterization of integrin beta6 and thrombospondin-1 double-null mice. J Cell Mol Med, 9, 421-37.

LUO, K. & LODISH, H. F. 1996. Signaling by chimeric erythropoietin-TGF-beta receptors: homodimerization of the cytoplasmic domain of the type I TGF-beta receptor and heterodimerization with the type II receptor are both required for intracellular signal transduction. EMBO J, 15, 4485-96.

LYONS, R. M., KESKI-OJA, J. & MOSES, H. L. 1988. Proteolytic activation of latent transforming growth factor-beta from fibroblast-conditioned medium. J Cell Biol, 106, 1659-65.

MA, L. J., YANG, H., GASPERT, A., CARLESSO, G., BARTY, M. M., DAVIDSON, J. M., SHEPPARD, D. & FOGO, A. B. 2003. Transforming growth factor-beta-dependent and -independent pathways of induction of tubulointerstitial fibrosis in beta6(-/-) mice. Am J Pathol, 163, 1261-73.

MACUNLUOGLU, B., ARIKAN, H., ATAKAN, A., TUGLULAR, S., ULFER, G., CAKALAGAOGLU, F., OZENER, C. & AKOGLU, E. 2008. Effects of spironolactone in an experimental model of chronic cyclosporine nephrotoxicity. Transplant Proc, 40, 273-8.

MARCEN, R., PASCUAL, J., TERUEL, J. L., VILLAFRUELA, J. J., RIVERA, M. E., MAMPASO, F., BURGOS, F. J. & ORTUNO, J. 2001. Outcome of cadaveric renal transplant patients treated for 10 years with cyclosporine: is chronic allograft nephropathy the major cause of late graft loss? Transplantation, 72, 57-62.

MARENHOLZ, I., LOVERING, R. C. & HEIZMANN, C. W. 2006. An update of the S100 nomenclature. Biochim Biophys Acta, 1763, 1282-3.

MARGETTS, P. J., BONNIAUD, P., LIU, L., HOFF, C. M., HOLMES, C. J., WEST-MAYS, J. A. & KELLY, M. M. 2005. Transient overexpression of TGF-{beta}1 induces epithelial mesenchymal transition in the rodent peritoneum. J Am Soc Nephrol, 16, 425-36.

MARKOVICS, J. A., ARAYA, J., CAMBIER, S., JABLONS, D., HILL, A., WOLTERS, P. J. & NISHIMURA, S. L. 2010. Transcription of the transforming growth factor beta activating integrin beta8 subunit is regulated by SP3, AP-1, and the p38 pathway. J Biol Chem, 285, 24695-706.

MASSARI, M. E. & MURRE, C. 2000. Helix-loop-helix proteins: regulators of transcription in eucaryotic organisms. Mol Cell Biol, 20, 429-40.

MATEVOSSIAN, E., KERN, H., HUSER, N., DOLL, D., SNOPOK, Y., NAHRIG, J., ALTOMONTE, J., SINICINA, I., FRIESS, H. & THORBAN, S. 2009. Surgeon Yurii Voronoy (1895-1961) - a pioneer in the history of clinical transplantation: in memoriam at the 75th anniversary of the first human kidney transplantation. Transpl Int, 22, 1132-9.

MATSUSHITA, A., GOTZE, T. & KORC, M. 2007. Hepatocyte growth factor-mediated cell invasion in pancreatic cancer cells is dependent on neuropilin-1. Cancer Res, 67, 10309-16.

MAZA, A., MONTAUDIE, H., SBIDIAN, E., GALLINI, A., ARACTINGI, S., AUBIN, F., BACHELEZ, H., CRIBIER, B., JOLY, P., JULLIEN, D., LE MAITRE, M., MISERY, L., RICHARD, M. A., ORTONNE, J. P. & PAUL, C. 2011. Oral cyclosporin in psoriasis: a systematic review on treatment modalities, risk of kidney toxicity and evidence for use in non-plaque psoriasis. J Eur Acad Dermatol Venereol, 25 Suppl 2, 19-27.

MCFARLAND, R. D., DOUEK, D. C., KOUP, R. A. & PICKER, L. J. 2000. Identification of a human recent thymic emigrant phenotype. Proc Natl Acad Sci U S A, 97, 4215-20.

MCMORROW, T., GAFFNEY, M. M., SLATTERY, C., CAMPBELL, E. & RYAN, M. P. 2005. Cyclosporine A induced epithelial-mesenchymal transition in human renal proximal tubular epithelial cells. Nephrol Dial Transplant, 20, 2215-25.

MEIER-KRIESCHE, H. U., SCHOLD, J. D. & KAPLAN, B. 2004. Long-term renal allograft survival: have we made significant progress or is it time to rethink our analytic and therapeutic strategies? Am J Transplant, 4, 1289-95.

MIAO, H. Q., SOKER, S., FEINER, L., ALONSO, J. L., RAPER, J. A. & KLAGSBRUN, M. 1999. Neuropilin-1 mediates collapsin-1/semaphorin III inhibition of endothelial cell motility: functional competition of collapsin-1 and vascular endothelial growth factor-165. J Cell Biol, 146, 233-42.

MIETTINEN, P. J., EBNER, R., LOPEZ, A. R. & DERYNCK, R. 1994. TGF-beta induced transdifferentiation of mammary epithelial cells to mesenchymal cells: involvement of type I receptors. J Cell Biol, 127, 2021-36.

MIGLIORE, A., BIZZI, E., MASSAFRA, U., VACCA, F., MARTIN MARTIN, L. S., FERLITO, C., PODESTA, E., GRANATA, M. & LAGANA, B. 2010. Can Cyclosporine-A associated to methotrexate maintain remission induced by anti-TNF agents in rheumatoid arthritis patients? (Cynar pilot study). Int J Immunopathol Pharmacol, 23, 783-90.

MIHATSCH, M. J., KYO, M., MOROZUMI, K., YAMAGUCHI, Y., NICKELEIT, V. & RYFFEL, B. 1998. The side-effects of ciclosporine-A and tacrolimus. Clin Nephrol, 49, 356-63.

MILPIED, P., RENAND, A., BRUNEAU, J., MENDES-DA-CRUZ, D. A., JACQUELIN, S., ASNAFI, V., RUBIO, M. T., MACINTYRE, E., LEPELLETIER, Y. & HERMINE, O. 2009. Neuropilin-1 is not a marker of human Foxp3+ Treg. Eur J Immunol, 39, 1466-71.

MINSKY, M. 1988. Memoir on inventing the confocal scanning microscope. Scanning, 10, 128-138.

MINOWADA, J., DREXLER, H. G., MENON, M., RUBINSTEIN, H., MESSMORE, H., KRASNOW, S., TAKEUCHI, J. & SANDBERG, A. A. 1985. A model scheme of hematopoietic cell differentiation based on multiple marker analysis of leukemia-lymphomas: T cell lineage. Haematol Blood Transfus, 29, 426-9.

MINOWADA, J. & MOORE, G. E. 1975. T-lymphocyte cell lines derived from patients with acute lymphoblastic leukemia. Bibl Haematol, 251-61.

MINOWADA, J., NONOYAMA, M., MOORE, G. E., RAUCH, A. M. & PAGANO, J. S. 1974. The presence of the Epstein-Barr viral genome in human lymphoblastoid B-cell lines and its absence in a myeloma cell line. Cancer Res, 34, 1898-903.

MIYAZAWA, K., SHINOZAKI, M., HARA, T., FURUYA, T. & MIYAZONO, K. 2002. Two major Smad pathways in TGF-beta superfamily signalling. Genes Cells, 7, 1191-204.

MIYAZONO, K., HELLMAN, U., WERNSTEDT, C. & HELDIN, C. H. 1988. Latent high molecular weight complex of transforming growth factor beta 1. Purification from human platelets and structural characterization. J Biol Chem, 263, 6407-15.

MIYAZONO, K., OLOFSSON, A., COLOSETTI, P. & HELDIN, C. H. 1991. A role of the latent TGF-beta 1-binding protein in the assembly and secretion of TGF-beta 1. EMBO J, 10, 1091-101.

MOHAMED, M. A., ROBERTSON, H., BOOTH, T. A., BALUPURI, S., GERSTENKORN, C., KIRBY, J. A. & TALBOT, D. 2000. Active TGF-beta1 expression in kidney transplantation: a comparative study of cyclosporin-A (CyA) and tacrolimus (FK506). Transpl Int, 13 Suppl 1, S295-8.

MOHAMED, M. A., WALMSLEY, M., ROBERTSON, H., KIRBY, J. A. & TALBOT, D. 1999. The effect of cyclosporin A and tacrolimus on cultured human epithelial cells: the role of TGF-beta. Transplant Proc, 31, 1173.

MOORE, G. E. & HOOD, D. B. 1993. Modified RPMI 1640 culture medium. In Vitro Cell Dev Biol Anim, 29A, 268.

MORALI, O. G., DELMAS, V., MOORE, R., JEANNEY, C., THIERY, J. P. & LARUE, L. 2001. IGF-II induces rapid beta-catenin relocation to the nucleus during epithelium to mesenchyme transition. Oncogene, 20, 4942-50.

MORISHIMA, N., MIZOGUCHI, I., TAKEDA, K., MIZUGUCHI, J. & YOSHIMOTO, T. 2009. TGF-beta is necessary for induction of IL-23R and Th17 differentiation by IL-6 and IL-23. Biochem Biophys Res Commun, 386, 105-10.

MU, D., CAMBIER, S., FJELLBIRKELAND, L., BARON, J. L., MUNGER, J. S., KAWAKATSU, H., SHEPPARD, D., BROADDUS, V. C. & NISHIMURA, S. L. 2002. The integrin alpha(v)beta8 mediates epithelial homeostasis through MT1-MMP-dependent activation of TGF-beta1. J Cell Biol, 157, 493-507.

MULLER, G. A., ZEISBERG, M. & STRUTZ, F. 2000. The importance of tubulointerstitial damage in progressive renal disease. Nephrol Dial Transplant, 15 Suppl 6, 76-7.

MUNGER, J. S., HUANG, X., KAWAKATSU, H., GRIFFITHS, M. J., DALTON, S. L., WU, J., PITTET, J. F., KAMINSKI, N., GARAT, C., MATTHAY, M. A., RIFKIN, D. B. & SHEPPARD, D. 1999. The integrin alpha v beta 6 binds and activates latent TGF beta 1: a mechanism for regulating pulmonary inflammation and fibrosis. Cell, 96, 319-28.

MURPHY-ULLRICH, J. E. & POCZATEK, M. 2000. Activation of latent TGF-beta by thrombospondin-1: mechanisms and physiology. Cytokine Growth Factor Rev, 11, 59-69.

MYERS, B. D., ROSS, J., NEWTON, L., LUETSCHER, J. & PERLROTH, M. 1984. Cyclosporine-associated chronic nephropathy. N Engl J Med, 311, 699-705.

MYERS, B. D., SIBLEY, R., NEWTON, L., TOMLANOVICH, S. J., BOSHKOS, C., STINSON, E., LUETSCHER, J. A., WHITNEY, D. J., KRASNY, D., COPLON, N. S. & ET AL. 1988. The long-term course of cyclosporine-associated chronic nephropathy. Kidney Int, 33, 590-600.

NAGATA, K. 2003. HSP47 as a collagen-specific molecular chaperone: function and expression in normal mouse development. Semin Cell Dev Biol, 14, 275-82.

NAKAMURA, K., KITANI, A. & STROBER, W. 2001. Cell contact-dependent immunosuppression by CD4(+)CD25(+) regulatory T cells is mediated by cell surface-bound transforming growth factor beta. J Exp Med, 194, 629-44.

NAKAO, A., IMAMURA, T., SOUCHELNYTSKYI, S., KAWABATA, M., ISHISAKI, A., OEDA, E., TAMAKI, K., HANAI, J., HELDIN, C. H., MIYAZONO, K. & TEN DIJKE, P. 1997. TGF-beta receptor-mediated signalling through Smad2, Smad3 and Smad4. EMBO J, 16, 5353-62.

NANKIVELL, B. J., BORROWS, R. J., FUNG, C. L., O'CONNELL, P. J., ALLEN, R. D. & CHAPMAN, J. R. 2003. The natural history of chronic allograft nephropathy. N Engl J Med, 349, 2326-33.

NANKIVELL, B. J., BORROWS, R. J., FUNG, C. L., O'CONNELL, P. J., CHAPMAN, J. R. & ALLEN, R. D. 2004. Calcineurin inhibitor nephrotoxicity: longitudinal assessment by protocol histology. Transplantation, 78, 557-65.

NANKIVELL, B. J., FENTON-LEE, C. A., KUYPERS, D. R., CHEUNG, E., ALLEN, R. D., O'CONNELL, P. J. & CHAPMAN, J. R. 2001. Effect of histological damage on long-term kidney transplant outcome. Transplantation, 71, 515-23.

NEUFELD, G., COHEN, T., SHRAGA, N., LANGE, T., KESSLER, O. & HERZOG, Y. 2002. The neuropilins: multifunctional semaphorin and VEGF receptors that modulate axon guidance and angiogenesis. Trends Cardiovasc Med, 12, 13-9.

NEUROHR, C., NISHIMURA, S. L. & SHEPPARD, D. 2006. Activation of transforming growth factor-beta by the integrin alphavbeta8 delays epithelial wound closure. Am J Respir Cell Mol Biol, 35, 252-9.

NEWTON, R. A. & HOGG, N. 1998. The human S100 protein MRP-14 is a novel activator of the beta 2 integrin Mac-1 on neutrophils. J Immunol, 160, 1427-35.

NICULESCU-DUVAZ, I., PHANISH, M. K., COLVILLE-NASH, P. & DOCKRELL, M. E. 2007. The TGFbeta1-induced fibronectin in human renal proximal tubular epithelial cells is p38 MAP kinase dependent and Smad independent. Nephron Exp Nephrol, 105, e108-16.

NIEVES-CINTRON, M., AMBERG, G. C., NICHOLS, C. B., MOLKENTIN, J. D. & SANTANA, L. F. 2007. Activation of NFATc3 down-regulates the beta1 subunit of large conductance, calcium-activated K+ channels in arterial smooth muscle and contributes to hypertension. J Biol Chem, 282, 3231-40.

NOBLE, P. B. & CUTTS, J. H. 1967. Separation of blood leukocytes by Ficoll gradient. Can Vet J, 8, 110-1.

OIDA, T. & WEINER, H. L. 2011. Murine CD4 T cells produce a new form of TGF-beta as measured by a newly developed TGF-beta bioassay. PLoS One, 6, e18365.

OIDA, T., ZHANG, X., GOTO, M., HACHIMURA, S., TOTSUKA, M., KAMINOGAWA, S. & WEINER, H. L. 2003. CD4+CD25- T cells that express latency-associated peptide on the surface suppress CD4+CD45RBhigh-induced colitis by a TGF-beta-dependent mechanism. J Immunol, 170, 2516-22.

OKADA, H., BAN, S., NAGAO, S., TAKAHASHI, H., SUZUKI, H. & NEILSON, E. G. 2000. Progressive renal fibrosis in murine polycystic kidney disease: an immunohistochemical observation. Kidney Int, 58, 587-97.

OKADA, H., DANOFF, T. M., KALLURI, R. & NEILSON, E. G. 1997. Early role of Fsp1 in epithelial-mesenchymal transformation. Am J Physiol, 273, F563-74.

OLIVER, J. A., BARASCH, J., YANG, J., HERZLINGER, D. & AL-AWQATI, Q. 2002. Metanephric mesenchyme contains embryonic renal stem cells. Am J Physiol Renal Physiol, 283, F799-809.

OSTERREICHER, C. H., PENZ-OSTERREICHER, M., GRIVENNIKOV, S. I., GUMA, M., KOLTSOVA, E. K., DATZ, C., SASIK, R., HARDIMAN, G., KARIN, M. & BRENNER, D. A. 2011. Fibroblast-specific protein 1 identifies an inflammatory subpopulation of macrophages in the liver. Proc Natl Acad Sci U S A, 108, 308-13.

OZDEMIR, B. H., OZDEMIR, F. N., DEMIRHAN, B. & HABERAL, M. 2005. TGF-beta1 expression in renal allograft rejection and cyclosporine A toxicity. Transplantation, 80, 1681-5.

PADDOCK, S. W. 2000. Principles and practices of laser scanning confocal microscopy. Mol Biotechnol, 16, 127-49.

PALLET, N., BOUVIER, N., LEGENDRE, C., GILLERON, J., CODOGNO, P., BEAUNE, P., THERVET, E. & ANGLICHEAU, D. 2008. Autophagy protects renal tubular cells against cyclosporine toxicity. Autophagy, 4, 783-91.

PARK, S. H., CHOI, H. J., LEE, J. H., WOO, C. H., KIM, J. H. & HAN, H. J. 2001. High glucose inhibits renal proximal tubule cell proliferation and involves PKC, oxidative stress, and TGF-beta 1. Kidney Int, 59, 1695-705.

PATEL, P., WEST-MAYS, J., KOLB, M., RODRIGUES, J. C., HOFF, C. M. & MARGETTS, P. J. 2010. Platelet derived growth factor B and epithelial mesenchymal transition of peritoneal mesothelial cells. Matrix Biol, 29, 97-106.

PATSENKER, E., POPOV, Y., STICKEL, F., JONCZYK, A., GOODMAN, S. L. & SCHUPPAN, D. 2008. Inhibition of integrin alphavbeta6 on cholangiocytes blocks

transforming growth factor-beta activation and retards biliary fibrosis progression. Gastroenterology, 135, 660-70.

PELLET-MANY, C., FRANKEL, P., JIA, H. & ZACHARY, I. 2008. Neuropilins: structure, function and role in disease. Biochem J, 411, 211-26.

PETCHER, T. J., WEBER, H. & RUEGGER, A. 1976. Crystal and molecular structure of an iodo-derivative of the cyclic undecapeptide cyclosporin A. Helv Chim Acta, 59, 1480-9.

PFAFFL, M. W., HORGAN, G. W. & DEMPFLE, L. 2002. Relative expression software tool (REST) for group-wise comparison and statistical analysis of relative expression results in real-time PCR. Nucleic Acids Res, 30, e36.

PHANISH, M. K., WAHAB, N. A., COLVILLE-NASH, P., HENDRY, B. M. & DOCKRELL, M. E. 2006. The differential role of Smad2 and Smad3 in the regulation of pro-fibrotic TGFbeta1 responses in human proximal-tubule epithelial cells. Biochem J, 393, 601-7.

PICARD, N., BAUM, O., VOGETSEDER, A., KAISSLING, B. & LE HIR, M. 2008. Origin of renal myofibroblasts in the model of unilateral ureter obstruction in the rat. Histochem Cell Biol, 130, 141-55.

PICHLER, R. H., FRANCESCHINI, N., YOUNG, B. A., HUGO, C., ANDOH, T. F., BURDMANN, E. A., SHANKLAND, S. J., ALPERS, C. E., BENNETT, W. M., COUSER, W. G. & ET AL. 1995. Pathogenesis of cyclosporine nephropathy: roles of angiotensin II and osteopontin. J Am Soc Nephrol, 6, 1186-96.

PIEK, E., JU, W. J., HEYER, J., ESCALANTE-ALCALDE, D., STEWART, C. L., WEINSTEIN, M., DENG, C., KUCHERLAPATI, R., BOTTINGER, E. P. & ROBERTS, A. B. 2001. Functional characterization of transforming growth factor beta signaling in Smad2- and Smad3-deficient fibroblasts. J Biol Chem, 276, 19945-53.

PIETRA, B. A., WISEMAN, A., BOLWERK, A., RIZEQ, M. & GILL, R. G. 2000. CD4 T cell-mediated cardiac allograft rejection requires donor but not host MHC class II. J Clin Invest, 106, 1003-10.

PILAT, N., SAYEGH, M. H. & WEKERLE, T. 2011. Costimulatory pathways in transplantation. Semin Immunol, 23, 293-303.

PROCTOR, J. M., ZANG, K., WANG, D., WANG, R. & REICHARDT, L. F. 2005. Vascular development of the brain requires beta8 integrin expression in the neuroepithelium. J Neurosci, 25, 9940-8.

RACUSEN, L. C., MONTEIL, C., SGRIGNOLI, A., LUCSKAY, M., MAROUILLAT, S., RHIM, J. G. & MORIN, J. P. 1997. Cell lines with extended in vitro growth potential from human renal proximal tubule: characterization, response to inducers, and comparison with established cell lines. J Lab Clin Med, 129, 318-29.

RACUSEN, L. C. & REGELE, H. 2010. The pathology of chronic allograft dysfunction. Kidney Int Suppl, S27-32.

RACUSEN, L. C., SOLEZ, K., COLVIN, R. B., BONSIB, S. M., CASTRO, M. C., CAVALLO, T., CROKER, B. P., DEMETRIS, A. J., DRACHENBERG, C. B., FOGO, A. B., FURNESS, P., GABER, L. W., GIBSON, I. W., GLOTZ, D., GOLDBERG, J. C., GRANDE, J., HALLORAN, P. F., HANSEN, H. E., HARTLEY, B., HAYRY, P. J., HILL, C. M., HOFFMAN, E. O., HUNSICKER, L. G., LINDBLAD, A. S., YAMAGUCHI, Y. & ET AL. 1999. The Banff 97 working classification of renal allograft pathology. Kidney Int, 55, 713-23.

RAMIREZ, C., OLMO, A., O'VALLE, F., MASSEROLI, M., AGUILAR, M., GOMEZ-MORALES, M., REVELLES, F., GARCIA-CHICANO, M. J., ARREBOLA, F., REGUERO, M. E. & DEL MORAL, R. G. 2000. Role of intrarenal endothelin 1, endothelin 3, and angiotensin II expression in chronic cyclosporin A nephrotoxicity in rats. Exp Nephrol, 8, 161-72.

RESCIGNO, M. 2010. Functional specialization of antigen presenting cells in the gastrointestinal tract. Curr Opin Immunol, 22, 131-6.

REYNOLDS, L. E., WYDER, L., LIVELY, J. C., TAVERNA, D., ROBINSON, S. D., HUANG, X., SHEPPARD, D., HYNES, R. O. & HODIVALA-DILKE, K. M. 2002. Enhanced pathological angiogenesis in mice lacking beta3 integrin or beta3 and beta5 integrins. Nat Med, 8, 27-34.

RIBEIRO, S. M., POCZATEK, M., SCHULTZ-CHERRY, S., VILLAIN, M. & MURPHY-ULLRICH, J. E. 1999. The activation sequence of thrombospondin-1 interacts with the latency-associated peptide to regulate activation of latent transforming growth factor-beta. J Biol Chem, 274, 13586-93.

ROBERTSON, H., ALI, S., MCDONNELL, B. J., BURT, A. D. & KIRBY, J. A. 2004. Chronic renal allograft dysfunction: the role of T cell-mediated tubular epithelial to mesenchymal cell transition. J Am Soc Nephrol, 15, 390-7.

ROBERTSON, H., MORLEY, A. R., TALBOT, D., CALLANAN, K. & KIRBY, J. A. 2000. Renal allograft rejection: beta-chemokine involvement in the development of tubulitis. Transplantation, 69, 684-7.

ROBERTSON, H., WHEELER, J., KIRBY, J. A. & MORLEY, A. R. 1996. Renal allograft rejection--in situ demonstration of cytotoxic intratubular cells. Transplantation, 61, 1546-9.

ROGERS, T. S., ELZINGA, L., BENNETT, W. M. & KELLEY, V. E. 1988. Selective enhancement of thromboxane in macrophages and kidneys in cyclosporine-induced nephrotoxicity. Dietary protection by fish oil. Transplantation, 45, 153-6.

ROMEO, P. H., LEMARCHANDEL, V. & TORDJMAN, R. 2002. Neuropilin-1 in the immune system. Adv Exp Med Biol, 515, 49-54.

RONCO, P., LELONGT, B., PIEDAGNEL, R. & CHATZIANTONIOU, C. 2007. Matrix metalloproteinases in kidney disease progression and repair: a case of flipping the coin. Semin Nephrol, 27, 352-62.

ROSS, R., EVERETT, N. B. & TYLER, R. 1970. Wound healing and collagen formation. VI. The origin of the wound fibroblast studied in parabiosis. J Cell Biol, 44, 645-54.

ROWSHANI, A. T., FLORQUIN, S., BEMELMAN, F., KUMMER, J. A., HACK, C. E. & TEN BERGE, I. J. 2004. Hyperexpression of the granzyme B inhibitor PI-9 in human renal allografts: a potential mechanism for stable renal function in patients with subclinical rejection. Kidney Int, 66, 1417-22.

RYAN, M. J., JOHNSON, G., KIRK, J., FUERSTENBERG, S. M., ZAGER, R. A. & TOROK-STORB, B. 1994. HK-2: an immortalized proximal tubule epithelial cell line from normal adult human kidney. Kidney Int, 45, 48-57.

RYFFEL, B. 1993. Cyclosporin binding proteins. Identification, distribution, function and relation to FK binding proteins. Biochem Pharmacol, 46, 1-12.

RYGIEL, K. A., ROBERTSON, H., MARSHALL, H. L., PEKALSKI, M., ZHAO, L., BOOTH, T. A., JONES, D. E., BURT, A. D. & KIRBY, J. A. 2008. Epithelial-mesenchymal transition contributes to portal tract fibrogenesis during human chronic liver disease. Lab Invest, 88, 112-23.

RYGIEL, K. A., ROBERTSON, H., WILLET, J. D., BRAIN, J. G., BURT, A. D., JONES, D. E. & KIRBY, J. A. 2010. T cell-mediated biliary epithelial-to-mesenchymal transition in liver allograft rejection. Liver Transpl, 16, 567-76.

SADY, S. P., GOYAL, M., THOMAS, P. E., WHARRAM, B. L. & WIGGINS, R. C. 1995. Fibronectin mRNA in the developing glomerular crescent in rabbit antiglomerular basement membrane disease. J Am Soc Nephrol, 5, 2087-90.

SAFINIA, N., AFZALI, B., ATALAR, K., LOMBARDI, G. & LECHLER, R. I. 2010. T-cell alloimmunity and chronic allograft dysfunction. Kidney Int Suppl, S2-12.

SAHARINEN, J., TAIPALE, J., MONNI, O. & KESKI-OJA, J. 1998. Identification and characterization of a new latent transforming growth factor-beta-binding protein, LTBP-4. J Biol Chem, 273, 18459-69.

SANFORD, L. P., ORMSBY, I., GITTENBERGER-DE GROOT, A. C., SARIOLA, H., FRIEDMAN, R., BOIVIN, G. P., CARDELL, E. L. & DOETSCHMAN, T. 1997. TGFbeta2 knockout mice have multiple developmental defects that are non-overlapping with other TGFbeta knockout phenotypes. Development, 124, 2659-70.

SAYEGH, M. H. 1999. Why do we reject a graft? Role of indirect allorecognition in graft rejection. Kidney Int, 56, 1967-79.

SCHENKEL, A. R., MAMDOUH, Z. & MULLER, W. A. 2004. Locomotion of monocytes on endothelium is a critical step during extravasation. Nat Immunol, 5, 393-400.

SCHMID, H., COHEN, C. D., HENGER, A., IRRGANG, S., SCHLONDORFF, D. & KRETZLER, M. 2003. Validation of endogenous controls for gene expression analysis in microdissected human renal biopsies. Kidney Int, 64, 356-60.

SCHMIDT-HANSEN, B., ORNAS, D., GRIGORIAN, M., KLINGELHOFER, J., TULCHINSKY, E., LUKANIDIN, E. & AMBARTSUMIAN, N. 2004. Extracellular S100A4(mts1) stimulates invasive growth of mouse endothelial cells and modulates MMP-13 matrix metalloproteinase activity. Oncogene, 23, 5487-95.

SCHMOUDER, R. L., STREITER, R. M., WALZ, A. & KUNKEL, S. L. 1995. Epithelial-derived neutrophil-activating factor-78 production in human renal tubule epithelial cells and in renal allograft rejection. Transplantation, 59, 118-24.

SCHNEIDER, M., HANSEN, J. L. & SHEIKH, S. P. 2008. S100A4: a common mediator of epithelial-mesenchymal transition, fibrosis and regeneration in diseases? J Mol Med (Berl), 86, 507-22.

SCHNEIDER, M., KOSTIN, S., STROM, C. C., APLIN, M., LYNGBAEK, S., THEILADE, J., GRIGORIAN, M., ANDERSEN, C. B., LUKANIDIN, E., LERCHE HANSEN, J. & SHEIKH, S. P. 2007. S100A4 is upregulated in injured myocardium and promotes growth and survival of cardiac myocytes. Cardiovasc Res, 75, 40-50.

SCHRAMEK, H., SARKOZI, R., LAUTERBERG, C., KRONBICHLER, A., PIRKLBAUER, M., ALBRECHT, R., NOPPERT, S. J., PERCO, P., RUDNICKI, M., STRUTZ, F. M. & MAYER, G. 2009. Neuropilin-1 and neuropilin-2 are differentially expressed in human proteinuric nephropathies and cytokine-stimulated proximal tubular cells. Lab Invest, 89, 1304-16.

SCHULTZ-CHERRY, S., CHEN, H., MOSHER, D. F., MISENHEIMER, T. M., KRUTZSCH, H. C., ROBERTS, D. D. & MURPHY-ULLRICH, J. E. 1995. Regulation of transforming growth factor-beta activation by discrete sequences of thrombospondin 1. J Biol Chem, 270, 7304-10.

SCHULTZ-CHERRY, S. & MURPHY-ULLRICH, J. E. 1993. Thrombospondin causes activation of latent transforming growth factor-beta secreted by endothelial cells by a novel mechanism. J Cell Biol, 122, 923-32.

SCOTTON, C. J., KRUPICZOJC, M. A., KONIGSHOFF, M., MERCER, P. F., LEE, Y. C., KAMINSKI, N., MORSER, J., POST, J. M., MAHER, T. M., NICHOLSON, A. G., MOFFATT, J. D., LAURENT, G. J., DERIAN, C. K., EICKELBERG, O. & CHAMBERS, R.

C. 2009. Increased local expression of coagulation factor X contributes to the fibrotic response in human and murine lung injury. J Clin Invest, 119, 2550-63.

SEMOV, A., MORENO, M. J., ONICHTCHENKO, A., ABULROB, A., BALL, M., EKIEL, I., PIETRZYNSKI, G., STANIMIROVIC, D. & ALAKHOV, V. 2005. Metastasis-associated protein S100A4 induces angiogenesis through interaction with Annexin II and accelerated plasmin formation. J Biol Chem, 280, 20833-41.

SEYMOUR, R. A., THOMASON, J. M. & ELLIS, J. S. 1996. The pathogenesis of drug-induced gingival overgrowth. J Clin Periodontol, 23, 165-75.

SHANG, M. H., YUAN, W. J., ZHANG, S. J., FAN, Y. & ZHANG, Z. 2008. Intrarenal activation of renin angiotensin system in the development of cyclosporine A induced chronic nephrotoxicity. Chin Med J (Engl), 121, 983-8.

SHEPPARD, D. 2005. Integrin-mediated activation of latent transforming growth factor beta. Cancer Metastasis Rev, 24, 395-402.

SHI, Y. & MASSAGUE, J. 2003. Mechanisms of TGF-beta signaling from cell membrane to the nucleus. Cell, 113, 685-700.

SHIAU, M. Y., TSAI, S. T., TSAI, K. J., HAUNG, M. L., HSU, Y. T. & CHANG, Y. H. 2006. Increased circulatory MMP-2 and MMP-9 levels and activities in patients with type 1 diabetes mellitus. Mt Sinai J Med, 73, 1024-8.

SHIHAB, F. S., ANDOH, T. F., TANNER, A. M. & BENNETT, W. M. 1997. Sodium depletion enhances fibrosis and the expression of TGF-beta1 and matrix proteins in experimental chronic cyclosporine nephropathy. Am J Kidney Dis, 30, 71-81.

SHIHAB, F. S., BENNETT, W. M., YI, H. & ANDOH, T. F. 2006. Effect of cyclosporine and sirolimus on the expression of connective tissue growth factor in rat experimental chronic nephrotoxicity. Am J Nephrol, 26, 400-7.

SHIHAB, F. S., WAID, T. H., CONTI, D. J., YANG, H., HOLMAN, M. J., MULLOY, L. C., HENNING, A. K., HOLMAN, J., JR., FIRST, M. R. & GROUP, C. S. 2008. Conversion from cyclosporine to tacrolimus in patients at risk for chronic renal allograft failure: 60-month results of the CRAF Study. Transplantation, 85, 1261-9.

SHIHAB, F. S., YI, H., BENNETT, W. M. & ANDOH, T. F. 2000. Effect of nitric oxide modulation on TGF-beta1 and matrix proteins in chronic cyclosporine nephrotoxicity. Kidney Int, 58, 1174-85.

SHIMIZU, H., BOLATI, D., ADIJIANG, A., MUTELIEFU, G., ENOMOTO, A., NISHIJIMA, F., DATEKI, M. & NIWA, T. 2011. NF-kappaB plays an important role in indoxyl sulfate-induced cellular senescence, fibrotic gene expression, and inhibition of proliferation in proximal tubular cells. Am J Physiol Cell Physiol, 301, C1201-12.

SHISHIDO, S., ASANUMA, H., NAKAI, H., MORI, Y., SATOH, H., KAMIMAKI, I., HATAYA, H., IKEDA, M., HONDA, M. & HASEGAWA, A. 2003. The impact of repeated subclinical acute rejection on the progression of chronic allograft nephropathy. J Am Soc Nephrol, 14, 1046-52.

SHUKLA, M. N., ROSE, J. L., RAY, R., LATHROP, K. L., RAY, A. & RAY, P. 2009. Hepatocyte growth factor inhibits epithelial to myofibroblast transition in lung cells via Smad7. Am J Respir Cell Mol Biol, 40, 643-53.

SIBBRING, J. S., SHARMA, A., MCDICKEN, I. W., SELLS, R. A. & CHRISTMAS, S. E. 1998. Localization of C-X-C and C-C chemokines to renal tubular epithelial cells in human kidney transplants is not confined to acute cellular rejection. Transpl Immunol, 6, 203-8.

SINGH, R. P., LA CAVA, A., WONG, M., EBLING, F. & HAHN, B. H. 2007. CD8+ T cell-mediated suppression of autoimmunity in a murine lupus model of peptide-induced immune tolerance depends on Foxp3 expression. J Immunol, 178, 7649-57.

SIS, B., MENGEL, M., HAAS, M., COLVIN, R. B., HALLORAN, P. F., RACUSEN, L. C., SOLEZ, K., BALDWIN, W. M., 3RD, BRACAMONTE, E. R., BROECKER, V., COSIO, F., DEMETRIS, A. J., DRACHENBERG, C., EINECKE, G., GLOOR, J., GLOTZ, D., KRAUS, E., LEGENDRE, C., LIAPIS, H., MANNON, R. B., NANKIVELL, B. J., NICKELEIT, V., PAPADIMITRIOU, J. C., RANDHAWA, P., REGELE, H., RENAUDIN, K., RODRIGUEZ, E. R., SERON, D., SESHAN, S., SUTHANTHIRAN, M., WASOWSKA, B. A., ZACHARY, A. & ZEEVI, A. 2010. Banff '09 meeting report: antibody mediated graft deterioration and implementation of Banff working groups. Am J Transplant, 10, 464-71.

SKALLI, O., PELTE, M. F., PECLET, M. C., GABBIANI, G., GUGLIOTTA, P., BUSSOLATI, G., RAVAZZOLA, M. & ORCI, L. 1989. Alpha-smooth muscle actin, a differentiation marker of smooth muscle cells, is present in microfilamentous bundles of pericytes. J Histochem Cytochem, 37, 315-21.

SLATTERY, C., CAMPBELL, E., MCMORROW, T. & RYAN, M. P. 2005. Cyclosporine A-induced renal fibrosis: a role for epithelial-mesenchymal transition. Am J Pathol, 167, 395-407.

SLATTERY, C., MCMORROW, T. & RYAN, M. P. 2006. Overexpression of E2A proteins induces epithelial-mesenchymal transition in human renal proximal tubular epithelial cells suggesting a potential role in renal fibrosis. FEBS Lett, 580, 4021-30.

SOLEZ, K., COLVIN, R. B., RACUSEN, L. C., SIS, B., HALLORAN, P. F., BIRK, P. E., CAMPBELL, P. M., CASCALHO, M., COLLINS, A. B., DEMETRIS, A. J., DRACHENBERG, C. B., GIBSON, I. W., GRIMM, P. C., HAAS, M., LERUT, E., LIAPIS, H., MANNON, R. B., MARCUS, P. B., MENGEL, M., MIHATSCH, M. J., NANKIVELL, B. J., NICKELEIT, V., PAPADIMITRIOU, J. C., PLATT, J. L., RANDHAWA, P., ROBERTS, I., SALINAS-MADRIGA, L., SALOMON, D. R., SERON, D., SHEAFF, M. & WEENING, J. J. 2007. Banff '05 Meeting Report: differential diagnosis of chronic allograft injury and elimination of chronic allograft nephropathy ('CAN'). Am J Transplant, 7, 518-26.

SOLOMON, B. D., MUELLER, C., CHAE, W. J., ALABANZA, L. M. & BYNOE, M. S. 2011. Neuropilin-1 attenuates autoreactivity in experimental autoimmune encephalomyelitis. Proc Natl Acad Sci U S A, 108, 2040-5.

SOULA-ROTHHUT, M., COISSARD, C., SARTELET, H., BOUDOT, C., BELLON, G., MARTINY, L. & ROTHHUT, B. 2005. The tumor suppressor PTEN inhibits EGF-induced TSP-1 and TIMP-1 expression in FTC-133 thyroid carcinoma cells. Exp Cell Res, 304, 187-201.

STAHELIN, H. F. 1996. The history of cyclosporin A (Sandimmune) revisited: another point of view. Experientia, 52, 5-13.

STEGALL, M. D., PARK, W. D., LARSON, T. S., GLOOR, J. M., CORNELL, L. D., SETHI, S., DEAN, P. G., PRIETO, M., AMER, H., TEXTOR, S., SCHWAB, T. & COSIO, F. G. 2011. The histology of solitary renal allografts at 1 and 5 years after transplantation. Am J Transplant, 11, 698-707.

STEINERT, P. M. & ROOP, D. R. 1988. Molecular and cellular biology of intermediate filaments. Annu Rev Biochem, 57, 593-625.

STRUTZ, F. & NEILSON, E. G. 1994. The role of lymphocytes in the progression of interstitial disease. Kidney Int Suppl, 45, S106-10.

STRUTZ, F., OKADA, H., LO, C. W., DANOFF, T., CARONE, R. L., TOMASZEWSKI, J. E. & NEILSON, E. G. 1995. Identification and characterization of a fibroblast marker: FSP1. J Cell Biol, 130, 393-405.

STRUTZ, F. & ZEISBERG, M. 2006. Renal fibroblasts and myofibroblasts in chronic kidney disease. J Am Soc Nephrol, 17, 2992-8.

SU, H., KIM, H., PAWLIKOWSKA, L., KITAMURA, H., SHEN, F., CAMBIER, S., MARKOVICS, J., LAWTON, M. T., SIDNEY, S., BOLLEN, A. W., KWOK, P. Y., REICHARDT, L., YOUNG, W. L., YANG, G. Y. & NISHIMURA, S. L. 2010. Reduced expression of integrin alphavbeta8 is associated with brain arteriovenous malformation pathogenesis. Am J Pathol, 176, 1018-27.

SUGIMOTO, T., HANEDA, M., SAWANO, H., ISSHIKI, K., MAEDA, S., KOYA, D., INOKI, K., YASUDA, H., KASHIWAGI, A. & KIKKAWA, R. 2001. Endothelin-1 induces cyclooxygenase-2 expression via nuclear factor of activated T-cell transcription factor in glomerular mesangial cells. J Am Soc Nephrol, 12, 1359-68.

TADA, H. & ISOGAI, S. 1998. The fibronectin production is increased by thrombospondin via activation of TGF-beta in cultured human mesangial cells. Nephron, 79, 38-43.

TAIPALE, J., MIYAZONO, K., HELDIN, C. H. & KESKI-OJA, J. 1994. Latent transforming growth factor-beta 1 associates to fibroblast extracellular matrix via latent TGF-beta binding protein. J Cell Biol, 124, 171-81.

TAKENAGA, K., NAKAMURA, Y. & SAKIYAMA, S. 1994. Cellular localization of pEL98 protein, an S100-related calcium binding protein, in fibroblasts and its tissue distribution analyzed by monoclonal antibodies. Cell Struct Funct, 19, 133-41.

TAN, R., HE, W., LIN, X., KISS, L. P. & LIU, Y. 2008. Smad ubiquitination regulatory factor-2 in the fibrotic kidney: regulation, target specificity, and functional implication. Am J Physiol Renal Physiol, 294, F1076-83.

TAPMEIER, T. T., FEARN, A., BROWN, K., CHOWDHURY, P., SACKS, S. H., SHEERIN, N. S. & WONG, W. 2010. Pivotal role of CD4+ T cells in renal fibrosis following ureteric obstruction. Kidney Int, 78, 351-62.

TARABYKINA, S., KRIAJEVSKA, M., SCOTT, D. J., HILL, T. J., LAFITTE, D., DERRICK, P. J., DODSON, G. G., LUKANIDIN, E. & BRONSTEIN, I. 2000. Heterocomplex formation between metastasis-related protein S100A4 (Mts1) and S100A1 as revealed by the yeast two-hybrid system. FEBS Lett, 475, 187-91.

TAYLOR, A. W. 2009. Review of the activation of TGF-beta in immunity. J Leukoc Biol, 85, 29-33.

TESSEUR, I., ZOU, K., BERBER, E., ZHANG, H. & WYSS-CORAY, T. 2006. Highly sensitive and specific bioassay for measuring bioactive TGF-beta. BMC Cell Biol, 7, 15.

THELLIN, O., ZORZI, W., LAKAYE, B., DE BORMAN, B., COUMANS, B., HENNEN, G., GRISAR, T., IGOUT, A. & HEINEN, E. 1999. Housekeeping genes as internal standards: use and limits. J Biotechnol, 75, 291-5.

THORNTON, A. M. & SHEVACH, E. M. 1998. CD4+CD25+ immunoregulatory T cells suppress polyclonal T cell activation in vitro by inhibiting interleukin 2 production. J Exp Med, 188, 287-96.

THURMAN, J. M. 2007. Triggers of inflammation after renal ischemia/reperfusion. Clin Immunol, 123, 7-13.

TORDJMAN, R., LEPELLETIER, Y., LEMARCHANDEL, V., CAMBOT, M., GAULARD, P., HERMINE, O. & ROMEO, P. H. 2002. A neuronal receptor, neuropilin-1, is essential for the initiation of the primary immune response. Nat Immunol, 3, 477-82.

TRAN, D. Q., ANDERSSON, J., HARDWICK, D., BEBRIS, L., ILLEI, G. G. & SHEVACH, E. M. 2009. Selective expression of latency-associated peptide (LAP) and IL-1 receptor type I/II (CD121a/CD121b) on activated human FOXP3+ regulatory T cells allows for their purification from expansion cultures. Blood, 113, 5125-33.

TRAVIS, M. A., REIZIS, B., MELTON, A. C., MASTELLER, E., TANG, Q., PROCTOR, J. M., WANG, Y., BERNSTEIN, X., HUANG, X., REICHARDT, L. F., BLUESTONE, J. A. & SHEPPARD, D. 2007. Loss of integrin alpha(v)beta8 on dendritic cells causes autoimmunity and colitis in mice. Nature, 449, 361-5.

TREVILLIAN, P., PAUL, H., MILLAR, E., HIBBERD, A. & AGREZ, M. V. 2004. alpha(v)beta(6) Integrin expression in diseased and transplanted kidneys. Kidney Int, 66, 1423-33.

TROXELL, M. L., GOPALAKRISHNAN, S., MCCORMACK, J., POTEAT, B. A., PENNINGTON, J., GARRINGER, S. M., SCHNEEBERGER, E. E., NELSON, W. J. & MARRS, J. A. 2000. Inhibiting cadherin function by dominant mutant E-cadherin expression increases the extent of tight junction assembly. J Cell Sci, 113 (Pt 6), 985-96.

TULCHINSKY, E., GRIGORIAN, M., TKATCH, T., GEORGIEV, G. & LUKANIDIN, E. 1995. Transcriptional regulation of the mts1 gene in human lymphoma cells: the role of DNA-methylation. Biochim Biophys Acta, 1261, 243-8.

TUNGGAL, J. A., HELFRICH, I., SCHMITZ, A., SCHWARZ, H., GUNZEL, D., FROMM, M., KEMLER, R., KRIEG, T. & NIESSEN, C. M. 2005. E-cadherin is essential for in vivo epidermal barrier function by regulating tight junctions. EMBO J, 24, 1146-56.

TURVEY, M. R., WANG, Y. & GU, Y. 2010. The effects of extracellular nucleotides on [Ca2+]i signalling in a human-derived renal proximal tubular cell line (HKC-8). J Cell Biochem, 109, 132-9.

USS, E., ROWSHANI, A. T., HOOIBRINK, B., LARDY, N. M., VAN LIER, R. A. & TEN BERGE, I. J. 2006. CD103 is a marker for alloantigen-induced regulatory CD8+ T cells. J Immunol, 177, 2775-83.

VALCOURT, U., KOWANETZ, M., NIIMI, H., HELDIN, C. H. & MOUSTAKAS, A. 2005. TGF-beta and the Smad signaling pathway support transcriptomic reprogramming during epithelial-mesenchymal cell transition. Mol Biol Cell, 16, 1987-2002.

VAN AMERONGEN, M. J., BOU-GHARIOS, G., POPA, E., VAN ARK, J., PETERSEN, A. H., VAN DAM, G. M., VAN LUYN, M. J. & HARMSEN, M. C. 2008. Bone marrow-derived myofibroblasts contribute functionally to scar formation after myocardial infarction. J Pathol, 214, 377-86.

VAN WAARDE, M. A., VAN ASSEN, A. J., KAMPINGA, H. H., KONINGS, A. W. & VUJASKOVIC, Z. 1997. Quantification of transforming growth factor-beta in biological material using cells transfected with a plasminogen activator inhibitor-1 promoter-luciferase construct. Anal Biochem, 247, 45-51.

VASCONCELLOS, L. M., SCHACHTER, A. D., ZHENG, X. X., VASCONCELLOS, L. H., SHAPIRO, M., HARMON, W. E. & STROM, T. B. 1998. Cytotoxic lymphocyte gene expression in peripheral blood leukocytes correlates with rejecting renal allografts. Transplantation, 66, 562-6.

VEERASAMY, M., NGUYEN, T. Q., MOTAZED, R., PEARSON, A. L., GOLDSCHMEDING, R. & DOCKRELL, M. E. 2009. Differential regulation of E-cadherin

and alpha-smooth muscle actin by BMP 7 in human renal proximal tubule epithelial cells and its implication in renal fibrosis. Am J Physiol Renal Physiol, 297, F1238-48.

VELDHOEN, M., HOCKING, R. J., FLAVELL, R. A. & STOCKINGER, B. 2006. Signals mediated by transforming growth factor-beta initiate autoimmune encephalomyelitis, but chronic inflammation is needed to sustain disease. Nat Immunol, 7, 1151-6.

VONGWIWATANA, A., TASANARONG, A., RAYNER, D. C., MELK, A. & HALLORAN, P. F. 2005. Epithelial to mesenchymal transition during late deterioration of human kidney transplants: the role of tubular cells in fibrogenesis. Am J Transplant, 5, 1367-74.

WAKEFIELD, L. M., SMITH, D. M., FLANDERS, K. C. & SPORN, M. B. 1988. Latent transforming growth factor-beta from human platelets. A high molecular weight complex containing precursor sequences. J Biol Chem, 263, 7646-54.

WALSH-REITZ, M. M. & TOBACK, F. G. 1992. Phenol red inhibits growth of renal epithelial cells. Am J Physiol, 262, F687-91.

WANG, B., KOH, P., WINBANKS, C., COUGHLAN, M. T., MCCLELLAND, A., WATSON, A., JANDELEIT-DAHM, K., BURNS, W. C., THOMAS, M. C., COOPER, M. E. & KANTHARIDIS, P. 2011. miR-200a Prevents renal fibrogenesis through repression of TGF-beta2 expression. Diabetes, 60, 280-7.

WANG, H., ZHANG, Y. & HEUCKEROTH, R. O. 2007. PAI-1 deficiency reduces liver fibrosis after bile duct ligation in mice through activation of tPA. FEBS Lett, 581, 3098-104.

WANG, L., DUTTA, S. K., KOJIMA, T., XU, X., KHOSRAVI-FAR, R., EKKER, S. C. & MUKHOPADHYAY, D. 2007. Neuropilin-1 modulates p53/caspases axis to promote endothelial cell survival. PLoS One, 2, e1161.

WANG, P. & HEITMAN, J. 2005. The cyclophilins. Genome Biol, 6, 226.

WANG, W., KOKA, V. & LAN, H. Y. 2005. Transforming growth factor-beta and Smad signalling in kidney diseases. Nephrology (Carlton), 10, 48-56.

WASSLER, M., JONASSON, I., PERSSON, R. & FRIES, E. 1987. Differential permeabilization of membranes by saponin treatment of isolated rat hepatocytes. Release of secretory proteins. Biochem J, 247, 407-15.

WEST, D. C., REES, C. G., DUCHESNE, L., PATEY, S. J., TERRY, C. J., TURNBULL, J. E., DELEHEDDE, M., HEEGAARD, C. W., ALLAIN, F., VANPOUILLE, C., RON, D. & FERNIG, D. G. 2005. Interactions of multiple heparin binding growth factors with neuropilin-1 and potentiation of the activity of fibroblast growth factor-2. J Biol Chem, 280, 13457-64.

WIPFF, P. J., RIFKIN, D. B., MEISTER, J. J. & HINZ, B. 2007. Myofibroblast contraction activates latent TGF-beta1 from the extracellular matrix. J Cell Biol, 179, 1311-23.

WITZGALL, R., BROWN, D., SCHWARZ, C. & BONVENTRE, J. V. 1994. Localization of proliferating cell nuclear antigen, vimentin, c-Fos, and clusterin in the postischemic kidney. Evidence for a heterogenous genetic response among nephron segments, and a large pool of mitotically active and dedifferentiated cells. J Clin Invest, 93, 2175-88.

WOLTMAN, A. M., DE FIJTER, J. W., VAN DER KOOIJ, S. W., JIE, K. E., MASSACRIER, C., CAUX, C., DAHA, M. R. & VAN KOOTEN, C. 2005. MIP-3alpha/CCL20 in renal transplantation and its possible involvement as dendritic cell chemoattractant in allograft rejection. Am J Transplant, 5, 2114-25.

WONG, M. L. & MEDRANO, J. F. 2005. Real-time PCR for mRNA quantitation. Biotechniques, 39, 75-85.

WONG, W. K., ROBERTSON, H., CARROLL, H. P., ALI, S. & KIRBY, J. A. 2003. Tubulitis in renal allograft rejection: role of transforming growth factor-beta and interleukin-15 in development and maintenance of CD103+ intraepithelial T cells. Transplantation, 75, 505-14.

WU, C. & DEDHAR, S. 2001. Integrin-linked kinase (ILK) and its interactors: a new paradigm for the coupling of extracellular matrix to actin cytoskeleton and signaling complexes. J Cell Biol, 155, 505-10.

WU, W., JIANG, X. Y., ZHANG, Q. L., MO, Y., SUN, L. Z. & CHEN, S. M. 2009. Expression and significance of TGF-beta1/Smad signaling pathway in children with IgA nephropathy. World J Pediatr, 5, 211-5.

WYNN, T. A. 2007. Common and unique mechanisms regulate fibrosis in various fibroproliferative diseases. J Clin Invest, 117, 524-9.

XU, J., LAMOUILLE, S. & DERYNCK, R. 2009. TGF-beta-induced epithelial to mesenchymal transition. Cell Res, 19, 156-72.

XU, Y., WAN, J., JIANG, D. & WU, X. 2010. BMP-7 blocks the cyclosporine-A-induced epithelial-to-mesenchymal transition in renal tubular epithelial cells. Nephron Exp Nephrol, 114, e23-31.

YANG, J. & LIU, Y. 2001. Dissection of key events in tubular epithelial to myofibroblast transition and its implications in renal interstitial fibrosis. Am J Pathol, 159, 1465-75.

YANG, Q., O'HANLON, D., HEIZMANN, C. W. & MARKS, A. 1999. Demonstration of heterodimer formation between S100B and S100A6 in the yeast two-hybrid system and human melanoma. Exp Cell Res, 246, 501-9.

YANG, Z., MU, Z., DABOVIC, B., JURUKOVSKI, V., YU, D., SUNG, J., XIONG, X. & MUNGER, J. S. 2007. Absence of integrin-mediated TGFbeta1 activation in vivo recapitulates the phenotype of TGFbeta1-null mice. J Cell Biol, 176, 787-93.

YANNARAKI, M., REBIBOU, J. M., DUCLOUX, D., SAAS, P., DUPERRIER, A., FELIX, S., RIFLE, G., CHALOPIN, J. M., HERVE, P., TIBERGHIEN, P. & FERRAND, C. 2006. Urinary cytotoxic molecular markers for a noninvasive diagnosis in acute renal transplant rejection. Transpl Int, 19, 759-68.

YOKOI, H., MUKOYAMA, M., NAGAE, T., MORI, K., SUGANAMI, T., SAWAI, K., YOSHIOKA, T., KOSHIKAWA, M., NISHIDA, T., TAKIGAWA, M., SUGAWARA, A. & NAKAO, K. 2004. Reduction in connective tissue growth factor by antisense treatment ameliorates renal tubulointerstitial fibrosis. J Am Soc Nephrol, 15, 1430-40.

YOUNG, B. A., BURDMANN, E. A., JOHNSON, R. J., ALPERS, C. E., GIACHELLI, C. M., ENG, E., ANDOH, T., BENNETT, W. M. & COUSER, W. G. 1995. Cellular proliferation and macrophage influx precede interstitial fibrosis in cyclosporine nephrotoxicity. Kidney Int, 48, 439-48.

YOUNG, G. D. & MURPHY-ULLRICH, J. E. 2004. The tryptophan-rich motifs of the thrombospondin type 1 repeats bind VLAL motifs in the latent transforming growth factor-beta complex. J Biol Chem, 279, 47633-42.

ZAMORA, R., DEREK, B. & YORAM, V. 2007. Differential activation of recombinant human latent transforming growth factor-β1 (TGF-β1) by acid and heat. Rev Fac Med, 15(2), 177-179.

ZAVADIL, J. & BOTTINGER, E. P. 2005. TGF-beta and epithelial-to-mesenchymal transitions. Oncogene, 24, 5764-74.

ZEISBERG, E. M., POTENTA, S. E., SUGIMOTO, H., ZEISBERG, M. & KALLURI, R. 2008. Fibroblasts in kidney fibrosis emerge via endothelial-to-mesenchymal transition. J Am Soc Nephrol, 19, 2282-7.

ZEISBERG, M., BONNER, G., MAESHIMA, Y., COLORADO, P., MULLER, G. A., STRUTZ, F. & KALLURI, R. 2001. Renal fibrosis: collagen composition and assembly regulates epithelial-mesenchymal transdifferentiation. Am J Pathol, 159, 1313-21.

ZEISBERG, M., HANAI, J., SUGIMOTO, H., MAMMOTO, T., CHARYTAN, D., STRUTZ, F. & KALLURI, R. 2003. BMP-7 counteracts TGF-beta1-induced epithelial-to-mesenchymal transition and reverses chronic renal injury. Nat Med, 9, 964-8.

ZEISBERG, M. & KALLURI, R. 2004. The role of epithelial-to-mesenchymal transition in renal fibrosis. J Mol Med (Berl), 82, 175-81.

ZEISBERG, M. & NEILSON, E. G. 2009. Biomarkers for epithelial-mesenchymal transitions. J Clin Invest, 119, 1429-37.

ZELENIKA, D., ADAMS, E., HUMM, S., GRACA, L., THOMPSON, S., COBBOLD, S. P. & WALDMANN, H. 2002. Regulatory T cells overexpress a subset of Th2 gene transcripts. J Immunol, 168, 1069-79.

ZHANG, H., TASNIM, F., YING, J. Y. & ZINK, D. 2009. The impact of extracellular matrix coatings on the performance of human renal cells applied in bioartificial kidneys. Biomaterials, 30, 2899-911.

ZHANG, L., BERTUCCI, A. M., RAMSEY-GOLDMAN, R., BURT, R. K. & DATTA, S. K. 2009. Regulatory T cell (Treg) subsets return in patients with refractory lupus following stem cell transplantation, and TGF-beta-producing CD8+ Treg cells are associated with immunological remission of lupus. J Immunol, 183, 6346-58.

ZHU, M. Q., DE BROE, M. E. & NOUWEN, E. J. 1996. Vimentin expression and distal tubular damage in the rat kidney. Exp Nephrol, 4, 172-83.

ZIYADEH, F. N. 2004. Mediators of diabetic renal disease: the case for tgf-Beta as the major mediator. J Am Soc Nephrol, 15 Suppl 1, S55-7.